

Tailored Synthesis of Complexes and Polymers Containing Organoiron and Organocobalt

by

Diana Joyce Winram

**A THESIS SUBMITTED IN PARTIAL FULFILLMENT OF THE REQUIREMENTS
FOR THE DEGREE OF**

Master of Science

in

The College of Graduate Studies

(Chemistry)

**THE UNIVERSITY OF BRITISH COLUMBIA
(Okanagan)**

February 2010

©Diana Joyce Winram 2010

Abstract

This thesis describes synthetic strategies for the incorporation of organoiron and organocobalt into polymers. Norbornene and methacrylate based polymers which contained μ -alkyne-bis(tricarbonylcobalt) complexes and either η^6 -(haloarene)- η^5 -cyclopentadienyliron(II) hexafluorophosphate or ferrocene moieties were synthesized. Norbornene monomers which contained both the organoiron and the organocobalt complexes were successfully polymerized using ring opening metathesis polymerization. Radical polymerization of methacrylate monomers which contained η^6 -(haloarene)- η^5 -cyclopentadienyliron(II) hexafluorophosphate moieties and alkyne functional groups, allowed for the coordination of dicobalt hexacarbonyl post polymerization. The monomers and their precursors were characterized through nuclear magnetic resonance spectroscopy, infrared spectroscopy and cyclic voltammetry. The molecular weights of the polymers were estimated using gel permeation chromatography and the thermal properties were studied with thermogravimetric analysis and differential scanning calorimetry.

Another class of organoiron monomers containing alkyne functional groups were polymerized through condensation of their η^6 -(haloarene)- η^5 -cyclopentadienyliron(II) hexafluorophosphate moieties with various dithiols. A monomer which contained both η^6 -(haloarene)- η^5 -cyclopentadienyliron(II) hexafluorophosphate and μ -alkyne-bis(tricarbonylcobalt) moieties was also combined with various dithiol linking groups.

Preliminary studies on the synthesis and characterization of three siloxane based polymers which contained η^6 -(arene)- η^5 -cyclopentadienyliron(II) hexafluorophosphate moieties were also explored.

Table of Contents

Abstract	ii
Table of Contents	iii
List of Tables	viii
List of Figures	ix
List of Schemes	xiii
List of Symbols and Abbreviations	xv
Acknowledgements	xviii
Chapter 1: Introduction	1
1.1 The chemistry of ferrocene	1
1.2 The synthesis and chemistry of η^6 -(arene)- η^5 -cyclopentadienyliron(II) hexafluorophosphate complexes	4
1.3 Synthesis and chemistry of μ -alkyne-bis(tricarbonylcobalt) complexes	9
1.4 Metal containing polymers.....	10
1.5 Scope of the present work.....	11
1.6 Materials and instrumentation.....	12
Chapter 2: Norbornene based polymers	14
2.1 Introduction.....	14
2.2 Synthesis and characterization of polynorbornenes containing organoiron and cobalt carbonyl.....	17
2.2.1 Synthesis of a norbornene monomer containing ferrocene.....	17
2.2.2 Polymerization of a norbornene monomer containing ferrocene.....	27
2.2.3 Synthesis of a norbornene monomer containing both ferrocene and cobalt	28

2.2.4 Polymerization of a norbornene monomer containing both ferrocene and cobalt.....	35
2.3 Synthesis and characterization of η^6 -arene- η^5 -cyclopentadienyliron(II) and cobalt containing polynorbornenes.....	37
2.3.1 Synthesis of a norbornene monomer containing alkyne-hexacarbonyl cobalt and two η^6 -chloroarene- η^5 -cyclopentadienyliron(II) moieties	37
2.3.2 Polymerization of a norbornene monomer containing cobalt carbonyl and two η^6 -arene- η^5 -cyclopentadienyliron(II) moieties	49
2.3.3 Synthesis of a norbornene monomer containing a single η^6 -arene- η^5 -cyclopentadienyliron(II) moiety and cobalt carbonyl.....	53
2.3.4 Polymerization of norbornene monomer containing a single η^6 -arene- η^5 -cyclopentadienyliron(II) moiety and cobalt carbonyl.....	62
2.4 Molecular weight determination of polymers.....	63
2.5 Thermal analysis of polymers.....	64
2.6 Cyclic voltammetry of norbornene complexes	66
2.7 Summary	67
2.8 Detailed experimental	69
Chapter 3: Methacrylate based polymers.....	83
3.1 Introduction.....	83
3.2 Synthesis and characterization of ferrocene and cobalt containing polymethacrylates.....	87
3.2.1 Synthesis of a methacrylate monomer that contains ferrocene.....	87
3.2.2 Synthesis of a model methacrylate complex that contains both ferrocene and cobalt carbonyl.....	92
3.2.3 Polymerization of a ferrocene-containing methacrylate monomer.....	96

3.2.4 Coordination of cobalt carbonyl to a ferrocene-containing methacrylate polymer	98
3.3 Synthesis and characterization of a polymethacrylate containing η^6 -arene- η^5 - cyclopentadienyliron and cobalt carbonyl	100
3.3.1 Synthesis of a methacrylate monomer containing two η^6 -arene- η^5 - cyclopentadienyliron(II) moieties	100
3.3.2 Polymerization of a methacrylate monomer containing two η^6 -arene- η^5 - cyclopentadienyliron(II) moieties	103
3.3.3 Coordination of cobalt carbonyl to a methacrylate polymer containing two η^6 -arene- η^5 -cyclopentadienyliron(II) moieties	105
3.3.4 Synthesis of a methacrylate monomer containing a single η^6 -arene- η^5 - cyclopentadienyliron(II) moiety	108
3.3.5 Polymerization of a methacrylate monomer containing a single η^6 -arene- η^5 - cyclopentadienyliron(II) moiety	111
3.3.6 Coordination of cobalt carbonyl to a methacrylate polymer monomer containing a single η^6 -arene- η^5 -cyclopentadienyliron(II) moiety	113
3.4 Molecular weight determination of polymers	114
3.5 Thermal analysis of polymers	115
3.6 Summary	117
3.7 Detailed experimental	118
Chapter 4: Condensation polymers.....	125
4.1 Introduction.....	125
4.2 Synthesis and characterization of condensation polymers containing η^6 -arene- η^5 - cyclopentadienyliron(II) and cobalt carbonyl.....	128

4.2.1 Synthesis of a monomer containing η^6 -arene- η^5 -cyclopentadienyliron(II) and alkyne moieties	128
4.2.2 Condensation polymerization of a monomer containing η^6 -arene- η^5 -cyclopentadienyliron(II) and alkyne moieties with dithiol linkers	131
4.2.3 Coordination of cobalt carbonyl to a monomer containing η^6 -arene- η^5 -cyclopentadienyliron(II) and alkyne moieties.....	132
4.2.4 Condensation polymerization of a monomer containing η^6 -arene- η^5 -cyclopentadienyliron(II) and dicobalt hexacarbonyl moieties with dithiol linkers	134
4.3 Thermal analysis of polymers	135
4.4 Cyclic voltammetry of complexes	137
4.5 Summary	137
4.6 Detailed experimental	138
Chapter 5: Preliminary work with polysiloxanes.	141
5.1 Introduction.....	141
5.2 Synthesis and characterization of polysiloxanes containing η^6 -arene- η^5 -cyclopentadienyliron.....	143
5.2.1 Nucleophilic substitution of η^6 -halo-arene- η^5 -cyclopentadienyliron with allylamine.....	143
5.2.2 Hydrosilation of allylamine complexes with methyldiethoxysilane.....	146
5.2.3 Cleavage of ethoxy groups from complexes 5.4 a-c.....	149
5.2.4 Polymerization	151
5.3 Thermal analysis of polymers	154
5.4 Cyclic voltammetry of complexes	155

5.5 Summary	156
5.6 Detailed experimental	157
Chapter 6: General conclusions.....	161
Chapter 7: References	163
Chapter 8: Appendices	171
8.1 X-ray structure report for complex 2.6	171
8.2 X-ray structure report for complex 3.3	190

List of Tables

Table 2.1: Molecular weight data for polymers.....	64
Table 2.2: Thermogravimetric analysis of polynorbornenes	65
Table 2.3: Differential scanning calorimetry of polynorbornenes.....	66
Table 2.4: Cyclic voltammetric studies of norbornene complexes.....	67
Table 3.1: Molecular weight data for polymers.....	115
Table 3.2: Thermogravimetric analysis of polymermethacrylates	116
Table 3.3: Differential scanning calorimetry of organoiron polymethacrylates.....	117
Table 4.1: Thermogravimetric analysis of polymers	136
Table 4.2: Differential scanning calorimetry of polymers.....	136
Table 4.3: Cyclic voltammetry of monomers	137
Table 5.1: Thermogravimetric analysis of polymers 5.6 a-c	155
Table 5.2: Differential scanning calorimetry of polymers 5.6 a-c	155
Table 5.3: Cyclic voltammetry of complexes	156

List of Figures

Figure 1.1: Proposed structures for ferrocene.....	1
Figure 1.2: The reactivity of ferrocene	2
Figure 1.3: Potentials for the oxidation states of ferrocene as determined by cyclic voltammetry.	3
Figure 1.4: General synthesis for η^6 -(arene)- η^5 -cyclopentadienyliron(II) hexafluorophosphate complexes	4
Figure 1.5: Reactivity of η^6 -(haloarene)- η^5 -cyclopentadienyliron(II) hexafluorophosphate salts..	5
Figure 1.6: Nucleophilic aromatic substitution of a η^6 -(haloarene)- η^5 -cyclopentadienyliron(II) ..	6
Figure 1.7: Potentials for the oxidation states of η^6 -(hexamethylbenzene)- η^5 -cyclopentadienyliron(II) as determined by cyclic voltammetry	6
Figure 1.8: Proposed sequence for the photolysis of η^6 -(arene)- η^5 -cyclopentadienyliron(II) complexes	8
Figure 1.9: General synthesis of alkyne-cobalt carbonyl complexes.....	9
Figure 2.1: Four strategies for norbornene polymerization	14
Figure 2.2: Ring opening metathesis of norbornene	15
Figure 2.3: A few examples of polynorbornenes with η^6 -aryl- η^5 -cyclopentadienyliron(II) hexafluorophosphate groups in their side chain.....	16
Figure 2.4: ^1H NMR spectrum of compound 2.6 acetone- d_6	19
Figure 2.5: APT ^{13}C NMR spectrum of compound 2.6 in CDCl_3	20
Figure 2.6: ORTEP diagram of complex 2.6	21
Figure 2.7: ^1H NMR spectrum of complex 2.8 in acetone- d_6	23
Figure 2.8: ^1H NMR spectral comparison of complexes 2.6 , 2.8 <i>exo</i> and 2.8 in acetone- d_6	24
Figure 2.9: APT ^{13}C NMR spectrum of complex 2.8 in acetone- d_6	25

Figure 2.10: HMBC NMR spectrum of complex 2.8 in acetone- d_6	26
Figure 2.11: HSQC NMR spectrum of complex 2.8 in acetone- d_6	27
Figure 2.12: ^1H NMR spectrum of complex 2.11 in acetone- d_6	30
Figure 2.13: Expansion of the ^1H NMR resonances in acetone- d_6 of the methylenes next to the coordinated cobalt moieties of 2.11 (<i>exo/endo</i> mixture) and 2.11 exo	31
Figure 2.14: APT ^{13}C NMR spectrum of complex 2.11 in acetone- d_6	32
Figure 2.15: HSQC NMR spectrum of complex 2.11 in acetone- d_6	33
Figure 2.16: HMBC NMR spectrum of complex 2.11 in acetone- d_6	34
Figure 2.17: IR spectral comparison of complexes 2.8 and 2.11	35
Figure 2.18: ^1H NMR spectrum of polymer 2.12 in CDCl_3	36
Figure 2.19: ^1H NMR spectrum of complex 2.17 in acetone- d_6	40
Figure 2.20: APT ^{13}C NMR spectrum of complex 2.17 in acetone- d_6	41
Figure 2.21: ^1H NMR spectrum of complex 2.18 in acetone- d_6	43
Figure 2.22: APT ^{13}C NMR spectrum of complex 2.18 in acetone- d_6	44
Figure 2.23: HSQC NMR spectrum of complex 2.18 in acetone- d_6	45
Figure 2.24: HMBC NMR spectrum for complex 2.18 in acetone- d_6	46
Figure 2.25: ^1H NMR spectrum of complex 2.19 in acetone- d_6	48
Figure 2.26: APT ^{13}C NMR spectrum of complex 2.19 in acetone- d_6	49
Figure 2.27: ^1H NMR of polymer 2.20 in $\text{DMSO-}d_6$	52
Figure 2.28: ^1H NMR spectrum of complex 2.23 in acetone- d_6	55
Figure 2.29: APT ^{13}C NMR spectrum of complex 2.23 in acetone- d_6	56
Figure 2.30: ^1H NMR spectrum of complex 2.24 in acetone- d_6	58
Figure 2.31: APT ^{13}C NMR spectrum of complex 2.24 in acetone- d_6	59

Figure 2.32: ^1H NMR spectrum of complex 2.25 in acetone- d_6	61
Figure 2.33: APT ^{13}C NMR spectrum of complex 2.25 in acetone- d_6	62
Figure 3.1: General polymerization of methacrylates.....	83
Figure 3.2: Initiation, propagation and termination of methylmethacrylate radical polymerization	84
Figure 3.3: Production of radicals from AIBN.....	85
Figure 3.4: Sample of methacrylates which contain organoiron moieties.....	86
Figure 3.5: ^1H NMR spectrum of complex 3.2 in CDCl_3	88
Figure 3.6: ^1H NMR spectral comparison for complexes 2.6 and 3.2 in CDCl_3	89
Figure 3.7: APT ^{13}C NMR spectrum of complex 3.2 in CDCl_3	90
Figure 3.8: HMBC NMR spectrum of complex 3.2 in CDCl_3	91
Figure 3.9: HSQC NMR spectrum of 3.2 in CDCl_3	92
Figure 3.10: ^1H NMR spectrum of complex 3.3 in acetone- d_6	94
Figure 3.11: APT ^{13}C NMR spectrum of complex 3.3 in acetone- d_6	95
Figure 3.12: ORTEP diagram for complex 3.3	96
Figure 3.13: ^1H NMR spectrum of polymer 3.4 in CDCl_3	98
Figure 3.14: ^1H NMR spectral comparison of polymers 3.4 and 3.5 in CDCl_3	99
Figure 3.15: ^1H NMR spectrum of complex 3.7 in acetone- d_6	102
Figure 3.16: APT ^{13}C NMR spectrum of complex 3.7 in acetone- d_6	103
Figure 3.17: ^1H NMR spectrum of polymer 3.8 in acetone- d_6	105
Figure 3.18: ^1H NMR spectral comparison of polymers 3.8 and 3.9 in acetone- d_6	108
Figure 3.19: ^1H NMR spectrum of complex 3.10 acetone- d_6	110
Figure 3.20: APT ^{13}C NMR spectrum of complex 3.10 in acetone- d_6	111

Figure 3.21: ^1H NMR spectrum of polymer 3.11	113
Figure 4.1: Previously reported condensation polymers of η^6 -arene- η^5 -cyclopentadienyliron(II) hexafluorophosphate salts	126
Figure 4.2: Previously reported condensation polymers of η^6 -arene- η^5 -cyclopentadienyliron(II) hexafluorophosphate salts	127
Figure 4.3: ^1H NMR spectrum of complex 4.1 in $\text{DMSO-}d_6$	129
Figure 4.4: APT ^{13}C NMR spectrum of complex 4.1 in $\text{DMSO-}d_6$	130
Figure 4.5: ^1H NMR of complex 4.4 in $\text{DMSO-}d_6$	133
Figure 4.6: APT ^{13}C NMR spectrum of complex 4.4 in $\text{DMSO-}d_6$	134
Figure 5.1: Hydrosilation of a terminal alkene	142
Figure 5.2: Deprotonation of the amine group to form a zwitterion.....	144
Figure 5.3: ^1H NMR spectrum of complex 5.2 b in acetone- d_6	145
Figure 5.4: APT ^{13}C NMR spectrum of complex 5.2 b in acetone- d_6	146
Figure 5.5: ^1H NMR spectrum of complex 5.4 b in acetone- d_6	148
Figure 5.6: APT ^{13}C NMR spectrum of complex 5.4 b in acetone- d_6	149
Figure 5.7: ^1H NMR spectral visualization of the cleavage of the ethoxy groups from complex 5.4 b through a reaction with D_2O in acetone- d_6	151
Figure 5.8: ^1H NMR spectrum of polymer 5.6 b in acetone- d_6	153
Figure 5.9: APT ^{13}C NMR spectrum of polymer 5.6 b in acetone- d_6	154

List of Schemes

Scheme 2.1: Synthesis of complex 2.4	17
Scheme 2.2: Synthesis of complex 2.6	18
Scheme 2.3: Synthesis of complex 2.8	22
Scheme 2.4: Synthesis of complex 2.9	28
Scheme 2.5: Synthesis of complex 2.11	29
Scheme 2.6: Synthesis of polymer 2.12	36
Scheme 2.7: Synthesis of complexes 2.14 a-c	37
Scheme 2.8: Synthesis of complex 2.16	38
Scheme 2.9: Synthesis of complex 2.17	39
Scheme 2.10: Synthesis of complex 2.18	42
Scheme 2.11: Synthesis of complex 2.19	47
Scheme 2.12: Synthesis of polymer 2.20	51
Scheme 2.13: Synthesis of complex 2.22	53
Scheme 2.14: Synthesis of complex 2.23	54
Scheme 2.15: Synthesis of complex 2.24	57
Scheme 2.16: Synthesis of complex 2.25	60
Scheme 2.17: Synthesis of polymer 2.26	63
Scheme 3.1: Synthesis of complex 3.2	87
Scheme 3.2: Synthesis of complex 3.3	93
Scheme 3.3: Synthesis of polymer 3.4	97
Scheme 3.4: Synthesis of polymer 3.5	99
Scheme 3.5: Synthesis of complex 3.7	101

Scheme 3.6: Synthesis of polymer 3.8	104
Scheme 3.7: Synthesis of polymer 3.9	107
Scheme 3.8: Synthesis of complex 3.10	109
Scheme 3.9: Synthesis of polymer 3.11	112
Scheme 3.10: Synthesis of polymer 3.12	114
Scheme 4.1: Synthesis of complex 4.1	128
Scheme 4.2: Synthesis of polymers 4.3 a-c	131
Scheme 4.3: Synthesis of complex 4.4	132
Scheme 4.4: Synthesis of polymers 4.5 a-c	135
Scheme 5.1: Synthesis of complexes 5.2 a-c	143
Scheme 5.2: Synthesis of complexes 5.4 a-c	147
Scheme 5.3: Cleavage of ethoxy groups from complexes 5.4 a-c	150
Scheme 5.4: Synthesis of polymers 5.6 a-c	152

List of Symbols and Abbreviations

°C	Degrees Celsius
¹³ C NMR	Carbon 13 nuclear magnetic resonance spectroscopy
¹ H NMR	Proton nuclear magnetic resonance spectroscopy
APT	Attached proton test
Ar	Aryl
bp	Boiling point
br.	broad
calc.	calculated
Cp	cyclopentadienyl ring
cm	centimetres
δ	NMR chemical shift in parts per million downfield from a standard
d	Doublet
<i>d</i> ₆	6 deuterium
DCC	Dicyclohexylcarbodiimide
DCM	Dichloromethane
DCU	Dicyclohexylurea
dd	doublet of doublets
ddd	doublet of doublets of doublets
DMAP	N,N'-dimethylaminopyridine
DMF	N,N'-dimethylformamide
DMSO	Dimethylsulfoxide
DSC	Differential scanning calorimetry

dt	Doublet of triplets
e ⁻	Electron
E _{1/2}	Half-wave potential
Et	Ethyl
g	grams
GPC	Gel permeation chromatography
<i>hν</i>	indicates light; <i>h</i> is Planks constant, and <i>v</i> is the photon frequency
HMBC	Heteronuclear correlation spectroscopy
HPLC	High performance liquid chromatography
IR	Infrared spectroscopy
<i>J</i>	<i>J</i> value
kcal	kilocalorie
λ	wavelength
M	Molar
m	multiplet
\overline{M}_n	number-average molecular weight
\overline{M}_w	weight-average molecular weight
MeOH	Methanol
MHz	Megahertz
min.	minute
mL	Millilitre
mM	Millimolar
mmol	Millimoles

mol	Moles
MS	Mass spectrometry
nm	Nanometer
NFO	Non-first order triplet
NMP	N-methyl-2-pyrrolidone
NMR	Nuclear magnetic resonance
Nu	Nucleophile
ORTEP	Oak Ridge thermal ellipsoid plot
<i>p</i>	Para
PDI	Polydispersity index
ppm	parts per million
q	Quartet
ROMP	Ring opening metathesis polymerization
s	Singlet
t	Triplet
T _g	Glass transition temperature
TGA	Thermogravimetric analysis
THF	Tetrahydrofuran
TM	Trademark
tt	Triplet of triplets
UV	Ultraviolet
UV-vis	Ultraviolet visible
V	Volts

Acknowledgements

I owe my deepest gratitude to my supervisor Dr. Alaa Abd-El-Aziz, for all of his inspiration, guidance and support, without whom this research would not have been possible. I would also like to thank the members of my committee Dr. Kevin Smith and Dr. Stephen McNeil for their excellent advice regarding the writing of this thesis. A huge thank you to Dr. Paul Shipley for always making time for my incessant questions regarding NMR interpretation and theory.

To the members of the lab both past and present, thank you for sharing your expertise and the fun times. Thank you, Chris Rock for your efforts in the Methacrylate project. In particular, I would like to thank my fiancé Patrick Oliver Shipman for all of his help completing this enormous task as well as for his excellent culinary skills.

I would also like to thank my family and friends, especially Lottie Joyce, Alexander Winram, Cynthia Winram, Christine McIntyre and Kelly Brodofske, for all of their encouragement. Patrick, I am not only grateful of your cooking skills but also for your patience and understanding during the whole thesis writing process.

Chapter 1: Introduction

1.1 The chemistry of ferrocene

In 1951, Peter Pauson and Tom Kealy reported the first synthesis of ferrocene.^{1,2} These two chemists were attempting to prepare fulvalene when they inadvertently prepared ferrocene; however, they proposed the wrong structure for the compound (Figure 1.1 a). Woodward and Wilkinson recognized that the proposed 10 e⁻ structure was unlikely and proposed the 18 e⁻ bis(η^5 -cyclopentadienyl)iron(II) structure which was confirmed through x-ray crystallography in 1952 (Figure 1.1 b). Ferrocene was determined to consist of two cyclopentadiene rings located in planes above and below an iron atom.^{2,3} Organometallic molecules that have this sort of “sandwich structure” are referred to as metallocenes.

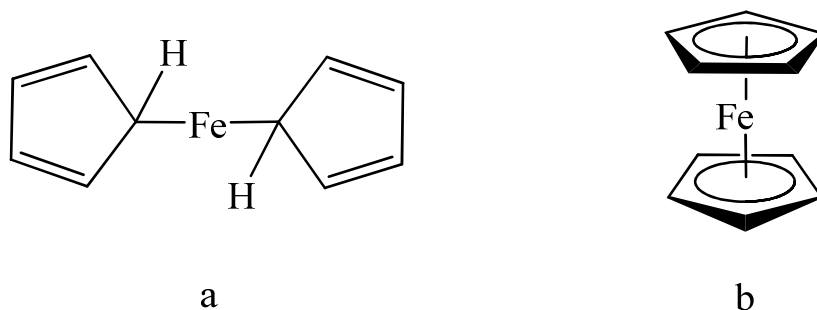


Figure 1.1: Proposed structures for ferrocene.

One of the more interesting features of ferrocene is that the cyclopentadiene rings can undergo chemical reactions similar to that of organic aromatic compounds. For example, Friedel-Crafts acylation of the cyclopentadiene rings proceeds in the presence of a Lewis acid.^{4,5} The chemistry of ferrocene is quite diverse and many derivatives can be prepared. This is illustrated in Figure 1.2 which shows a sample of the different ferrocene derivatives that can be

synthesized.

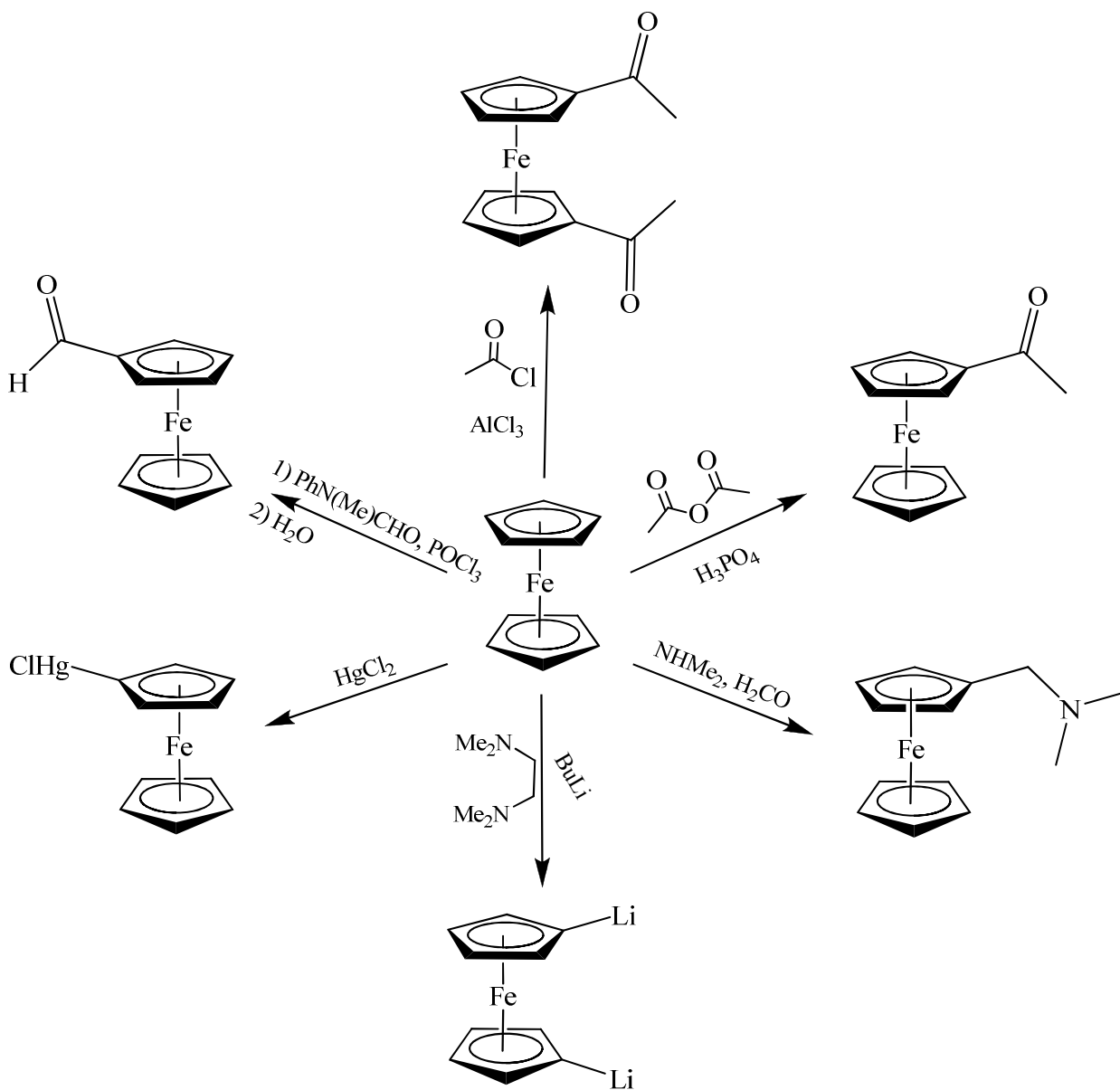


Figure 1.2: The reactivity of ferrocene. ^{6,7}

Four oxidation states have been demonstrated for ferrocene, the $18 e^-$ ferrocene is an electron rich species that can be oxidized to form its $17 e^-$ ferrocenium ion by either chemical or electro-oxidation (Figure 1.3).⁶ Using cyclic voltammetry more extreme oxidation states have been demonstrated by the groups of Laviron (reduction to $19 e^-$, DMF) and Bard (oxidation to $16 e^-$, SO_2). Studies of the $18 e^-$ ferrocene to the $17 e^-$ ferrocenium ion cyclic voltammetry wave

shows that the oxidation of ferrocene is not only reversible but highly reproducible.^{8,9} The reproducibility of this reaction is such that ferrocene is often used as an internal reference for cyclic voltammetric studies. Investigations into the electrochemical behaviour of a number of substituted ferrocenes has revealed that electron donating substituents lead to lower redox potentials while electron withdrawing substituents lead to increased redox potentials.¹⁰

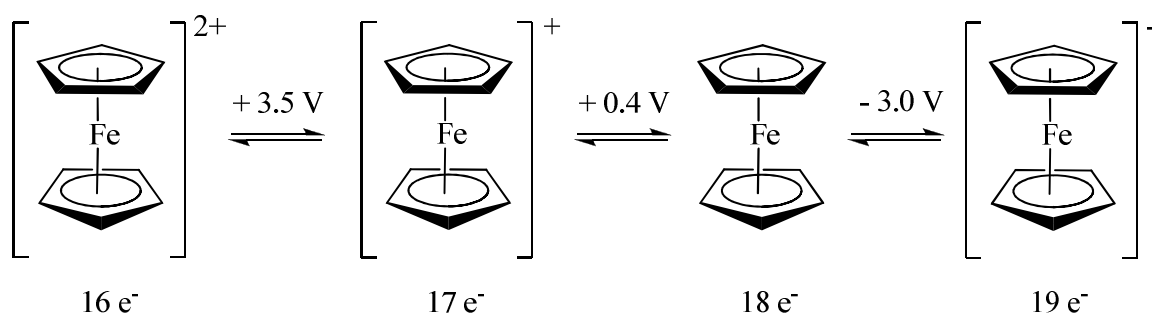


Figure 1.3: Potentials for the oxidation states of ferrocene as determined by cyclic voltammetry. (Potentials are given versus a saturated calomel reference electrode.)⁶

The development of ferrocene derivatives with reactive functional groups has led to the incorporation of these complexes into large molecules and polymers.^{2,3,11} Arimoto and Haven were the first to produce polymers containing ferrocene with the polymerization of vinyl ferrocene.¹¹ Since then numerous polymers with ferrocene in the side chain or backbone have been prepared.¹²⁻¹⁴ The continued interest in the incorporation of ferrocene into polymers stems from its high stability towards heat, UV radiation and γ -radiation as well as the electrochemical behaviour.^{1,11,13,15}

Ferrocene compounds are some of the most studied organometallic compounds in chemistry. Their diamagnetic nature allows for thorough characterization through nuclear magnetic spectroscopy (NMR). In a 1H NMR spectrum, ferrocene shows up as a singlet at 4.2 ppm while in a ^{13}C NMR spectrum it shows up as a singlet at 68 ppm (in $CDCl_3$). The shielding

and deshielding effects of substituents on cyclopentadienyl rings of ferrocene, mirror the trends found for aromatic organic compounds.

1.2 The synthesis and chemistry of η^6 -(arene)- η^5 -cyclopentadienyliron(II) hexafluorophosphate complexes

Ferrocene is capable of exchanging one of its cyclopentadiene rings with an arene; this type of ligand exchange was first reported in 1963 by Nesmeyanov, Vol'kenau and Bolesova.¹⁶ They reacted ferrocene with arene ligands using aluminum chloride in the presence of powdered aluminum at temperatures between 80-165 °C (Figure 1.4). The aluminum was used to prevent the oxidation of ferrocene to the ferricinium-cation. The reaction gave 30-66% yield of the η^6 -(arene)- η^5 -cyclopentadienyliron(II) which can be isolated as the tetrafluoroborate or hexafluorophosphate salt. While many examples of this reaction use decalin as a solvent, an additional solvent is not necessary for arenes which are liquid at reaction temperature.

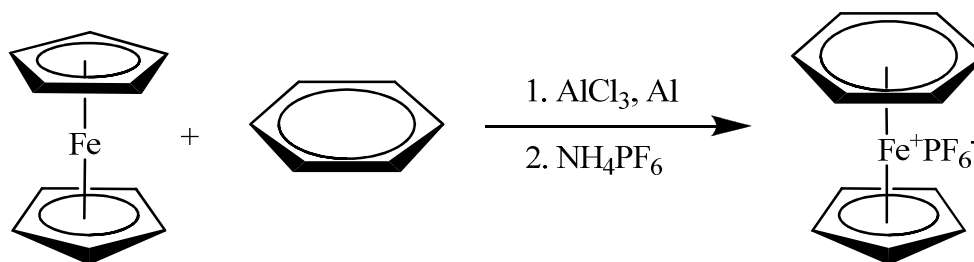


Figure 1.4: General synthesis for η^6 -(arene)- η^5 -cyclopentadienyliron(II) hexafluorophosphate complexes.

η^6 -(haloarene)- η^5 -cyclopentadienyliron(II) hexafluorophosphate salts can be synthesized by reacting ferrocene with the appropriate halo-benzene compounds using the general conditions described above. These η^6 -(haloarene)- η^5 -cyclopentadienyliron(II) hexafluorophosphate salts are able to undergo many reactions utilizing the haloarene ring (Figure 1.5).⁶ One of the most useful

properties of η^6 -(haloarene)- η^5 -cyclopentadienyliron(II) compounds is that they can undergo metal mediated nucleophilic aromatic substitution reactions under mild reaction conditions (Figure 1.6).^{6, 17, 18} The susceptibility of the complexed arene to nucleophilic aromatic substitution is due to the strong electron withdrawing capabilities of the cyclopentadienyliron. In substitution reactions, the nucleophile (amine, alcohol or thiol) attacks the *ipso* carbon halo-arene ligand forming a cyclohexadienyl intermediate which is very acidic (Figure 1.6). Dehydrohalogenation of the cyclohexadienyl intermediate is easily accomplished using a weak base such as K_2CO_3 .

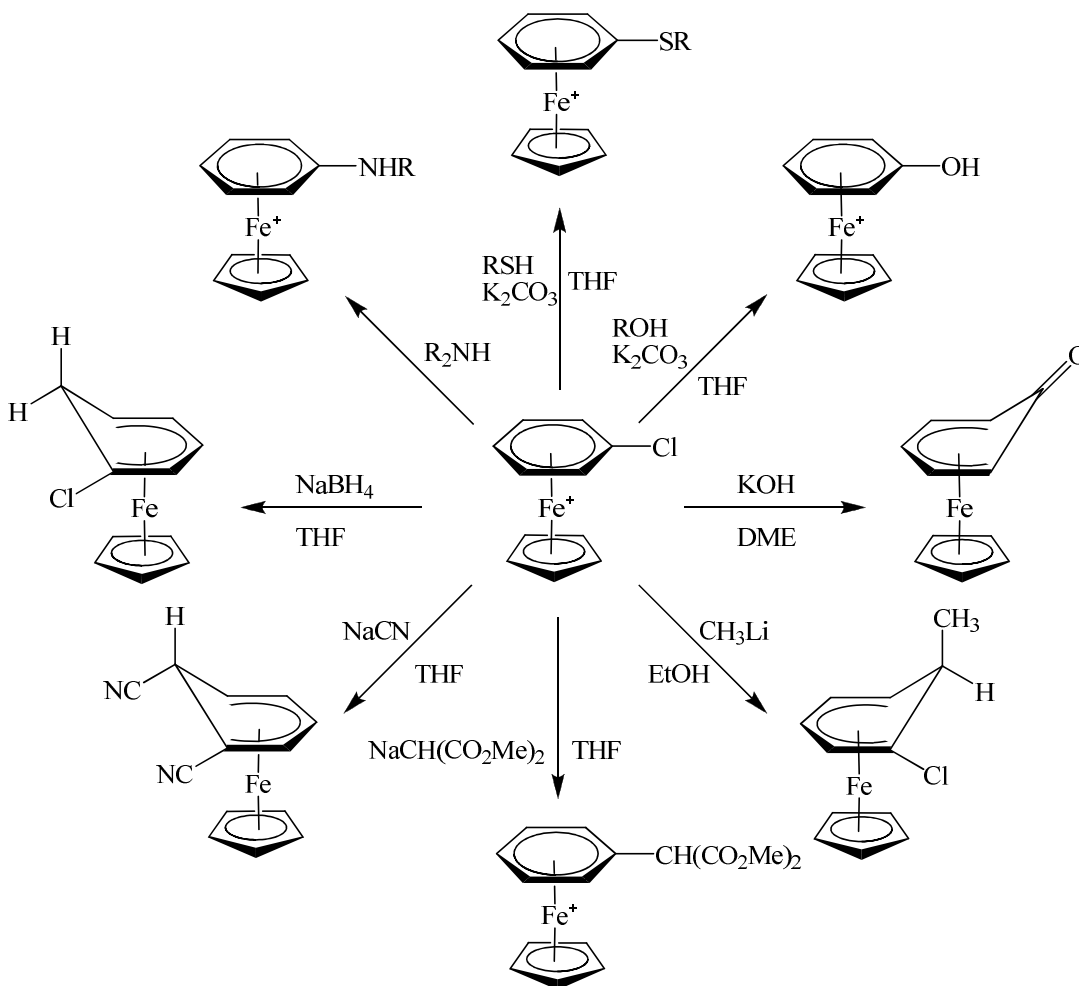


Figure 1.5: Reactivity of η^6 -(haloarene)- η^5 -cyclopentadienyliron(II) hexafluorophosphate salts.⁶

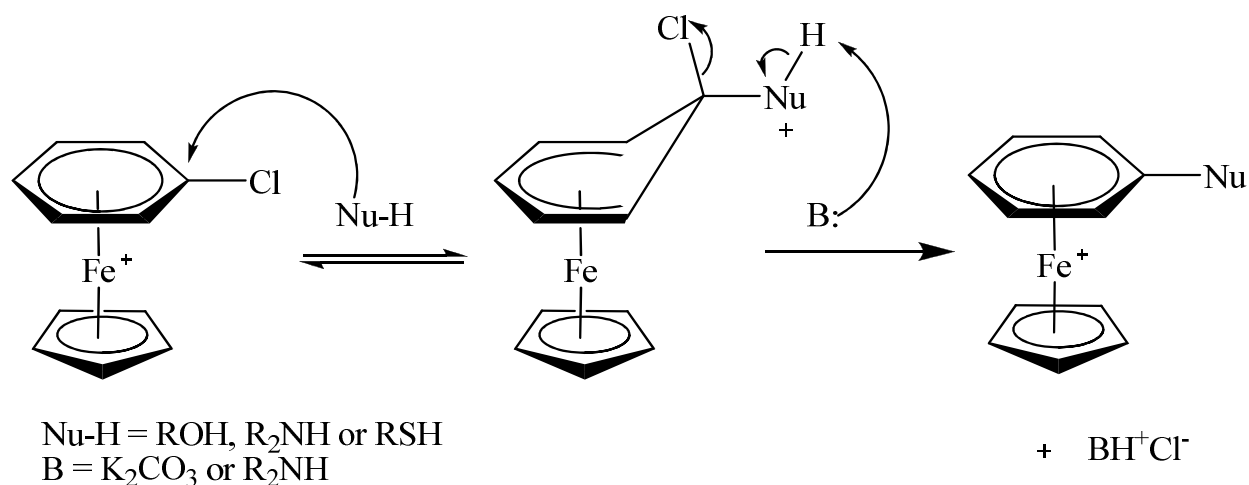


Figure 1.6: Nucleophilic aromatic substitution of a η^6 -(haloarene)- η^5 -cyclopentadienyliron(II) (hexafluorophosphate counter ion omitted for clarity).⁶

Cyclic voltammetric studies of η^6 -(arene)- η^5 -cyclopentadienyliron(II) hexafluorophosphate complexes have revealed up to 4 possible oxidation states (Figure 1.7).⁶ For complexes where the arene is hexamethylbenzene the cyclic voltammetry waves of the four oxidation states are electrochemically and chemically reversible, and the $17 e^-$, $18 e^-$ and $19 e^-$ states have all been isolated in their crystalline form. For other η^6 -(arene)- η^5 -cyclopentadienyliron(II) hexafluorophosphate salts the first reduction to the $19 e^-$ species is typically reversible, while the second reduction is reversible only when a suitable arene ring is chosen. This is due to the relative instability of the $20 e^-$ species.¹⁹

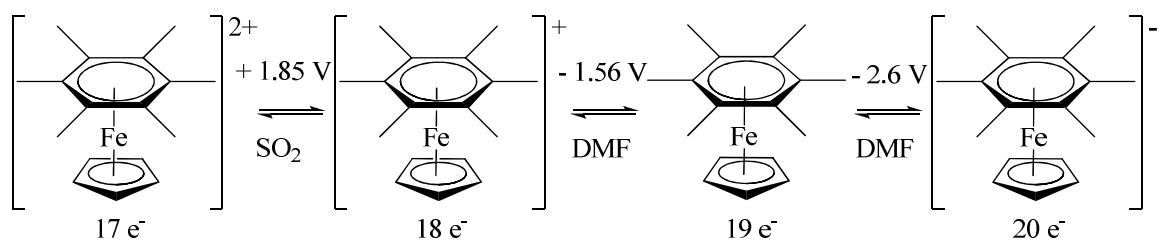


Figure 1.7: Potentials for the oxidation states of η^6 -(hexamethylbenzene)- η^5 -cyclopentadienyliron(II) as determined by cyclic voltammetry. (Potentials are given versus a saturated calomel reference electrode.)⁶

The mild reaction conditions permitted by the use of η^6 -(haloarene)- η^5 -cyclopentadienyliron(II) to form aryl ethers, allows for the synthesis of molecules that would otherwise (without the iron) be difficult to obtain.^{17, 18, 20, 21} Decomplexation of the cationic cyclopentadienyliron moiety to give the organic arene is easily performed, making the η^6 -(arene)- η^5 -cyclopentadienyliron(II) moiety a useful tool for organic synthesis. There are three strategies for the removal of the cyclopentadienyliron(II) moiety from various η^6 -(arene)- η^5 -cyclopentadienyliron(II) complexes; pyrolysis, electrolysis and photolysis.²¹ Pyrolysis is the most harsh method for the removal of the cyclopentadienyliron(II) moiety, requiring temperatures above 200°C. This strategy is not commonly used as it requires thermally stable arenes and often yields less of the arene compared to the other two methods. Advantages of pyrolysis include short reaction times and compounds do not need to be soluble. Electrolysis is less harsh than pyrolysis requiring potentials of -1.5 to -2.5 V. While this method is quite effective, the presence of reducible substituents on the arene can lead to side reactions. Photolysis is often the best strategy for the removal of the cyclopentadienyliron(II) moiety; as it can be used with arenes that are heat sensitive as well as arenes with reducible substituents.

The photolytic cleavage of the cyclopentadienyliron moiety was thoroughly studied by Schuster *et al* who proposed that irradiation caused ring slippage from η^6 to η^4 .²² The iron could then be nucleophilically attacked by the solvent acetonitrile, displacing the arene ligand. At -40 °C the product of this reaction is the tris(acetonitrile)cyclopentadienyl iron species seen in Figure 1.8; however, at 20 °C the reaction continues to give the organic product, iron salts and ferrocene.^{23, 24}

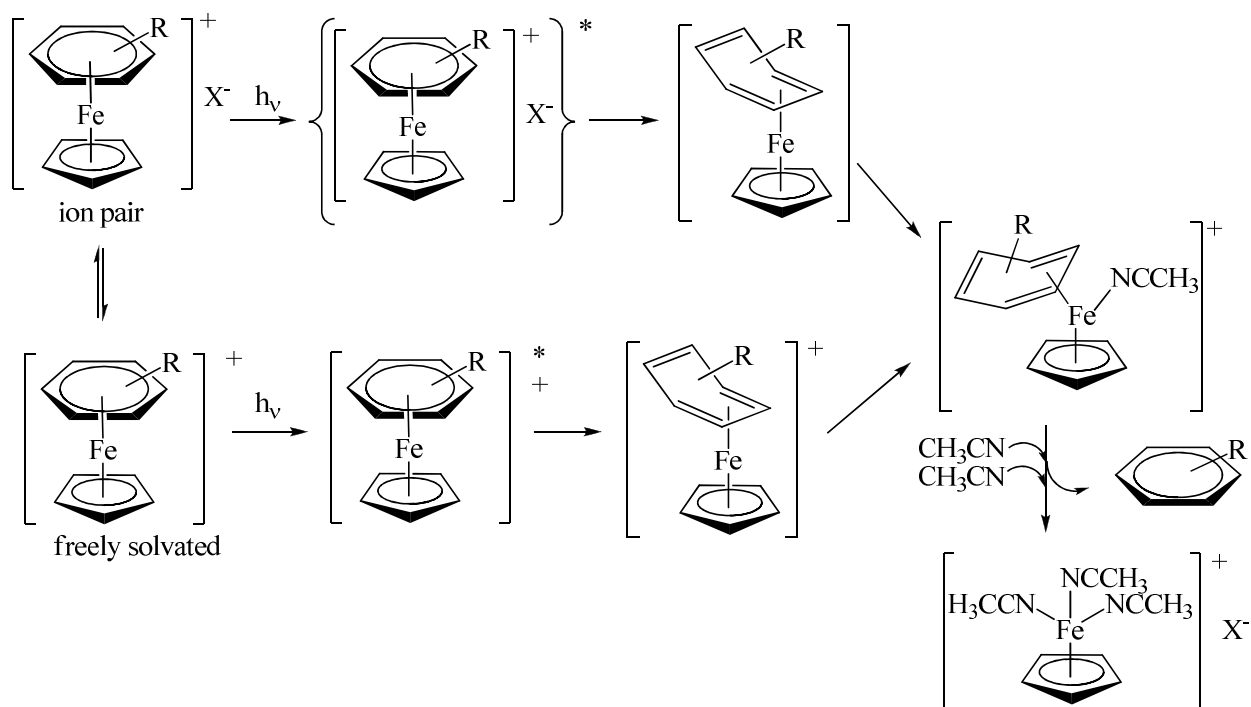


Figure 1.8: Proposed sequence for the photolysis of η^6 -(arene)- η^5 -cyclopentadienyliron(II) complexes.²² X^- is a counter ion such as PF_6^- .

Characterization of η^6 -(arene)- η^5 -cyclopentadienyliron(II) complexes can be performed using several different methods including IR, MS, UV-vis spectrophotometry, X-ray crystallography and NMR spectroscopy.²¹ Unfortunately, these species often have a low volatility making MS difficult and it is very difficult to grow crystals of these structures that are of adequate quality for crystallography. While many transition metal complexes are paramagnetic, η^6 -(arene)- η^5 -cyclopentadienyliron(II) complexes are diamagnetic allowing for their characterization through NMR. Compared to ferrocene which appears at approximately 4.2 ppm, the cyclopentadiene ring of η^6 -(arene)- η^5 -cyclopentadienyliron(II) complexes shows a significant downfield shift appearing at approximately 4.9-5.6 ppm in ^1H NMR spectra. This shift is possibly due to the delocalization of the positive charge throughout the cyclopentadiene ring.²⁵ The complexed arene appears at approximately 6.0 -7.0 ppm, which is upfield compared

to free arenes, this is due to increased shielding resulting from metal to ligand π backbonding. In ^{13}C NMR spectra the complexed arenes appear at 70-95 ppm for $\text{C}_{\text{Ar-H}}$ and 100-135 ppm for quaternary carbons, which is farther upfield than non-complexed arenes.

1.3 Synthesis and chemistry of μ -alkyne-bis(tricarbonylcobalt) complexes

The replacement of the bridging carbonyl groups of dicobalt octacarbonyl ($\text{Co}_2(\text{CO})_8$) has been known since the mid 1950's (Figure 1.9).²⁶ This complex can form an intermediate in cyclicization reactions such as the Pauson-Khand reaction. The alkyne- $(\text{Co}_2(\text{CO})_6)$ complex can also stabilize a carbonium ion center and allow for regio-specific nucleophilic coupling reactions.²⁷ The cobalt carbonyl can also act as a protecting group for triple bonds and can be removed using oxidative cleavage with ceric(IV) ammonium nitrate ($(\text{NH}_4)_2\text{Ce}(\text{NO}_3)_6$) in acetone.²⁸

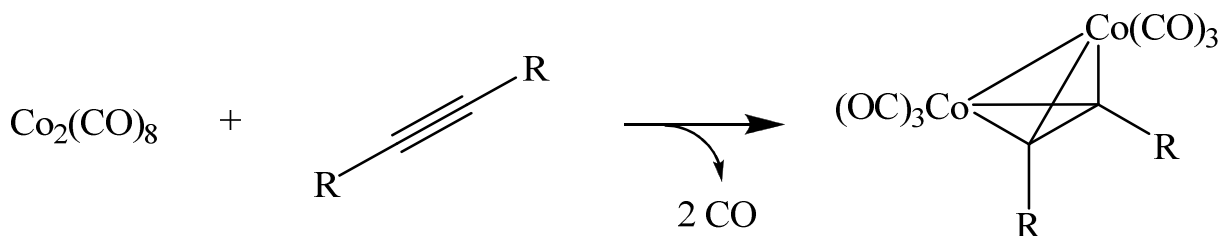


Figure 1.9: General synthesis of alkyne-cobalt carbonyl complexes.

Purification of μ -alkyne-bis(tricarbonylcobalt) complexes usually involves chromatography on alumina or silica.²⁹ The incorporation of the cobalt carbonyl is usually confirmed with IR spectroscopy, where the disappearance of the $\text{C}\equiv\text{C}$ stretching vibration (weak band $2260\text{-}2100 \text{ cm}^{-1}$) and the appearance of three sharp bands between $2100\text{-}2000 \text{ cm}^{-1}$ indicate coordination of the cobalt to the alkyne.^{26, 30} The absence of a bridging carbonyl band at 1859 cm^{-1} can be used to indicate that no excess cobalt carbonyl is present in a sample.

Cyclic voltammetric studies of $\text{PhC}_2\text{Co}_2(\text{CO})_6$ were done by Arewgoda *et al.* using Ag/AgCl electrode in acetone at $-30\text{ }^\circ\text{C}$ found two one electron waves at -0.82 V and -1.56 V .³⁷⁷ However, at higher temperatures the anodic peak current decreased indicating decomposition of the radical anion. Complex $(t\text{-Bu})_2\text{C}_2\text{Co}_2(\text{CO})_6$ under the same conditions also found two one electron waves at -1.03 V and -1.8 V as well as, a smaller wave at -1.9 V .

1.4 Metal containing polymers

Metal containing polymeric materials are a desired synthetic goal due to their potential use as electronic or magnetic materials or as precursors for ceramics and metallic nanoparticles.³¹ Iron and cobalt containing polymers are important classes of metal containing materials due to their possible magnetic and redox properties.³¹ Cobalt nanomaterials are often prepared by the thermolysis of $\text{Co}_2(\text{CO})_8$ in the presence of phosphines or carboxylic acids, which prevent aggregation into larger agglomerates; however, this stabilization can also be achieved by directly incorporating the organometallic components into polymers. Shi and coworkers have recently reported on the pyrolytic ceramization of hyperbranched poly(ferrocenylphenylenes) containing cobalt carbonyl to produce soft ferromagnetic ceramics with high magnetizability.³²

While ferrocene and $\eta^6\text{-(arene)-}\eta^5\text{-cyclopentadienyliron(II)}$ are usually incorporated into monomers which are then polymerized, there are two possible strategies for the inclusion of cobalt into polymers. The most common strategy is coordination of the cobalt carbonyl post polymerization; however, the cobalt can also be added prior to polymerization.

1.5 Scope of the present work

This thesis focuses on the incorporation of transition metals into the backbone or side chains of various classes of polymers and oligomers. Small changes to a monomer, such as change of functional group or incorporation of dyes or metals can result in large property changes in the resulting polymers. This well known adage is a driving force for the production of new polymeric materials where the incorporation of functional groups or other structural moieties provides materials with useful properties.

Chapters two and three focus on the synthesis of norbornene and methacrylic ester polymers and oligomers with iron and cobalt in the side chain. To this end three different polymers will be discussed in each chapter, polymers containing a ferrocene moiety as well as an μ -alkyne-bis(tricarbonylcobalt) moiety. The next two polymers incorporate one or two η^6 -(arene)- η^5 -cyclopentadienyliron(II) hexafluorophosphate moieties as well as an μ -alkyne-bis(tricarbonylcobalt) moiety.

Chapter four presents the synthesis of two different types of condensation polymers synthesized utilizing the nucleophilic aromatic substitution reaction. The first type has η^6 -(arene)- η^5 -cyclopentadienyliron(II) hexafluorophosphate moieties as well as a alkyne group, while the second type has the alkyne group complexed to cobalt carbonyl.

Chapter 5 details the synthesis of silyloxane polymers that incorporate η^6 -(arene)- η^5 -cyclopentadienyliron(II) hexafluorophosphate moieties. This project lays the foundation for future work within the Abd-El-Aziz group with polysiloxanes and the incorporation of transition metals.

1.6 Materials and instrumentation

All reagents were purchased from Sigma-Aldrich and used without further purification. All general solvents were HPLC grade and used without further purification. The dry dichloromethane and the dry THF, used in water and oxygen sensitive reactions, were HPLC grade solvents that were dried and degassed using established procedures.³³

¹H and ¹³C NMR spectra were recorded at 400 MHz and 100 MHz respectively on a Varian Mercury Plus spectrometer equipped with a gradient field probe. The chemical shifts were referenced to residual solvent peaks and coupling constants reported in Hz. Infrared (IR) spectroscopy was recorded on a Nicolet IR200 FT-IR by making thin layer films of each compound on NaCl plates or by making KBr pellets.

Thermogravimetric analysis (TGA) was performed on a Mettler–Toledo TGA/SDTA851e with a heating rate of 20 °C/min under a steady stream of nitrogen (50 mL/min). Differential scanning calorimetry (DSC) was performed on a Mettler DSC821° with a heating rate of 20°C/min under a 50mL/min flow of nitrogen. Cyclic voltammetric experiments were performed using a conventional three-electrode cell. In these studies the working electrode was a glassy carbon disk electrode (ca. 2 mm diameter), the auxiliary electrode was a Pt wire, and a (Ag/AgCl) reference electrode was utilized. Temperatures at -40 °C were obtained using an acetone/dry ice mixture. The concentration of the analyte was 2.0 mM in propylene carbonate, while that of the supporting electrolyte, Tetrabutylammonium perchlorate, was 0.1 M. The solutions were deoxygenated with nitrogen prior to use and an EG&G Princeton Applied Research model 263 A potentiostat was used in all experiments with a scanning rate of 0.2 V/s.

GPC was performed on a Polymer Labs PL-GPC 50 plus with a PL-AS RT auto-sampler and PL-RI detector. The eluent was THF flowing at 1 mL/min at 30 °C. Two PLgel mixC columns were setup in series. The molecular weights were calculated against PS-H polystyrene standards.

All crystallographic materials and instrumentation are described in the appendices (p. 171).

Chapter 2: Norbornene based polymers

2.1 Introduction

Norbornene is a highly strained bicyclic olefin that is often used for the synthesis of polymeric materials. Norbornene, which is also known as bicyclo[2.2.1]hept-2-ene, can be polymerized in four ways: radical polymerization, cationic polymerization, ring opening metathesis polymerization (ROMP) or vinyl polymerization (Figure 2.1).³⁴ Each type of polymerization provides products with different structures and properties. However, this thesis focuses on ROMP as it is known to give a more uniform polymer.

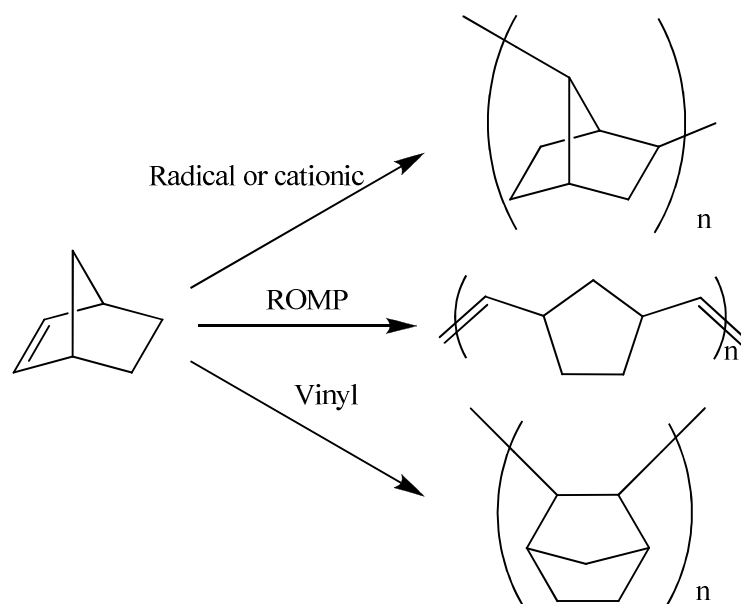


Figure 2.1: Four strategies for norbornene polymerization.

Ring opening metathesis polymerization is a process by which highly strained cyclic olefins are opened to form polymeric materials. Catalysts containing transition metals such as ruthenium, molybdenum and tungsten are known to be quite useful for this process.³⁵ ROMP is an olefin metathesis reaction where a transition metal alkylidene complex reacts with the

norbornene alkene in a [2+2] fashion to give a metalacyclobutane ring as an unstable intermediate (Figure 2.2). A cycloreversion reaction of the metalacyclobutane ring leaves a cyclopentane ring with a metal alkylidene. This complex can then react repeatedly with norbornene to form a growing chain. Many of the catalysts used for ROMP can also catalyze ring closing metathesis; this means that eventually a reaction equilibrium may be reached where both processes are occurring simultaneously. It is often beneficial to terminate the polymerization before this equilibrium is established so that the polymers are more uniform in size (have a lower polydispersity index, PDI). ROMP can be terminated by adding ethyl vinyl ether, which reacts with the metal to cleave off the polymer chain forming a $M=CHOEt$ carbene complex. This complex is unreactive toward further metathesis reactions.

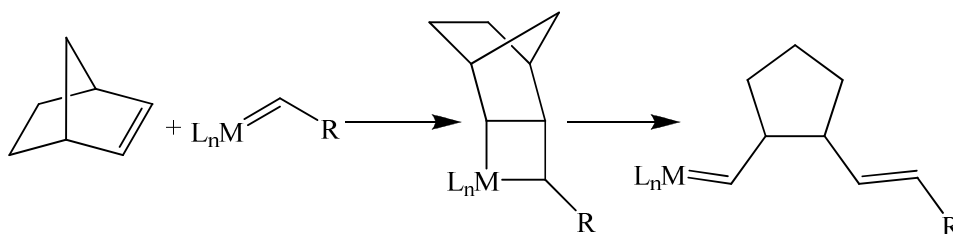


Figure 2.2: Ring opening metathesis of norbornene.

Ruthenium catalysts such as those developed by Grubbs are very useful for the ROMP of norbornene derivatives due to their high level of tolerance for various functional groups and pendent moieties.³⁶ ROMP with the Grubbs catalysts has been demonstrated for norbornenes with pendent carboxylic acid,³⁷ amino acid,³⁸ ether, ester,^{39, 40} decaboranes,⁴¹ and siloxanes.⁴²

Previous work done by Abd-El-Aziz *et al.* has shown that the first generation of Grubbs catalyst can be used to prepare polynorbornenes with η^6 -aryl- η^5 -cyclopentadienyliron(II) hexafluorophosphate groups in their side chain (Figure 2.3).^{39, 40} Polynorbornenes that contained azo dyes and η^6 -aryl- η^5 -cyclopentadienyliron(II) hexafluorophosphate groups in their side chain, were also prepared. The present work builds on previous research by showing that alkyne

coordinated dicobalt hexacarbonyl can also be incorporated into polymers (pre-polymerization). In this chapter, three different classes of highly metallated polynorbornenes were synthesized, one with neutral ferrocene and cobalt carbonyl-alkyne moieties and two that contained cationic η^6 -arene- η^5 -cyclopentadienyliron(II) and cobalt carbonyl-alkyne moieties. All of the polymerizations utilized Grubbs 2nd generation catalyst.

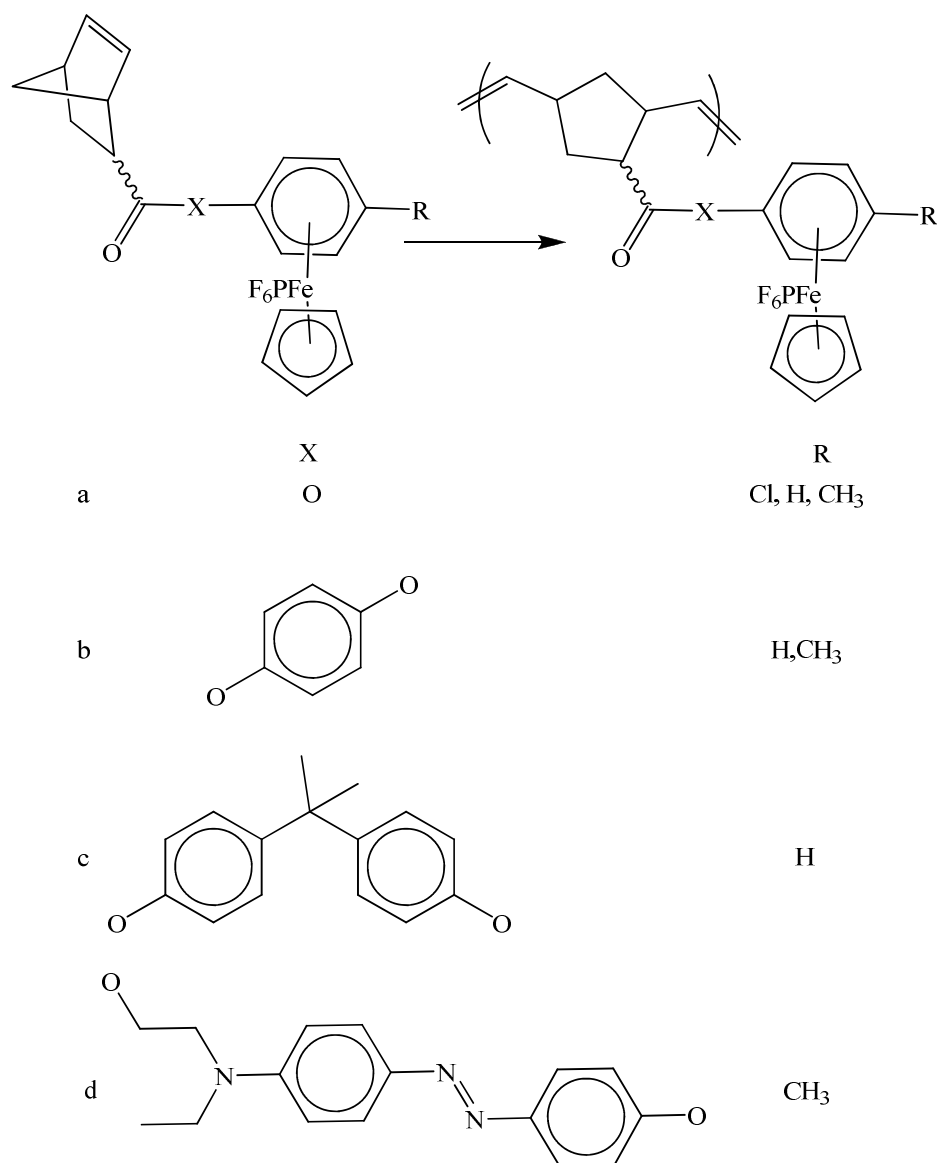
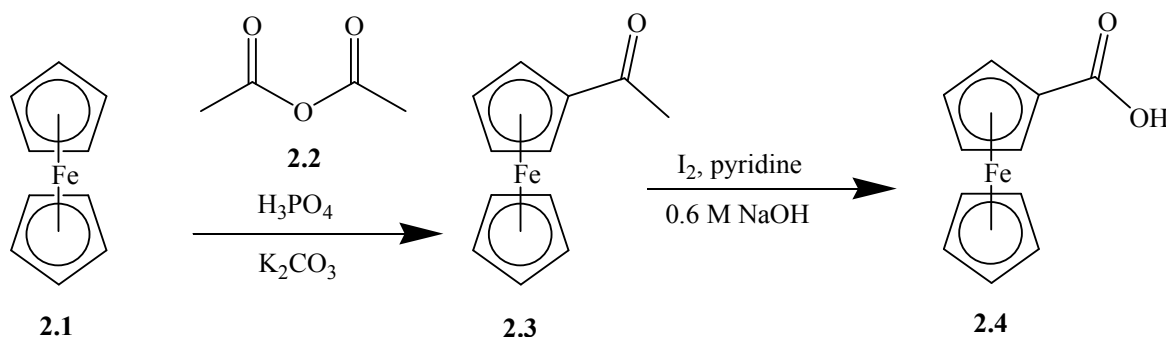


Figure 2.3: A few examples of polynorbornenes with η^6 -aryl- η^5 -cyclopentadienyliron(II) hexafluorophosphate groups in their side chain.

2.2 Synthesis and characterization of polynorbornenes containing organoiron and cobalt carbonyl

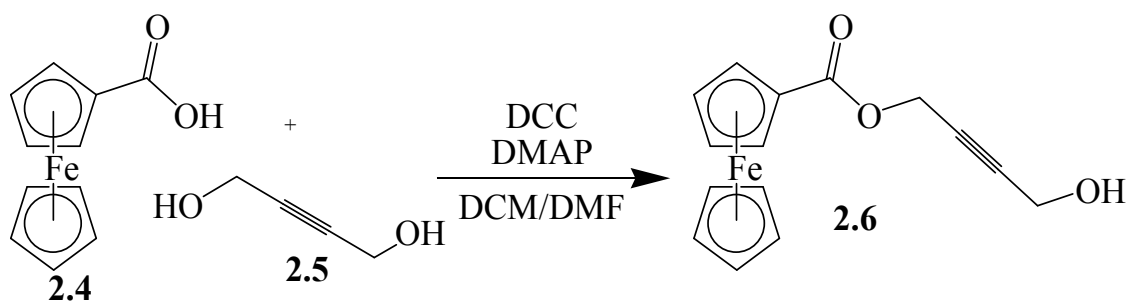
2.2.1 Synthesis of a norbornene monomer containing ferrocene

The first step in the 5 step synthesis of the ferrocene-containing norbornene monomer was to prepare mono-acetyl ferrocene (**2.3**) through the acetylation of ferrocene (**2.1**) (Scheme 2.1). This was accomplished using acetic anhydride (**2.2**) in concentrated phosphoric acid according to standard methods.⁷ Treatment of the mono-acetyl ferrocene with iodine and pyridine followed with the addition of 0.6 M NaOH afforded carboxylic acid ferrocene (**2.4**) (Scheme 2.1).⁴



Scheme 2.1: Synthesis of complex **2.4**.

Steglich esterification between mono-carboxylic acid ferrocene and 2-butyne-1,4-diol (**2.5**) was accomplished using DCC and DMAP in a DCM/DMF solvent mixture (Scheme 2.2). Attempts to perform this reaction in DCM alone gave a mixture of starting material and product due to the poor solubility of the 2-butyne-1,4-diol. Purification of the crude product on silica using ether and hexanes for the mobile phase gave the product in the second fraction, which was isolated as an orange-red solid.



Scheme 2.2: Synthesis of complex **2.6**.

The ^1H NMR spectrum for compound **2.6** can be seen in Figure 2.4. The substituted cyclopentadiene ring gives two NFO triplets at 4.79 and 4.48 ppm. Between 4.20 and 4.29 ppm there are two overlapping peaks, one resonance is a singlet which is due to the non-substituted cyclopentadiene while the other is a triplet due to the methylene next to the alcohol. The methylene of the ester appears at 4.86 ppm. It is interesting to note that the methylenes of the butyne-diol moiety appear as triplets due to long range coupling to each other through the triple bond ($J=1.8$ Hz).

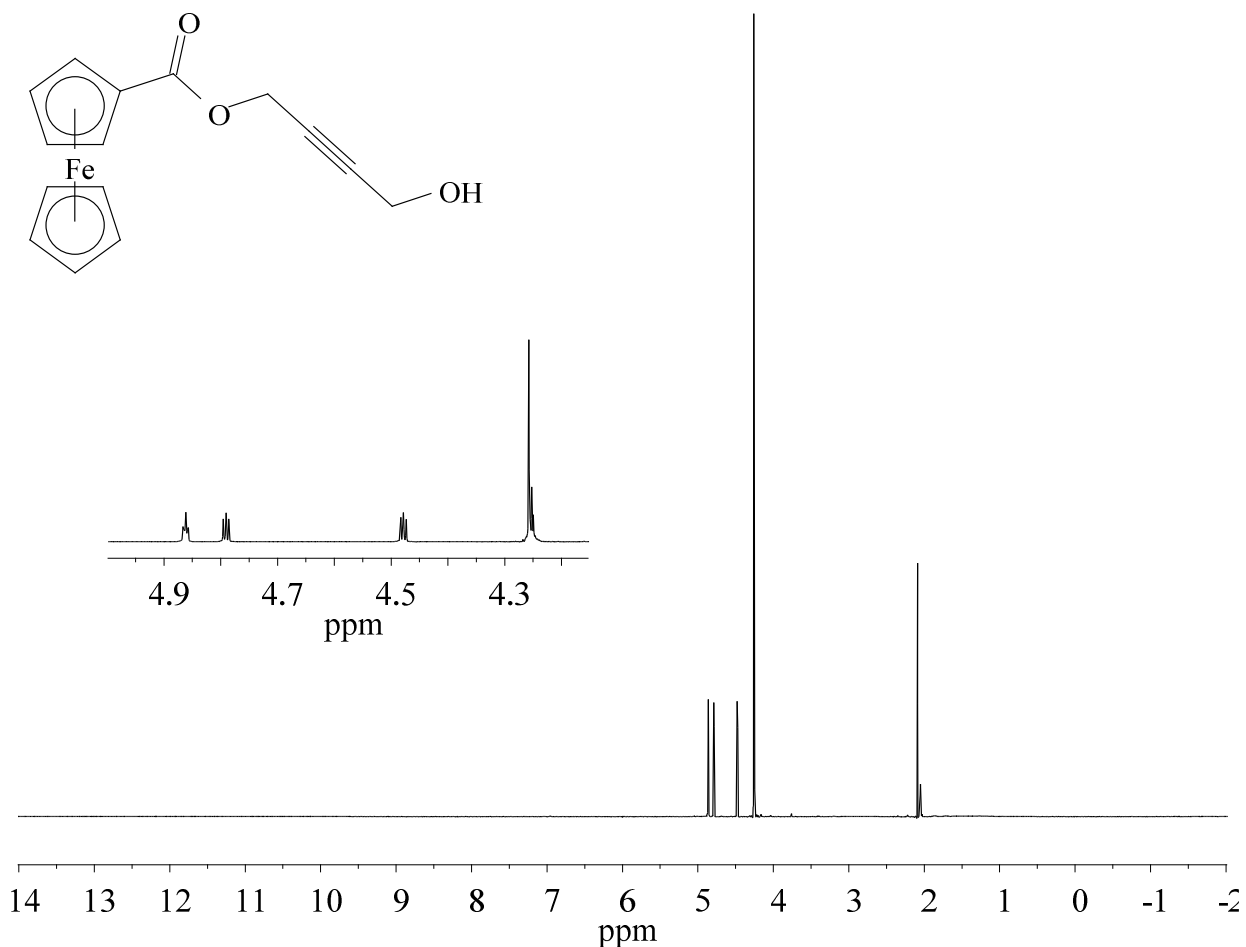


Figure 2.4: ^1H NMR spectrum of compound **2.6** $\text{acetone-}d_6$.

The ^{13}C NMR spectrum of complex **2.6** in chloroform shows the three expected resonances for the mono-substituted ferrocene at 71.9, 70.5 and 70.1 ppm (Figure 2.5). The quaternary carbon of the substituted ferrocene cannot be clearly seen as it overlaps with one of the other resonances. The carbonyl carbon is visible at 171.4 ppm, while the alkyne carbons appear at 84.8 and 81.0 ppm. Finally the methylenes appear at 52.1 and 51.4 ppm.

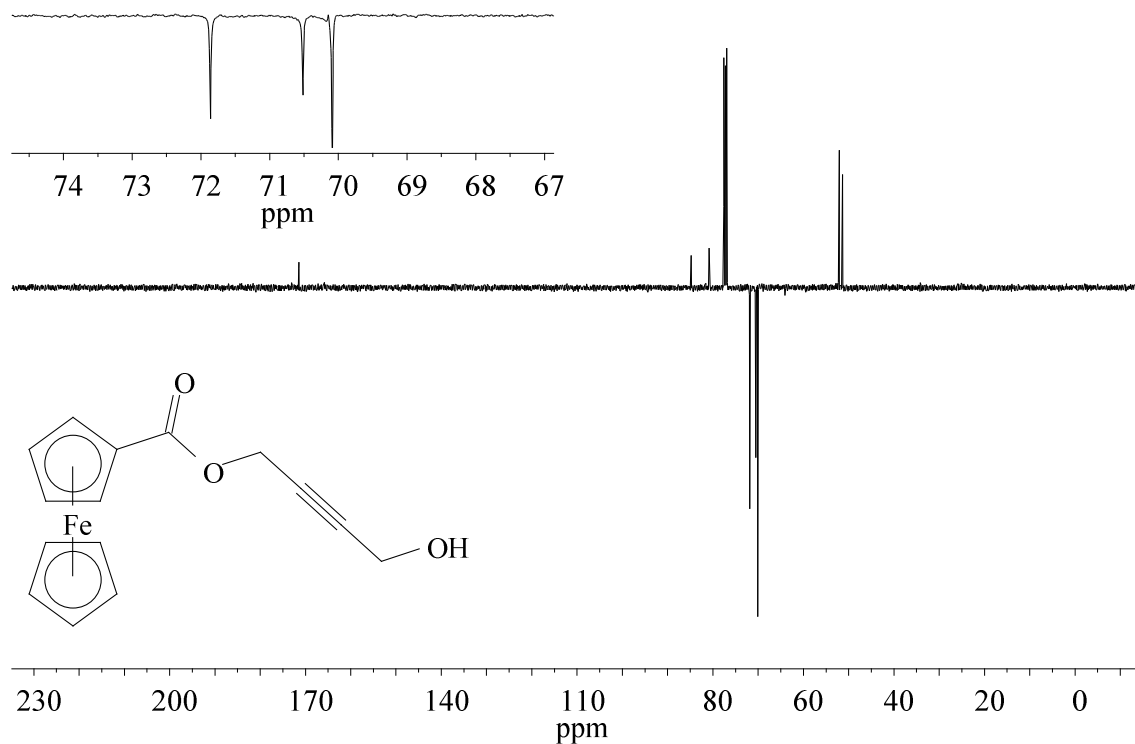


Figure 2.5: APT ^{13}C NMR spectrum of compound **2.6** in CDCl_3 .

Crystals of complex **2.6**, suitable for X-ray crystallography, were grown from an ether/hexanes solvent mixture(60/30); the ORTEP diagram for this complex can be seen in Figure 2.6. Lists of structural factors and other crystallographic data can be found in the appendix on page 171. The cyclopentadiene rings are coplanar and eclipsed as was previously seen for complex **2.4**.⁴³

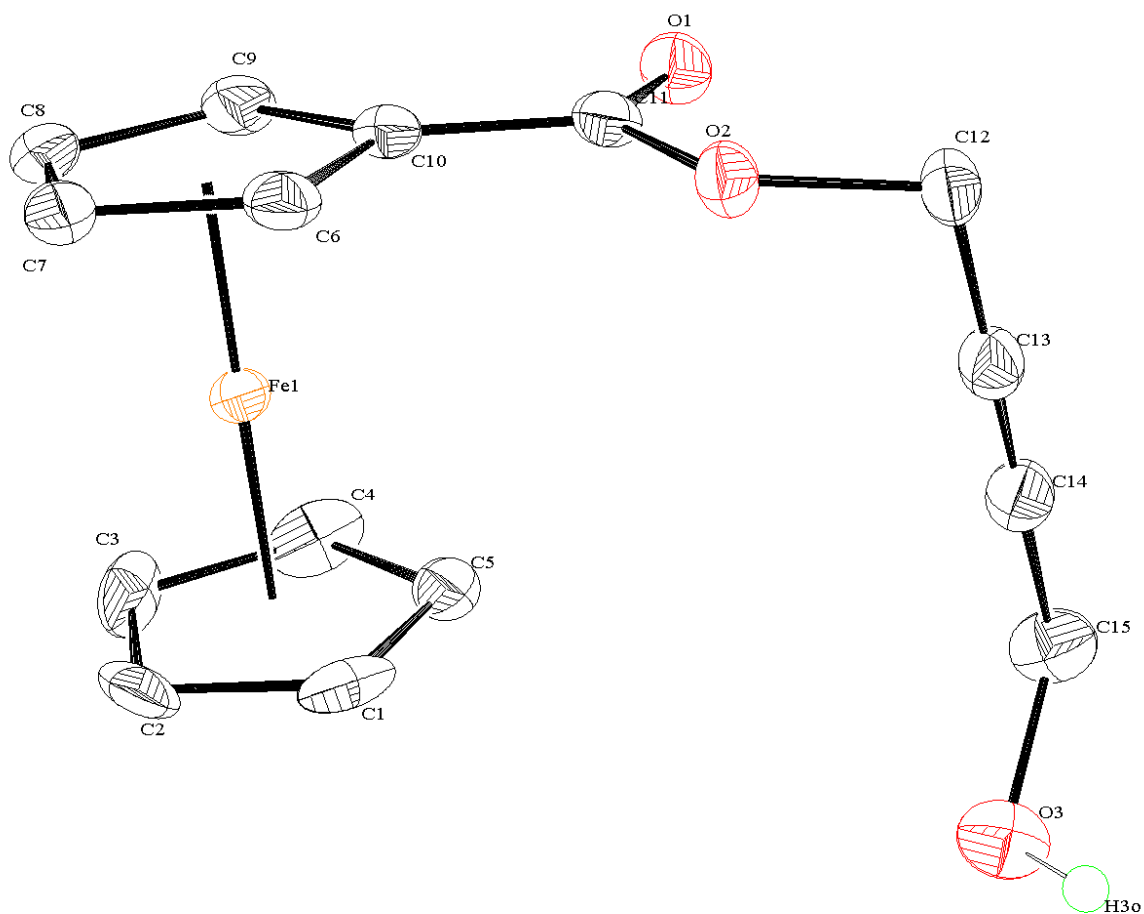
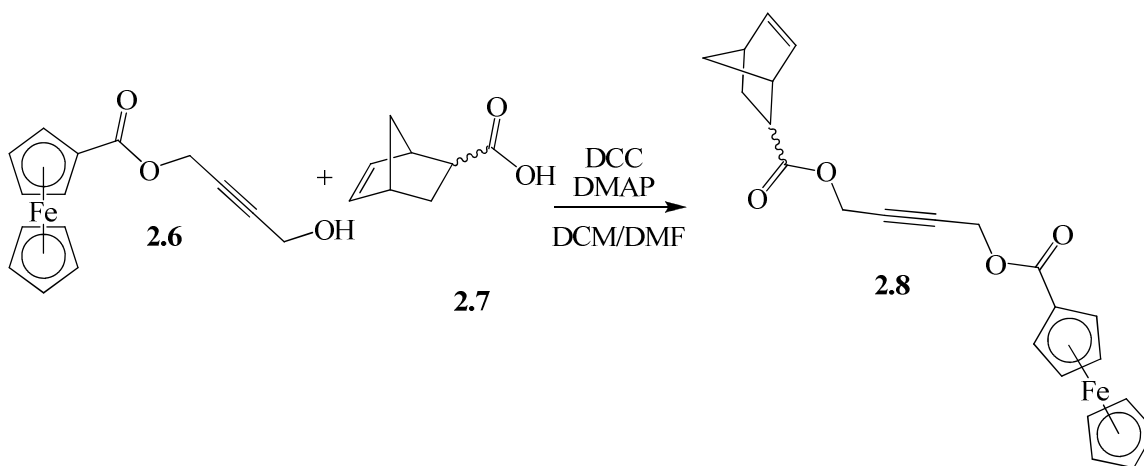


Figure 2.6: ORTEP diagram of complex **2.6**.

The next step in the preparation of the target monomer was to incorporate norbornene. A mixture of *endo* and *exo* 5-norbornene-2-carboxylic acid (**2.7**) was reacted with complex **2.6** via the Steglich esterification reaction giving the norbornene monomer **2.8** (Scheme 2.3). As the analysis of complex **2.8** is quite complicated it was also necessary to synthesize a single isomer, **2.8 exo**, in order to fully elucidate the spectral analysis. Complex **2.8 exo** was synthesized using the *exo*-5-norbornene-2-carboxylic (**2.7 exo**) acid that was prepared according to standard techniques. Both complex **2.8** and complex **2.8 exo** were isolated as dark orange solids.



Scheme 2.3: Synthesis of complex **2.8**.

The ^1H NMR of complex **2.8** clearly shows the incorporation of the norbornene (Figure 2.7). The olefinic hydrogens of the norbornene appeared between 5.90 and 6.20 ppm, while the aliphatic resonances (complicated by the mixture of *endo* and *exo* norbornene) were seen between 3 and 1 ppm. An expanded view of the norbornene olefinic hydrogen resonances can be seen in Figure 2.7. Integration of the *endo* and *exo* peaks that appear 5.93 and 6.10 ppm, respectively, clearly indicate that the compound mixture is 78 % *endo* and 22 % *exo*. Due to the complexity of the NMR spectra of the *endo* and *exo* mixture of complex **2.8** a pure sample of complex **2.8** *exo* was synthesized to help elucidate the spectra. It is beneficial to compare the spectrum for the *endo/exo* mixture of complex **2.8** with its single *exo* isomer (**2.8** *exo*) and the starting material (**2.6**) (Figure 2.8). For the complex **2.8** *exo* the formation of the ester can be confirmed by the downfield shift of one of the methylenes from beneath the non-substituted cyclopentadiene peak at ~4.25 ppm (complex **2.6**) to beneath one of the substituted cyclopentadiene peaks at ~4.8 ppm. The overlapping of the methylene peak and one of the substituted cyclopentadiene peaks is confirmed through the integration of 4 for that peak. For the *endo* portion of complex **2.8** the methylene protons appear as two doublets of triplets between 4.91–4.87 ppm.

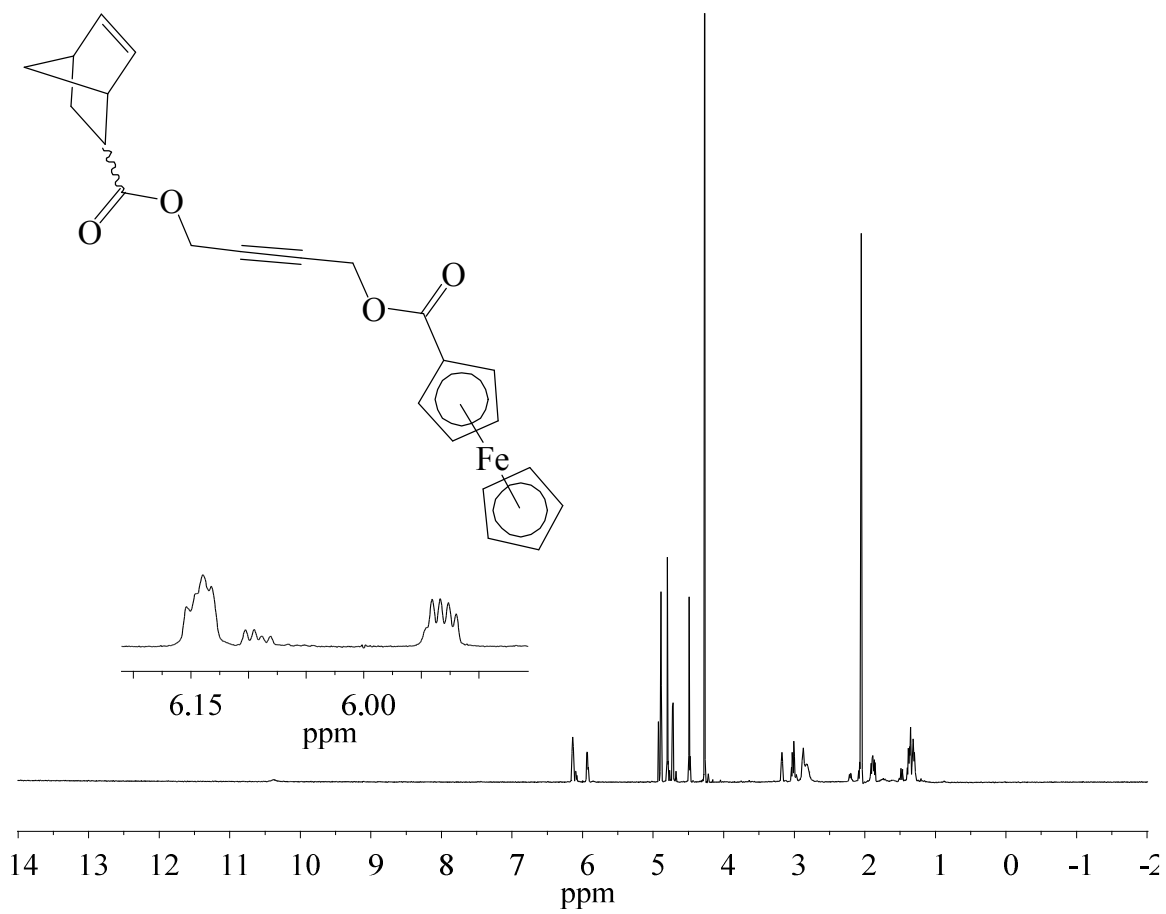


Figure 2.7: ^1H NMR spectrum of complex **2.8** in $\text{acetone-}d_6$.

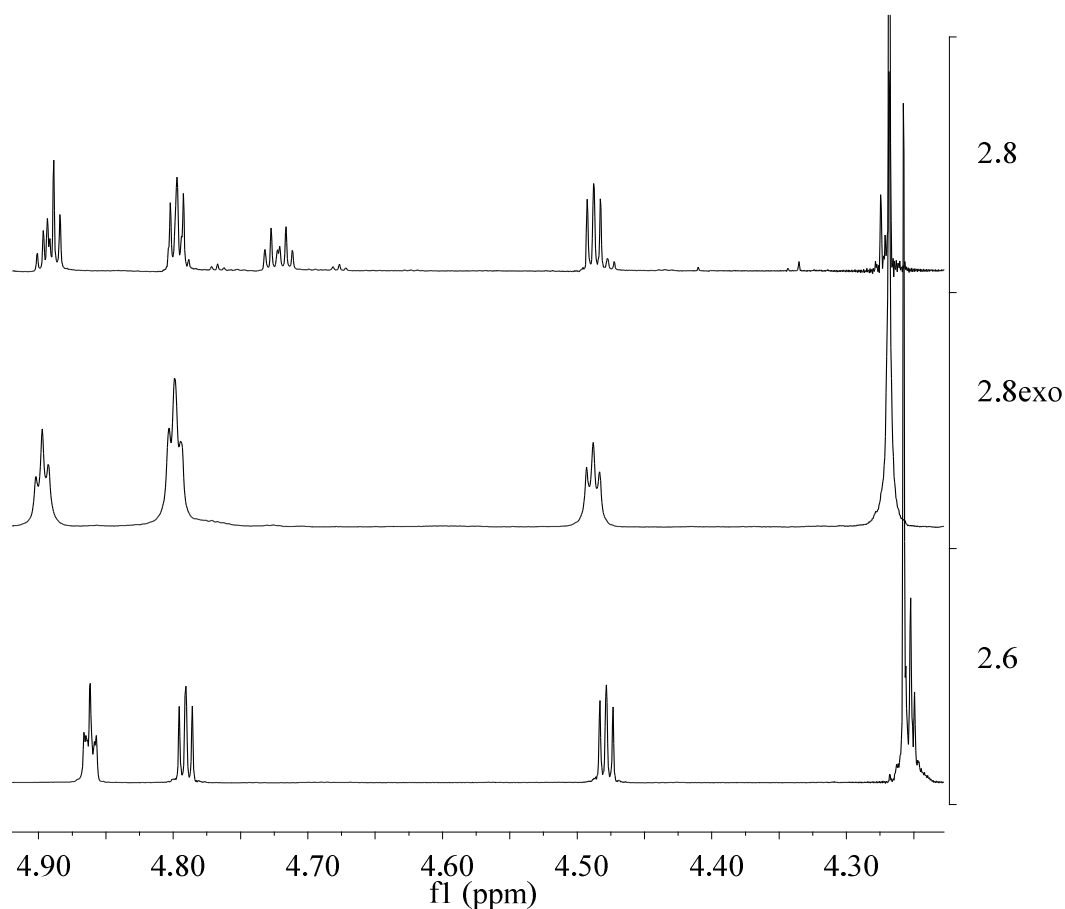


Figure 2.8: ^1H NMR spectral comparison of complexes **2.6**, **2.8 exo** and **2.8** in acetone- d_6 .

The ^{13}C NMR spectrum for complex **2.8** in acetone, like the ^1H NMR spectrum indicates a mixture of both *endo* and *exo* structures (Figure 2.9). The carbon atoms that are more distant from the norbornene start to overlap, in fact the methylene furthest from the norbornene has only one resonance for both the *endo* and the *exo* isomers. The ferrocene carbons and adjacent carbonyl carbon are also distant enough from the norbornene that the *endo* and *exo* resonances appeared as a single peak. The resonances for the *endo* and *exo* norbornene olefin carbons appeared as four peaks between 134 and 140 ppm, while the other ten norbornene resonances appeared between 29 and 51 ppm (one overlapped with the solvent peak). The four alkyne resonances appeared between 80 and 85 ppm, while the three resonances for the adjacent methylenes were found between 51 and 53 ppm. The quaternary carbon of the ferrocene was

found at 71.0 ppm. However, only two of the expected carbonyl carbons are apparent, 173.88 and 170.93. A quick analysis of the HMBC NMR spectrum (Figure 2.10) reveals that the resonance at 173.88 show secondary coupling to the methylene of the *endo* complex at 4.72 ppm and to a norbornene peak at 1.36 ppm, indicating that it belongs to the norbornene ester carbonyl. The exo norbornene ester carbonyl at 175.61 ppm is only evident in the HMBC NMR spectrum, where coupling to the methylene at 4.79 ppm and to the norbornene peak at 1.36 ppm is apparent. It is useful at this point to examine a small portion of the HSQC NMR spectrum for complex **2.8** as it confirms the overlapping of the methylene protons and cyclopentadiene protons at 4.88 ppm (Figure 2.11).

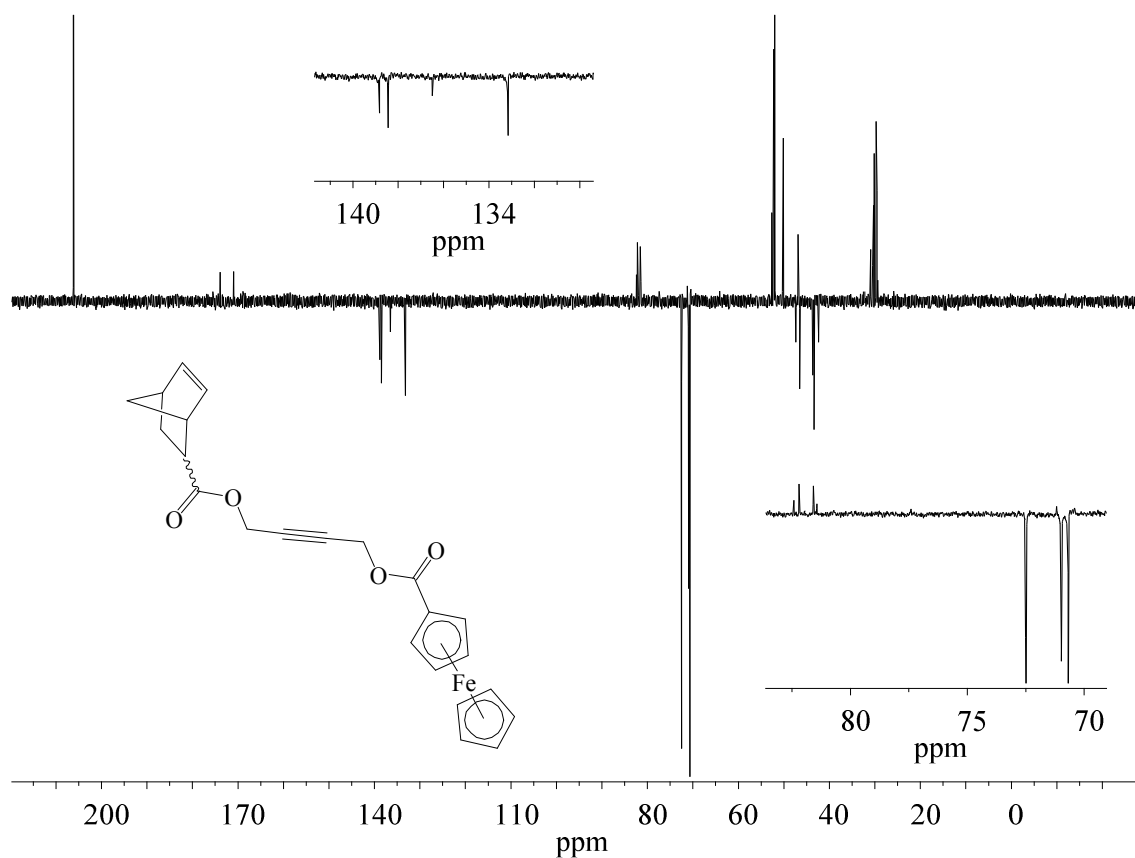


Figure 2.9: APT ^{13}C NMR spectrum of complex **2.8** in acetone- d_6 .

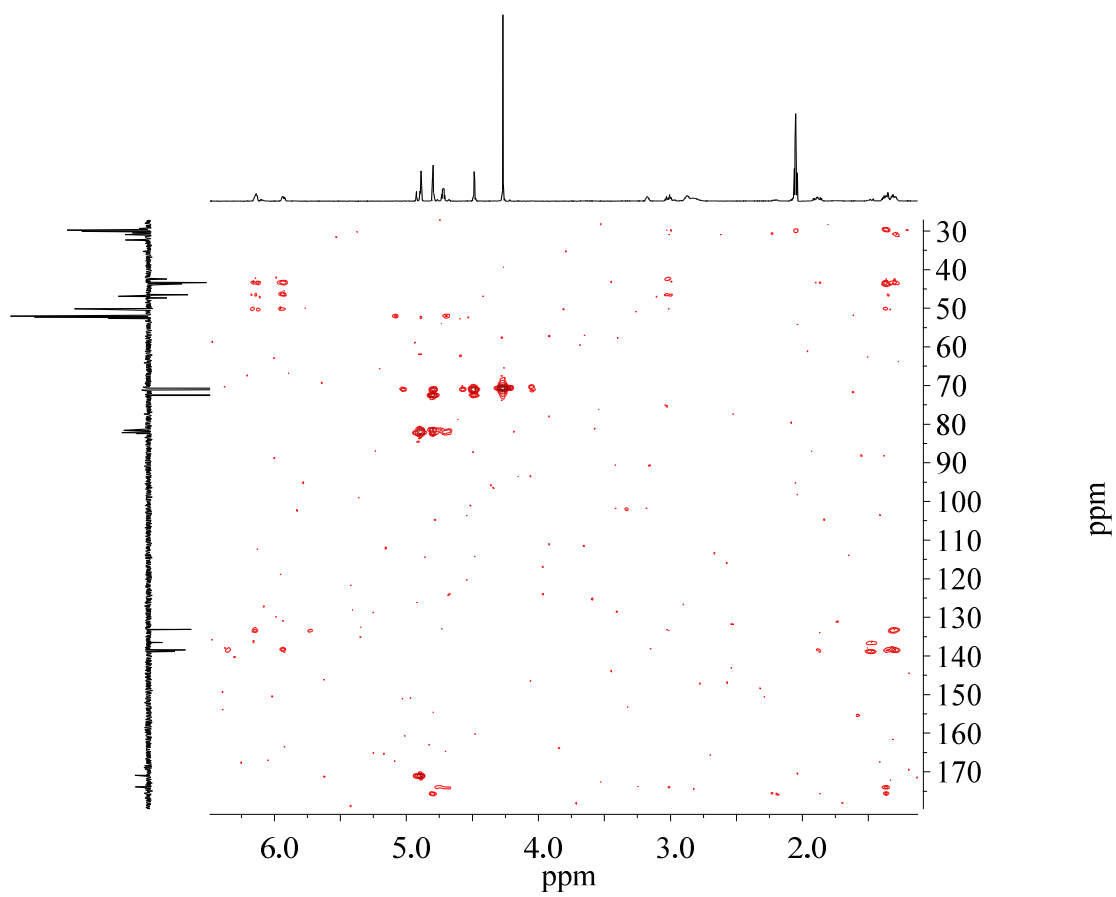


Figure 2.10: HMBC NMR spectrum of complex **2.8** in acetone- d_6 .

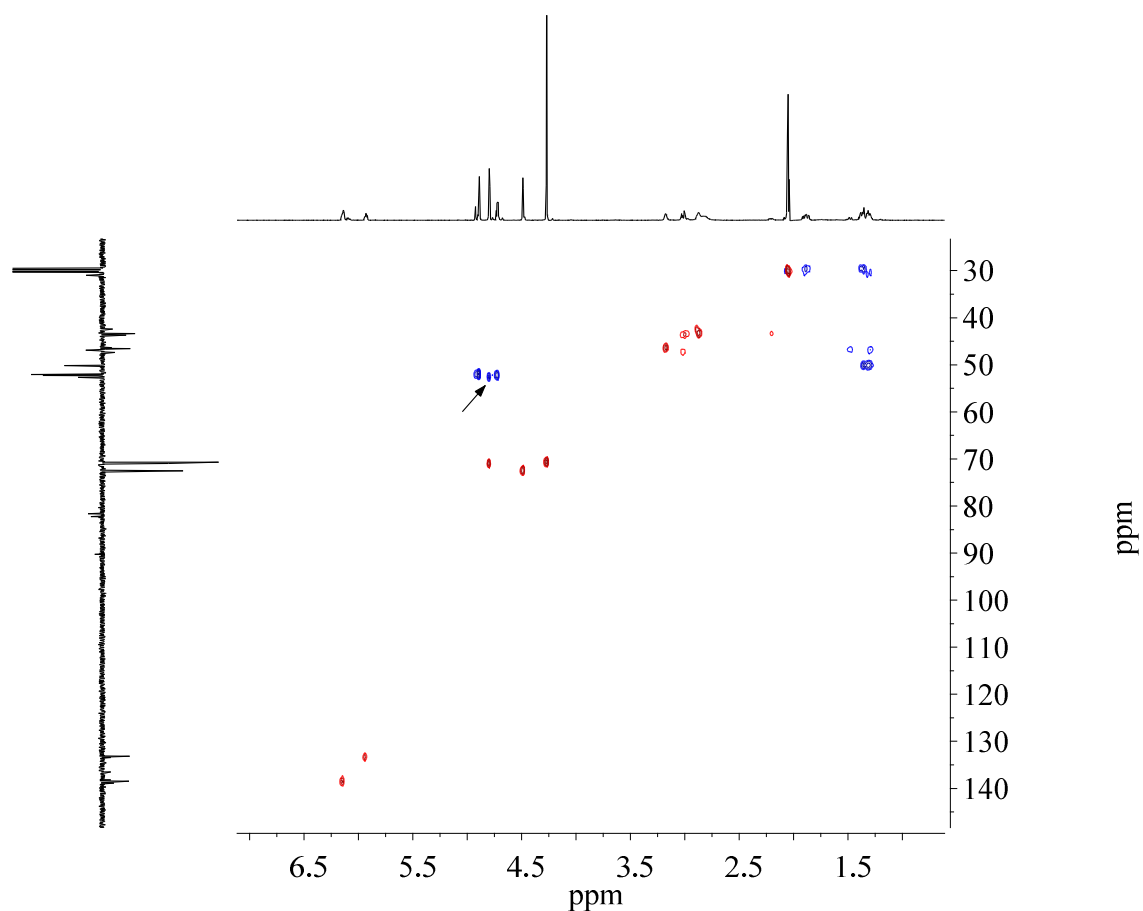
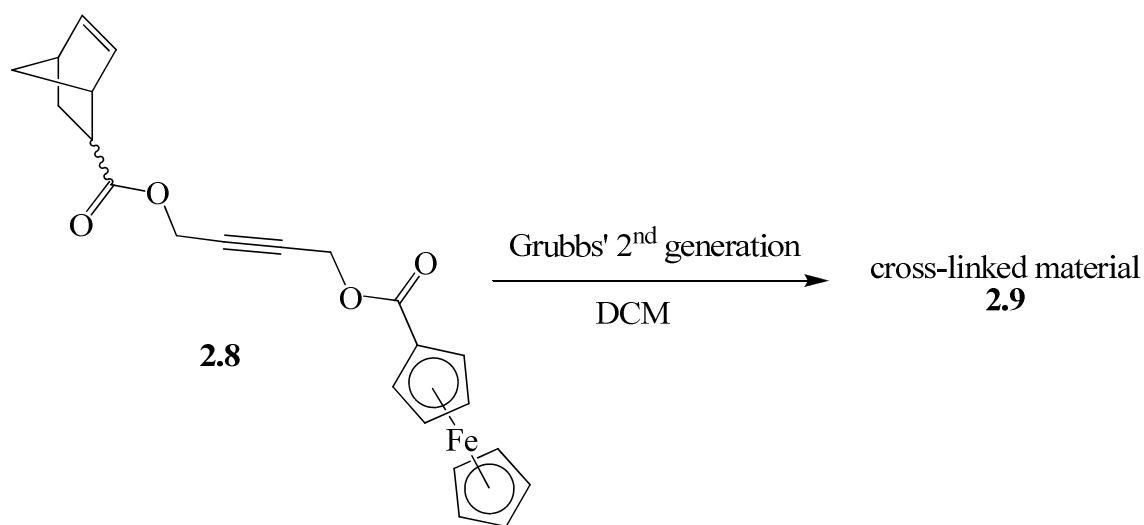


Figure 2.11: HSQC NMR spectrum of complex **2.8** in acetone- d_6 . Arrow indicates the overlapping methylene resonance.

2.2.2 Polymerization of a norbornene monomer containing ferrocene

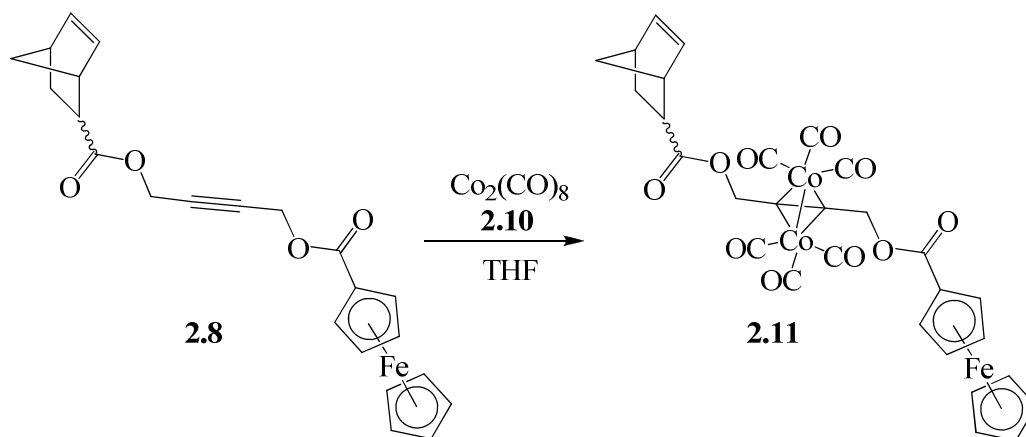
Polymerization of complex **2.8** was done using Grubbs 2nd generation catalyst in DCM. While this catalyst is known to react both with alkene and alkyne functional groups, we were curious to see how it performed with a monomer that contained both an alkyne group and norbornene.^{44, 45} This polymerization produced what appeared to be a cross linked polymer (Scheme 2.4). This material was observed to swell without dissolving in organic solvents such as acetone, DCM, chloroform, DMSO, THF and DMF as is typical of cross-linked materials.⁴⁶



Scheme 2.4: Synthesis of complex **2.9**.

2.2.3 Synthesis of a norbornene monomer containing both ferrocene and cobalt

Since the attempts to polymerize complex **2.8** directly resulted in a cross linked material (**2.9**), it was necessary to coordinate the cobalt carbonyl to the alkyne moiety of complex **2.8** prior to polymerization (Scheme 2.5). During the synthesis of **2.11**, the bridging carbonyl groups of the two cobalt atoms were exchanged for the alkyne resulting in the evolution of carbon monoxide. Once the reaction reached completion, the excess cobalt carbonyl needed to be removed from the reaction. This is especially important as the degradative products of $\text{Co}_2(\text{CO})_8$ are paramagnetic and greatly affect the NMR spectral analysis. When complex **2.11** was dissolved in acetone and left open to the atmosphere, a precipitate formed in the solution. This precipitate was easily removed by filtration through celite. After the precipitate was removed the product was isolated by removal of the solvent *in vacuo*.



Scheme 2.5: Synthesis of complex **2.11**.

The ^1H NMR spectrum of **2.11** showed a noticeable shift of the methylene resonances nearest the triple bond from ~ 4.9 and ~ 4.7 ppm to ~ 5.4 ppm due to electron deshielding caused by the coordination of the cobalt carbonyl to the alkyne (Figure 2.12). The methylene region that appears from 5.25 -5.53 ppm is fairly complicated due to the two isomers of the complex. In order to fully understand why there are 10 peaks in this region it was necessary to synthesize the *exo* isomer of complex **2.11** (**2.11** *exo*). A comparison of **2.11** and **2.11** *exo* (Figure 2.13) allowed for the full analysis of this region. The ^1H NMR spectrum for **2.11** *exo* shows that one of the methylenes (presumably the one closest to the norbornene) is affected by the chiral nature of the norbornene, causing the two protons to appear as 2 doublets at 5.49 and 4.43 ppm. The other methylene is not as affected by the proximity to the norbornene causing it to appear as a singlet at 5.50 ppm overlapping with one of the doublets. This same pattern of multiplicity is also seen for the *endo* form of complex **2.11** in the isomeric mixture (*endo* peaks indicated by

arrows).

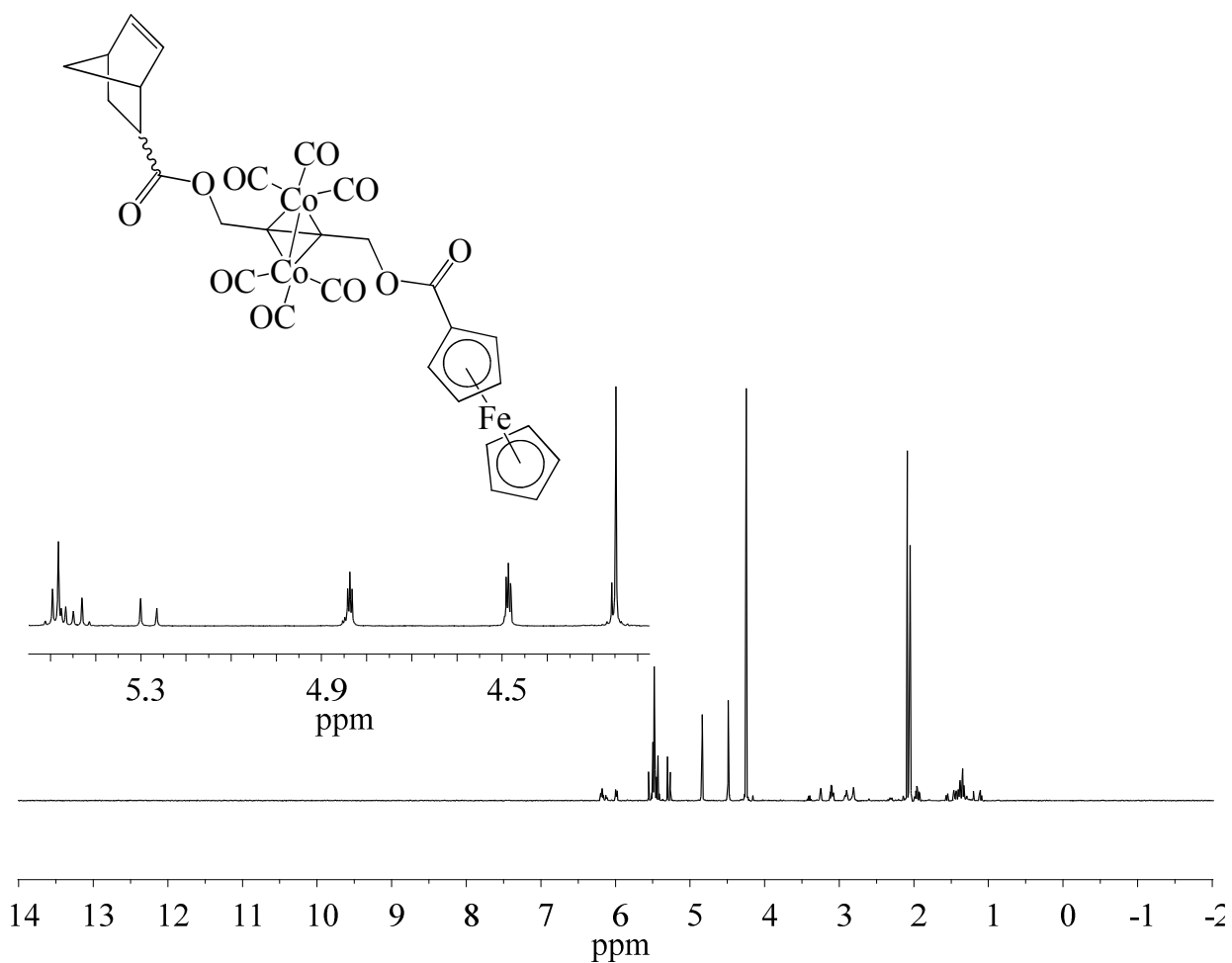


Figure 2.12: ^1H NMR spectrum of complex **2.11** in acetone- d_6 .

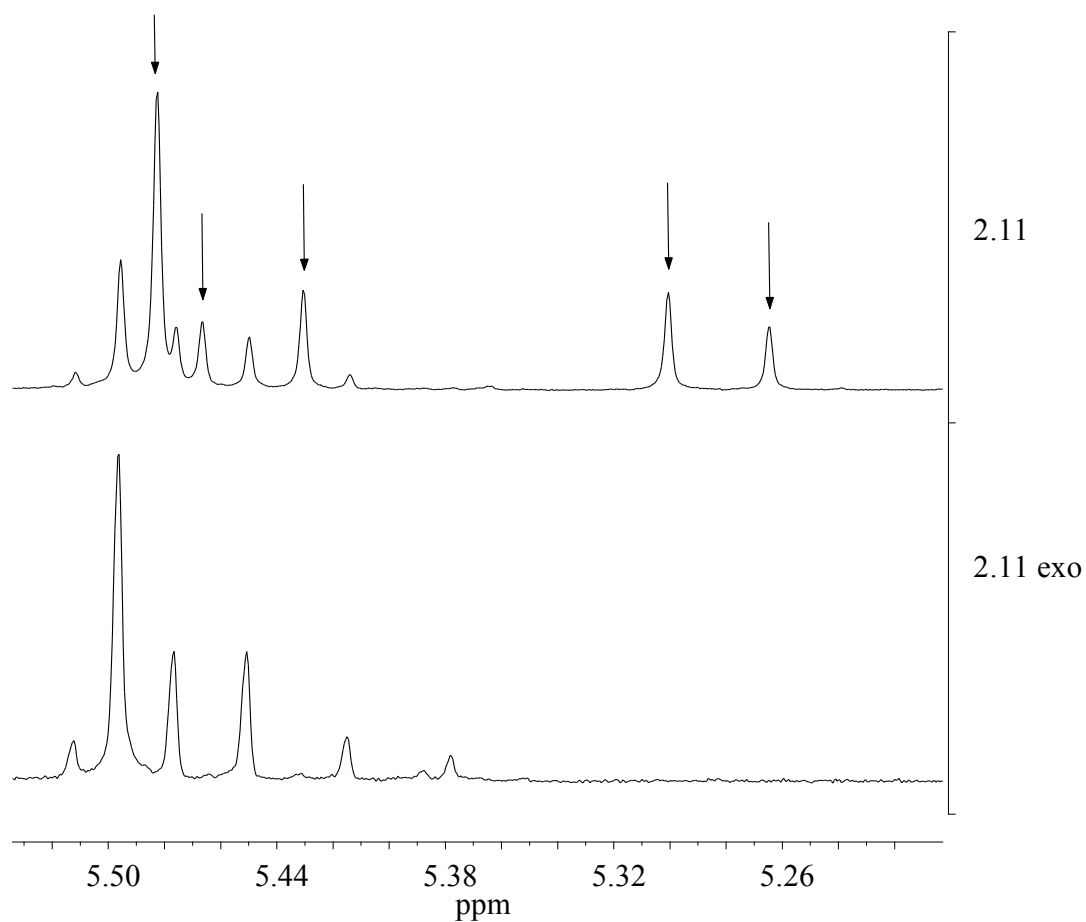


Figure 2.13: Expansion of the ^1H NMR resonances in acetone- d_6 of the methylenes next to the coordinated cobalt moieties of **2.11** (*exo/endo* mixture) and **2.11 exo**. *Arrows indicate *endo* resonances.

Deshielding of the methylene groups adjacent to the alkyne cobalt complex is apparent in the ^{13}C NMR spectrum of the complex **2.11**, where the four representative peaks shift from 52.63, 52.25, 52.02 and 50.12 ppm (complex **2.8**) to 65.79, 65.76, 65.56 and 65.45 ppm (complex **2.11**, Figure 2.14). This is confirmed in the HSQC NMR spectrum of complex **2.11** (Figure 2.15). It can be seen that the proton resonances due to the methylenes at 5.53-5.25 ppm are directly connected to the carbon resonances between 65.4 and 65.8 ppm. The carbon

resonances of the alkyne and carbonyl carbons coordinated to the cobalt are not readily apparent in the ^{13}C NMR spectrum due to broadening caused by the presence of the cobalt. However, the alkyne carbon resonances can be visualized in the HMBC NMR spectrum for complex **2.11** as the peaks at 5.46 and 90.84 ppm (Figure 2.16).

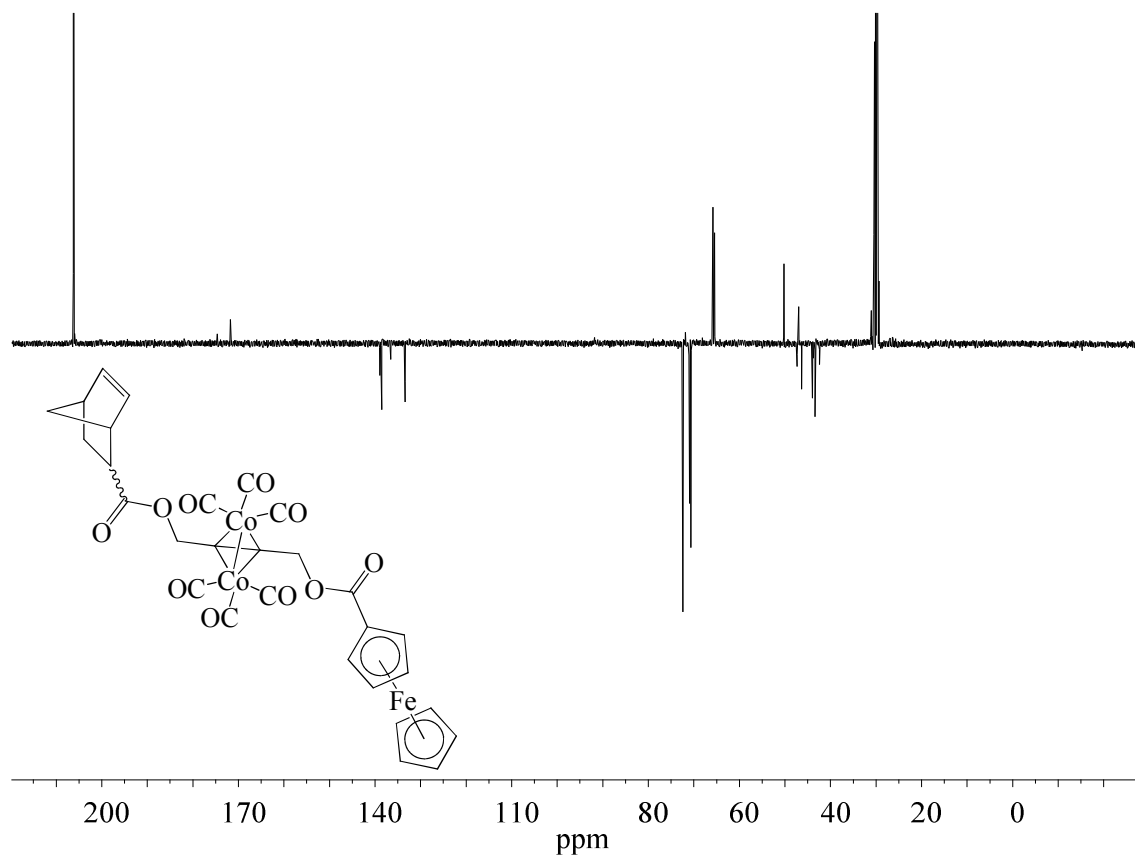


Figure 2.14: APT ^{13}C NMR spectrum of complex **2.11** in $\text{acetone-}d_6$.

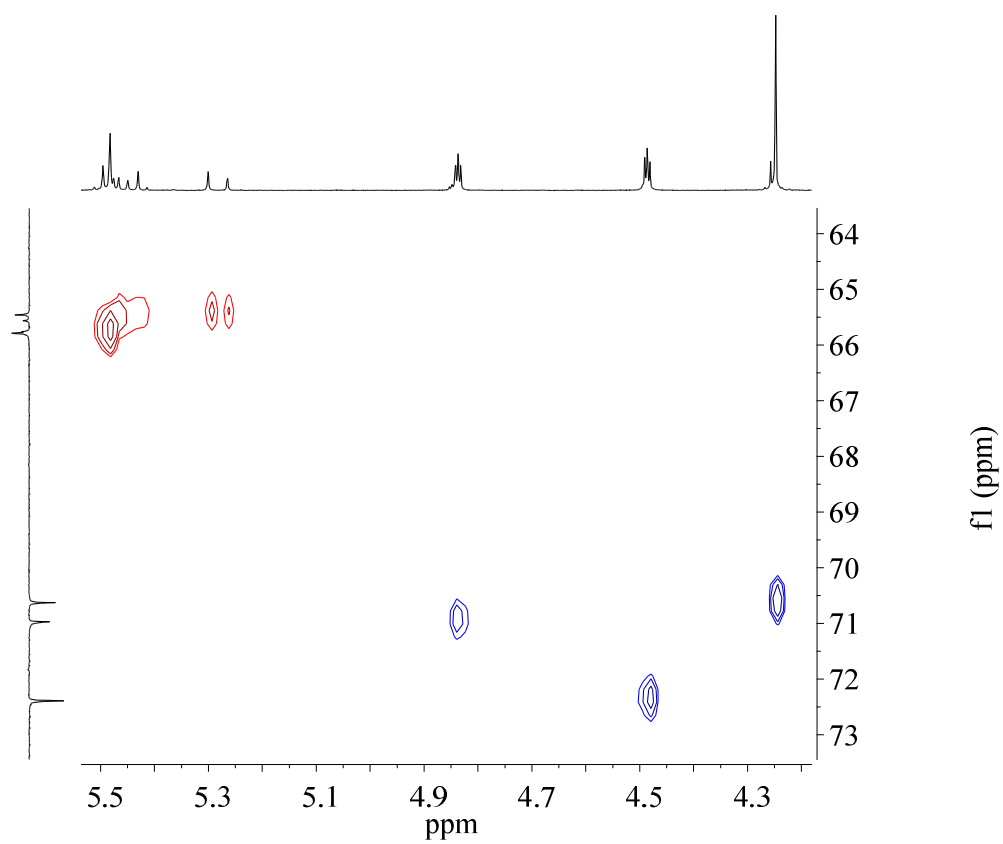


Figure 2.15: HSQC NMR spectrum of complex **2.11** in acetone- d_6 .

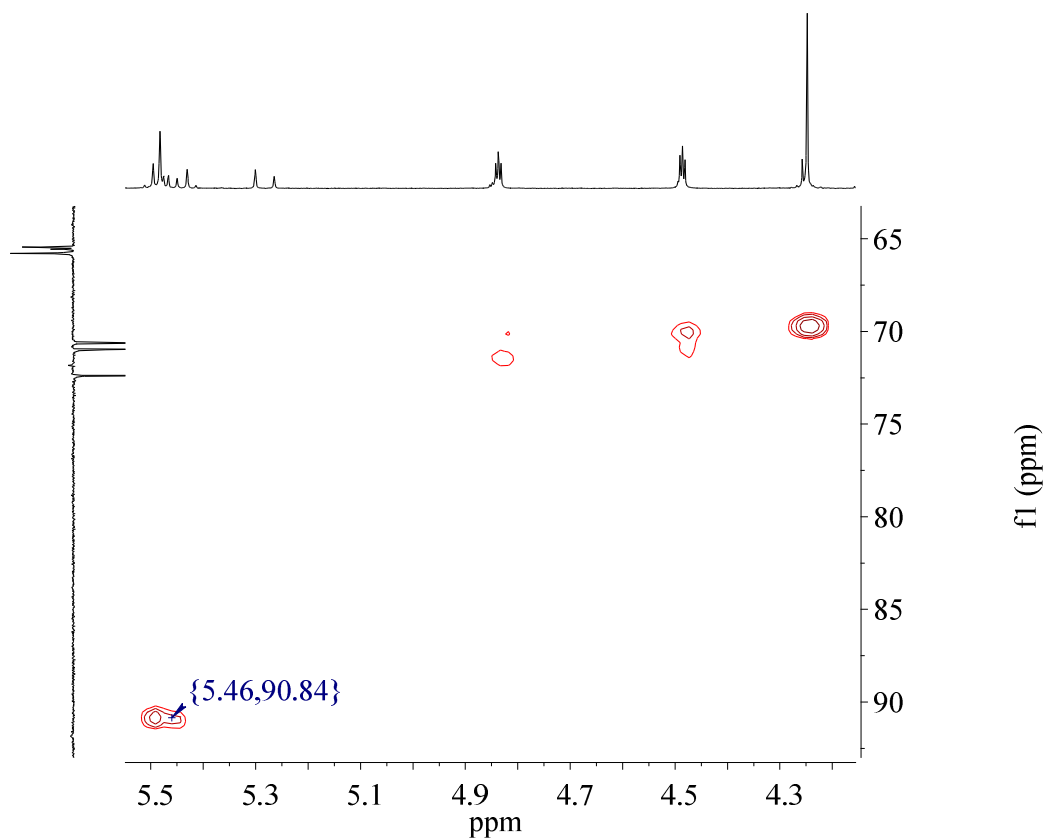


Figure 2.16: HMBC NMR spectrum of complex **2.11** in acetone- d_6 .

The carbonyl carbons coordinated to the cobalt cannot be seen in the various NMR spectra shown (Figure 2.14-Figure 2.16). However, IR spectroscopy can be used to indicate their presence. The IR spectrum for complex **2.11** shows three distinct bands in the 2100 cm^{-1} region of the IR spectrum which is a typical band pattern for the carbonyl stretches of an alkyne cobalt carbonyl structure (Figure 2.17).^{26, 47}

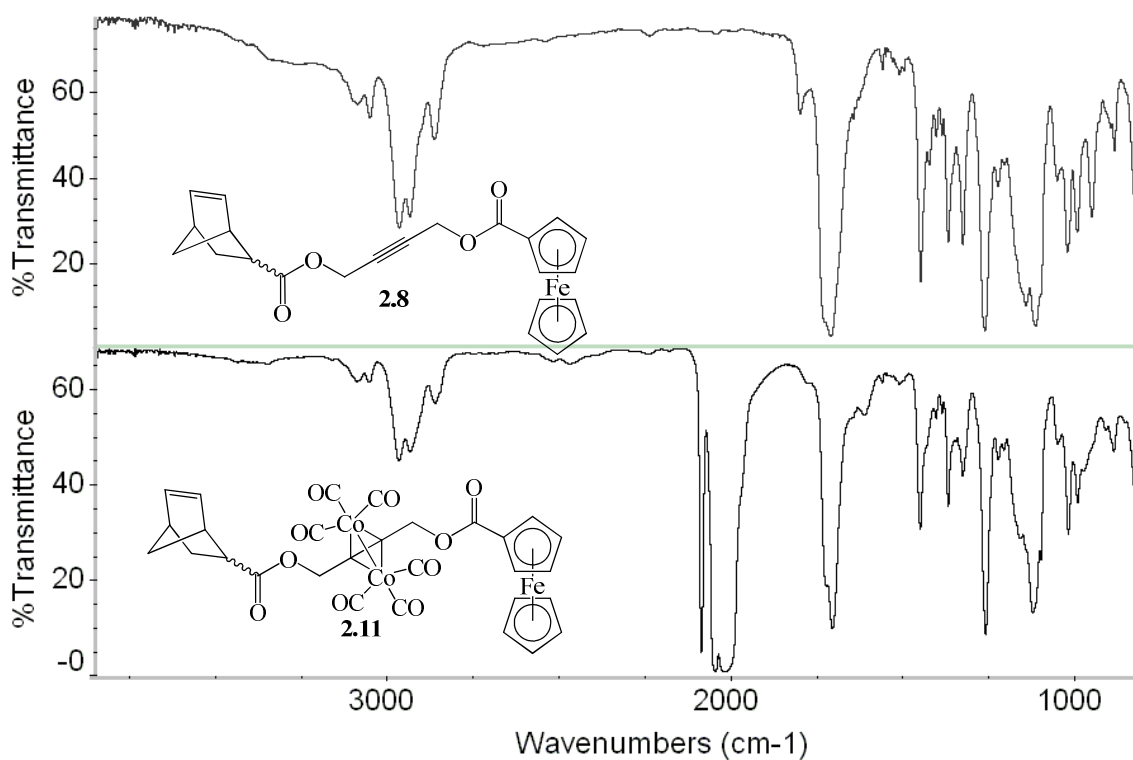
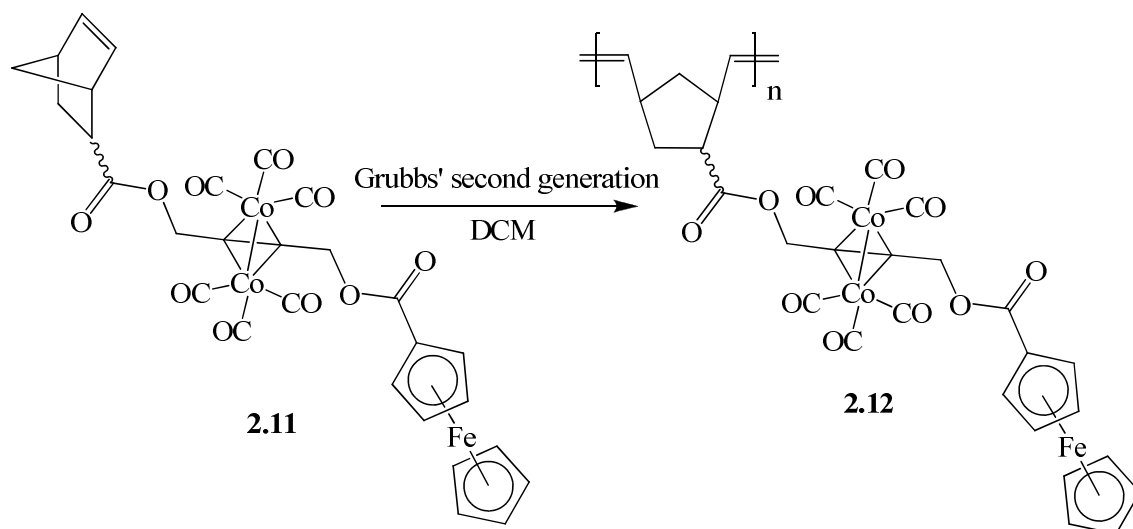


Figure 2.17: IR spectral comparison of complexes **2.8** and **2.11**.

2.2.4 Polymerization of a norbornene monomer containing both ferrocene and cobalt

Polymerization of the multiple metal containing complex **2.11** was achieved using Grubbs 2nd generation catalyst in DCM (Scheme 2.6). The success of the polymerization is supported by the ¹H NMR with an upfield shift of the norbornene olefinic protons from a multiplet at 5.90-6.25 ppm to a broad peak at 5.00-5.55 ppm overlapping with the methylene resonances. There is also broadening of many of the resonances as is typical for the ¹H NMR spectra of polymers (Figure 2.18). The polymers were not soluble enough to acquire a ¹³C NMR spectrum. The molecular weights of this polymer will be discussed later in section 2.4.



Scheme 2.6: Synthesis of polymer **2.12**.

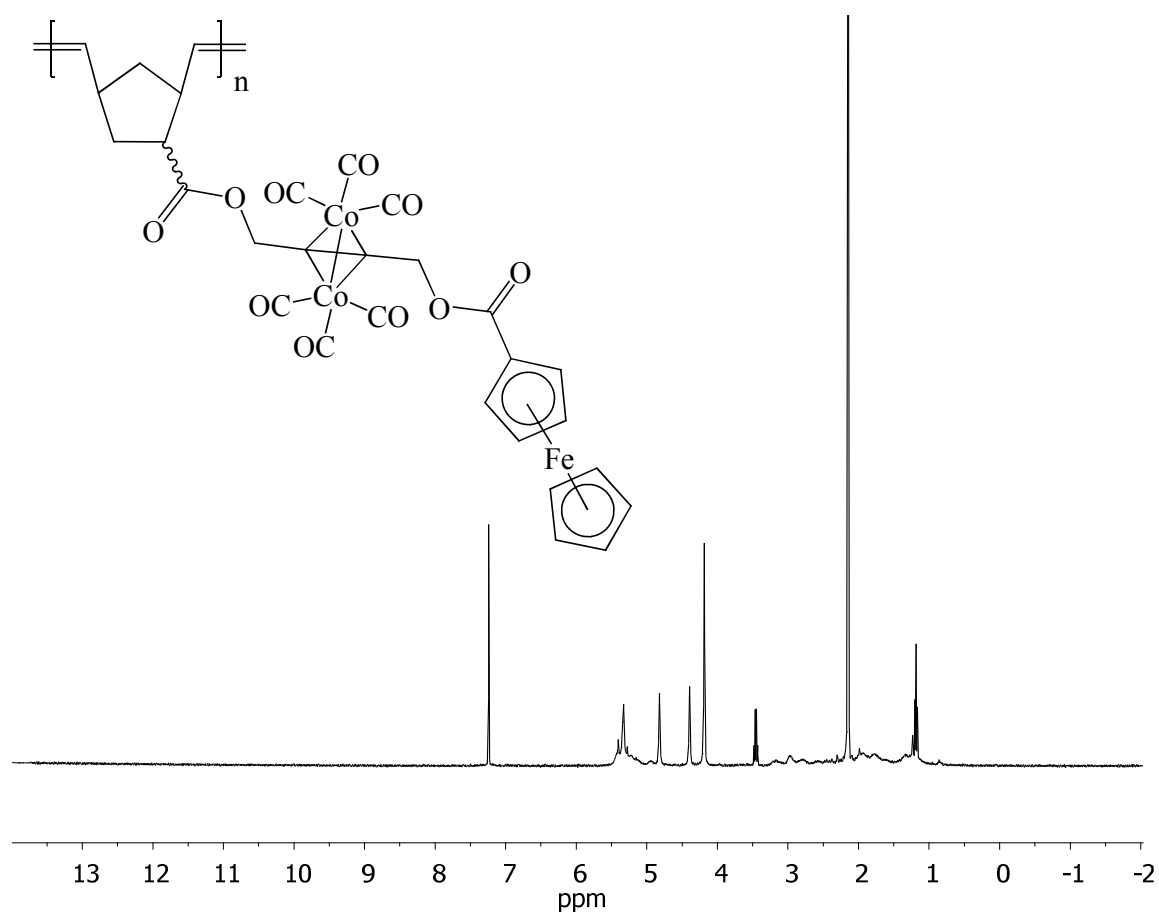
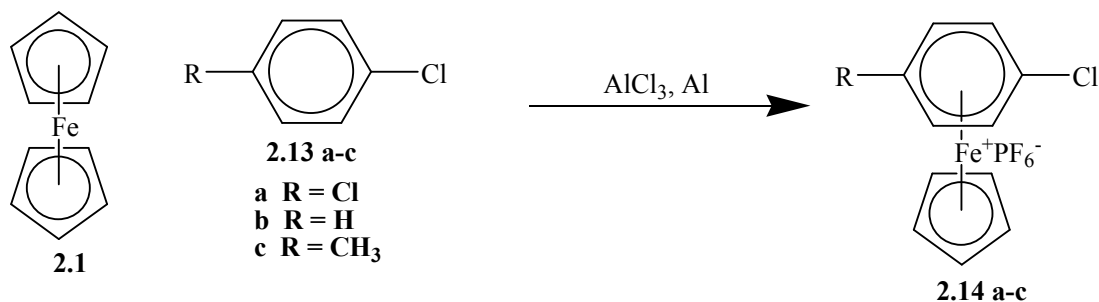


Figure 2.18: ^1H NMR spectrum of polymer **2.12** in CDCl_3 .

2.3 Synthesis and characterization of η^6 -arene- η^5 -cyclopentadienyliron(II) and cobalt containing polynorbornenes

2.3.1 Synthesis of a norbornene monomer containing alkyne-hexacarbonyl cobalt and two η^6 -chloroarene- η^5 -cyclopentadienyliron(II) moieties

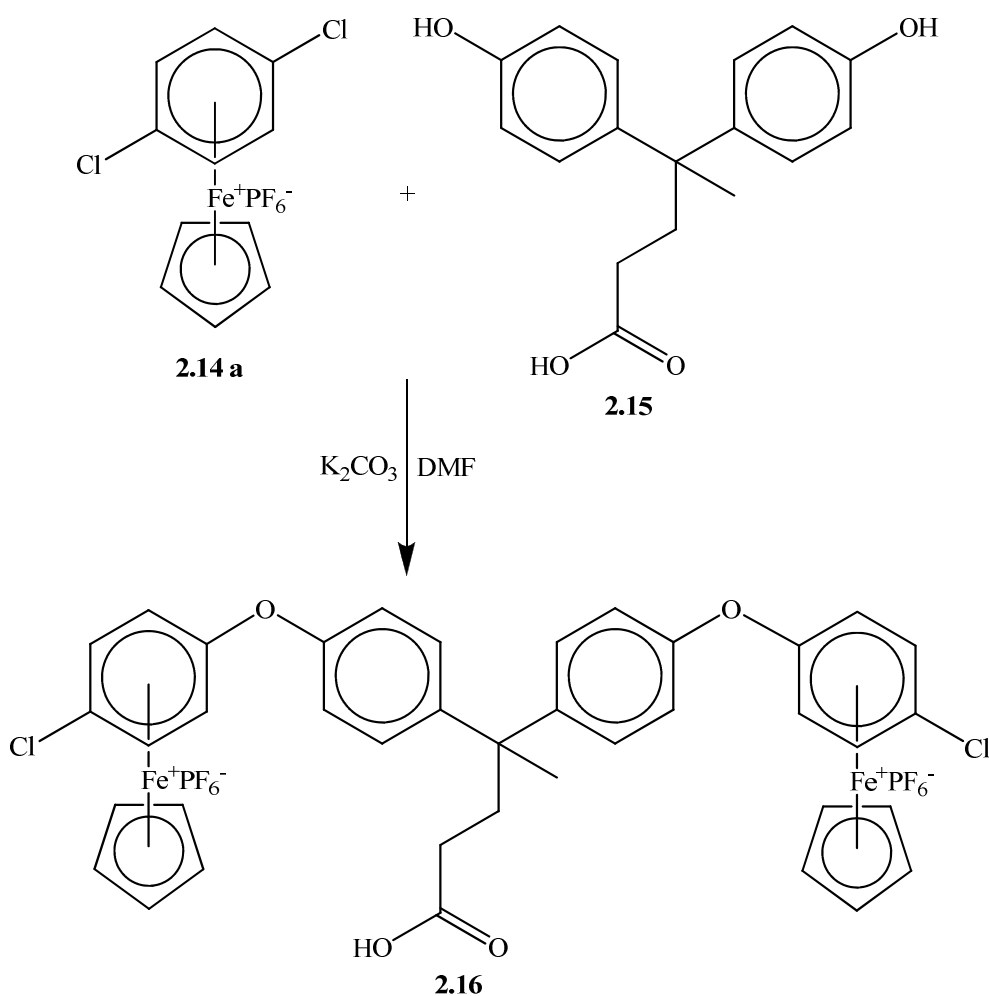
In the previous section, ferrocene and cobalt carbonyl were incorporated into norbornene which was then polymerized. This section of chapter 2 details the synthesis of norbornene monomers which contain η^6 -arene- η^5 -cyclopentadienyliron(II) moieties as well as an alkyne-hexacarbonylcobalt moiety. Using a similar procedure as developed by Nesmeyanov et al. complexes **2.14 a-c** were prepared (Scheme 2.7).¹⁶ Compounds that contain these η^6 -chloroarene- η^5 -cyclopentadienyliron(II) hexafluorophosphate salts can decompose when exposed to light, so complexes **2.14 a-c** and all subsequent derivatives were stored and reacted in the dark.



Scheme 2.7: Synthesis of complexes **2.14 a-c**.

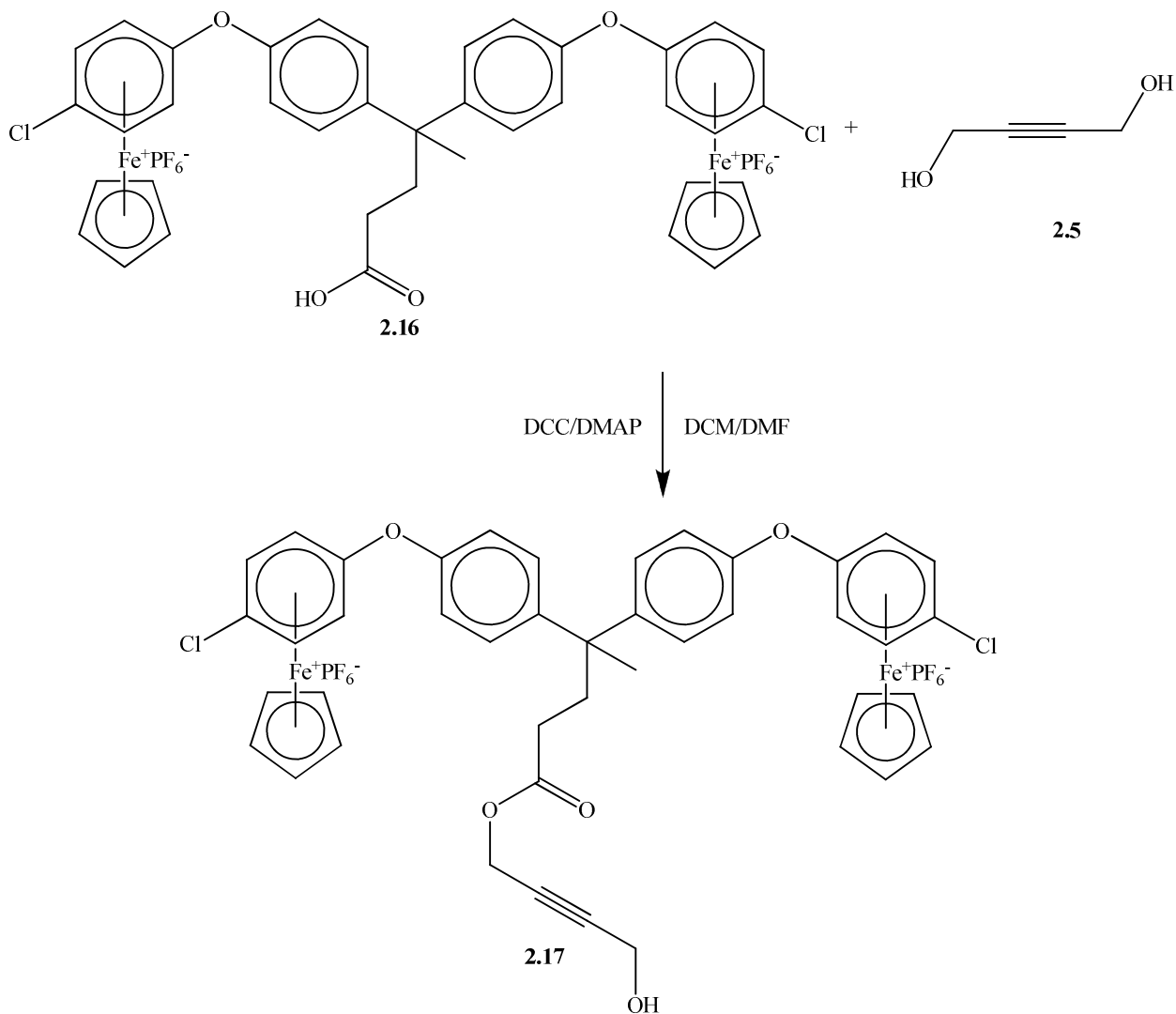
Norbornene monomers containing two η^6 -chloroarene- η^5 -cyclopentadienyliron(II) hexafluorophosphate moieties and dicobalt hexacarbonyl were prepared, to determine if increasing the amount of cationic iron in the polymers would have any effect on their synthesis or thermal properties. As shown previously, η^6 -chloroarene- η^5 -cyclopentadienyliron(II) hexafluorophosphate salts are known to undergo nucleophilic aromatic substitution. Complex

2.14 a possesses two positions where substitution can occur and is highly reactive towards alcohol, amine and thiol nucleophiles. The incorporation of two η^6 -chloroarene- η^5 -cyclopentadienyliron(II) hexafluorophosphate moieties was accomplished by first finding a compound that had three reactive sites. 4,4-bis(4-hydroxyphenyl)valeric acid (**2.15**) is ideal for the incorporation of two iron centers due to its two phenolic alcohols which were reacted with complex **2.14 a** leaving the carboxylic acid free for further reactions (Scheme 2.8). Previous reports on the synthesis of complex **2.16** used a THF/DMF solvent mixture at 50 °C; however, using DMF alone at room temperature works as well.⁴⁸ The DMF is easily removed when the product is precipitated into 1.2 M HCl and washed with water.



Scheme 2.8: Synthesis of complex **2.16**.

Complex **2.17** was synthesized using the Steglich esterification between the valeric acid complex **2.16** and 2-butyne-1,4-diol (**2.5**) (Scheme 2.9). Complex **2.17** has a free alcohol which can allow for its incorporation into various monomers.



Scheme 2.9: Synthesis of complex **2.17**.

The ^1H NMR of complex **2.17** shows all of the expected resonances (Figure 2.19). The non-complexed arene resonances appear at 7.48 and 7.34 ppm, while the complexed arene resonances are found at 6.82 and 6.52 ppm. The cyclopentadiene resonance appears at 5.38 ppm

and the two methylenes adjacent to the triple bonded carbons are at 4.71 and 4.23 ppm. The other two methylenes appear as triplets at 2.56 and 2.24 ppm and finally the methyl group appears at 1.76 ppm.

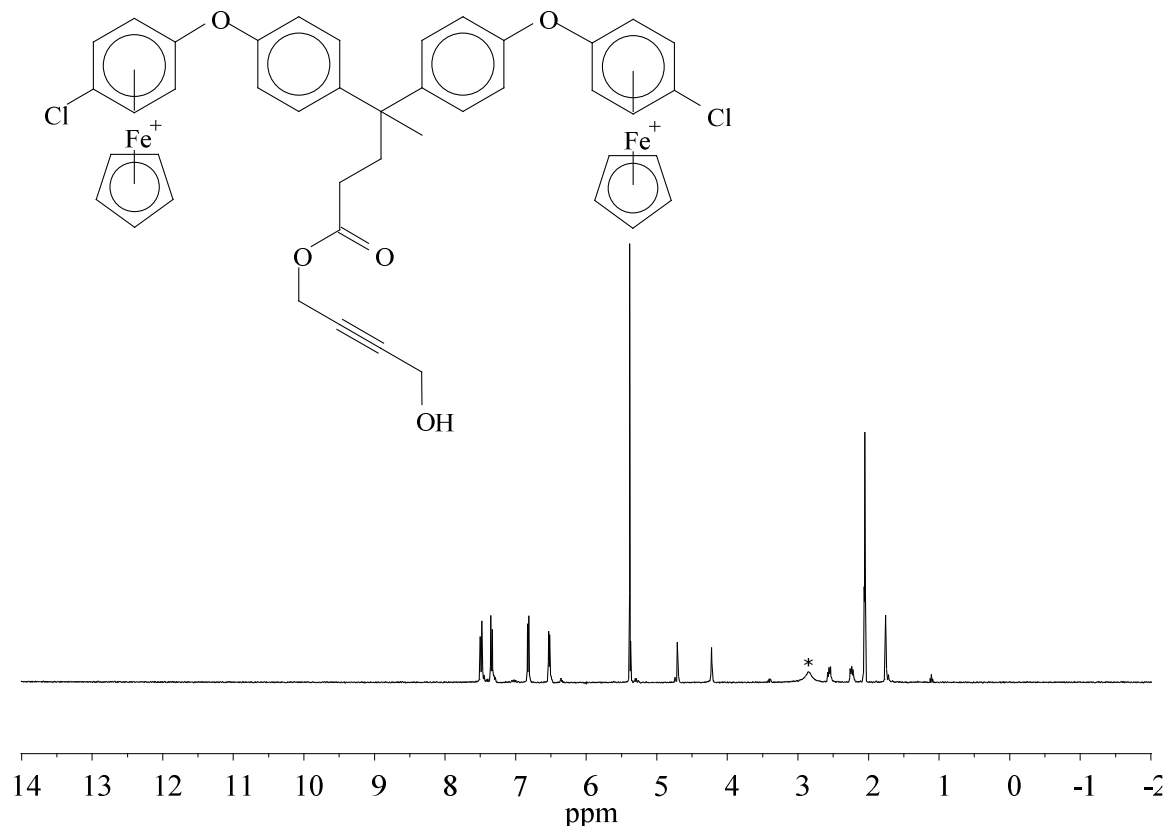


Figure 2.19: ^1H NMR spectrum of complex **2.17** in acetone- d_6 . * denotes H_2O .

The ^{13}C NMR spectrum for complex **2.17** (Figure 2.20) contains all 18 of the expected peaks plus acetone at 30.6 and 206.9 ppm.⁴⁹ The carbonyl carbon resonated at 172.9 ppm. While the non-complexed arene resonances were observed at 151.7, 147.6, 130.4 and 121.1 ppm. The complexed arenes were found at 133.6, 104.5, 87.5 and 76.7 ppm while the cyclopentadiene resonances appeared at 80.3 ppm. The alkyne carbon resonances were found at 86.6 and 79.3 ppm while the adjacent methylene carbons resonated at 52.5 and 50.3 ppm. The methylene carbon next to the carbonyl carbon of the organometallic moiety resonates at 30.2 ppm and is

actually found within the solvent residue peak. The final methylene was found at 36.8 ppm, the quaternary carbon sandwiched between the arenes appeared at 46.0 ppm and the methyl resonated at 27.7 ppm.

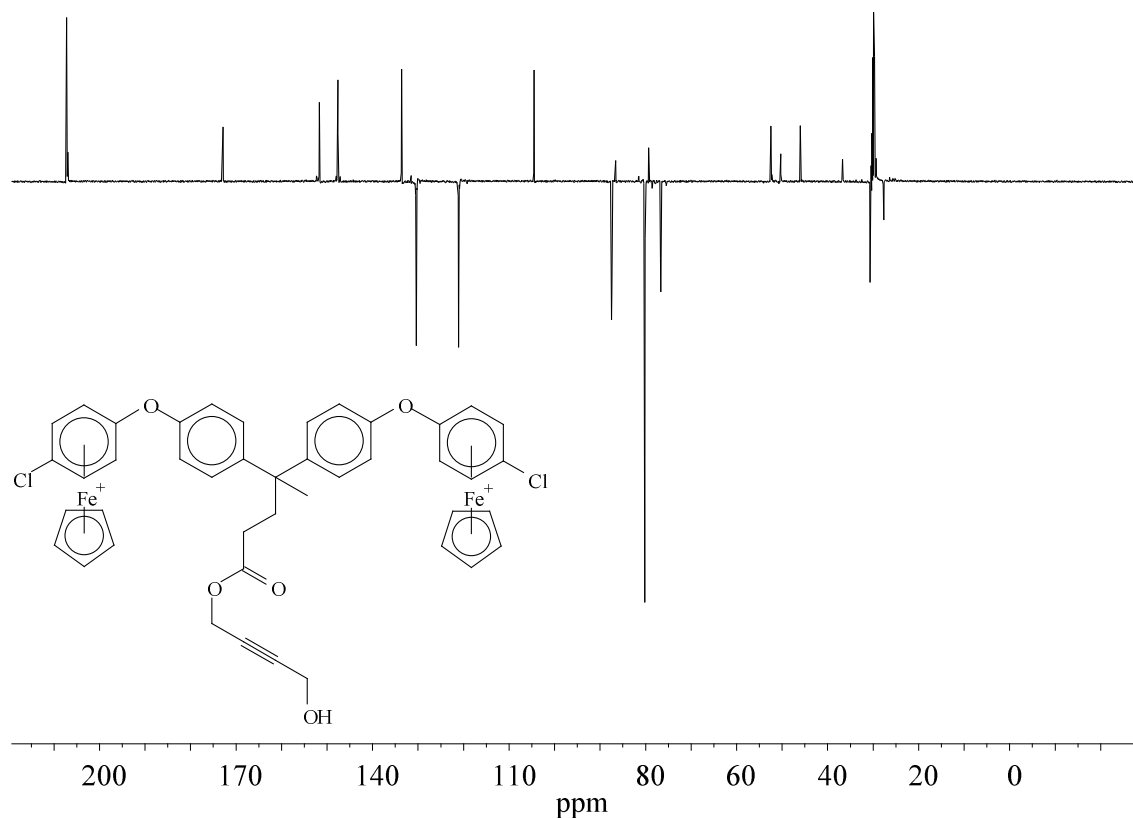
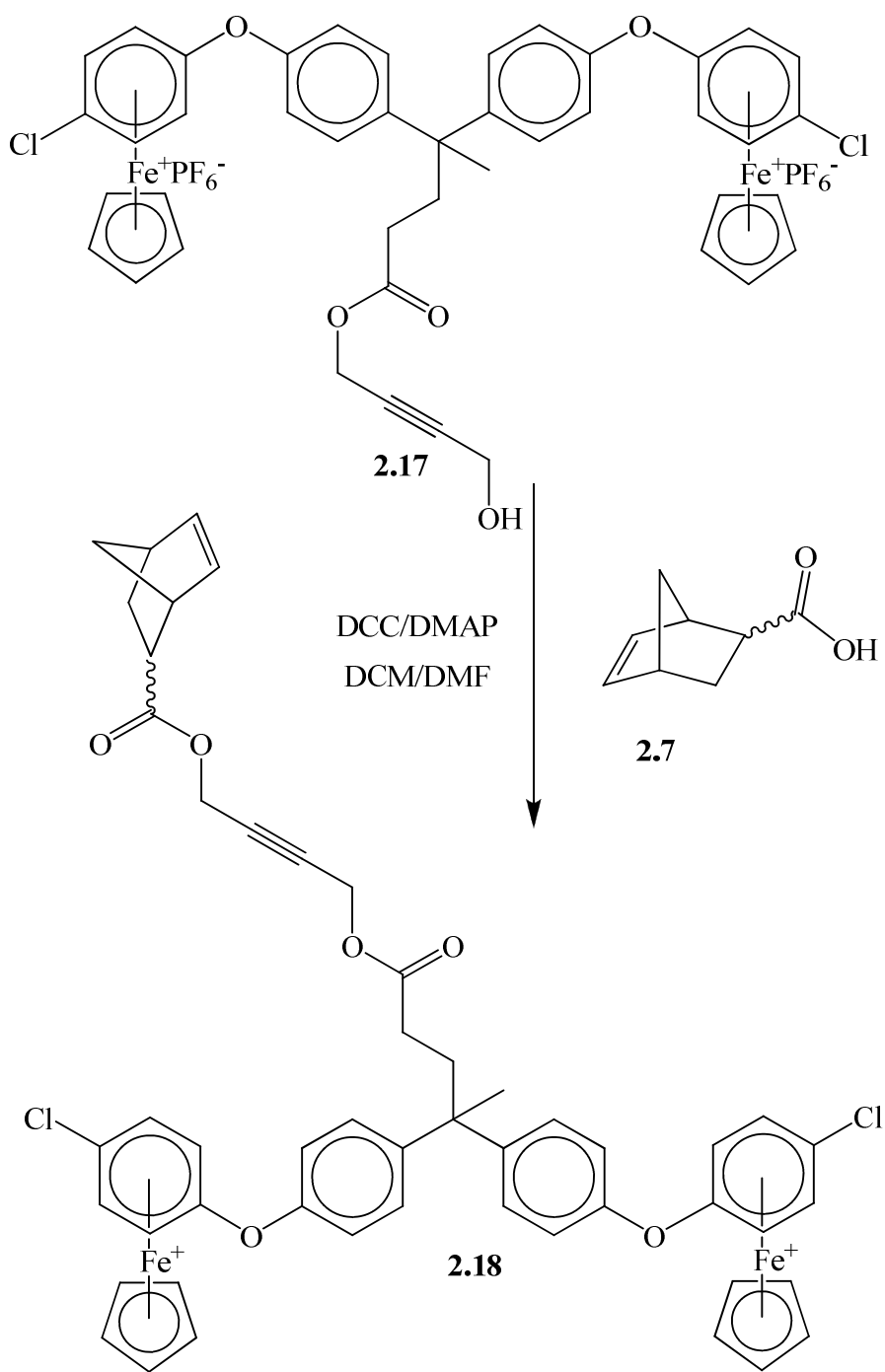


Figure 2.20: APT ^{13}C NMR spectrum of complex **2.17** in acetone- d_6 .

Steglich esterification between complex **2.17** and 5-norbornene-2-carboxylic acid (**2.7**) produced complex **2.18**. The success of the reaction between complex **2.17** and the 5-norbornene-2-carboxylic acid (**2.7**) was determined through NMR spectroscopy. The ^1H NMR spectrum of complex **2.18** (Figure 2.21) shows both the appearance of the norbornene peaks at 6.19-5.87, 2.18-2.88, 1.95-1.85, and 1.48-1.26 ppm as well as the downfield shift of the methylene protons adjacent to the newly formed ester to 4.76-4.64 ppm. Unfortunately, the *endo* *exo* ratio of the sample could not be determined due to overlapping of the olefin peaks.



Scheme 2.10: Synthesis of complex **2.18**.

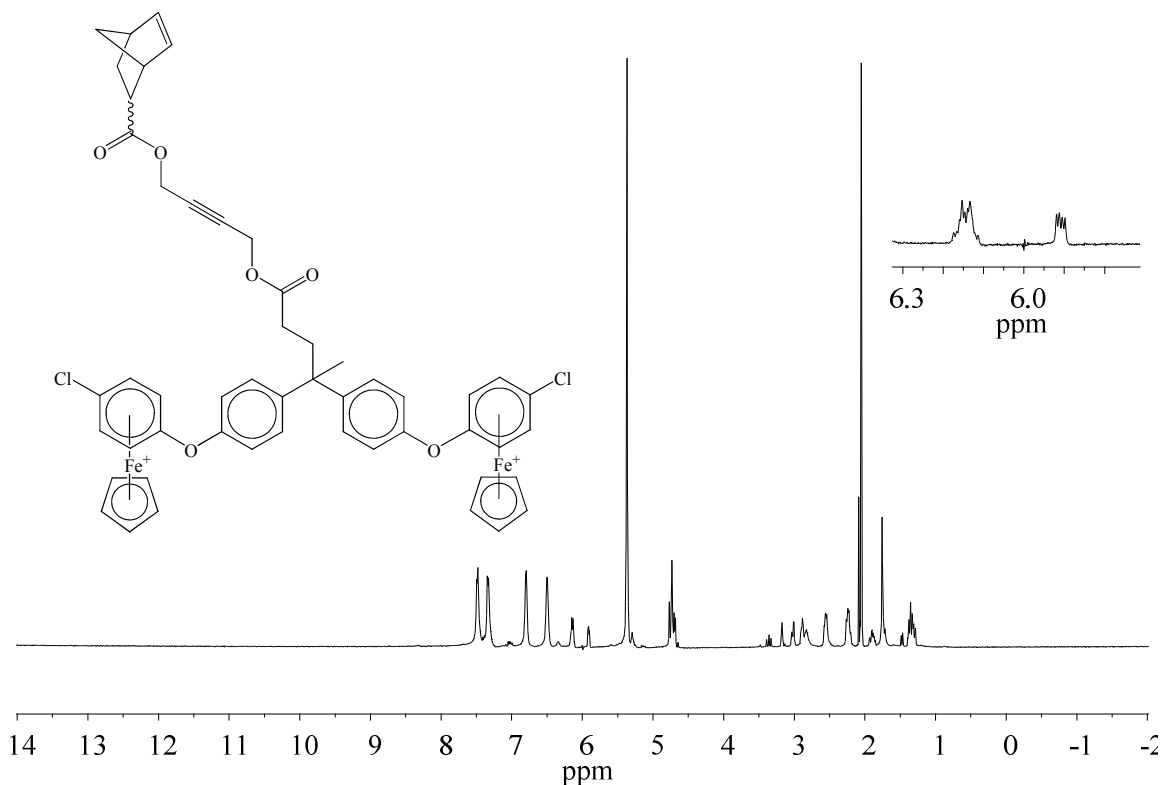


Figure 2.21: ^1H NMR spectrum of complex **2.18** in acetone- d_6 .

The ^{13}C NMR spectrum of **2.18** also shows the appearance of the norbornene olefin resonances at 138.92, 138.52, 136.47 and 133.10 ppm (Figure 2.22). Ten resonances can be seen for the other five carbons of the norbornene. The formation of the ester is further confirmed by the upfield shift of the methylene carbons from 50.3 ppm to 52.56 and 52.59. Of the forty five peaks in the ^{13}C NMR spectrum thirty eight can be attributed to an *endo/exo* mixture of complex **2.18**. Upon a full analysis of the HSQC and HMBC NMR spectra for complex **2.18** it is possible to determine the identities of the *exo* and *endo* carbon resonances (Figure 2.23 and Figure 2.24). The *endo* and *exo* resonances for each carbon get closer and closer together as the distance from the norbornene increases to the point where the methylene carbon between the alkyne and the valeric ester appears only as one peak at 52.16 ppm. The convergence of the *endo* and *exo* resonances at this point in the molecule was also seen for complexes **2.8**. The seven

other peaks in the ^{13}C NMR spectrum are of quite low intensity and can be attributed to a slight amount of starting material in the sample.

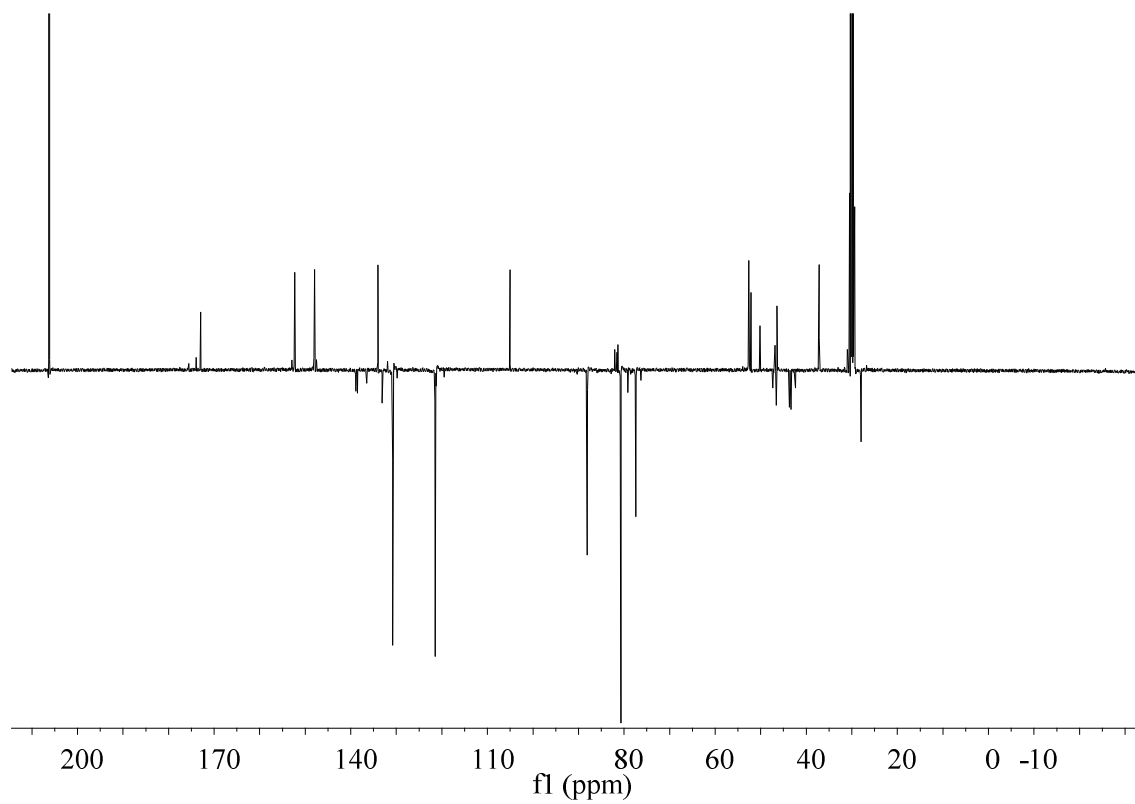


Figure 2.22: APT ^{13}C NMR spectrum of complex **2.18** in acetone- d_6 .

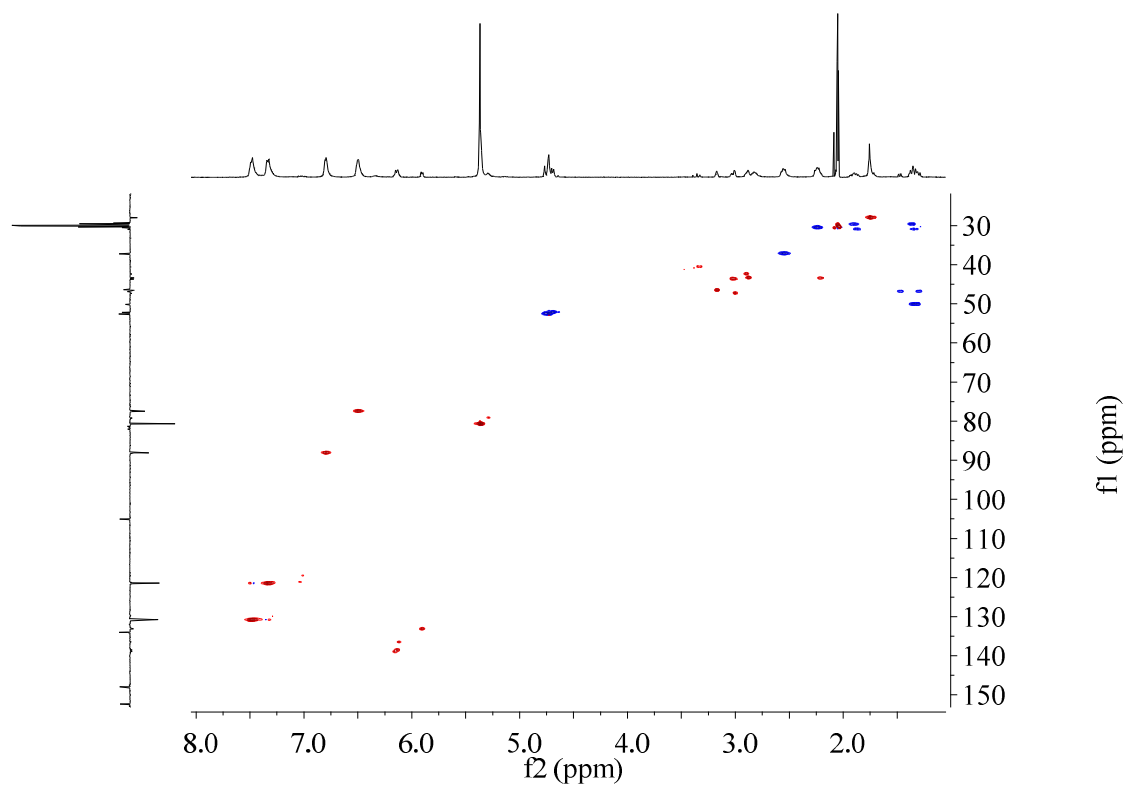


Figure 2.23: HSQC NMR spectrum of complex **2.18** in acetone-*d*₆.

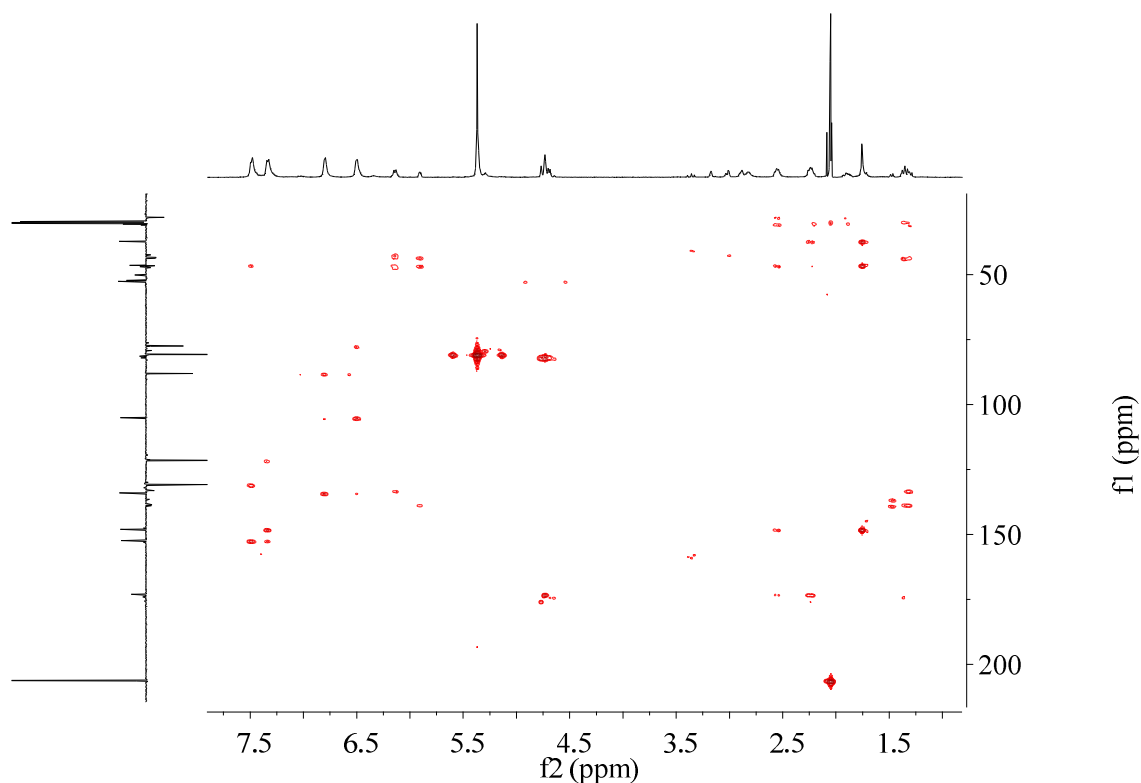
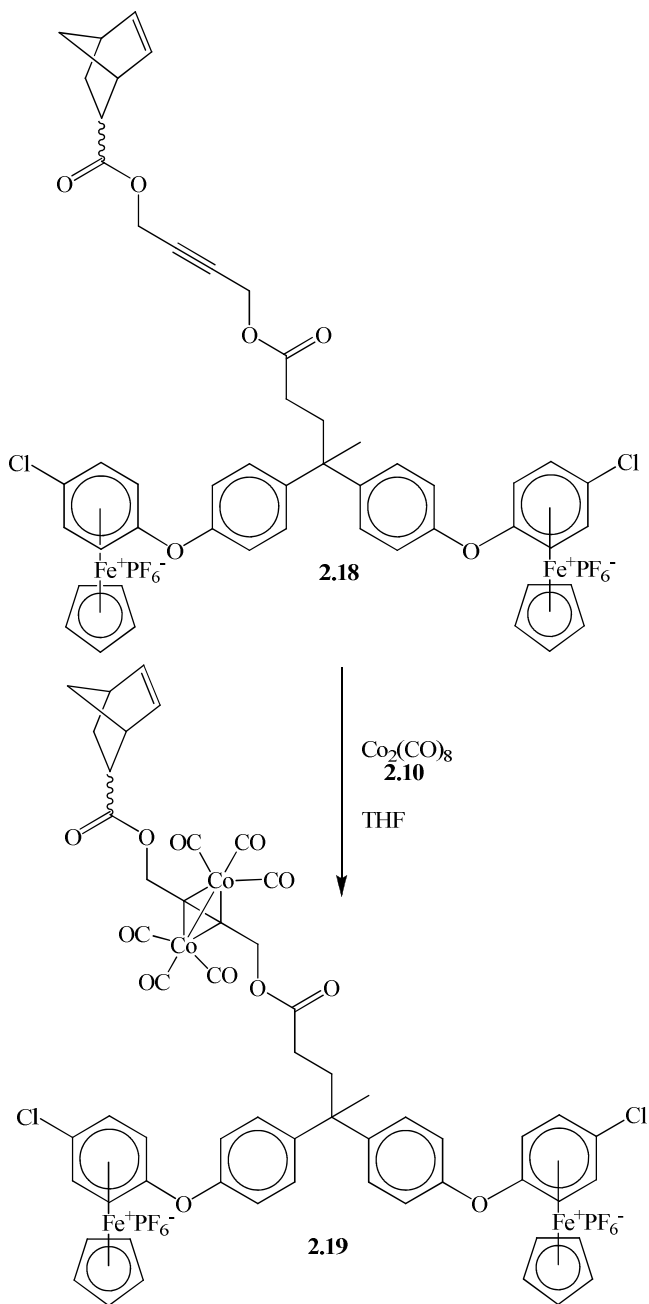


Figure 2.24: HMBC NMR spectrum for complex **2.18** in acetone- d_6 .

Coordination of dicobalt octacarbonyl (**2.10**) to complex **2.18** gave the tetra metallic complex **2.19** (Scheme 2.11). The success of the reaction was determined through NMR and IR spectroscopies. The IR showed the presence of the cobalt carbonyl bands situated around 2100 cm^{-1} . In the ^1H NMR spectra of complex **2.19**, the resonances of the methylenes adjacent to the alkyne have shifted downfield from 4.76-4.64 ppm (complex **2.18**) to 5.48-5.17 ppm (complex **2.19**) (Figure 2.25). The splitting pattern of these resonances cannot be seen as they overlap with the cyclopentadiene peak. The olefin resonances of the *endo/exo* mixture appear as discrete peaks in this spectrum, allowing for the ratio of isomers to be determined (63% *endo* and 37% *exo*). The ^{13}C NMR spectrum of complex **2.19** also shows a downfield shift from 52.59, 52.55 and 52.16 ppm (complex **2.18**), to 65.60, 65.40 and 65.38 ppm (complex **2.19**) for the methylene carbons adjacent to the alkyne (Figure 2.27). Unfortunately, not all of the carbon resonances are

visible in the ^{13}C NMR spectrum; the alkyne and carbonyl carbons coordinated to the cobalt cannot be seen due to broadening, also the two *endo* and *exo* carbonyl carbons of the norbornene are not visible.



Scheme 2.11: Synthesis of complex **2.19**.

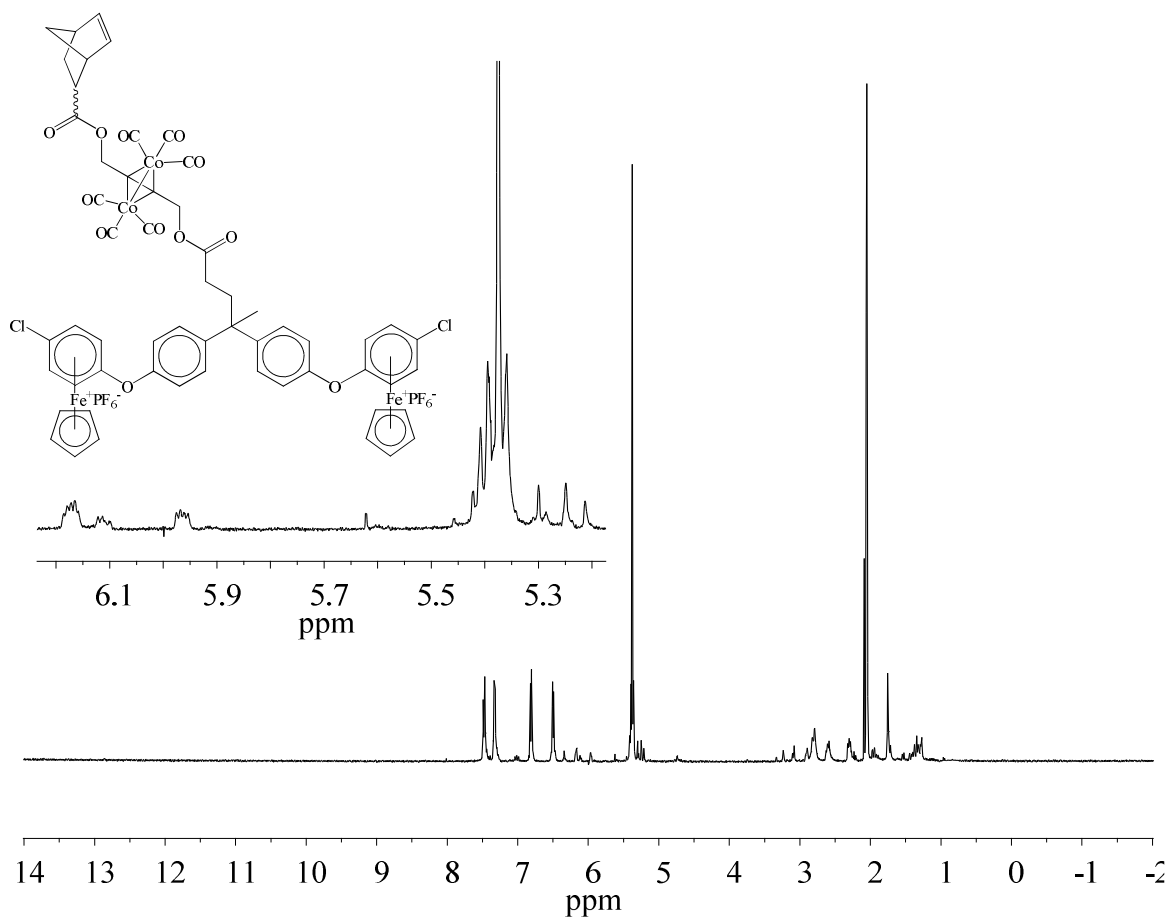


Figure 2.25: ^1H NMR spectrum of complex **2.19** in $\text{acetone-}d_6$.

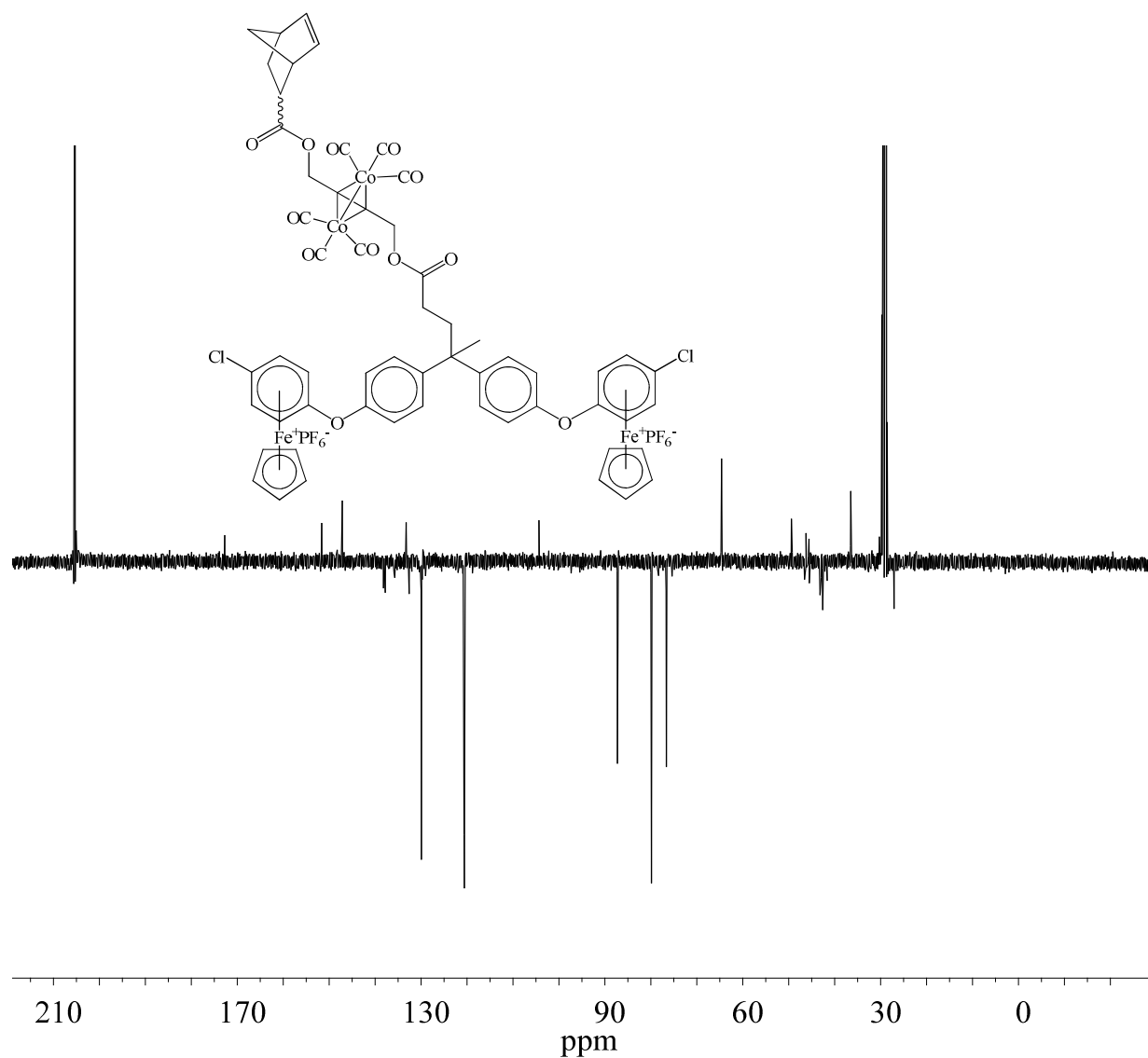
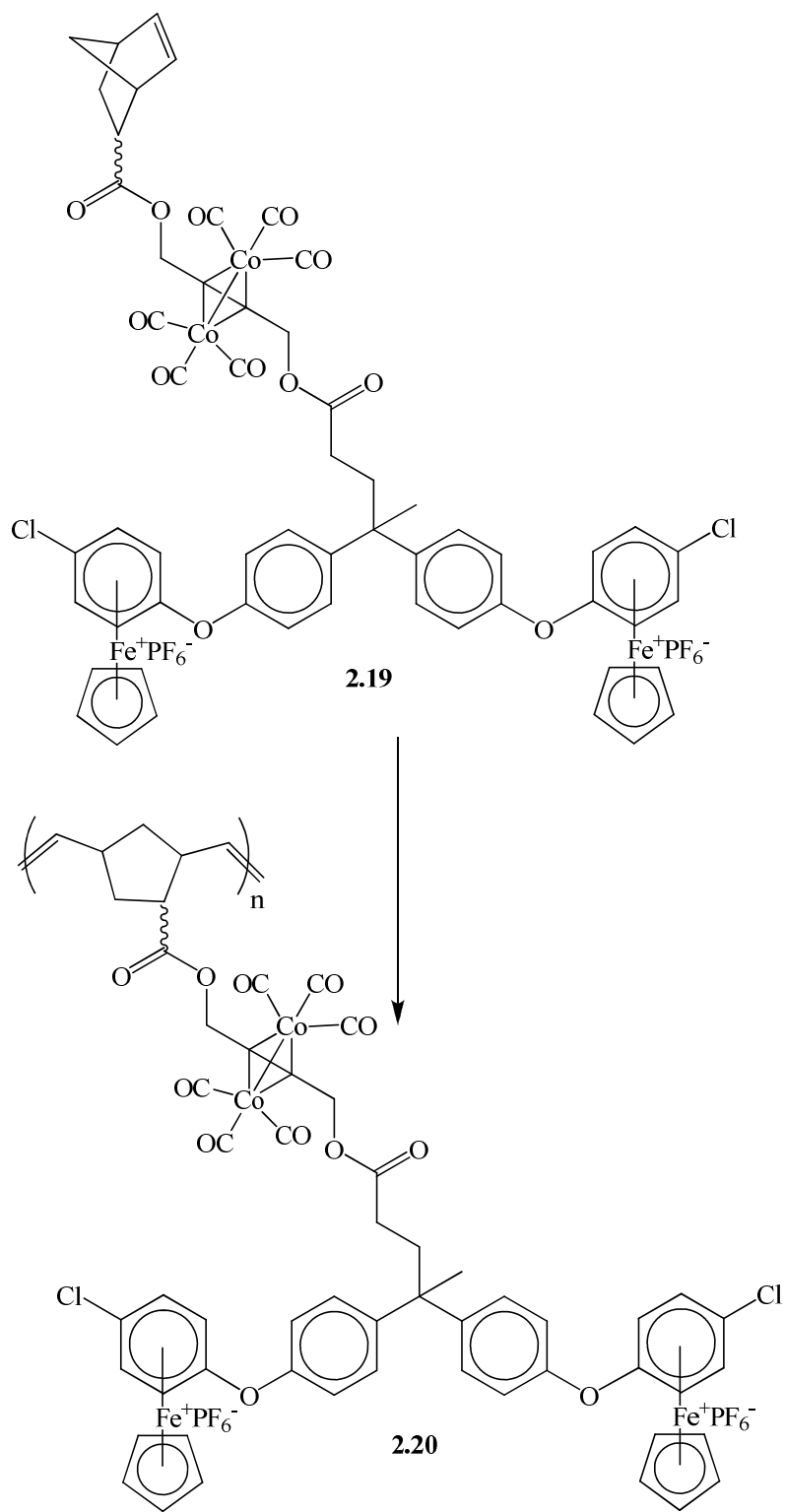


Figure 2.26: APT ^{13}C NMR spectrum of complex **2.19** in acetone- d_6 .

2.3.2 Polymerization of a norbornene monomer containing cobalt carbonyl and two η^6 -arene- η^5 -cyclopentadienyliron(II) moieties

Polymerization of complex **2.19** was done using Grubbs 2nd generation catalyst in a 50:1 ratio giving polymer **2.20** (Scheme 2.12). After 45 min. the polymers had mostly precipitated out

of solution and ethylvinylether was added to end cap any polymers still in solution. The polymers were red in colour and displayed very different solubility than the monomer. The monomers had been soluble in DCM, acetone, DMSO, acetonitrile and DMF; however, the polymers showed no solubility in acetone or DCM, and were only partially soluble in acetonitrile, DMSO and DMF.



Scheme 2.12: Synthesis of polymer **2.20**.

The ^1H -NMR of polymer **2.20** shows the typical broadened peaks expected from a slightly soluble polymer (Figure 2.27). It is important to note that the olefinic hydrogens of the norbornene do not appear in the region as they did in the monomer (5.9-6.2 ppm). These olefinic hydrogens have shifted upfield to reside as a part of the very broad resonance at 5.28 ppm, which also includes the cyclopentadiene and methylene resonances. There is a significant water peak in this spectrum that hides some of the polymer backbone peaks as well as some diethyl ether, which causes the aliphatic peak at 1.28 ppm to integrate for 3 extra protons.

The ^{13}C -NMR analysis of polymer **2.20** could not be obtained because the polymer would not stay in solution long enough to obtain a good spectrum.

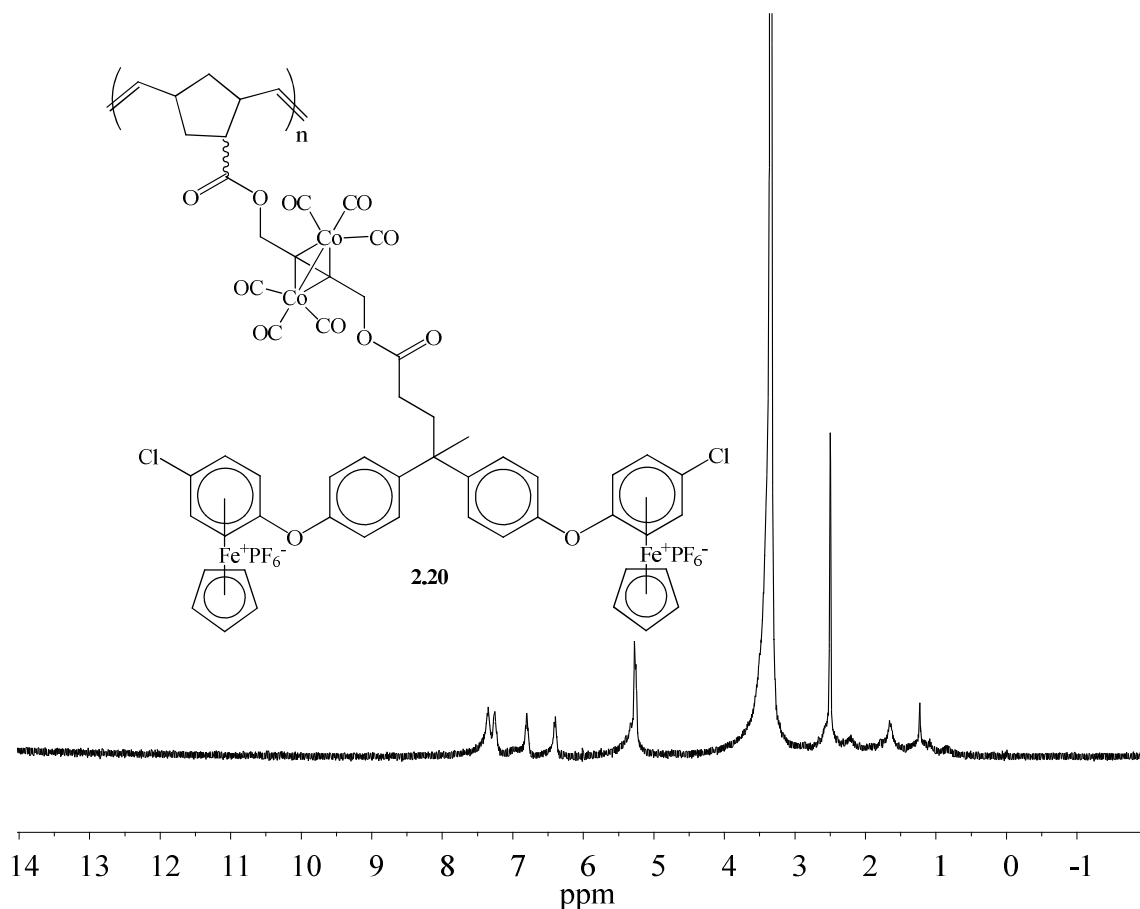
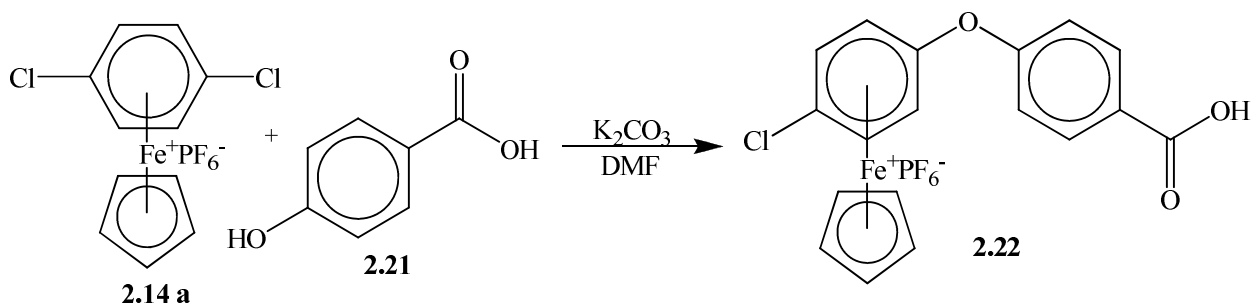


Figure 2.27: ^1H NMR of polymer **2.20** in $\text{DMSO-}d_6$.

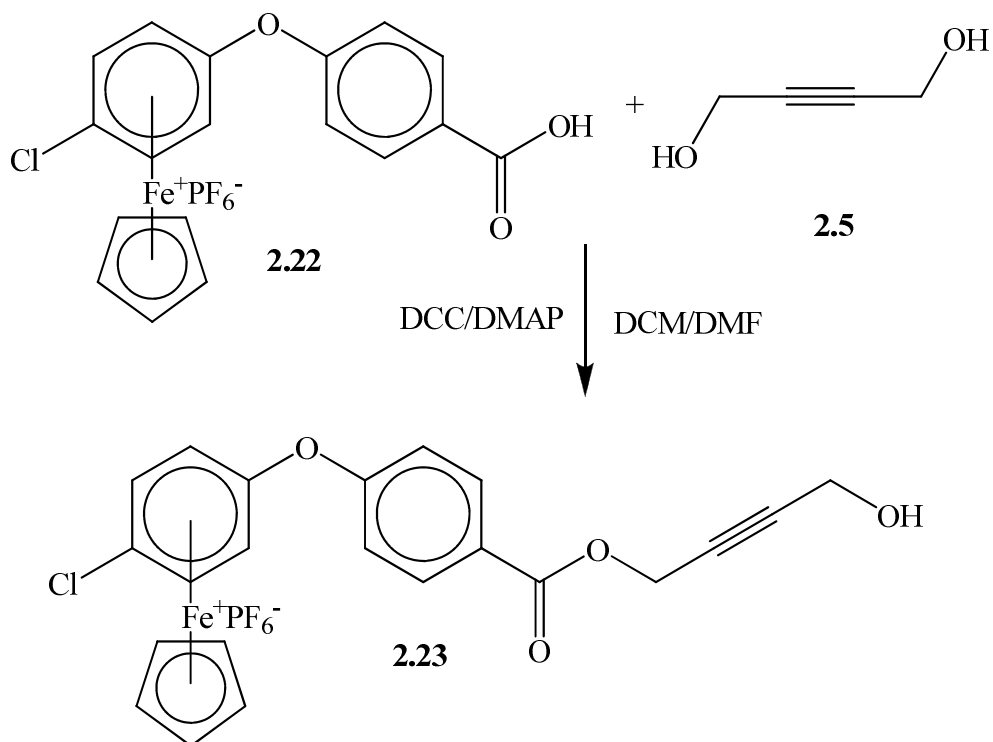
2.3.3 Synthesis of a norbornene monomer containing a single η^6 -arene- η^5 -cyclopentadienyliron(II) moiety and cobalt carbonyl

In an effort to synthesize a monomer which contained a single η^6 -arene- η^5 -cyclopentadienyliron(II) hexafluorophosphate moiety, complex **2.14 a** was reacted with 4-hydroxybenzoic acid (**2.21**). Complex **2.22** was synthesized through modification to previously published procedures (Scheme 2.13).⁵⁰ Previously, this reaction was done in a THF/DMF solvent mixture at an elevated temperature (60 °C) for 16 hours. However this reaction works quite well at room temperature in pure DMF for 18 hours. Keeping the temperature between 20-25 °C is very important to the success of the reaction because higher temperatures lead to partial disubstitution of the arene and decreased temperatures can lead to a mixture of starting material and product.



Scheme 2.13: Synthesis of complex **2.22**.

As in the previous sections, the 2-butyne-1,4-diol (**2.5**) was reacted with complex **2.22** through a Steglich esterification reaction (Scheme 2.14). By using a very large excess of the diol (**2.5**) it is possible to make complex **2.23** which has a terminal alcohol. After purification, complex **2.23** was isolated as a yellow solid.



Scheme 2.14: Synthesis of complex **2.23**.

The ^1H NMR spectrum of complex **2.23** is consistent with the proposed structure (Figure 2.28). The non-complexed arene resonances appear as doublets at 8.17 and 7.46 ppm, while the complexed arene resonances are at 6.84 and 6.61 ppm. The cyclopentadiene resonance appears as a singlet at 5.39 ppm and the two methylene resonances are at 5.01 and 4.26 ppm. The ^1H NMR spectrum shows evidence of a second complex, with two very low intensity doublets at 7.7 and 7.4 ppm, as well as a second low intensity cyclopentadiene just slightly upfield of the complex **2.23** cyclopentadiene at 5.38 ppm. This slight impurity is most likely some residual starting material (**2.22**).

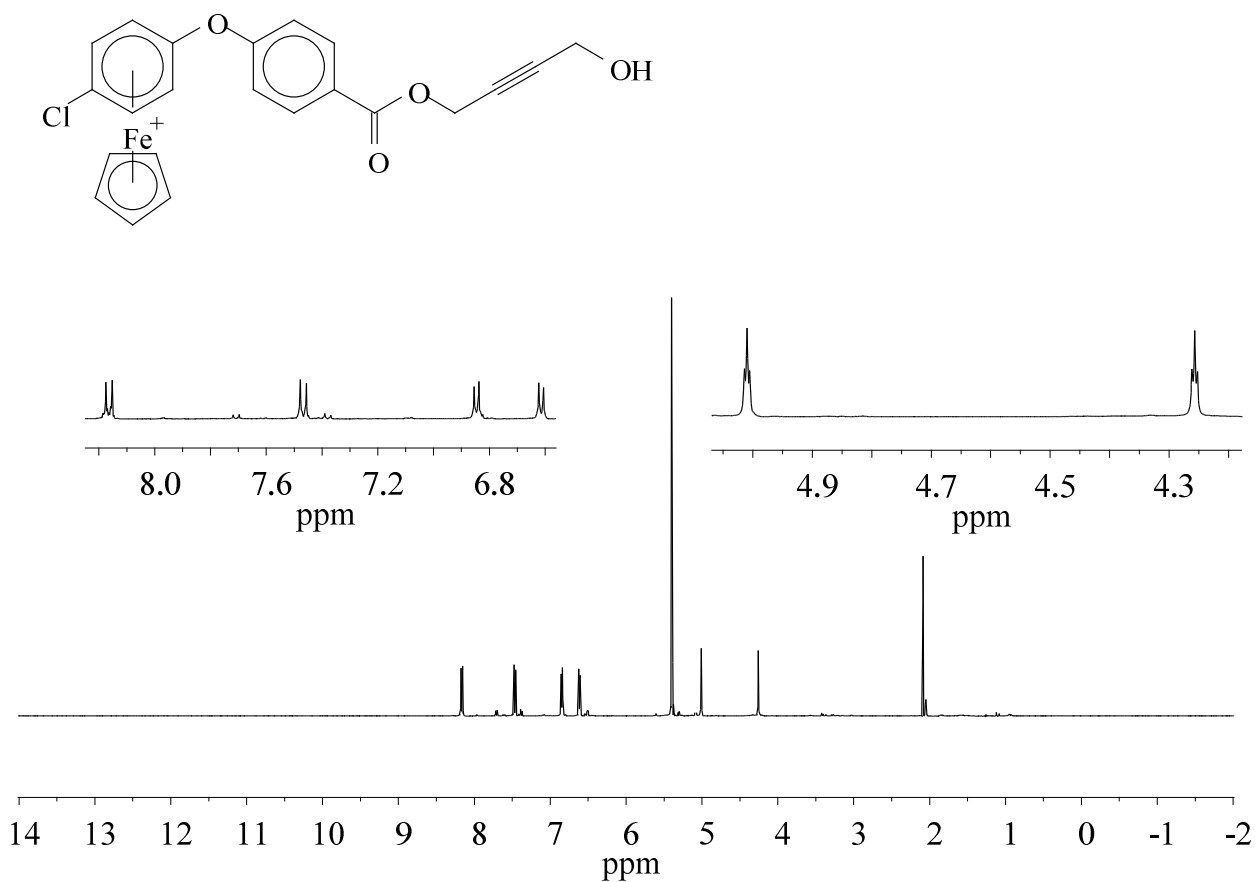


Figure 2.28: ^1H NMR spectrum of complex **2.23** in acetone- d_6 .

The ^{13}C NMR spectrum also confirms the expected structure (Figure 2.29). The carbonyl carbon resonance is visible at 165.51 ppm. There are four resonances for the non complexed arene at 158.95, 133.52, 128.74 and 121.55 ppm. The four resonances for the complexed arene, which are shielded by the iron, appear at 132.66, 105.83, 88.41 and 79.03 ppm. The two resonances for the alkyne carbons appear at 87.55 and 79.43 ppm while the CH_2 resonances can be seen at 53.89 and 50.81 ppm. As in the ^1H NMR spectrum, the ^{13}C NMR spectrum also shows evidence of a second organoiron complex (**2.22**). The low intensity residual starting material resonances appear at 131.19, 121.37, 88.30, 81.01 and 78.14.

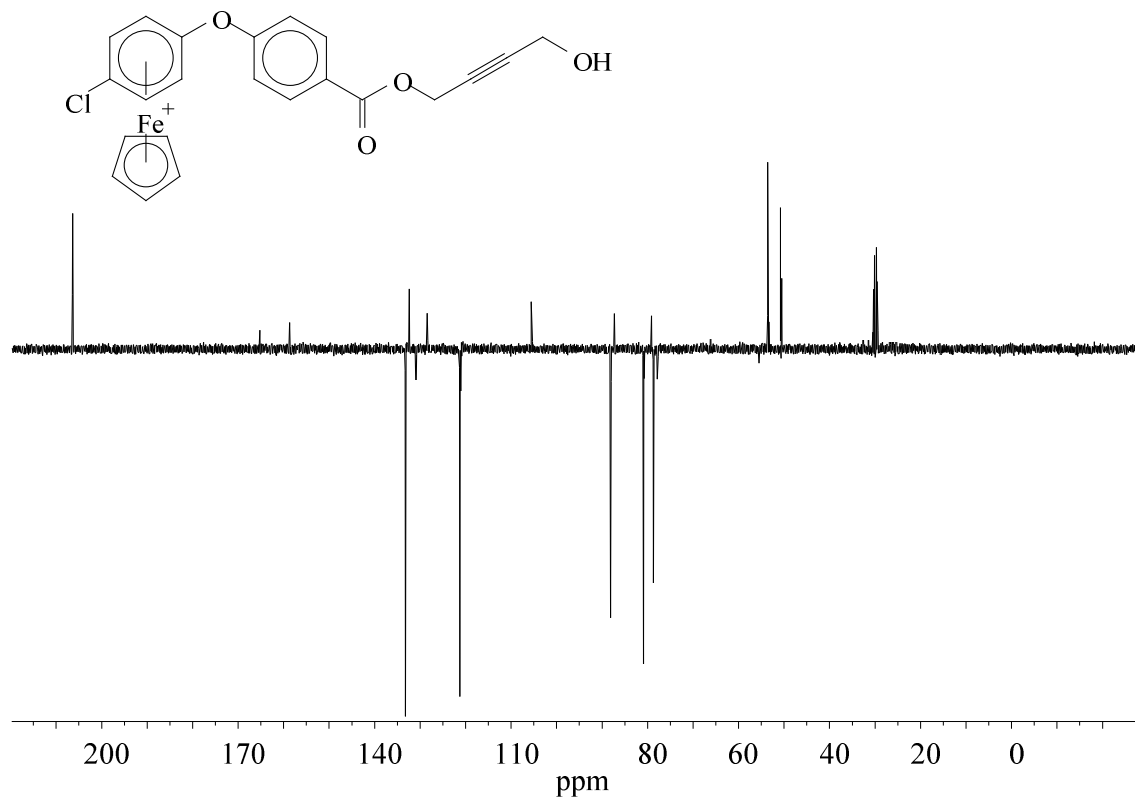
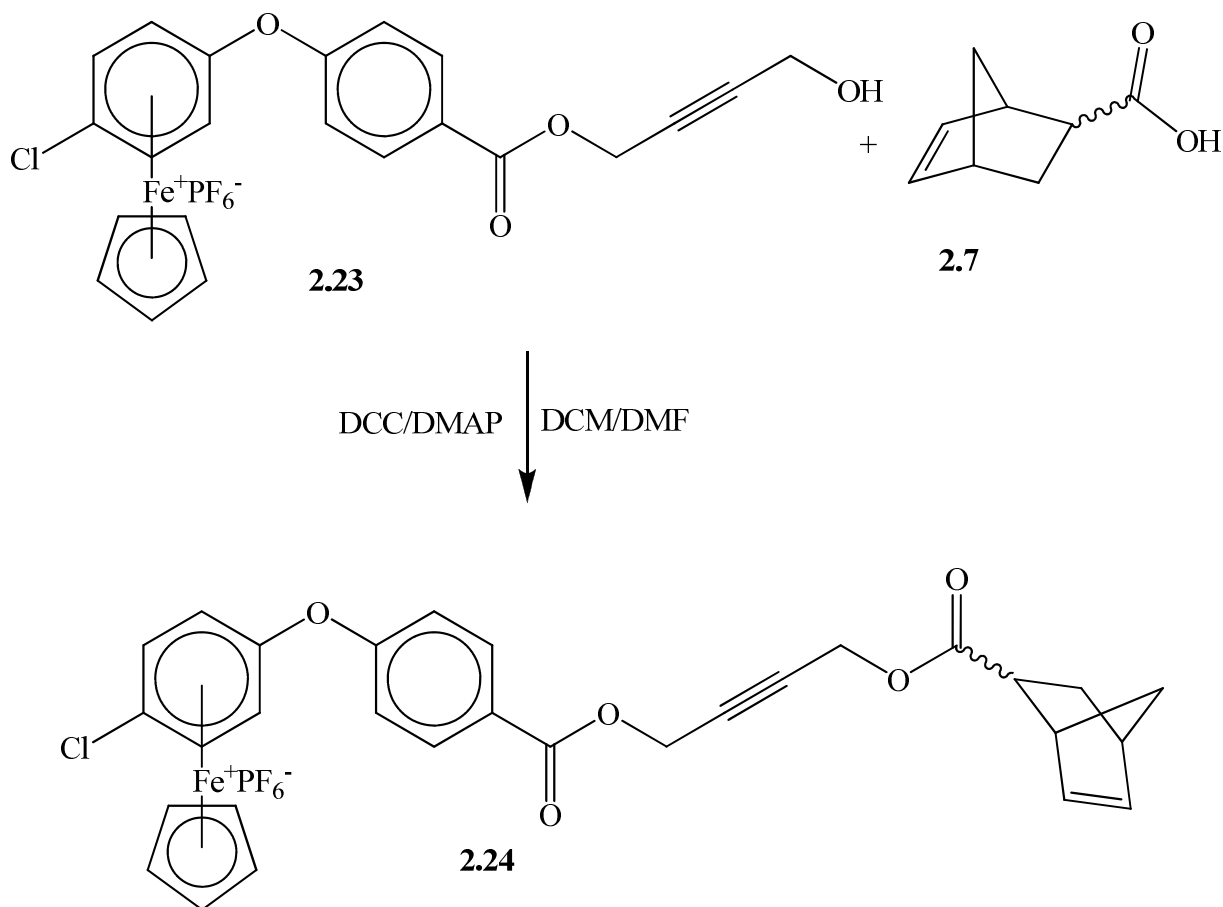


Figure 2.29: APT ^{13}C NMR spectrum of complex **2.23** in acetone- d_6 .

Attempts to further purify complex **2.23** were hampered by the presence of the η^6 -chloroarene- η^5 -cyclopentadienyliron(II) hexafluorophosphate moiety in both of the complexes. Chromatography was unsuccessful as no solvent system could be found which would separate the complex from the impurity using either neutral alumina or silica as the solid phase. Indeed, both silica and alumina decomposed the sample.

The reaction between complex **2.23** and 5-norbornene-2-carboxylic acid (**2.7**) (Scheme 2.15) gave a yellow solid (complex **2.24**) which showed the same solubilities as its precursor (**2.23**). NMR and IR spectroscopies were used to determine if complex **2.24** was successfully synthesized.



Scheme 2.15: Synthesis of complex **2.24**.

The ^1H NMR spectrum for complex **2.24** can be viewed in Figure 2.30. The ^1H NMR shows the appearance of the *endo* and *exo* norbornene peaks. The most easily identified norbornene resonances are the alkene hydrogens which can be seen at 6.18-5.90 ppm. While the ester formation is confirmed by the shift from 4.26 ppm (in complex **2.23**) to ~4.75 ppm (in complex **2.24**) for the methylene resonances. It is important to note that the same coupling pattern (ddt) can be seen for the *endo* methylene resonances of complex **2.24** as was seen for complex **2.8** and **2.18**. The integration of this particular set of methylene peaks shows that the complex was isolated as 65% *endo* and 35% *exo*. There are two impurities that need to be mentioned, water and diethyl ether. The water causes the multiplet at 3.23-2.88 ppm integrates for five protons rather than the expected three and the ether is clearly visible at 1.1 and 3.4 ppm.

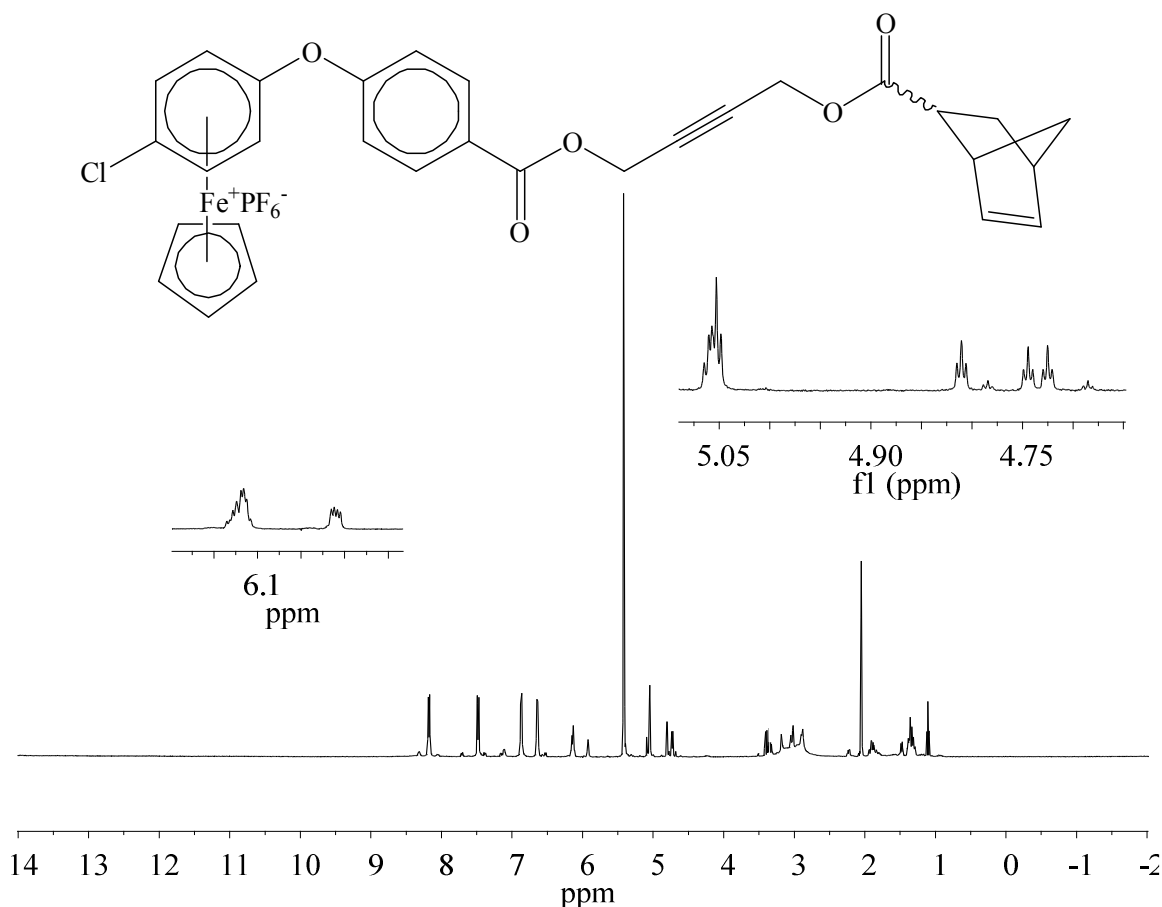
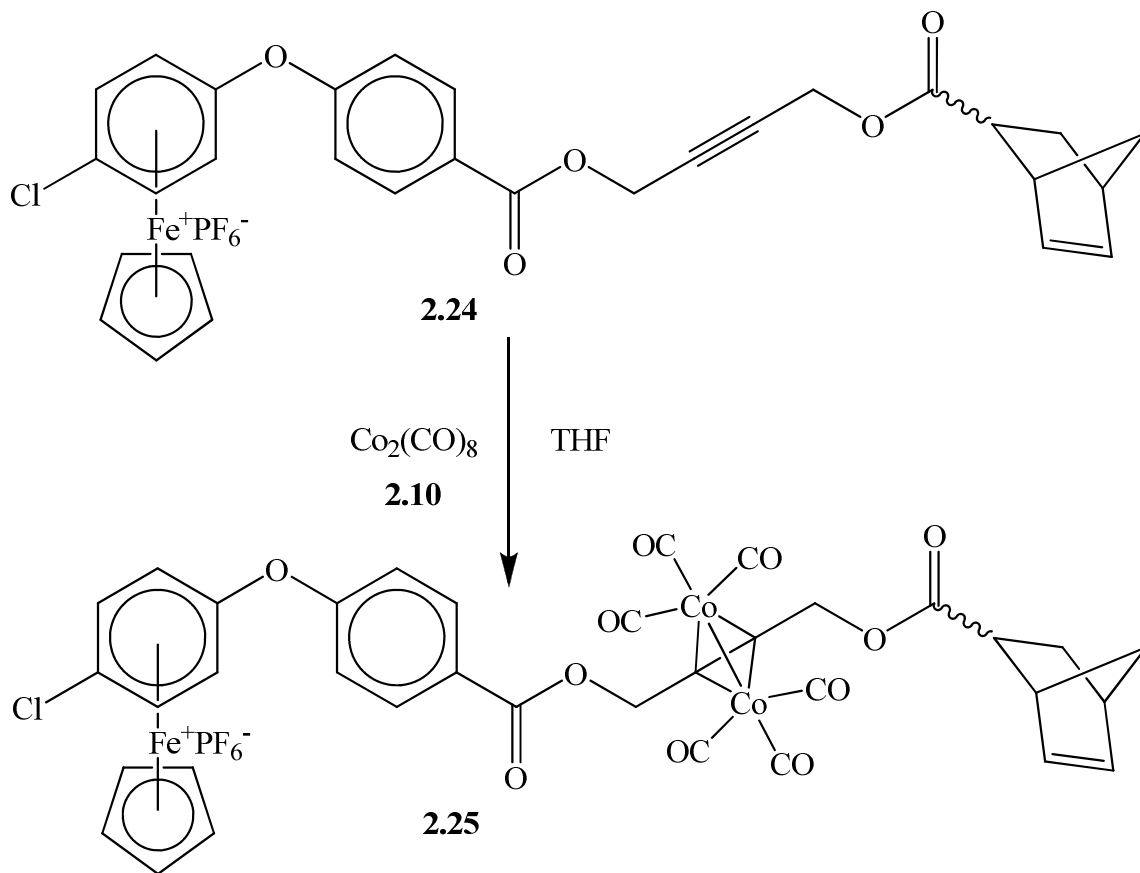


Figure 2.30: ^1H NMR spectrum of complex **2.24** in acetone- d_6 .

The ^{13}C NMR spectrum also shows incorporation of the norbornene moiety. The methylene resonance shifted from 50.81 ppm when it was next to an alcohol to 52.51 and 52.10 ppm (*endo* and *exo*) with the formation of the ester linkage. In this spectrum the resonances of the norbornene and alkyne part of the complex show up at almost the same chemical shift as they did for complexes **2.8** and **2.18**. While the rest of the molecule appears very similar to the starting material **2.23** and the impurity persisted in this spectrum as well. As with complexes **2.8** and **2.18**, the different *exo* and *endo* peaks are less apparent for the carbons more distant from the norbornene. Unlike the ^1H NMR of this compound, the ether did not show up in the ^{13}C



Scheme 2.16: Synthesis of complex **2.25**.

The ^1H NMR spectrum for complex **2.25** shows the downfield shift of the CH_2 resonances from 5.05 and 4.75 ppm (complex **2.24**) to between 5.40-6.00 ppm (complex **2.25**) where some of the resonances overlap with the cyclopentadiene resonance at 5.64 (Figure 2.32). This shift is also seen for the carbon atoms of the methylenes have shifted downfield by approximately 10 ppm (Figure 2.33). It is interesting to note that the broadened resonance of the $\text{CoC}\equiv\text{O}$ carbons at 199 ppm and the broadened alkyne resonances at approximately 91 ppm are visible for this complex.

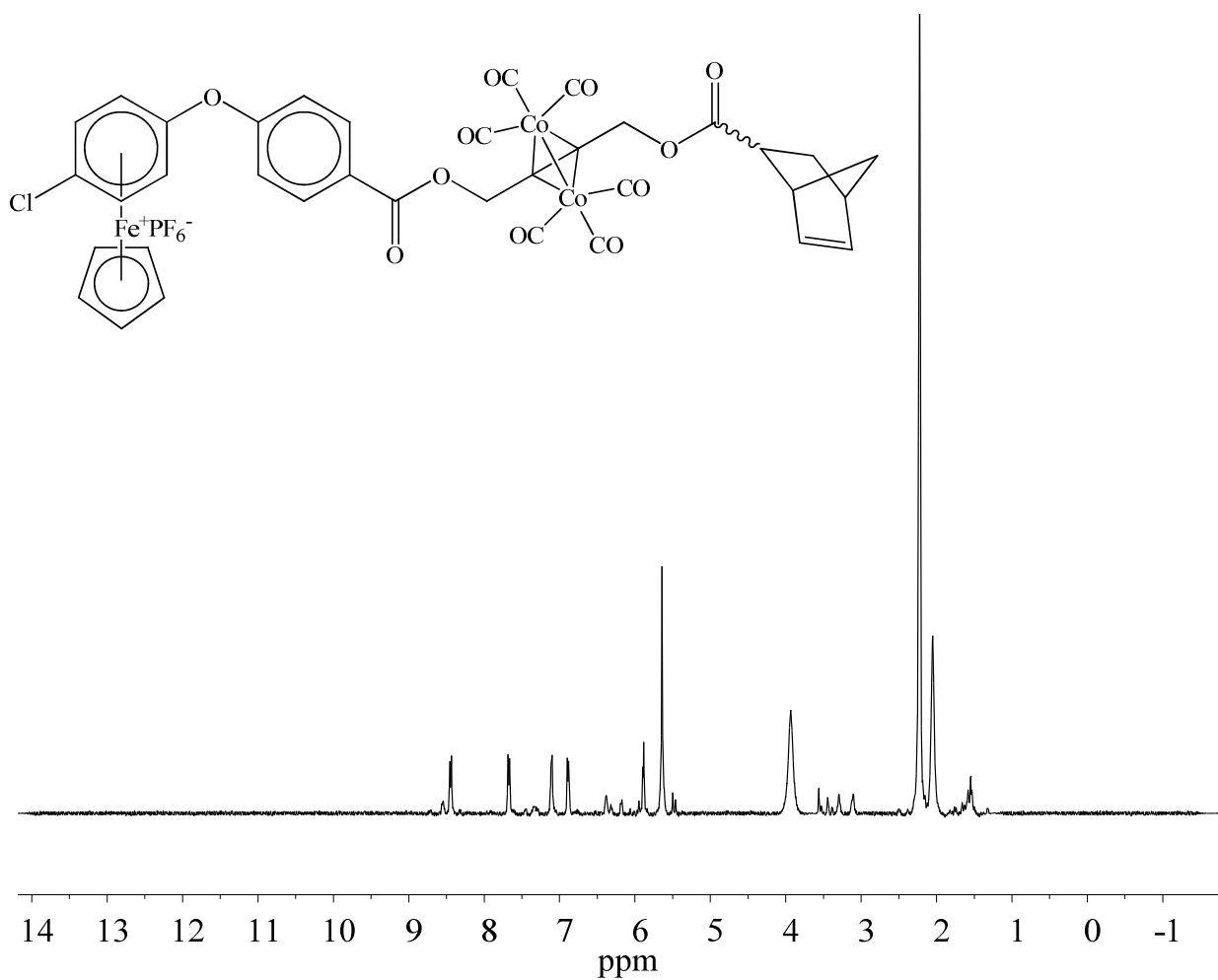


Figure 2.32: ^1H NMR spectrum of complex **2.25** in acetone- d_6 .

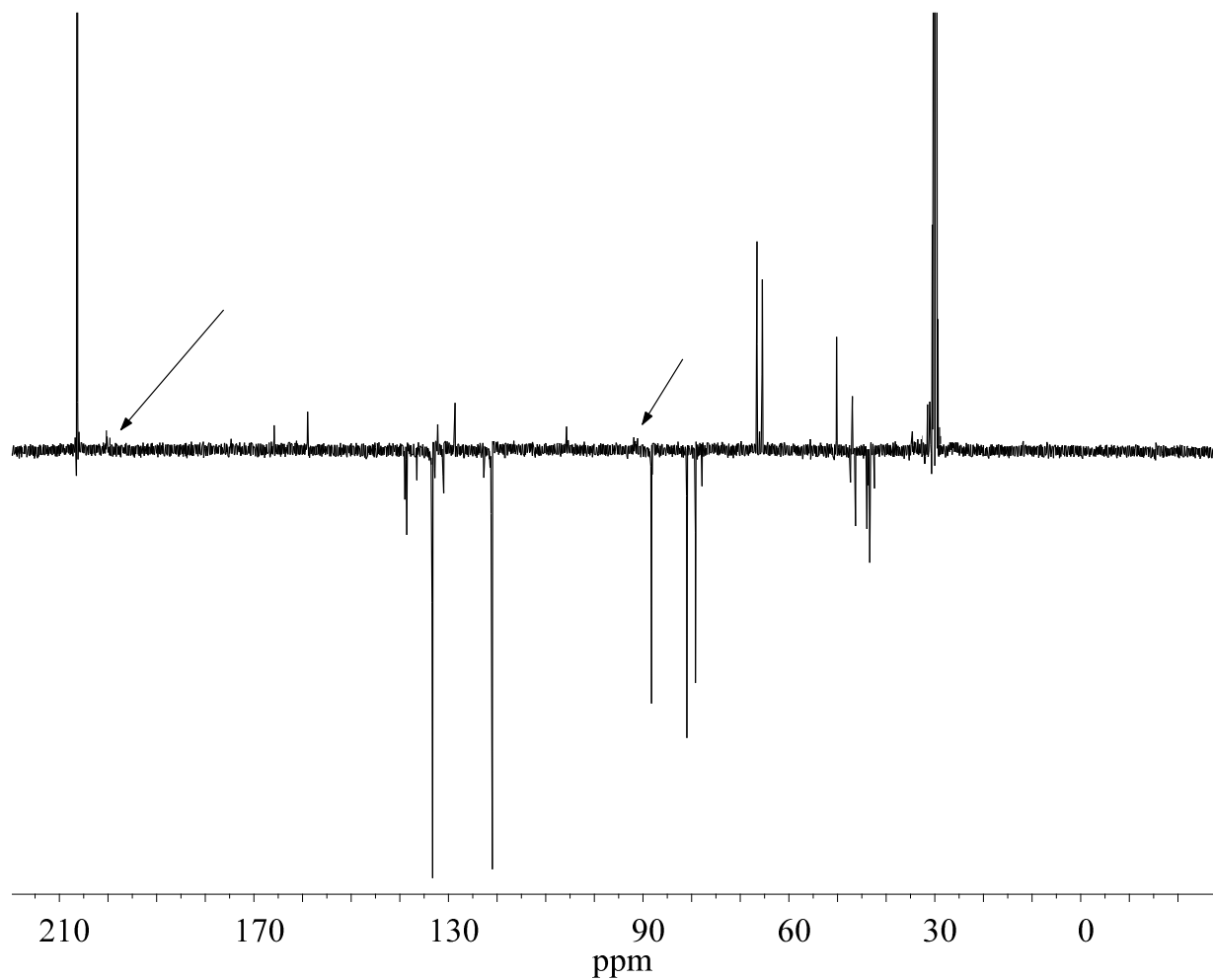
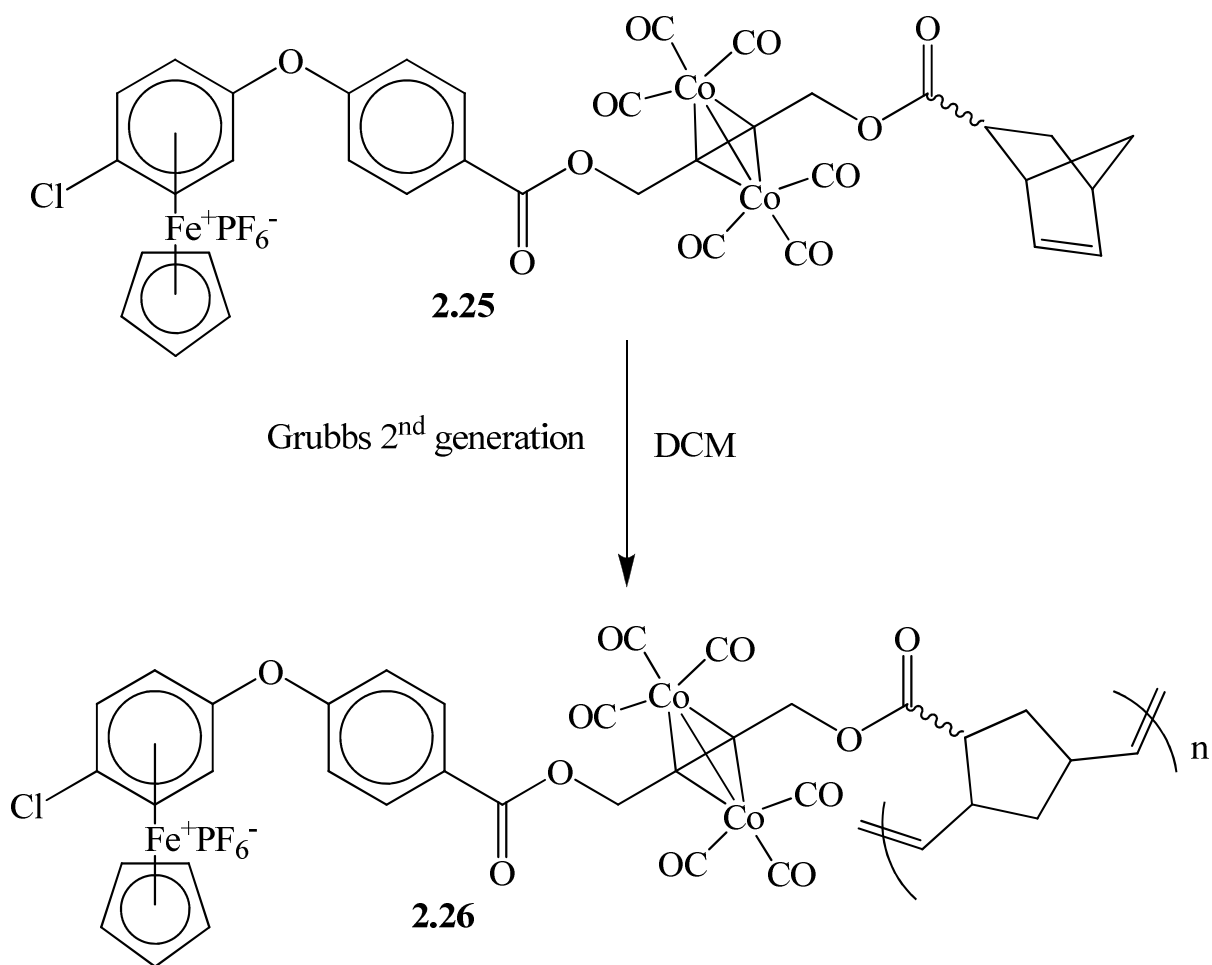


Figure 2.33: APT ¹³C NMR spectrum of complex **2.25** in acetone-*d*₆. Arrows indicate the broadened resonances of the carbon atoms coordinated to cobalt.

2.3.4 Polymerization of norbornene monomer containing a single η^6 -arene- η^5 -cyclopentadienyliron(II) moiety and cobalt carbonyl

Polymerization of complex **2.25** using Grubbs' second generation catalyst was done using the same procedures as for the polymerization of the ferrocene containing complex (**2.11**)

(Scheme 2.17). Unfortunately, polymer **2.26** proved to be either insoluble or only slightly soluble in most common laboratory solvents including acetone, DCM, acetonitrile, chloroform, THF and DMSO. In fact, the only solvent that it showed any appreciable solubility was DMF. Due to the insolubility of this complex no useful NMR spectra could be obtained, however IR did show the continued presence of the cobalt carbonyl bands.



Scheme 2.17: Synthesis of polymer **2.26**.

2.4 Molecular weight determination of polymers

The molecular weight of the ferrocene based polymer **2.12** could be determined using GPC, however the η^6 -arene- η^5 -cyclopentadienyliron(II) hexafluorophosphate moiety is not

compatible with the HPLC column. It was therefore necessary to cleave the cyclopentadienyliron hexafluorophosphate salts from the polymers **2.20** and **2.26** to form their iron free analogues. This was accomplished by dissolving the polymers in a mixture of DMF and acetonitrile (75:25) and irradiating the sample with 300 nm light. The soluble portions of these polymers were then dissolved in THF and analyzed using GPC to give their molecular weight data. The molecular weight of the polymers, before irradiation, was then calculated to give the values presented in Table 2.1. Unfortunately the iron free analogue of polymer **2.26** was completely insoluble in THF, so no molecular weight data could be obtained.

Table 2.1: Molecular weight data for polymers

Polymer	Catalyst : monomer	\overline{M}_w	\overline{M}_n	PDI
2.12	1:50	49 500	39 600	1.2
2.20*	1:50	55 300	29 800	1.9

* The molecular weights of the polymers are estimated from molecular weights of the soluble portions of their analogs after removal of the cationic cyclopentadienyliron moieties.

2.5 Thermal analysis of polymers

Thermogravimetric analysis of the polymers indicated the the polymers were thermally stable to 125 °C and had 3-4 main degradative steps (Table 2.2). Polymer **2.12** had four degradative steps, the first one was probably due to the loss of the COs off the cobalt, while the second step was likely due to the loss of the ester. The third degradative step for polymer **2.12** was from 419-472 °C and is the degradation of the ferrocene and the final degradative step from 480-1000 °C would be due to the slow breakdown of the polymer backbone. For the other two

polymers, **2.20** and **2.26**, the first degradative step which occurred between 125-160 °C, was likely due to the evolution of the CO groups from the alkyne cobalt carbonyl moieties. This loss of the CO groups from the cobalt occurred at a lower temperature for the cationic organoiron polymers (**2.20** and **2.26**) as compared to the polymers which contained ferrocene (**2.12**). This difference may be due to destabilization of the cobalt complexes due to the η^6 -aryl- η^5 -cyclopentadienyliron(II) hexafluorophosphate salts or could be an effect of the higher molecular weight of the ferrocene polymer. The second degradative step for each polymer occurred from 220-240 °C and was due to the breakdown of the the cyclopentadiene moieties. For polymer **2.20** the third step (417-464 °C) is likely due to the breakdown of the the ester groups while the fourth step (575-802 °C) represents the breakdown of the polymer backbone. For polymer **2.26** the esters and the backbone both degrade in 3rd step (382-472 °C).

Table 2.2: Thermogravimetric analysis of polynorbornenes.

Polymer	Step 1	Step 2	Step 3	Step 4
2.12	176-218 °C, 33 %	330-360 °C, 10 %	419-472 °C, 8 %	480-1000 °C, %
2.20	127-148 °C, 8 %	223-232 °C, 11 %	382-472 °C, 57 %	
2.26	132-158 °C, 6 %	221-242 °C, 14 %	417-464 °C, 12 %	575-802 °C, 26 %

Differential scanning calorimetry of each polymer indicated that the glass transition temperatures for polymers **2.12** and **2.26** was 61 and 63 °C respectively, while a glass transition temperature could not be found for polymer **2.20** (Table 2.3). Above the glass transition temperature polymer chains can slide past each other when a force is applied. It is therefore important to know the glass transition temperature of polymers as it gives information about the

processability and thermal stability of the polymers. For each of the polymers the glass transition temperature changed after the CO had been thermally driven off. For example, in the DSC of polymer **2.26**, the evolution of the CO from the polymer was observed from 120-150 °C. A second DSC scan of polymer **2.26** revealed a higher T_g by over 20 °C. This was also seen for polymers **2.12** and **2.20**, where the glass transition temperatures were found to be 82 and 84 °C respectively, after loss of the CO.

Table 2.3: Differential scanning calorimetry of polynorbornenes.

Polymer	T_g	T_g^*
2.12	61 °C	92 °C
2.20	63 °C	84 °C
2.26	Not found.	82 °C

T_g^* was taken from a second run, after the CO groups had been removed.

2.6 Cyclic voltammetry of norbornene complexes

Since ferrocene, η^6 -benzene- η^5 -cyclopentadienyliron and alkyne-cobalt carbonyl complexes are known to possess electrochemical behaviour, we used cyclic voltammetry to determine if this would be evident in our structures (Table 2.4). Cyclic voltammetric studies were done on the norbornene complexes, but due to solubility issues were not done on polymers. The cyclic voltammogram of complex **2.8** displayed an $E_{1/2} = 0.69$ V corresponding to the reversible oxidation of the ferrocene moiety to a ferrocinium ion moiety. When complex **2.11** was investigated, both the reversible oxidation of the ferrocene and the irreversible reduction of the cobalt was also seen $E_{1/2} = 0.71$ V (ferrocene) and $E_{p,c} = -0.97$ V (cobalt). The cyclic

voltammogram of complexes **2.18** and **2.24** displayed a reversible redox couples at $E_{1/2} = -1.55$ V and $E_{1/2} = -1.27$ V respectively, due to the reduction of the cationic η^6 -benzene- η^5 -cyclopentadienyliron 18 electron moieties to the neutral 19 e- moieties. The irreversible reduction of the cobalt was seen for complex **2.19** $E_{p,c} = -1.28$ V; however, for complex **2.25** the cobalt reduction overlapped with the redox couple of the cationic η^6 -benzene- η^5 -cyclopentadienyliron moiety. Two cobalt reduction waves were observed by Arewgoda *et al.* for smaller alkyne-cobalt carbonyl complexes which ranged from -0.82 V to -1.8 V. {{377 Arewgoda, M. 1982}} However, only one reduction wave was observed for for the alkyne-cobalt carbonyl complexes presented here, this may be due to differences in experimental procedure such as solvent and temperature.

Table 2.4: Cyclic voltammetric studies of norbornene complexes.

Complex	1 st $E_{1/2}$	2 nd $E_{1/2}$	$E_{p,c}$
2.8	+ 0.69		
2.11	+ 0.71	-0.97	
2.18	- 1.55		
2.19	- 1.51		- 1.28
2.24	- 1.27		
2.25	- 1.30		

2.7 Summary

A number of neutral and cationic organoiron based norbornene compounds were prepared through esterification with 2-butyne-1,4-diol. The presence of alkyne moieties in these

complexes allowed for the generation of mixed organoiron/cobalt norbornene monomers through reaction with dicobalt octacarbonyl. The monomers displayed varying electrochemical properties based on the type of organoiron groups present. The monomer containing ferrocene showed reversible oxidation at $E_{1/2} = + 0.71 \text{ V}$; the monomers containing cationic cyclopentadienyliron moieties displayed a reversible reduction between -1.28 and -1.55 V . The cobalt moieties in these monomers displayed a reduction at -1.30 V , which was reversible for the ferrocene monomer $E_{1/2} = -0.97 \text{ V}$. The monomers underwent ROMP in the presence of Grubbs' 2nd generation catalyst to give polynorbornenes containing organoiron and organocobalt moieties in their side chains. The soluble portions of the polymers possessed \overline{M}_w between 49 500 and 55 300 with PDIs between 1.2 and 1.9. The molecular weights of the cationic organoiron polymers were determined from the soluble portions of demetallated samples resulting in lower reported molecular weights. Thermal analysis of the polymers showed that the cobalt units decomposed between $125 \text{ }^\circ\text{C}$ and $220 \text{ }^\circ\text{C}$; the cationic cyclopentadienyliron moieties decomposed between $220 \text{ }^\circ\text{C}$ and $245 \text{ }^\circ\text{C}$. The backbones of the polymers decomposed between $380 \text{ }^\circ\text{C}$ and $1000 \text{ }^\circ\text{C}$. Differential scanning calorimetry showed that the polymers **2.12** and **2.26** possessed T_g s of $61 \text{ }^\circ\text{C}$ and $63 \text{ }^\circ\text{C}$ respectively; interestingly, when the samples were heated above $150 \text{ }^\circ\text{C}$ and allowed to cool and scanned again the T_g s shifted to higher temperatures ($92 \text{ }^\circ\text{C}$ and $84 \text{ }^\circ\text{C}$ respectively) presumably due to the decomposition of the cobalt carbonyl moieties. For polymer **2.20** a T_g of $82 \text{ }^\circ\text{C}$ was only found for after the cobalt carbonyl decomposed. This shift in the glass transition temperature may prove useful in manufacturing as it allows for the control of glass transition post manufacturing.

2.8 Detailed experimental

All reactions and complexes containing a η^6 -aryl- η^5 -cyclopentadienyl iron hexafluorophosphate moiety were kept in the dark to prevent decomposition.

Synthesis of acetylferrocene (2.3)⁷

Ferrocene (18.16 g, 100 mmol) (2.1), acetic anhydride (53.75 mL, 570 mmol) (2.2), and 4 mL of phosphoric acid were stirred under nitrogen at 100 °C for 20 minutes. This reaction mixture was then poured into 100 mL of ice and neutralized with the addition of potassium carbonate (~40 g). An orange precipitate was filtered out of the solution and dried before purification by column chromatography on silica using hexanes to remove residual ferrocene followed by diethyl ether to elute the product. (14.98 g, 66 % yield)

¹H NMR (400 MHz, acetone-*d*₆) δ = 4.77 (NFO t, 2H), 4.52 (NFO t, 2H), 4.22 (s, 5H), 2.35 (s, 3H).

Synthesis of carboxylic acid ferrocene (2.4)⁷

Acetyl ferrocene (2.3) (5.47 g, 24 mmol), iodine (6.34 g, 25 mmol) and 11 mL of pyridine were stirred for 15 hours under nitrogen. The reaction was then heated to 100 °C until the solution became viscous (35 minutes) followed by the addition of 180 mL of 0.6 M NaOH. This mixture was then allowed to stir overnight exposed to the atmosphere. The reaction mixture was gravity filtered and glacial acetic acid was added to the filtrate until a orange precipitate was formed. The product was then collected by vacuum filtration as a orange powder that was rinsed with water. 2.56 g, 46 %

¹H NMR (400 MHz, acetone-*d*₆) δ = 4.75 (NFO t, 2H), 4.42 (NFO t, 2H), 4.21 (s, 5H).

Synthesis of compound 2.6

Carboxylic ferrocene (**2.4**) (2.4305 g, 9.7 mmol), 2-butyne-1,4-diol (**2.5**) (4.1709 g, 48 mmol), DCC (2.2515 g, 10.9 mmol), DMAP (1.3090 g, 10.7 mmol), 25 mL DCM and 5 mL DMF were stirred under nitrogen for 5 hours. The reaction was then cooled to -10 °C and a fine white precipitate of DCU and excess 2-butyne-1,4-diol were filtered out of the solution. The filtrate was diluted with 150 mL of DCM, washed with 200 mL of 1.2 M HCl solution, dried with MgSO₄ and the DCM was removed *in vacuo* leaving a dark red liquid that was purified using silica chromatography using ether:hexanes 6:4 as the eluent. The solvent mixture was removed *in vacuo* leaving an orange-red solid with a 2.1891 g yield (71 % yield). Crystals suitable for X-ray crystallography were grown from ether/hexanes solvent mixture (60/30).

¹H NMR (400 MHz, acetone-*d*₆) δ = 4.86 (t, *J*=1.8, 2H), 4.79 (NFO t, 2H), 4.48 (NFO t, 2H), 4.29 – 4.20 (m, 7H). ¹H NMR (400 MHz, CDCl₃) δ = 4.84 (t, *J*=1.8, 2H), 4.82 (NFO t, 2H), 4.41 (NFO t, 2H), 4.30-4.33 (dt, *J*=6.2, 1.8, 2H), 4.22 (s, 5H), 1.82 (t, *J*=6.2, 1H).

¹³C NMR (100 MHz, CDCl₃) δ = 171.43, 84.79, 80.95, 71.86, 70.52, 70.09, 52.09, 51.35.

IR 1706 cm⁻¹ (-C=O), 3400 cm⁻¹ (-O-H).

Synthesis of compound 2.7 *exo*⁵¹

In order to fully identify and understand the complexity of the *endo-exo* mixtures of compounds containing norbornene, the pure 5-norbornene-*exo*-2-carboxylic acid (**2.7 *exo***) was synthesized according to published procedures.⁵¹

¹H NMR (400 MHz, CDCl₃) δ = 6.15-6.11 (m, 2 H), 3.09 (s, 1 H), 2.92 (s, 1 H), 2.27-2.22 (m, 1 H), 1.93 (dt, *J*=11.8, 3.9, 1 H), 1.52 (d, *J*=10.1, 1 H), 1.42-1.35 (m, 2 H).

Synthesis of compound 2.8 and 2.8 *exo*

Compound **2.6** (1.8276 g, 6.1 mmol), 5-norbornene-2-carboxylic acid (**2.7** or **2.7 *exo***) (0.85 mL, 6.9 mmol), DCC (1.4209 g, 6.9 mmol), DMAP (0.7932 g, 6.5 mmol), 15 mL DCM and 3 mL of DMF were stirred under nitrogen for 5 hours. The reaction was then cooled to -10 °C and a fine white precipitate of DCU was filtered out of the solution. The filtrate was diluted with 150 mL of DCM, washed with 200 mL of 1.2 M HCl solution, dried with MgSO₄ and the DCM was removed *in vacuo* leaving an orange solid that was purified using silica chromatography using ether:hexanes 6:4 as the eluent. The solvent mixture was removed *in vacuo* leaving an orange solid.

2.8 2.0110 g yield (79 % yield).

¹H NMR (400 MHz, acetone-*d*₆) δ = 6.23-5.86 (m, 2H), 4.89 (dt, *J*=3.0, 1.9, 2H), 4.80 (NFO t, 2H), 4.72 (ddt, *J*= 20.3, 15.9, 1.9, 2H), 4.48 (NFO t, 2H), 4.27 (s, 5H), 3.18 (s, 1H) 3.05-2.94 (m, 1H), 2.88 (s, 1H) 2.25-2.16 (m, 0H), 1.94-1.83 (m, 1H), 1.48 (d, *J*=8.3 0H), 1.42-1.25 (m, 4H).

¹³C NMR (101 MHz, acetone-*d*₆) δ = 175.01, 173.88, 170.93, 138.83, 138.44, 136.50, 133.16, 82.43, 82.20, 81.58, 81.44, 72.49, 71.0, 70.98, 70.68, 52.63, 52.25, 52.02, 50.12, 47.35, 46.86, 46.53, 43.69, 43.50, 43.37, 42.40, 30.95, 29.69.

IR 1710 cm⁻¹ (C=O).

2.8 *exo* (85% yield)

¹H NMR (400 MHz, acetone-*d*₆) δ = 6.19 – 6.05 (m, 2H), 4.90 (NFO t, 2H), 4.80 (t, *J*=1.7, 4H), 4.49 (NFO t, 2H), 4.27 (s, 5H), 3.04-2.75 (m, 3H), 2.21 (dd, *J*=9.6, 3.7, 1H), 1.93 – 1.82 (m, 1H), 1.48 (d, *J*=8.3, 1H), 1.41-1.23 (m, 2H).

Synthesis of complex 2.9

Complex **2.8** (0.8376 g, 2 mmol) dissolved in 1 mL of DCM was stirred under N₂ while Grubbs' 2nd generation catalyst (0.01709 g, 0.02 mmol in 1 mL DCM) was added to the mixture. After 30 min the reaction mixture turned viscous and the reaction was quenched with the addition of ethylvinyl ether (1 mmol). The orange red compound, which had a jelly like appearance, was washed with acetone and dried in a crucible. The yield appeared to be over 100% possibly due to solvent molecules being trapped in the cross linked polymer. 0.8543 g, 102 % yield.

Synthesis of complexes 2.11 and 2.11 *exo*

Under N₂, 0.8369 g (2 mmol) of complex **2.8** was dissolved in 10 mL dry THF and stirred. When 0.8442 g (2.5 mmol) of Co₂(CO)₈ (**2.10**) was added to the stirring solution CO_(g) was evolved. This evolution of gas lasted for 20 min. To ensure that the reaction went to completion the reaction was allowed to continue stirring, under N₂, for an additional 15 hours. The solvent was then removed *in vacuo* leaving a red film which was dissolved in 20 mL of acetone. After 1 hour of being exposed to the atmosphere, a fine precipitate formed which was filtered out of the solution through Celite. The filtrate was collected and the solvent removed *in vacuo* leaving 1.2670 g of the pure complex (**2.11**).

2.11 1.2670 g yield (90 % yield).

¹H NMR (400 MHz, acetone-*d*₆) δ = 6.23 – 5.93 (m, 2H), 5.53 – 5.39 (m, 4H), 4.84 (NFO t, 2H), 4.49 (NFO t, 2H), 4.25 (s, 5H), 3.25 (s, 1H), 3.10 (dt, *J*=9.3, 4.0, 1H), 2.90 (s, 1H), 2.33 – 2.28 (m, 0H), 2.00-1.89 (m, 1H), 1.59 – 1.26 (m, 3H).

^{13}C NMR (101 MHz, acetone- d_6) δ = 174.61, 171.72, 138.92, 138.55, 136.52, 133.39, 91.85, 72.39, 71.83, 70.97, 70.63, 65.79, 65.76, 65.56, 65.45, 50.20, 47.34, 46.99, 46.33, 44.00, 43.72, 43.37, 42.43.

IR 2106 cm^{-1} , 2067 cm^{-1} and 2040 cm^{-1} (CoC \equiv O) 1718 cm^{-1} (C=O).

2.11 *exo* (92 %)

^1H NMR (400 MHz, acetone- d_6) δ = 6.14 (m, 2H), [5.50 (s), 5.49 (d, $J=14.3$), 5.43 (d, $J=14.3$), 4H], 4.85 (NFO t, 2H), 4.50 (NFO t, 2H), 4.25 (s, 5H), 3.10 (s, 1H), 2.92 (s, 1H), 2.30 (d, $J=8.5$, 1H), 1.99 – 1.72 (m, 1H), 1.56 (d, $J=8.3$, 1H), 1.46 – 1.06 (m, 3H).

Synthesis of polymer 2.12

Under N_2 , complex **2.11** (1.0565 g, 1.5 mmol) was dissolved in 1 mL of DCM and stirred, Grubbs' 2nd generation catalyst (0.0257 g 0.03 mmol) dissolved in 1.4 mL of DCM was then added. After 30 min. 5 mL of methanol was added causing the polymer to precipitate out of solution. The precipitate was collected and triturated with DCM and diethyl ether to remove the lower molecular weight polymers and monomer leaving 0.9972 g of red solid.

^1H NMR (400 MHz, CDCl_3) δ = 5.48-5.06 (m, 6H), 4.82 (s, 2H), 4.39 (s, 2H), 4.18 (s, 5H), 3.16 (br. s, 1H), 2.95 (br. s, 1H), 2.80 (br. s, 1H), 1.95 (br. s, 2H), 1.76 (br. s, 2H), 1.60 (br. s, 1H), 1.34 (br. s, 1H).

Synthesis of η^6 -chlorobenzene- η^5 -cyclopentadienyliron(II) complexes (2.14 a-c)¹⁶

A magnetic stir bar, the appropriate arene (**2.13 a-c**) (277 mmol), ferrocene (**2.1**) (277 mmol), aluminum (159 mmol) and aluminum chloride (306 mmol) respectively, were placed in a 3-necked 500 mL round bottom flask. The flask was fitted with a condenser and a thermometer.

The reaction was stirred at 135 °C, under nitrogen, in the dark for 5 hours. The reaction was then allowed to cool to 85 °C before it was poured into 700 mL of ice. This solution was then filtered through sand in a Buchner funnel. The filtrate was washed with diethyl ether until the ether layer was a pale yellow colour. 12 g of NH₄PF₆ was then added to the water layer, resulting in the formation of a green precipitate. The product was then extracted using DCM and then was washed with water. The product DCM mixture was dried using magnesium sulphate followed by gravity filtration. The filtrate was concentrated using a rotary evaporator and then added to diethyl ether forming a yellow precipitate. The precipitate was collected in a Buchner funnel and dried over vacuum with a 30-45% yield.

2.14 a ¹H NMR (400 MHz, acetone-*d*₆) δ = 6.90 (s, 4H), 5.39 (s, 5H).

2.14 b ¹H NMR (400 MHz, acetone-*d*₆) δ = 6.81 (d, *J*=6.1, 2H), 6.57 (t, *J*=6.0, 2H), 6.46 (t, *J*=5.8, 1H), 5.30 (s, 5H).

2.14 c ¹H NMR (400 MHz, acetone-*d*₆) δ = 6.80 (d, *J*=6.7, 2H), 6.56 (d, *J*=6.7, 2H), 5.31 (s, 5H), 2.55 (s, 3H).

Synthesis of complex **2.16**⁵²

Complex **2.14 a** (3.3044 g, 8 mmol), 4,4-bis(4-hydroxyphenyl)valeric acid (**2.15**) (1.0353 g, 3.6 mmol), K₂CO₃ (1.3845 g, 10 mmol) and 40 mL of DMF were combined in a 100 mL round bottom flask with a magnetic stir bar. The reaction was stirred in a nitrogen environment for 48 hours. The product was precipitated in 600 mL 1.2 M HCl and NH₄PF₆ (1.3211 g, 8 mmol). The pale yellow precipitate was collected in a Buchner funnel and dried over vacuum. Once dry the product was dissolved in 5-10 mL of acetone and a white precipitate was filtered

out. The filtrate was then re-precipitated in to 1.2 M HCl , collected in a Buchner funnel and dried over vacuum. This gave 3.2776 g, 87 % yield.

^1H NMR (400 MHz, DMSO- d_6) δ = 7.38 (d, J =8.9, 4H), 7.28 (d, J =8.9, 4H), 6.81 (d, J =6.9, 4H), 6.42 (d, J =6.9, 4H), 5.28 (s, 10H), 2.46 – 2.38 (m, 2H), 2.12 – 2.04 (m, 2H), 1.68 (s, 3H).

Synthesis of complex 2.17

Complex **2.16** (3.0129 g, 2.9 mmol), 2-butyne-1,4-diol (**2.5**) (0.7771 g, 9 mmol), DCC (0.6679 g, 3 mmol), DMAP (0.3741 g, 3 mmol), 15 mL DCM and 5 mL DMF were stirred for 18 hours under nitrogen. The reaction was then placed in the freezer for 3 h and filtered to remove DCU. The 60 mL of DCM was added to the filtrate which was then washed with 200 mL of 1.2 M HCl and 6 mmol of NH_4PF_6 . The organic layer was then was dried using magnesium sulphate followed by gravity filtration. The DCM was removed from the filtrate using a rotary evaporator, leaving a mixture of product and DCU in DMF. This mixture was placed in the freezer for 3 hours, resulting in the precipitation of DCU crystals which were then filtered out. The filtrate was then added to 200 mL of water and 0.9850 g (6 mmol) of NH_4PF_6 forming a yellow precipitate, which was collected in a Buchner funnel and dried over vacuum. 2.860 g yield (89 % yield).

^1H NMR (400 MHz, acetone- d_6) δ = 7.48 (t, J =8.8, 4H), 7.34 (d, J =8.7, 4H), 6.82 (d, J =6.6, 4H), 6.52 (d, J =6.3, 4H), 5.38 (s, 10H), 4.71 (s, 2H), 4.23 (s, 2H), 2.60 – 2.50 (m, 2H), 2.29 – 2.19 (m, 2H), 1.76 (s, 3H).

^{13}C NMR (101 MHz, acetone- d_6) δ = 172.85, 151.68, 147.61, 133.59, 130.37, 121.09, 104.53, 87.47, 86.58, 80.15, 79.32, 76.68, 52.49, 50.33, 46.02, 36.75, 30.20, 27.68.

IR 1738 cm^{-1} (C=O), 3580 cm^{-1} (OH)

Synthesis of complex 2.18

Complex **2.17** (2.770 g, 2.5 mmol), 5-norbornene-2-carboxylic acid (**2.7**) (0.35 mL, 2.8 mmol), DCC (0.6680 g 3 mmol), DMAP (0.3741 g, 3 mmol), 15 mL DCM and 5 mL DMF were stirred for 18 hours, in the dark, under nitrogen. The reaction was then placed in the freezer for 3 h and filtered to remove DCU. 100 mL of DCM was added to the filtrate which was then washed with 100 mL of 1.2 M HCl and 0.9840 g (6 mmol) of NH_4PF_6 . The organic layer was then dried using magnesium sulphate followed by gravity filtration. The DCM was removed from the filtrate using a rotary evaporator, leaving a mixture of product and DCU in DMF. This mixture was placed in the freezer for 3 hours, resulting in the precipitation of DCU crystals which were then filtered out. The filtrate was then added to 200 mL of water and 6 mmol of NH_4PF_6 forming a yellow precipitate, which was collected in a Buchner funnel and dried over vacuum. 2.5166 g yield (82 % yield).

^1H NMR (400 MHz, acetone- d_6) δ = 7.49 (d, $J=7.7$, 5H), 7.34 (d, $J=7.8$, 4H), 6.81 (d, $J=5.6$, 4H), 6.52 (d, $J=5.5$, 4H), 6.35 (m, 0H), 6.19-5.87 (m, 2H), 5.38 (s, 10H), 4.76-4.64 (m, 4H), 3.18 (s, 1H), 3.07-2.97 (m, 1H), 2.88 (s, 2H), 2.62-2.50 (m, 2H), 2.30-2.18 (m, 2H), 1.95-1.85 (m, 1H), 1.76 (s, 3H), 1.48 (d, $J=8.2$, 0H), 1.41-1.26 (m, 3H).

^{13}C NMR (101 MHz, acetone- d_6) δ = 175.57, 173.92, 172.96, 152.92*, 152.33, 147.96, 147.51*, 138.92, 138.52, 136.47, 134.01, 133.10, 131.94*, 130.78, 129.85*, 121.44, 119.48*, 105.05, 88.09, 82.05, 81.96, 81.79, 81.60, 81.36, 80.68, 79.17*, 77.45, 76.26*, 52.59, 52.55, 52.16, 50.13, 47.33, 46.87, 46.55, 46.41, 43.68, 43.50, 43.37, 42.40, 37.18, 30.96, 30.53, 29.74, 27.98.*denotes starting material peaks.

IR 1733 cm^{-1} , 1730 cm^{-1} (C=O)

Synthesis of complex 2.19

Under N₂, 0.8585 g (2.5 mmol) of dicobalt octacarbonyl (**2.10**) was added to a stirring solution of 2.3331 g (1.9 mmol) of complex **2.18** in 10 mL of THF. For the first 30 min, bubbles appeared in the reaction flask indicating the evolution of carbon monoxide from the reaction. To ensure the full incorporation of the cobalt, the reaction was stirred for an additional 14 hours. The THF was removed *in vacuo* leaving a red residue that was dissolved in acetone and allowed to sit on the bench top until a small amount of precipitate formed (30 min - 1 hour). The solution was then filtered through Celite and the acetone was concentrated to ~5 mL *in vacuo*. The solution was then added to 200 mL of water containing 0.3280 g NH₄PF₆, forming a pink precipitate that was collected and dried for 24-48 hours over vacuum. 2.5889 g yield (90 % yield).

¹H NMR (400 MHz, acetone-*d*₆) δ = 7.48 (d, *J*=8.6, 4H), 7.33 (d, *J*=8.6, 4H), 6.81 (d, *J*=6.4, 4H), 6.51 (d, *J*=6.6, 4H), 6.23 – 5.92 (m, 2H), 5.48 – 5.17 (m, 14H), 3.23 (s, 1H), 3.15-3.04 (m, 1H), 2.90 (s, 1H), 2.66 – 2.52 (m, 2H), 2.37 – 2.18 (m, 2H), 2.01 – 1.88 (m, 1H), 1.73 (s, 4H), 1.54 (d, *J*=7.9, 0H), 1.49 – 1.22 (m, 4H).

¹³C NMR (101 MHz, acetone-*d*₆) δ = 173.49, 152.41, 147.95, 138.96, 138.60, 136.47, 134.01, 133.35, 130.69, 121.40, 105.12, 88.03, 80.64, 77.42, 65.50, 65.40, 65.38, 50.21, 47.33, 47.00, 46.35, 46.33, 44.00, 43.73, 43.36, 42.96, 42.43, 37.29, 31.06, 30.62, 27.87. The alkyne and carbonyl carbons coordinated to the cobalt cannot be seen due to broadening, also the two endo and exo carbonyl carbons of the norbornene are not visible.

IR 2100 cm⁻¹, 2067 cm⁻¹ and 2034 cm⁻¹ (CoC≡O) 1725 cm⁻¹ (C=O)

Synthesis of polymer 2.20

For the synthesis of the polymers all chemicals and solvents were kept under nitrogen. 0.0257 g of 2nd generation Grubbs catalyst dissolved in 1.4 mL of dry DCM was added to complex **2.19** (2.2701 g, 1.5 mmol) dissolved in 2 mL of dry DCM and stirred. After 45 minutes, the polymer had precipitated out of solution and 5 mL of ethylvinyl ether was added to the reaction mixture to terminate any residual polymer growth, end capping the polymers. The polymer was then triturated with DCM to remove any residual monomer leaving higher molecular weight polymers in a 2.2107 g yield

¹H NMR (400 MHz, DMSO-*d*₆) δ = 7.35 (bs, 4H), 7.25 (bs, 4H), 6.80 (bs, 4H), 6.40 (bs, 4H), 5.28 (bs, 16H), 2.18 (bs, 1H), 1.66 (bs, 3H), 1.23 (bs, 6H).

¹³C NMR: not soluble enough to obtain.

Synthesis of complex 2.22 (modified procedure from reference 50)

Complex **2.14 a** (3.3249 g, 8 mmol), 4-hydroxy benzoic acid (**2.21**) (4.4081 g, 32 mmol) (19), K₂CO₃ (11.0437 g, 80 mmol) and 65 mL of DMF were combined in a 100 mL round bottom flask with a magnetic stir bar. The reaction was stirred in a dark nitrogen environment for 18 hours. The reaction mixture was then poured into 300 mL 1.2 M HCl and NH₄PF₆ (8 mmol). The product DCM mixture was dried using magnesium sulphate followed by gravity filtration. The filtrate was concentrated using a rotary evaporator and then added to diethyl ether forming a yellow precipitate. The pale yellow precipitate was collected in a Buchner funnel and dried over vacuum. 3.5058 g yield (85 % yield).

¹H NMR (400 MHz, acetone-*d*₆) δ = 8.19 (d, *J*=8.8, 2H), 7.47 (d, *J*=8.8, 2H), 6.90 (d, *J*=7.0, 2H), 6.66 (d, *J*=6.9, 2H), 5.44 (s, 5H).

Synthesis of complex 2.23

Complex **2.22** (4.9393, 9.58 mmol), 2-butyne-1,4-diol (**2.5**) (45 mmol), DCC (2.2075 g, 10.6 mmol), DMAP (1.2282 g, 10 mmol), 30 mL DCM and 10 mL DMF were stirred for 18 hours under nitrogen and in the dark. The reaction was then placed in the freezer for 3 h and filtered to remove DCU. 100 mL of DCM was added to the filtrate which was then washed with 200 mL of 1.2 M HCl and 1.64 g (10 mmol) of NH_4PF_6 . The organic layer was dried using magnesium sulphate followed by gravity filtration. The DCM was removed from the filtrate using a rotary evaporator, leaving a mixture of product and DCU in DMF. This mixture was placed in the freezer for 3 hours, resulting in the precipitation of DCU crystals which were then filtered out. The filtrate was then added to 200 mL of water and 4 mmol of NH_4PF_6 forming a yellow precipitate, which was collected in a Buchner funnel and dried over vacuum. 4.9724 g yield (89 % yield).

^1H NMR (400 MHz, acetone- d_6) δ = 8.17 (d, J=8.8, 2H), 7.46 (d, J=8.8, 2H), 6.84 (d, J=6.8, 2H), 6.61 (d, J=6.8, 2H), 5.39 (s, 5H), 5.01 (t, J=1.8, 2H), 4.26 (t, J=1.8, 2H).

^{13}C NMR (101 MHz, acetone- d_6) δ = 165.51, 158.95, 133.52, 132.66, 131.19*, 128.74, 121.55, 121.37*, 105.83, 88.41, 88.30*, 87.55, 81.16, 81.01*, 79.43, 79.03, 78.14*, 53.89, 50.81. *

denotes impurity peaks.

IR 1720 cm^{-1} (C=O), 3398 cm^{-1} (OH)

Synthesis of complex 2.24

Complex **2.23** (4.8524 g 8.3 mmol), 5-norbornene-2-carboxylic acid (1.6 mL, 13 mmol) (**2.7**), DCC (2.9005 g, 14 mmol), DMAP (1.5336 g, 12.5 mmol), 15 mL DCM and 5 mL DMF

were stirred for 18 hours, in the dark, under nitrogen. The reaction was then placed in the freezer for 3 h and filtered to remove DCU. 150 mL of DCM was added to the filtrate which was then washed with 1.4765 g (9 mmol) of NH_4PF_6 dissolved in 200 mL of 1.2 M HCl and once with 200 mL of 1.2 M HCl. The organic layer was then dried using magnesium sulphate followed by gravity filtration. The DCM was removed from the filtrate *in vacuo*, leaving a mixture of product and DCU in DMF. This mixture was placed in the freezer for 3 hours, resulting in the precipitation of DCU crystals which were then filtered out. The filtrate was then added to 150 mL of diethyl ether forming a brown viscous oil which was isolated by decanting off the DMF/ether and allowing to dry for 24 hours. 2.073 g yield (36 % yield).

^1H NMR (400 MHz, acetone- d_6) δ = 8.18 (d, J = 8.4, 2H), 7.48 (d, J = 8.5, 2H), 6.87 (d, J = 6.5, 2H), 6.64 (d, J = 6.5, 2H), 6.18-5.90 (m, 2H), 5.42 (s, 5H), 5.11-5.02 (m, 2H), 4.81 (t, J = 1.8, 0H), 4.73 (ddt, J = 23.65, 15.9, 1.8, 1H), 3.23-2.88 (m, 5H), 2.28 – 2.18 (m, 0H), 1.97-1.84 (m, 1H), 1.52 – 1.23 (m, 3H).

^{13}C NMR (101 MHz, acetone- d_6) δ = 175.55, 173.89, 165.16, 158.71, 138.88, 138.46, 136.46, 133.32, 133.10, 132.45, 130.96*, 128.41, 121.37, 121.18*, 105.60, 105.34*, 88.25, 88.13, 82.40, 82.30, 81.39*, 81.15, 80.97*, 80.80, 78.85, 77.90*, 53.42, 52.53, 52.13, 50.10, 47.32, 46.83, 46.53, 43.66, 43.48, 43.36, 42.41, 30.93, 29.65. * denotes slight impurities

IR 1728 cm^{-1} (C=O).

Synthesis of complex **2.25**

Under N_2 , 0.9961 g (2.9 mmol) of dicobalt octacarbonyl (**2.10**) was added to a stirring solution of 1.7710 g (2.5 mmol) of complex **2.24** in 10 mL of THF. For the first 30 min, bubbles appeared in the reaction flask indicating the evolution of carbon monoxide from the

reaction. To ensure the full incorporation of the cobalt the reaction was stirred for an additional 12.5 hours. The THF was removed *in vacuo* leaving a red residue that was dissolved in acetone and allowed to sit on the bench top until a small amount of precipitate formed (20-30 min). The solution was then filtered through celite and the acetone was concentrated to 5 mL *in vacuo*. The solution was then added to water containing NH_4PF_6 forming a pink precipitate that was collected. 2.3418 g yield (95 % yield).

^1H NMR (400 MHz, acetone- d_6) δ = 7.48 (d, $J=8.6$, 4H), 7.33 (d, $J=8.6$, 4H), 6.81 (d, $J=6.4$, 4H), 6.50 (d, $J=6.5$, 4H), 6.21-5.92 (m, 2H), 5.48 – 5.17 (m, 14H), 3.23 (s, 1H), 3.08 (s, 1H), 2.89 (s, 1H), 2.58 (s, 2H), 2.30 (s, 3H), 1.99-1.87 (m, 2H), 1.78-1.70 (m, 4H), 1.52 (d, 1H), 1.47-1.23 (m, 5H), 0.98 – 0.80 (m, 2H).

^{13}C NMR (101 MHz, acetone- d_6) δ = 200.31, 165.83, 158.96, 138.95, 138.57, 136.48, 133.27, 132.82*, 132.21, 130.99*, 128.61, 122.73*, 120.96, 105.71, 91.88, 91.16, 88.27, 88.09*, 80.98, 80.77*, 79.21, 77.83*, 66.55, 65.53, 65.43, 50.20, 47.32, 46.98, 46.32, 43.98, 43.70, 43.36, 42.42, 30.95, 29.64. * denotes slight impurities

IR 2103 cm^{-1} , 2067 cm^{-1} and 2033 cm^{-1} ($\text{CoC}\equiv\text{O}$) 1720 cm^{-1} ($\text{C}=\text{O}$).

Synthesis of polymer 2.26

For the synthesis of the polymers all chemicals and solvents were kept under nitrogen. 0.0257 g of 2nd generation Grubbs catalyst dissolved in 1.4 mL of dry DCM was added to 1.4831 g (1.5 mmol) complex **2.25** dissolved in 2 mL of dry DCM and stirred. After 30 minutes 5 mL of ethylvinyl ether was added to the reaction mixture to terminate polymer growth and endcap the polymers. The polymer was then precipitated into ether, collected by vacuum filtration and allowed to dry over vacuum for 24 hours giving a 1.3644 g yield.

IR 2103 cm^{-1} , 2067 cm^{-1} and 2033 cm^{-1} ($\text{CoC}\equiv\text{O}$) 1722 cm^{-1} ($\text{C}=\text{O}$).

Chapter 3: Methacrylate based polymers

3.1 Introduction

There is a plethora of literature and commercial examples of polymers based on the polymerization of methacrylic esters (Figure 3.1). The simplest of these would be poly(methylmethacrylate) which was first synthesized in the 1880's by Fittig and Paul.⁵³ Methacrylates can be polymerized using anionic chain polymerization and radical polymerization.⁵⁴ The anionic methods require very pure monomer and stringently purified and degassed solvents. Radical polymerization is more robust allowing for the use of monomers with trace impurities. Radical scavengers such as oxygen can cause premature chain termination; however, if enough initiator is added, polymers can be obtained even in the presence of trace amounts of oxygen or without the removal of the stabilizers present in commercially available monomers.

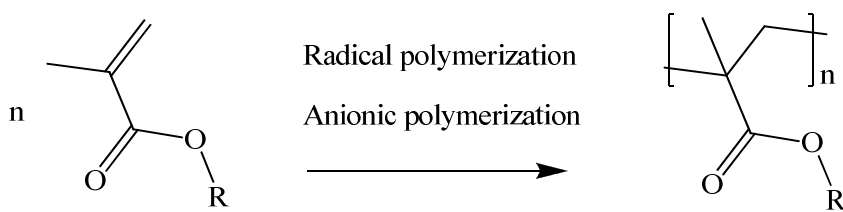


Figure 3.1: General polymerization of methacrylates.

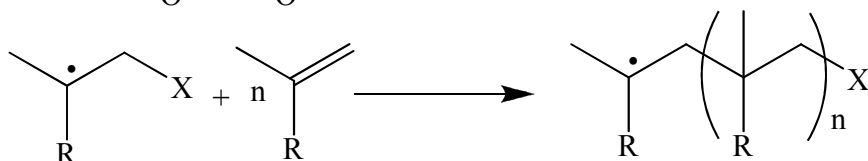
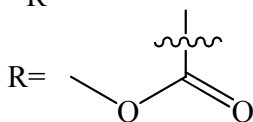
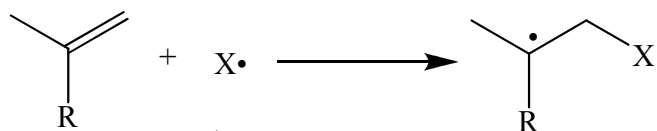
Radical polymerization occurs in three steps: initiation, propagation and termination (Figure 3.2). Initiation involves a reaction that produces radicals. This is often achieved using peroxides or alkyl azo compounds. For example AIBN is an excellent source of radicals through its thermal or photochemical decomposition (Figure 3.3). Propagation is the process by which a radical reacts with monomer to give a radical product. Termination is when two radical species

come together to make a single non-radical product. This could be two radical polymer ends or a radical polymer end and an initiator radical.

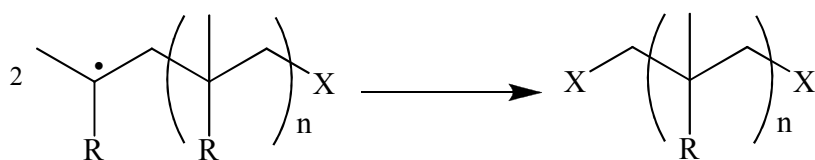
Initiation



Propagation



Termination



or

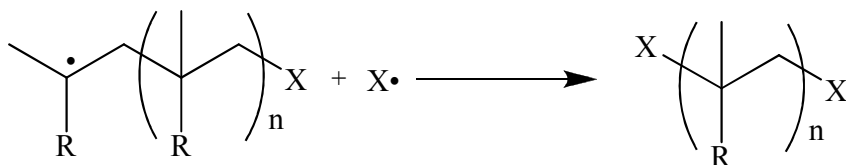


Figure 3.2: Initiation, propagation and termination of methylmethacrylate radical polymerization.

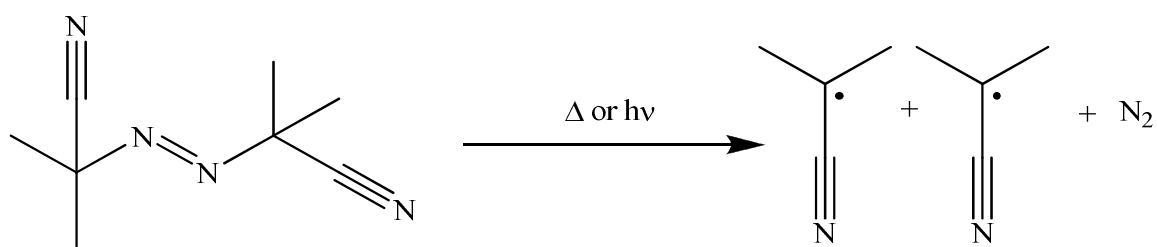


Figure 3.3: Production of radicals from AIBN.

The incorporation of various types of organoiron into methacrylate polymers has been studied mainly by Pittman *et al* and Abd-El-Aziz *et al.*⁵⁵⁻⁶⁶ In the 1970s, Pittman *et al.* reported on the synthesis of methacrylate polymers containing ferrocene (Figure 3.4, complex a). The main goal of their research was to make charge transfer polymers. To this end, the ferrocene polymers were treated with tetracyanoethylene, dichlorodicyanoquinone, and chloranil.⁵⁸⁻⁶² Unfortunately, the ferrocene polymers were not shown to have any charge transfer properties. Previous work done by Abd-El-Aziz *et al.* has shown that AIBN can be used to prepare polymethacrylates with η^6 -aryl- η^5 -cyclopentadienyliron(II) hexafluorophosphate groups in their side chain (Figure 3.4, complexes b and c).^{64, 66-68} It is important to note that the presence of the cationic cyclopentadienyliron was found to increase the solubility of these polymers, which would increase their processability.

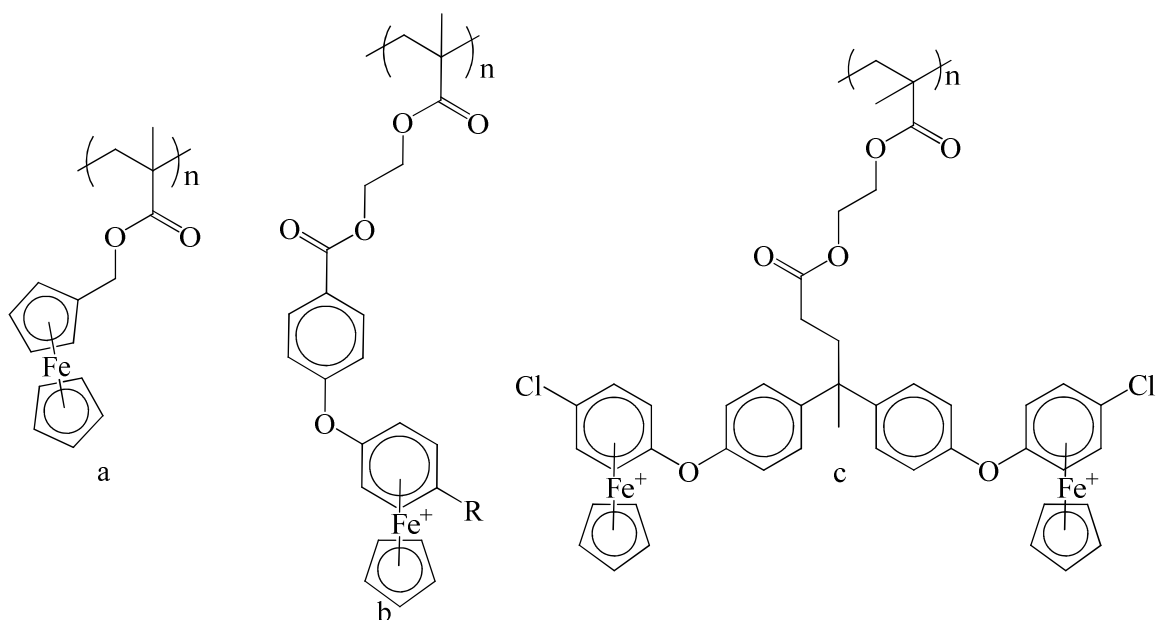


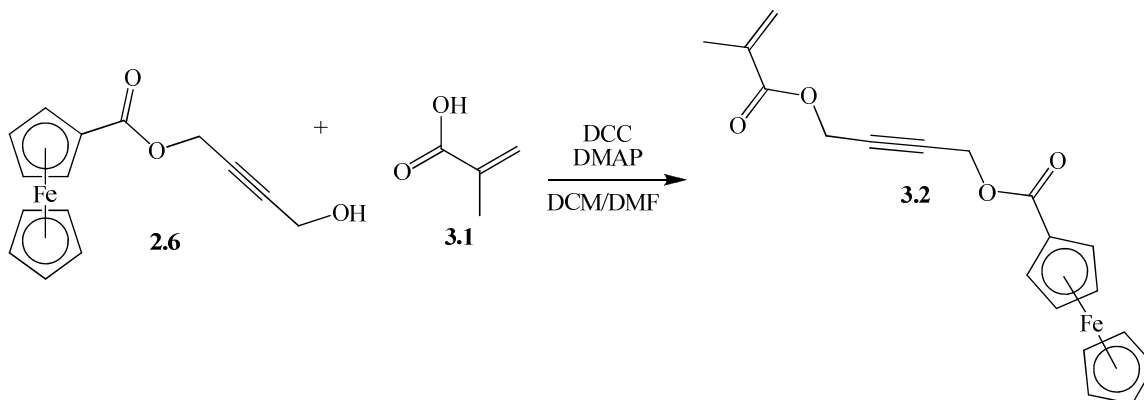
Figure 3.4: Sample of methacrylates which contain organoiron moieties.

This chapter describes the synthesis of methacrylic ester based organoiron/cobalt polymers. Unlike chapter 2 the cobalt was incorporated into these molecules post polymerization the reason for this will be discussed herein. The present work builds on both the previous research in the Abd-El-Aziz lab, as well as, the previous chapter of this thesis by showing that alkyne coordinated dicobalt hexacarbonyl can also be incorporated into polymethacrylates containing organoiron (post-polymerization). In this chapter three different classes of polymethacrylates were synthesized, one with neutral ferrocene and cobalt carbonyl-alkyne moieties and two containing cationic η^6 -aryl- η^5 -cyclopentadienyliron(II) and cobalt carbonyl-alkyne moieties.

3.2 Synthesis and characterization of ferrocene and cobalt containing polymethacrylates

3.2.1 Synthesis of a methacrylate monomer that contains ferrocene

Synthesis of the methacrylate ferrocene complex **3.2** was accomplished through Steglich esterification between methacrylic acid (**3.1**) and the alcohol of complex **2.6** (Scheme 3.1). After purification by column chromatography, the complex was isolated as an orange oil.



Scheme 3.1: Synthesis of complex **3.2**.

The ^1H NMR spectrum of complex **3.2** (Figure 3.5) shows the appearance of the diastereotopic protons of the terminal olefin carbon at 6.14 and 5.58 ppm as well as the appearance of the methyl resonance at 1.92 ppm. Upon closer inspection, the methylene protons of the butyne unit nearest to the newly formed ester have shifted from 4.32 ppm to 4.80 ppm (Figure 3.6). One can also see that these methylene protons are no longer coupled to the alcohol proton going from a doublet of triplets (when in CDCl_3) to a triplet.

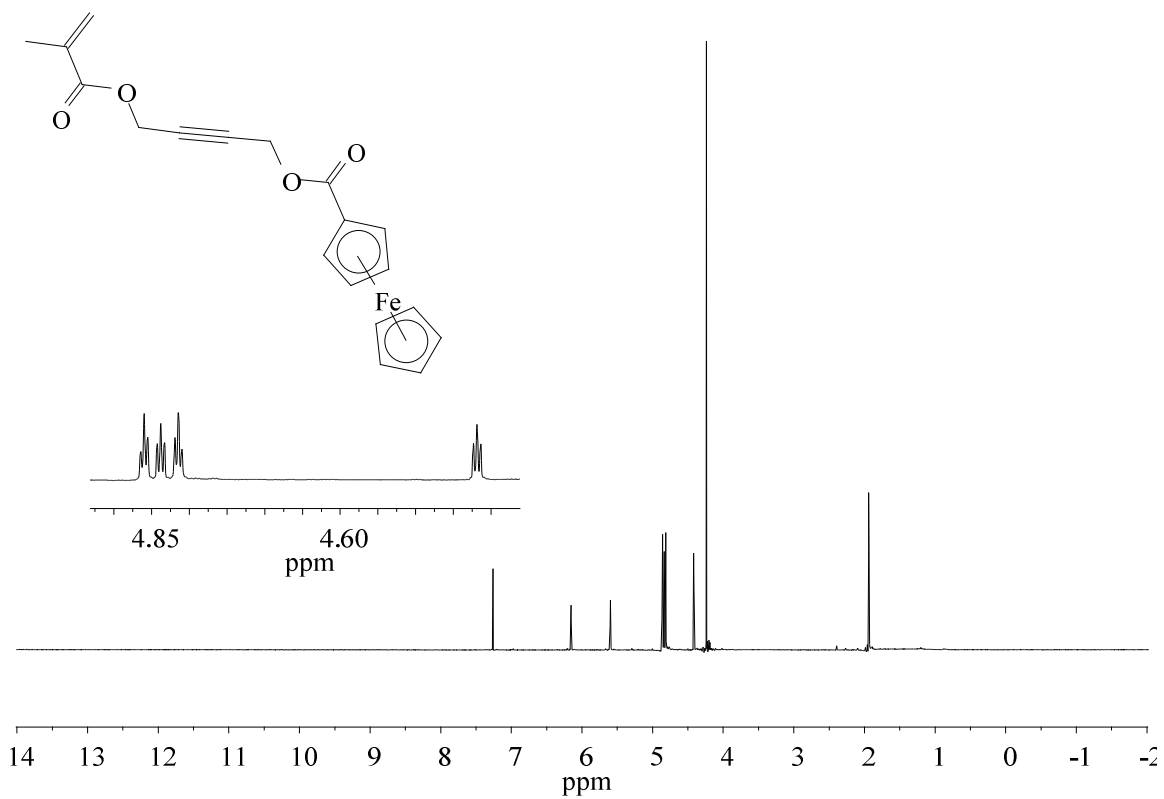


Figure 3.5: ^1H NMR spectrum of complex **3.2** in CDCl_3 .

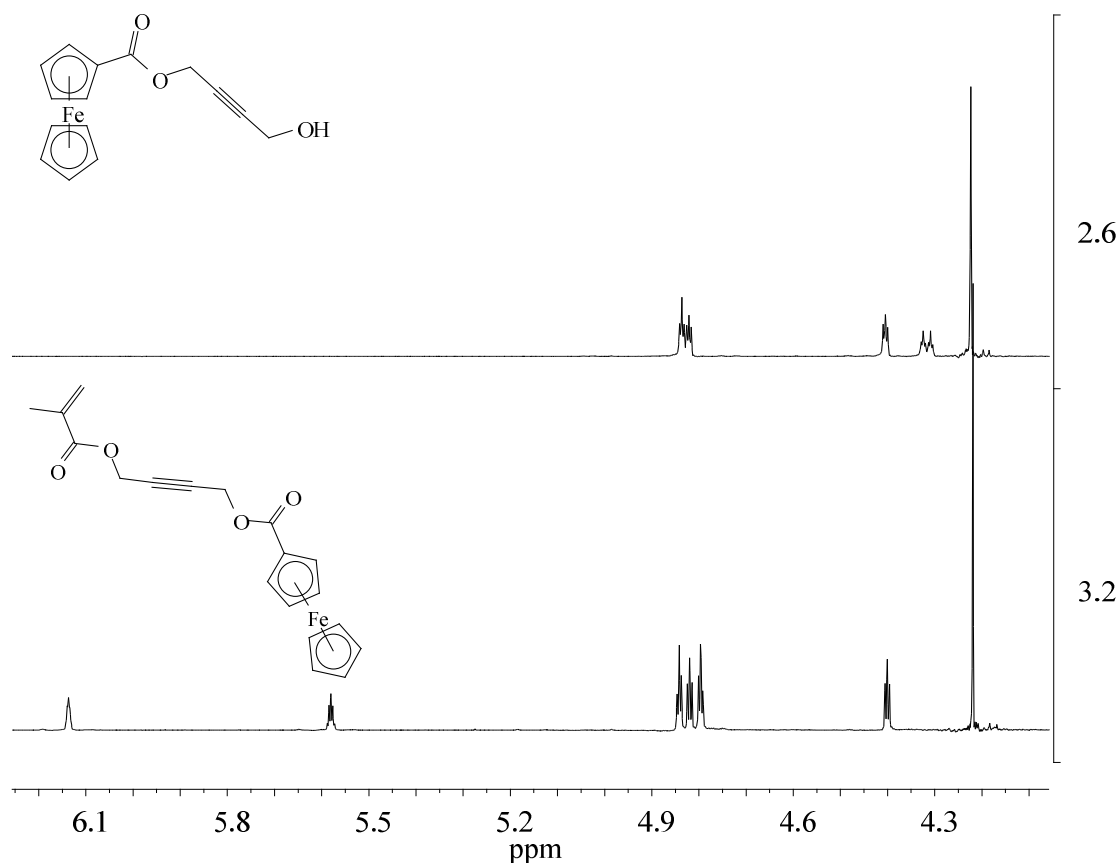


Figure 3.6: ¹H NMR spectral comparison for complexes **2.6** and **3.2** in CDCl₃.

The incorporation of the methacrylate moiety can also be seen in the ¹³C NMR spectrum of complex **3.2** (Figure 3.7). The carbonyl carbon of the newly formed ester can be seen at 167 ppm, the quaternary carbon appears at 136 ppm, the methylene carbon is at 127 ppm and the methyl resonance is at 18.5 ppm. Identification of these resonances was determined through analysis of the HMBC and HSQC spectra for complex **3.2** (Figure 3.8 and Figure 3.9 respectively). The HMBC spectrum also shows that there is connectivity between one of the carbonyl carbons to the methyl of the methacrylate and the methylene on the other side of the newly formed ester. This connectivity allowed for the identification of the two carbonyl carbons.

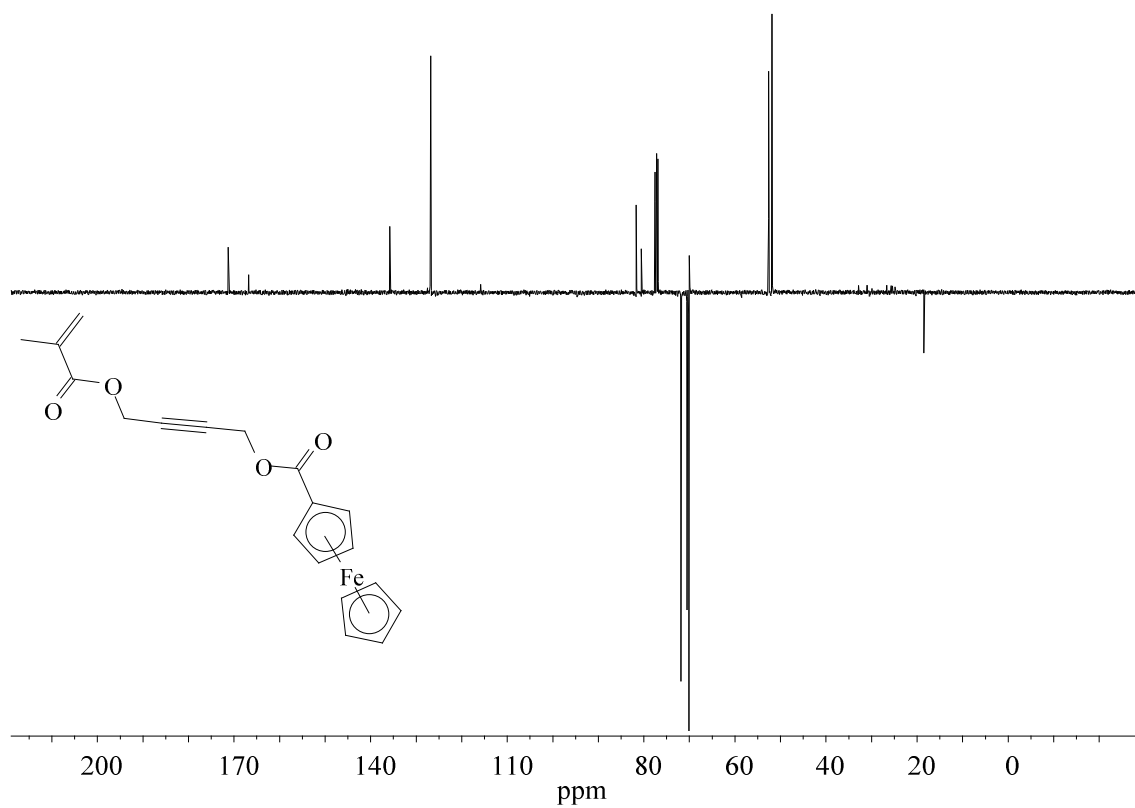


Figure 3.7: APT ^{13}C NMR spectrum of complex **3.2** in CDCl_3 .

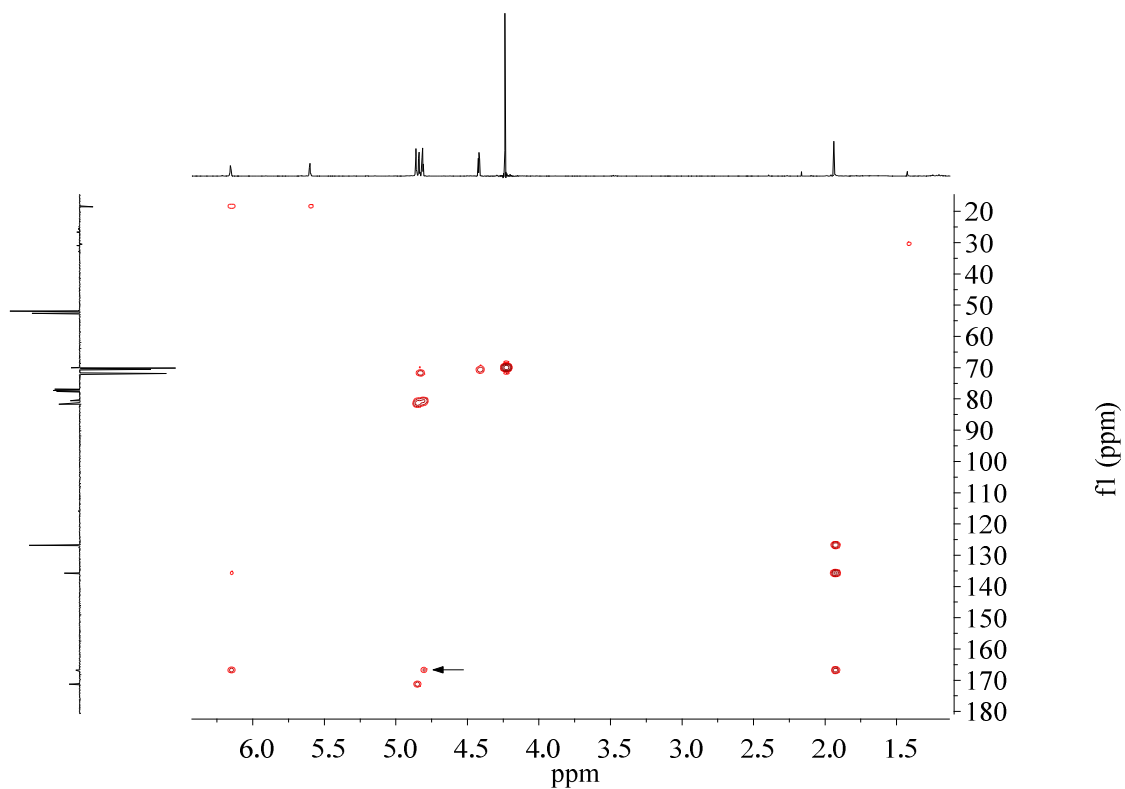


Figure 3.8: HMBC NMR spectrum of complex **3.2** in CDCl_3 . Resonance indicating connectivity between the carbonyl of the methacrylate and the methylene on the other side of the ester is indicated by the arrow.

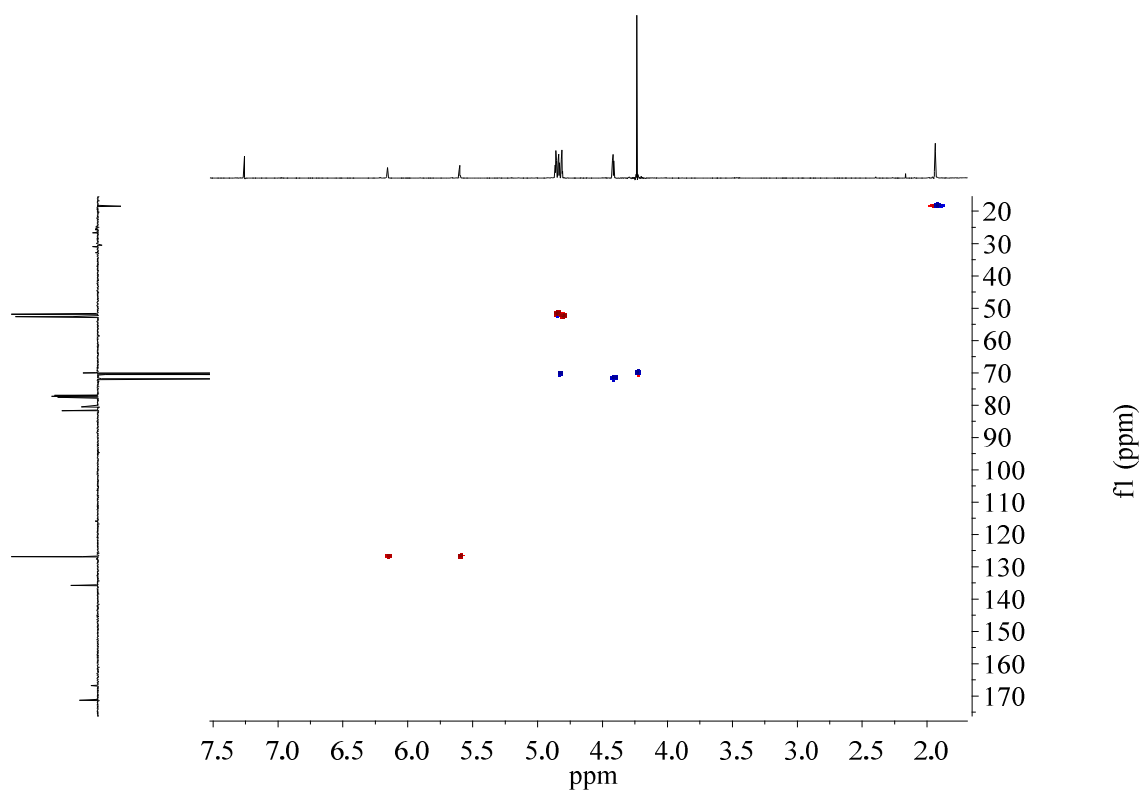
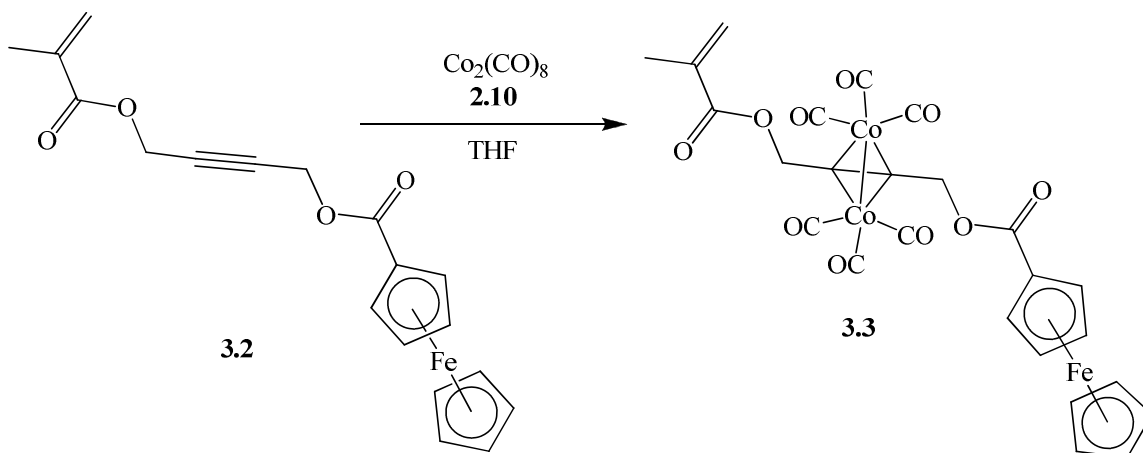


Figure 3.9: HSQC NMR spectrum of **3.2** in CDCl_3 .

3.2.2 Synthesis of a model methacrylate complex that contains both ferrocene and cobalt carbonyl

Cobalt carbonyl was added across the triple bond in a THF solution to make the model complex **3.3** (Scheme 3.2). This complex was isolated as a red crystalline solid that was characterized through IR, NMR spectroscopies and X-ray crystallography.



Scheme 3.2: Synthesis of complex **3.3**.

The IR for complex **3.3** shows three characteristic bands for the C≡O stretch at 2096, 2053 and 2022 cm^{-1} , indicating that there is some cobalt carbonyl in the sample. There is also no alkyne stretching band or bridging carbonyl band visible in the spectrum.

The ^1H NMR spectrum of complex **3.3** can be seen in Figure 3.10 where the methylene resonances have shifted downfield to 5.51 and 5.54 ppm. This downfield shift is due to the deshielding effects of the cobalt and was accompanied with a loss of coupling between the two methylenes. The ^{13}C NMR spectrum also shows a downfield shift of the methylenes to two very close peaks at 65.8 ppm (Figure 3.11). Also the alkyne carbons are now resonating together at 91.7 ppm as a broadened peak due to the broadening effect of the cobalt.

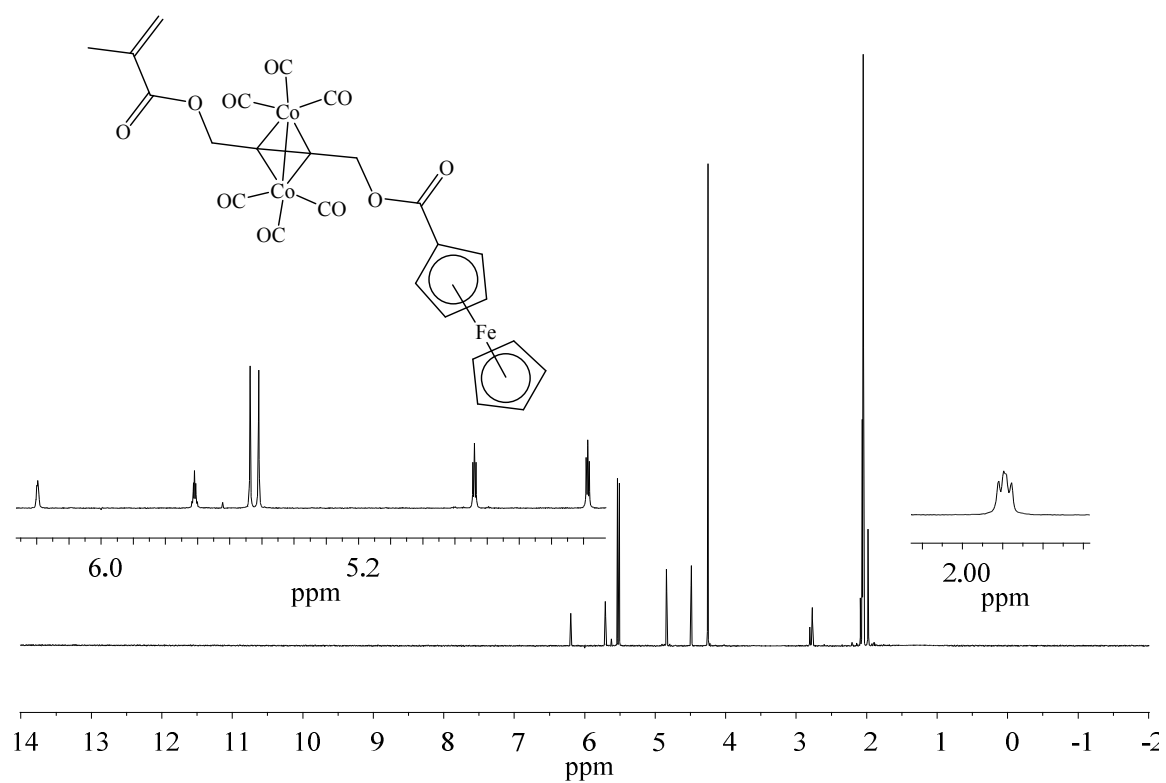


Figure 3.10: ^1H NMR spectrum of complex **3.3** in $\text{acetone-}d_6$.

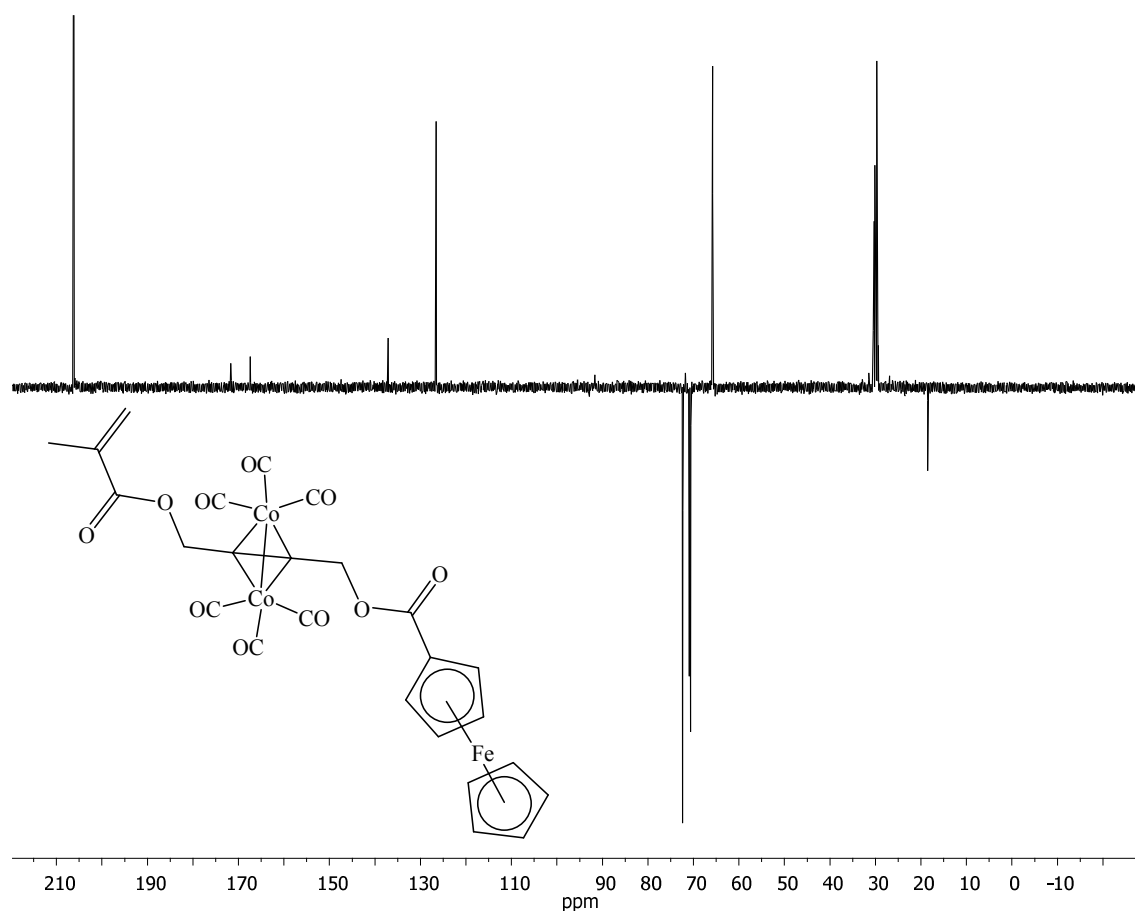


Figure 3.11: APT ^{13}C NMR spectrum of complex **3.3** in $\text{acetone-}d_6$.

Complex **3.3** formed beautiful red crystals that were characterized through X-ray crystallography. As can be seen in Figure 3.12 there is coordination between the acetylene carbons and each cobalt atom. This pseudo saw horse structure is similar to typical M_2L_6 -acetylenes.⁶⁹ The pseudo saw horse structure has a nearly linear dihedral C21-Co1-Co2-C24 angle (6°) and a Co-Co bond length of 2.48 \AA , that lie within normal ranges for this type of structure. The bulkiness of the cobalt carbonyl cluster forces the rest of the molecule into a pseudo *cis* formation at the acetylene moiety leaving the methylene carbons (C15 and C12) and ester atoms in a parallel orientation where they are nearly in the same plane. The alkyne C13-

C14 bond (1.338 Å) and the C-C≡C-C “bend back” angles (142.47° and 143.25°) were fairly typical.⁷⁰

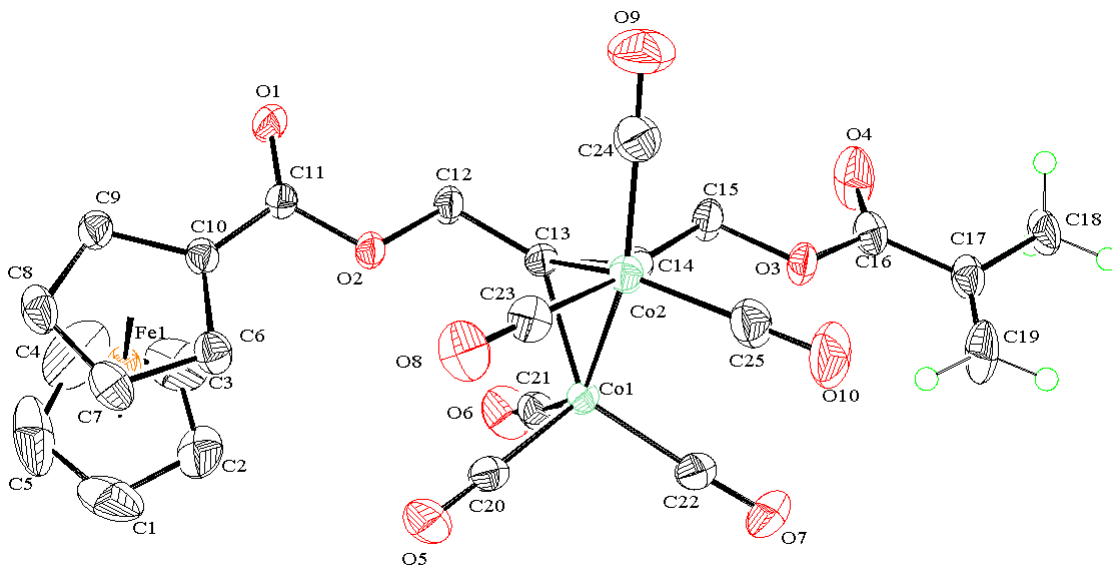


Figure 3.12: ORTEP diagram for complex **3.3**.

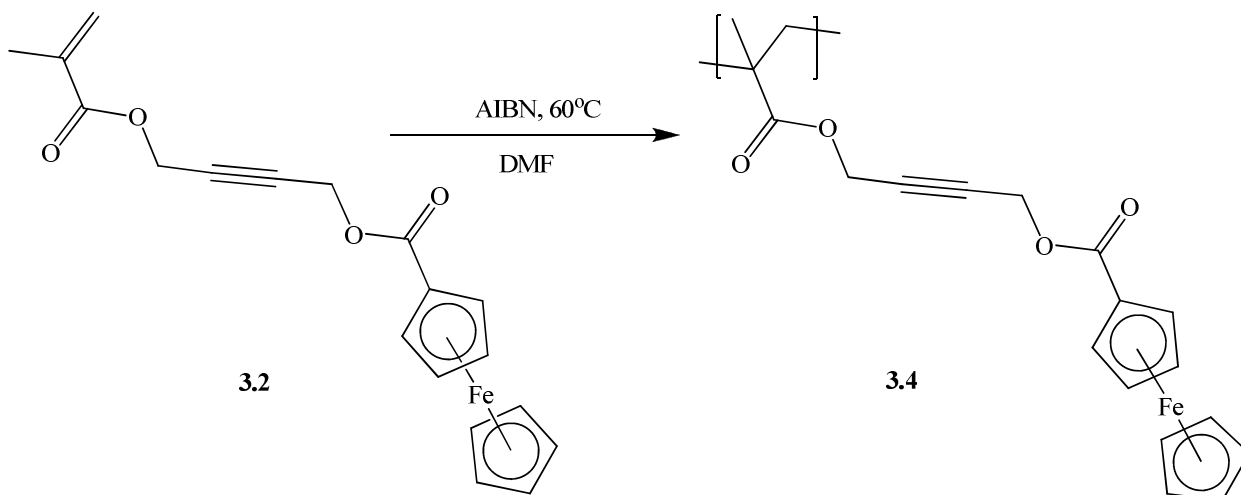
Attempts to polymerize complex **3.3** using AIBN was unsuccessful. This failure was likely due to a radical reaction involving the cobalt carbonyl. The ¹H-NMR of the products showed a complicated spectrum with inadequate characterization data.

Complex **3.3** was useful as a model complex for alkyne dicobalt hexacarbonyl complexes indicating the effect of the cobalt on NMR resonances.

3.2.3 Polymerization of a ferrocene-containing methacrylate monomer

While attempts to polymerize complex **3.3** were unsuccessful, the precursor compound **3.2** was easily polymerized using AIBN (Scheme 3.3). The best conditions for this polymerization proved to be in dry DMF using 7:1 monomer to AIBN ratio. The successful

polymerization of compound **3.2** was confirmed through GPC and NMR spectroscopy. The molecular weight of the polymer will be discussed in section 3.4.



Scheme 3.3: Synthesis of polymer **3.4**.

The ^1H NMR spectrum of polymer **3.4** indicates that the polymerization was successful (Figure 3.13). All of the resonances have broadened as is typical for polymer spectra and there is no longer any evidence of the olefin hydrogen atoms of the methacrylate at 6.14 and 5.58 ppm.

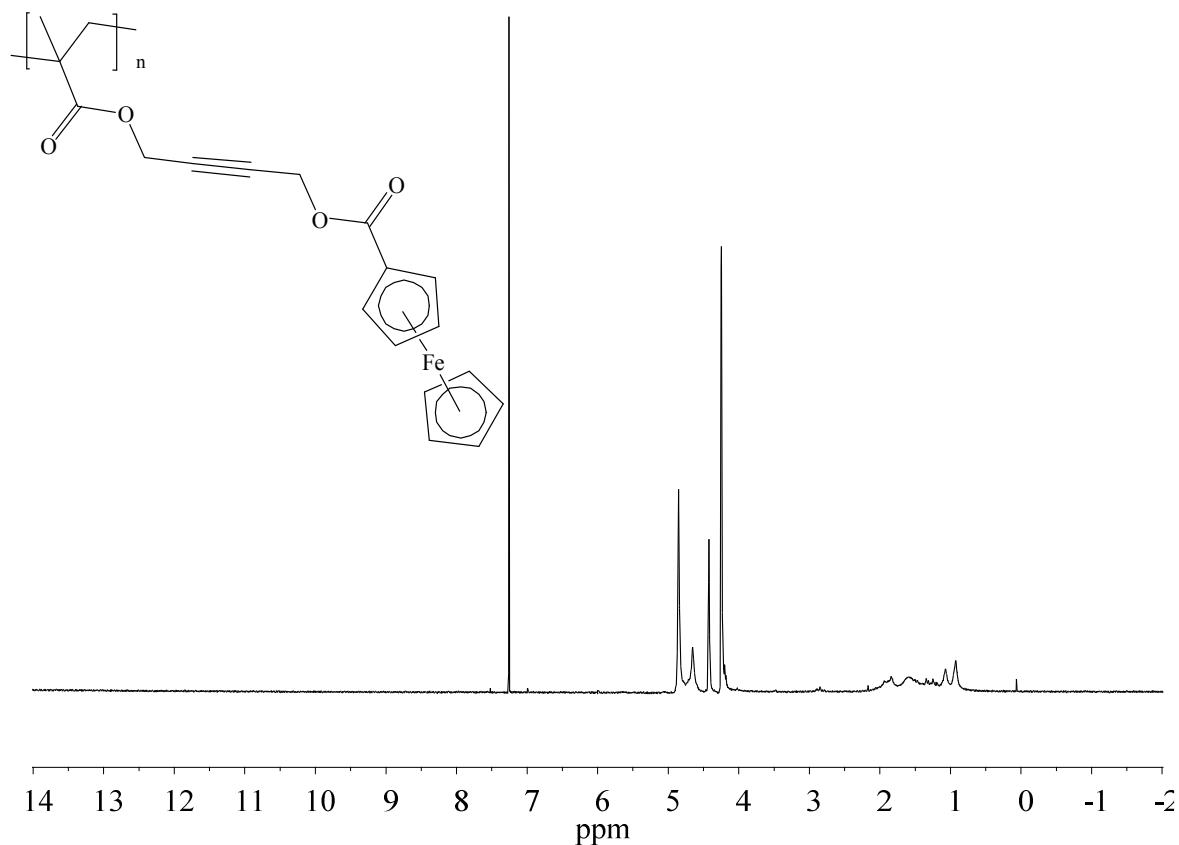
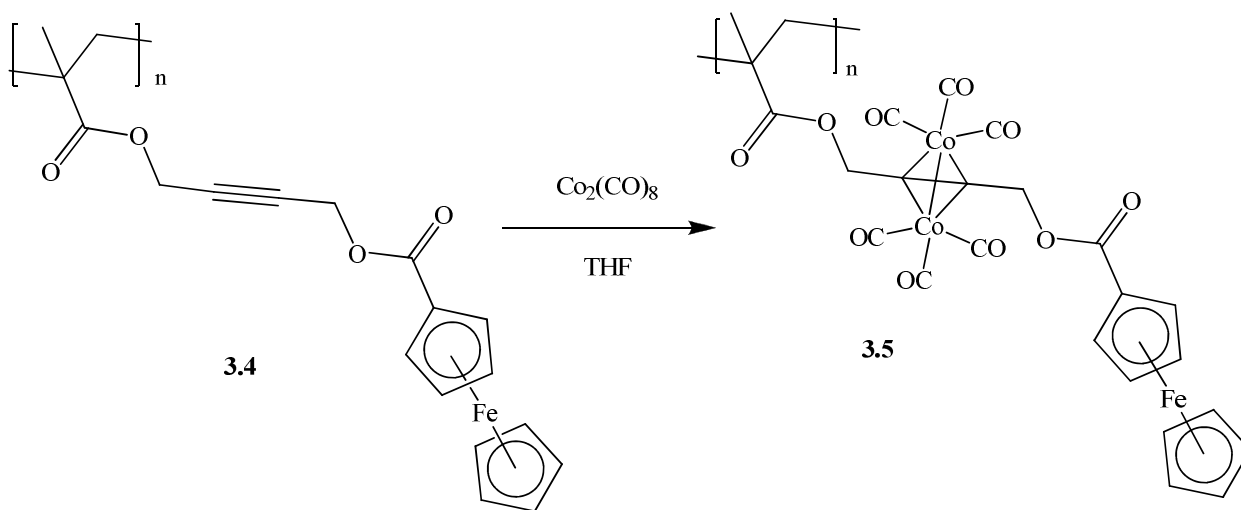


Figure 3.13: ^1H NMR spectrum of polymer **3.4** in CDCl_3 .

3.2.4 Coordination of cobalt carbonyl to a ferrocene-containing methacrylate polymer

The incorporation of cobalt into the polymer was achieved by first dissolving polymer **3.4** into THF and adding dicobalt octacarbonyl (Scheme 3.4). Converting the polymer from an orange color to a dark red color. The incorporation of the cobalt can be seen through IR and NMR. For IR 3 characteristic bands appear at 2023, 2054 and 2096 cm^{-1} representing the $\text{C}\equiv\text{O}$ bonds of the cobalt carbonyls. ^1H NMR confirms the full incorporation of the cobalt into the polymer with the shift of the methylene hydrogens from 4.65 and 4.85 ppm to 5.04 and 5.35 ppm respectively (Figure 3.14).



Scheme 3.4: Synthesis of polymer **3.5**.

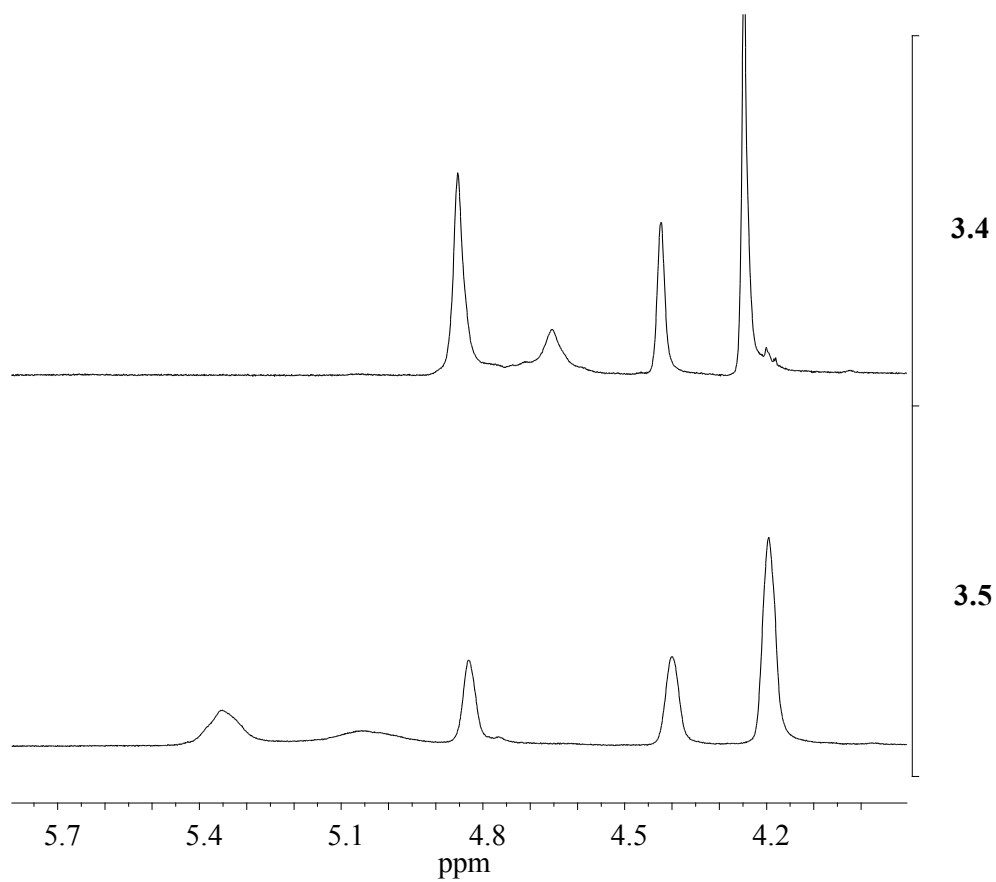
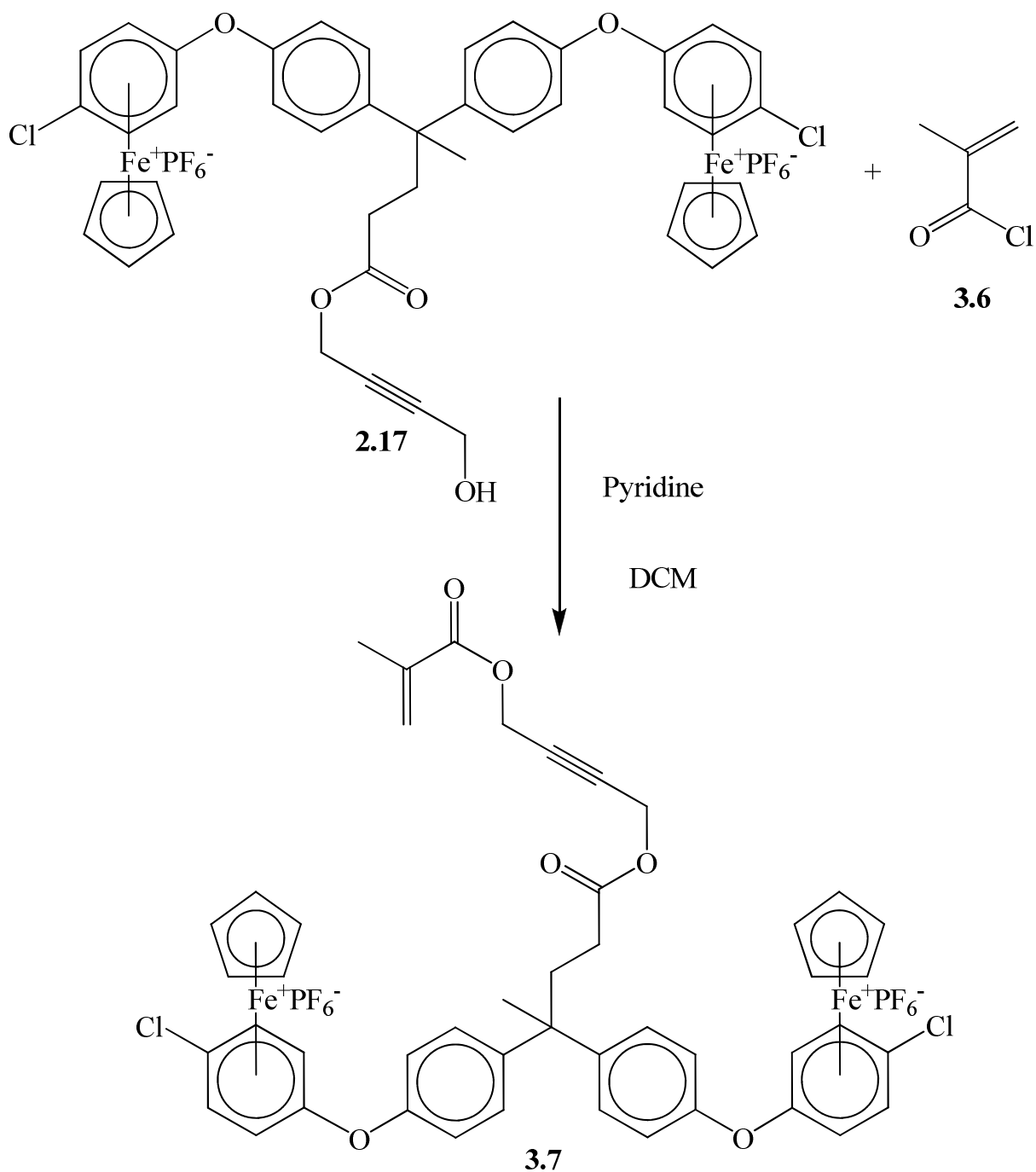


Figure 3.14: ^1H NMR spectral comparison of polymers **3.4** and **3.5** in CDCl_3 .

3.3 Synthesis and characterization of a polymethacrylate containing η^6 -arene- η^5 -cyclopentadienyliron and cobalt carbonyl

3.3.1 Synthesis of a methacrylate monomer containing two η^6 -arene- η^5 -cyclopentadienyliron(II) moieties

The first step in the synthesis of a polymethacrylate polymer containing containing two η^6 -arene- η^5 -cyclopentadienyliron hexafluorophosphate moieties and alkyne coordinated cobalt carbonyl was to react complex **2.17** with methacryloyl chloride (**3.6**) (Scheme 3.5). As polymerization of methacrylate monomers can be both thermal- and photo-initiated this complex was carefully kept in a cool dark place.



Scheme 3.5: Synthesis of complex **3.7**.

The full incorporation of the methacrylate is evidenced in the ^1H NMR and ^{13}C NMR spectra. The ^1H NMR spectrum shows the appearance of methacrylate resonances at 1.92, 5.70 and 6.09 ppm as well as the shift of the methylene groups adjacent to the alkyne from 4.22 and

4.71 ppm (complex **2.17**) to 4.74 and 4.84 ppm (complex **3.7**) (Figure 3.15). The ^{13}C NMR spectrum also shows the four methacrylate resonances at 164.06, 136.83, 126.70 and 18.39 ppm (Figure 3.16).

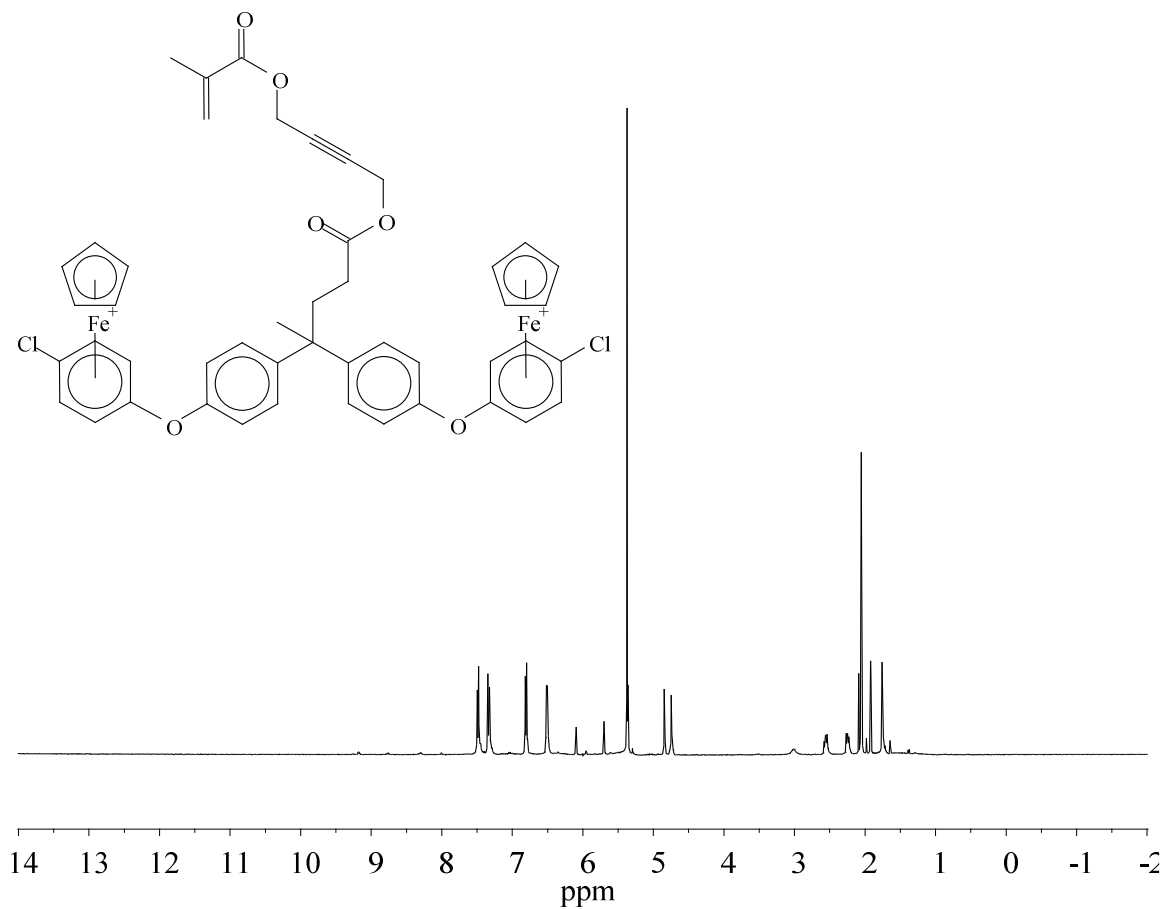


Figure 3.15: ^1H NMR spectrum of complex **3.7** in acetone- d_6 .

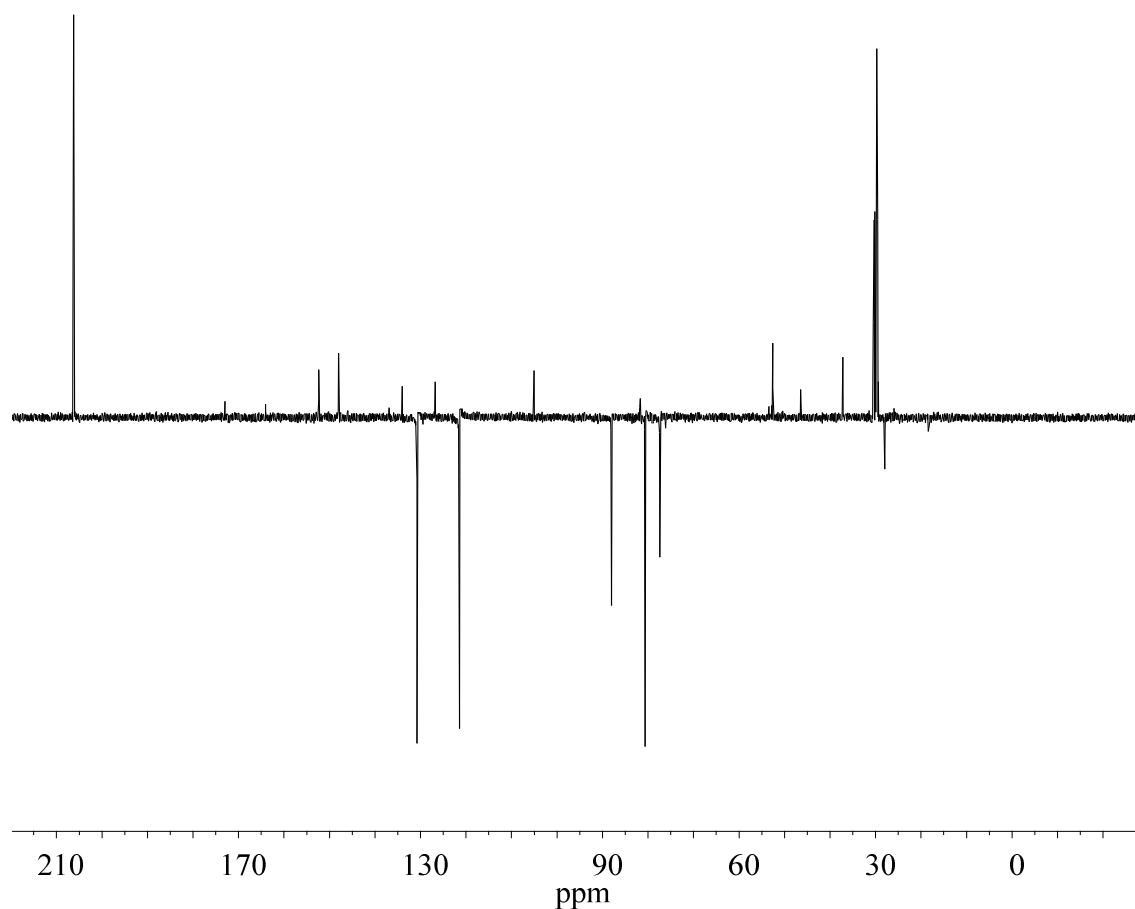
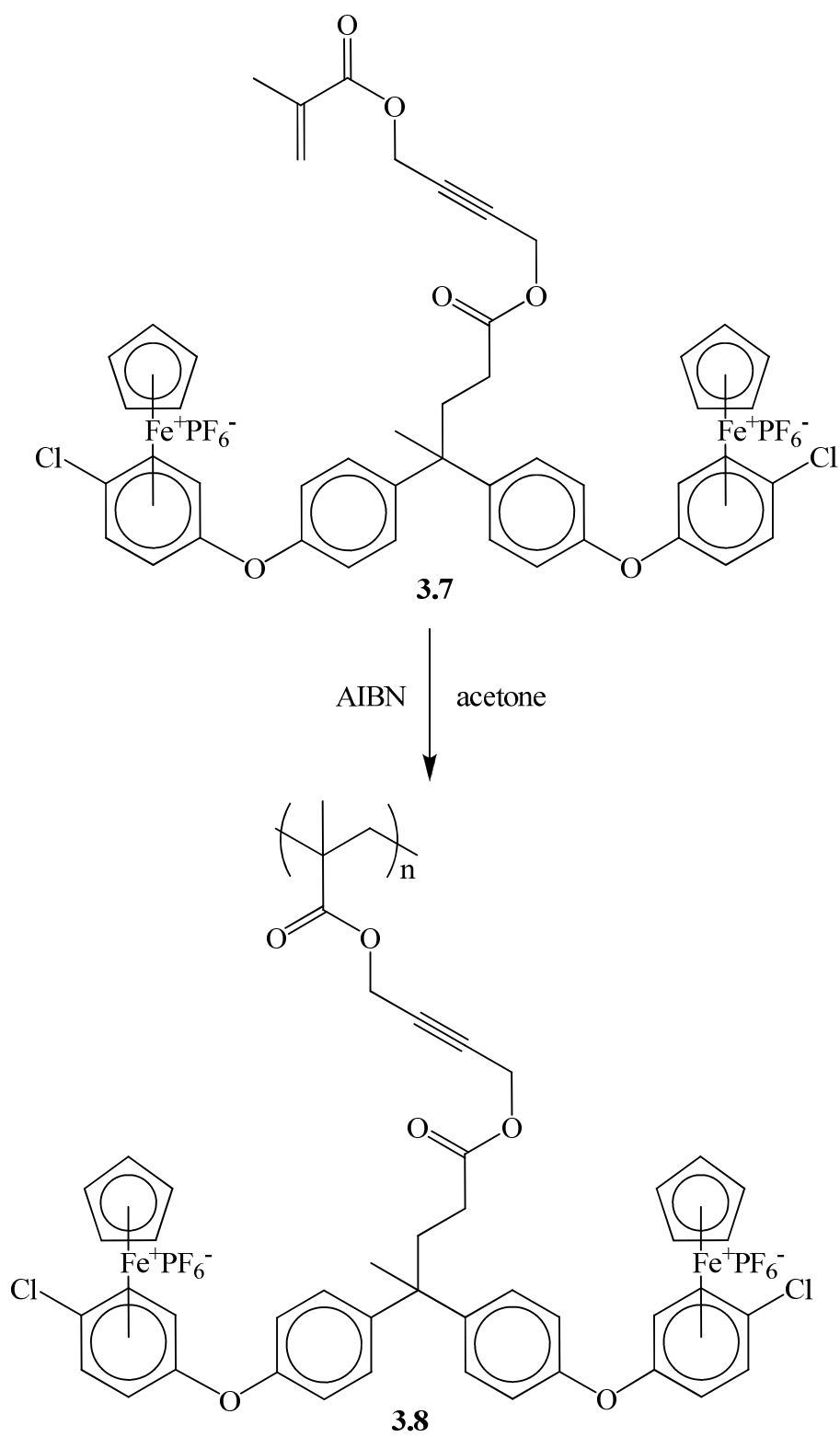


Figure 3.16: APT ^{13}C NMR spectrum of complex **3.7** in acetone- d_6 .

3.3.2 Polymerization of a methacrylate monomer containing two η^6 -arene- η^5 -cyclopentadienyliron(II) moieties

Radical polymerization of complex **3.7** was initiated with AIBN, giving polymer **3.8** (Scheme 3.6). The polymerization was confirmed using ^1H NMR spectroscopy, which shows the disappearance of the olefin peaks of the methacrylate monomer and broadening of all resonances (Figure 3.17).



Scheme 3.6: Synthesis of polymer **3.8**.

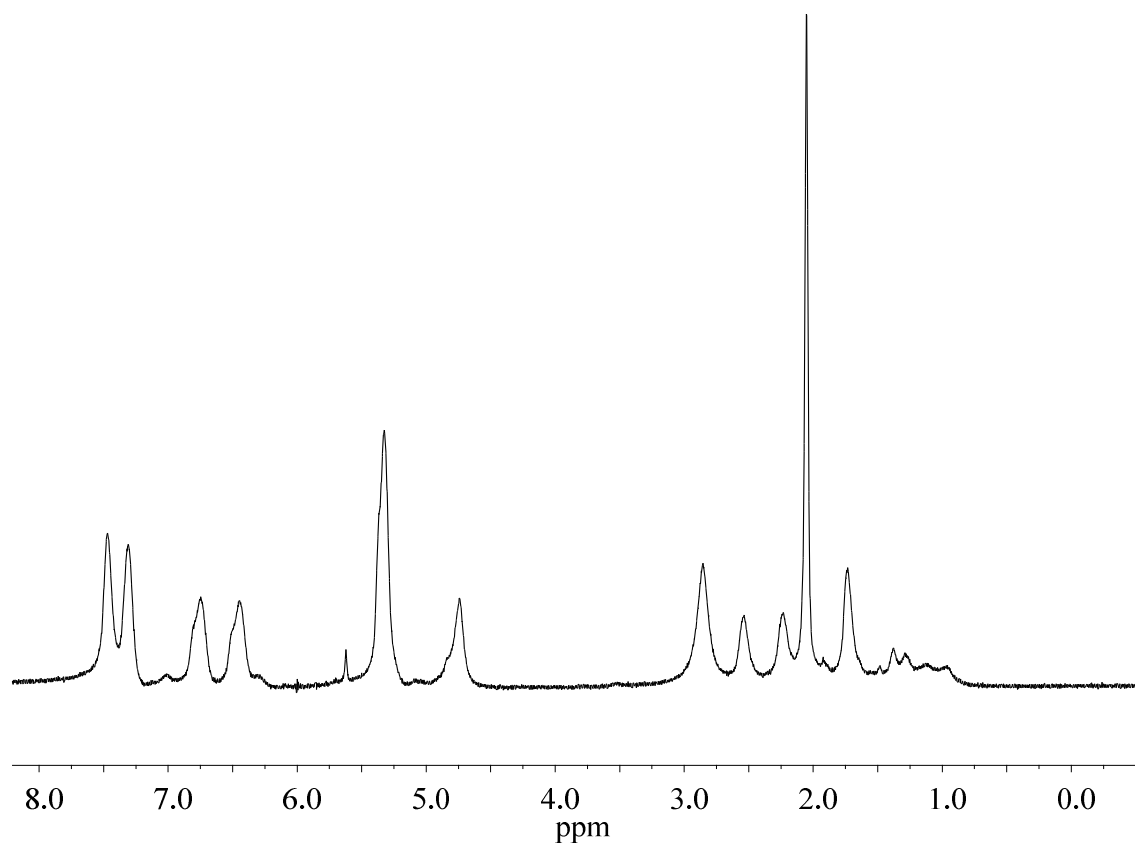
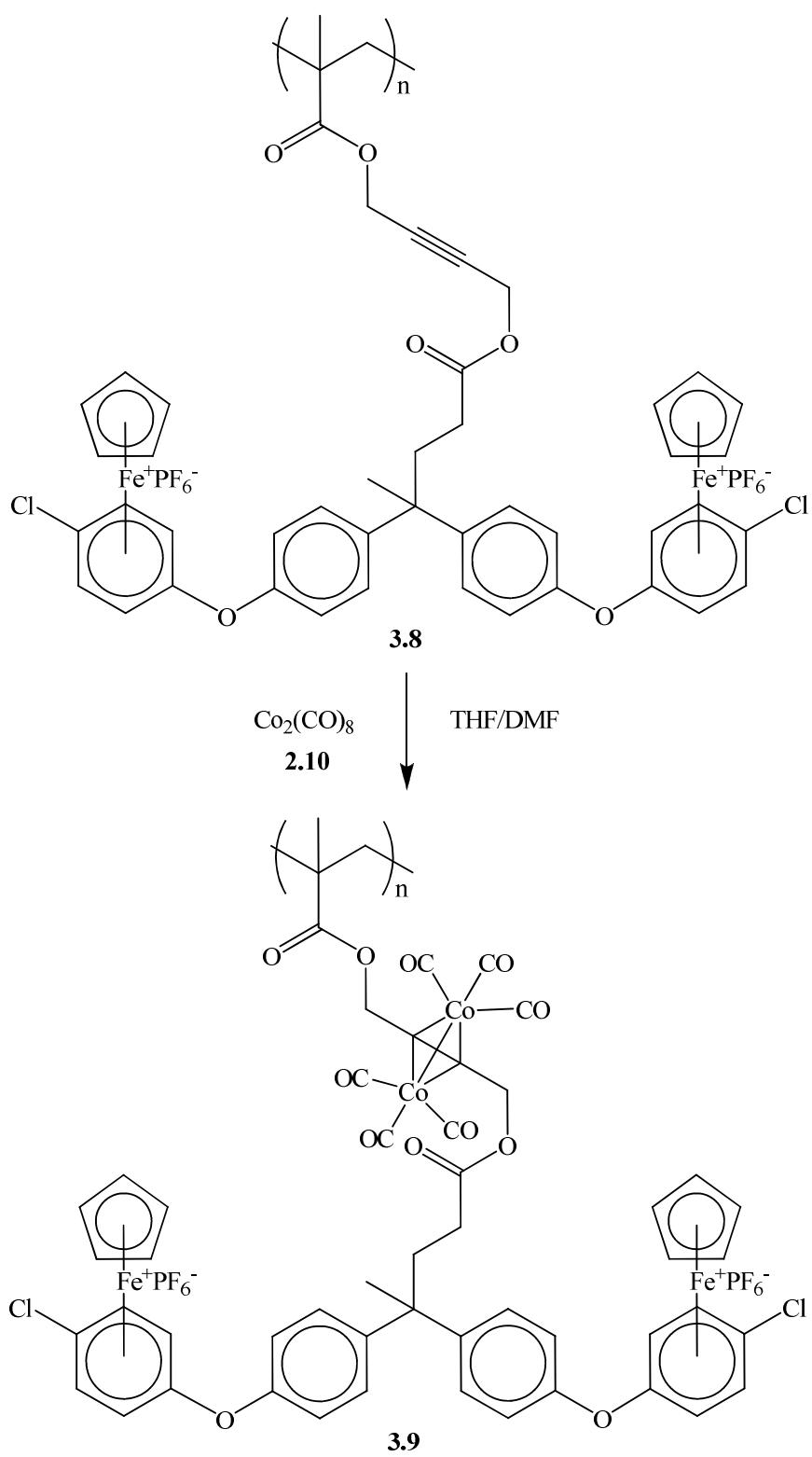


Figure 3.17: ^1H NMR spectrum of polymer **3.8** in acetone- d_6 .

3.3.3 Coordination of cobalt carbonyl to a methacrylate polymer containing two η^6 -arene- η^5 -cyclopentadienyliron(II) moieties

The incorporation of cobalt into the polymer was achieved by first dissolving polymer **3.8** into a THF/DMF mixture and adding dicobalt octacarbonyl (Scheme 3.7), which converted the polymer from a yellow colour to a pink colour. The incorporation of the cobalt was seen with the appearance of the three characteristic IR bands at 2098, 2057 and 2026 cm^{-1} representing the carbonyl groups off the cobalt. The ^1H NMR spectrum indicates that the cobalt was not fully incorporated into the polymer (Figure 3.18). The resonances due to the methylenes

adjacent to alkynes which are complexed to cobalt have shifted to beneath the cyclopentadiene peak, increasing its integration to ~12. The other methylenes which are not influenced by the cobalt remain at ~4.7 ppm. The integrations of these peaks suggest that the cobalt was incorporated into approximately half of the alkyne units of the polymers.



Scheme 3.7: Synthesis of polymer **3.9**.

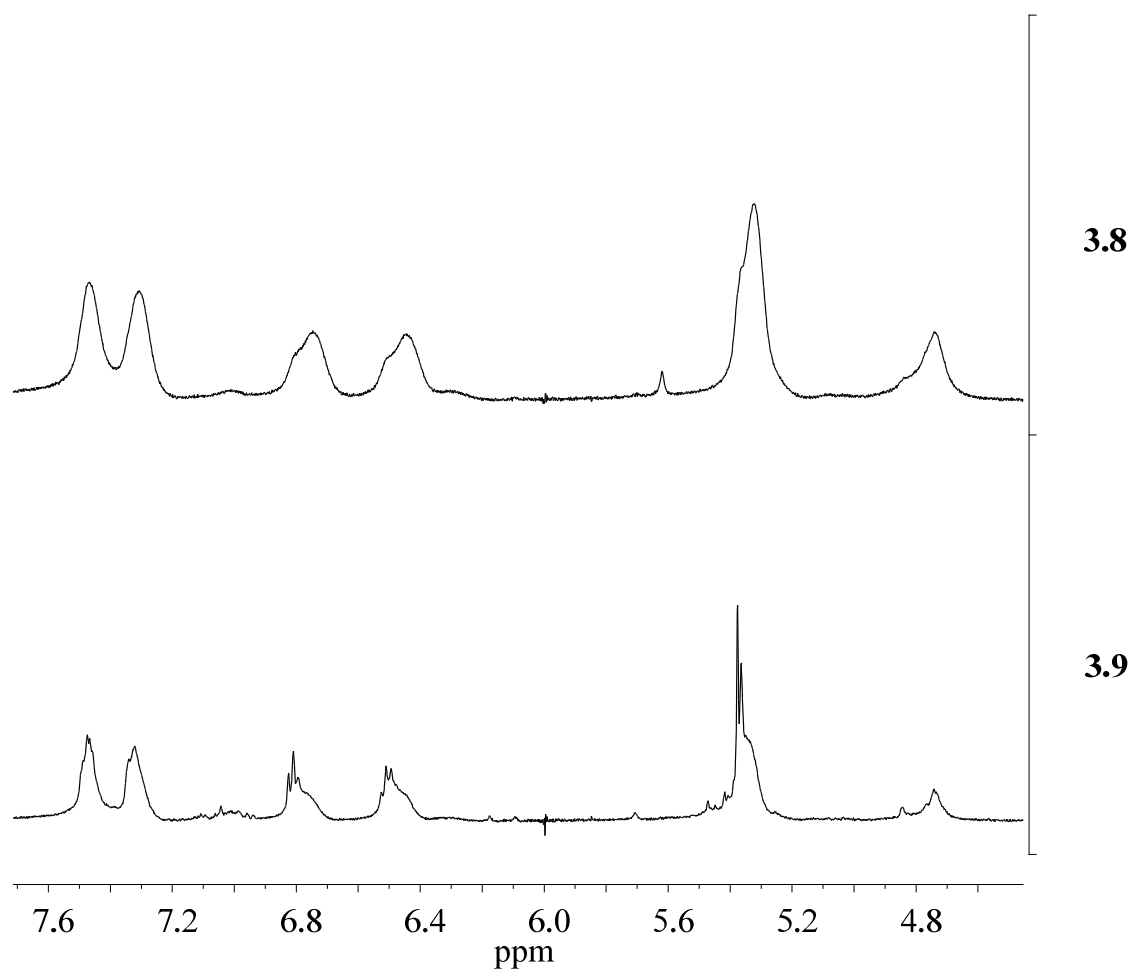
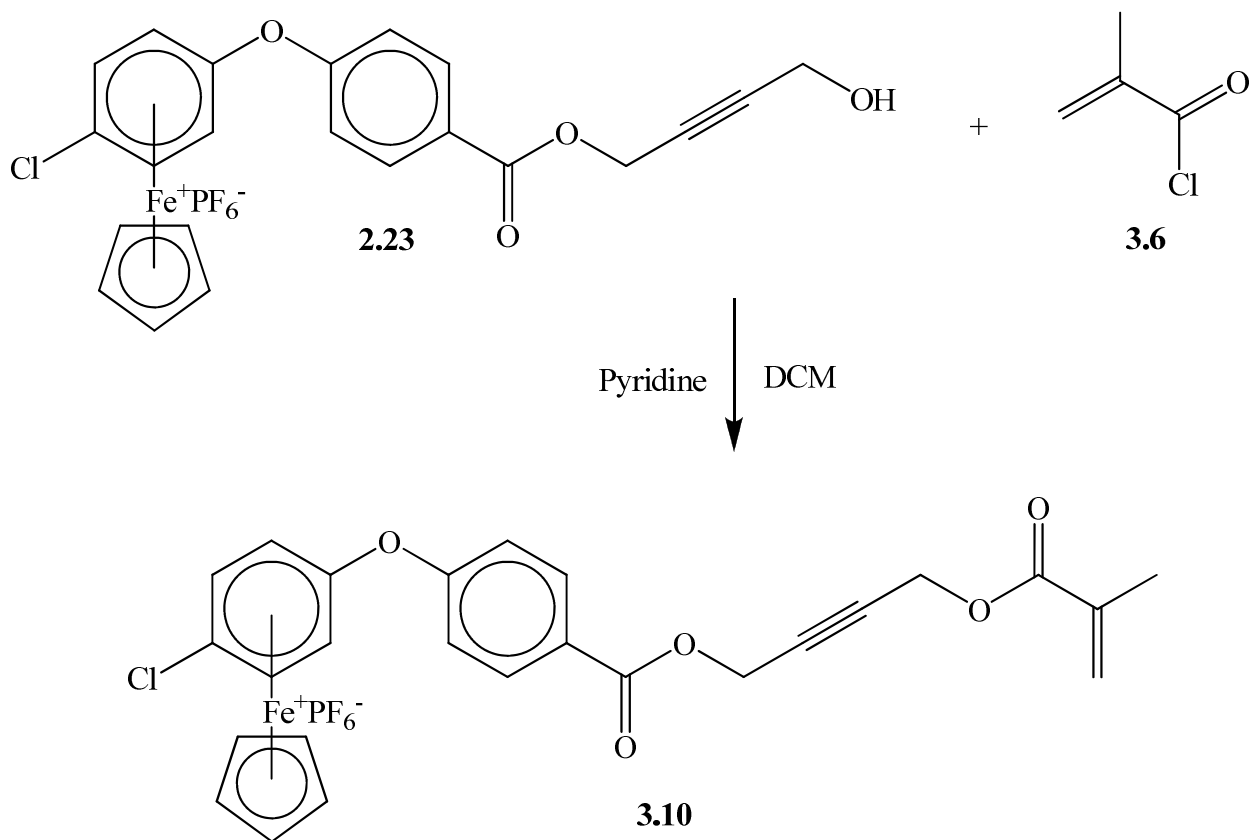


Figure 3.18: ^1H NMR spectral comparison of polymers **3.8** and **3.9** in acetone- d_6 .

3.3.4 Synthesis of a methacrylate monomer containing a single η^6 -arene- η^5 -cyclopentadienyliron(II) moiety

The first step in the synthesis of a polymethacrylate polymer containing containing a single η^6 -arene- η^5 -cyclopentadienyliron moiety and cobalt carbonyl was to react complex **2.23** with methacryloyl chloride (**3.6**) (Scheme 3.8). As polymerization of methacrylate monomer can be initiated both thermally and photically this complex was carefully kept out of the light.



Scheme 3.8: Synthesis of complex **3.10**.

The ^1H NMR spectrum of complex **3.10** appeared as expected for this type of molecule (Figure 3.19). The methacrylate resonances are found at 6.11, 5.72 and 1.92 ppm. The success of the esterification reaction is indicated by the shift of the methylene resonances from 4.26 and 5.01 ppm (complex **2.23**) to 4.88 and 5.06 ppm (complex **3.10**). The sample was not completely pure as it contained a small amount of DCU from the previous reaction and a small amount of starting material. The DCU appeared from 1.00-1.90 ppm and at 2.27 ppm and some starting material is apparent as small peaks in the aromatic and complexed aromatic regions.

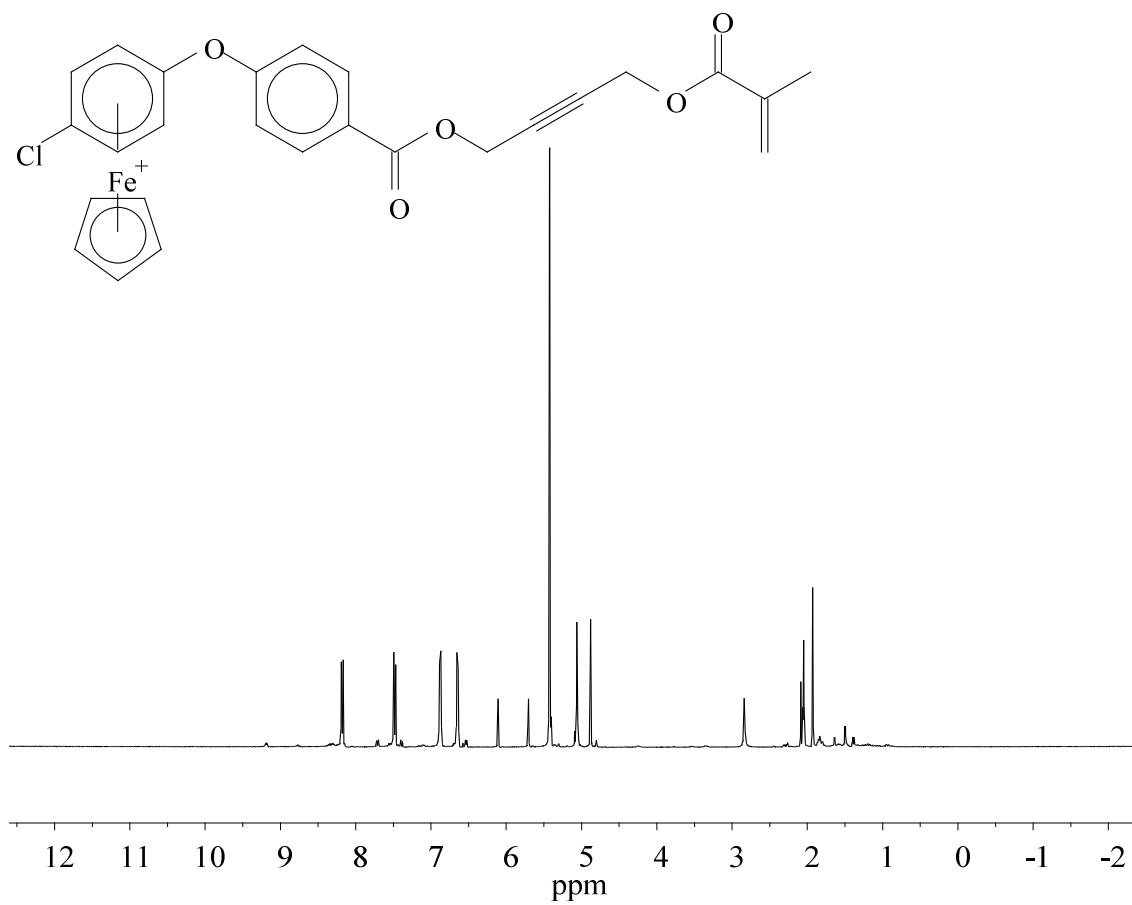


Figure 3.19: ^1H NMR spectrum of complex **3.10** acetone- d_6 .

The ^{13}C NMR spectrum for complex **3.10** also shows the appearance of the four resonances due to the methacrylic ester at 166.01, 136.87, 126.74 and 18.39 ppm (Figure 3.20). The carbon resonance of one of the methylenes was also seen to shift from 53.89 and 50.81 ppm for complex **2.23** to 53.31 and 52.79 ppm for complex **3.10**. The residual DCU and starting material that were seen in the ^1H NMR spectrum are even more obvious in the ^{13}C NMR spectrum. The very small amount of starting material resonates as peaks adjacent to the aromatic peaks while the DCU has resonances at 31.98, 30.76, 26.12, 25.42, 25.20 and 24.69 ppm.

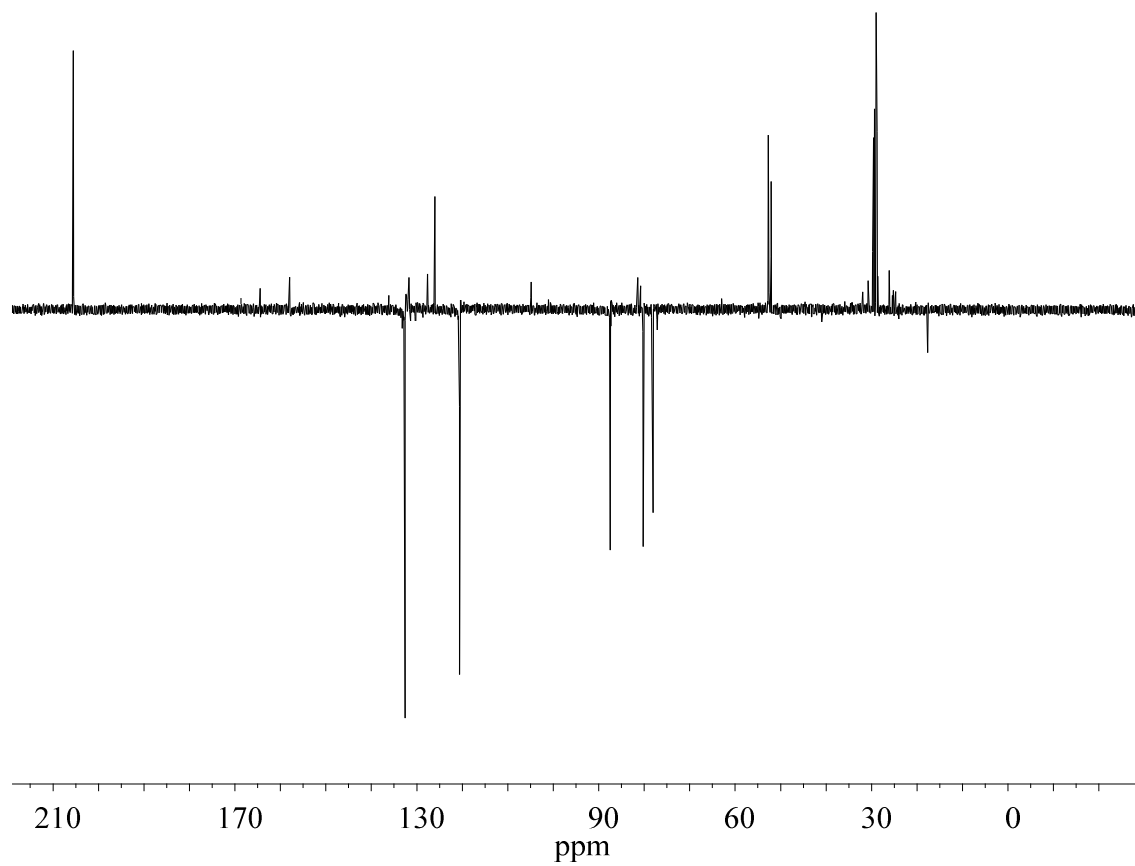
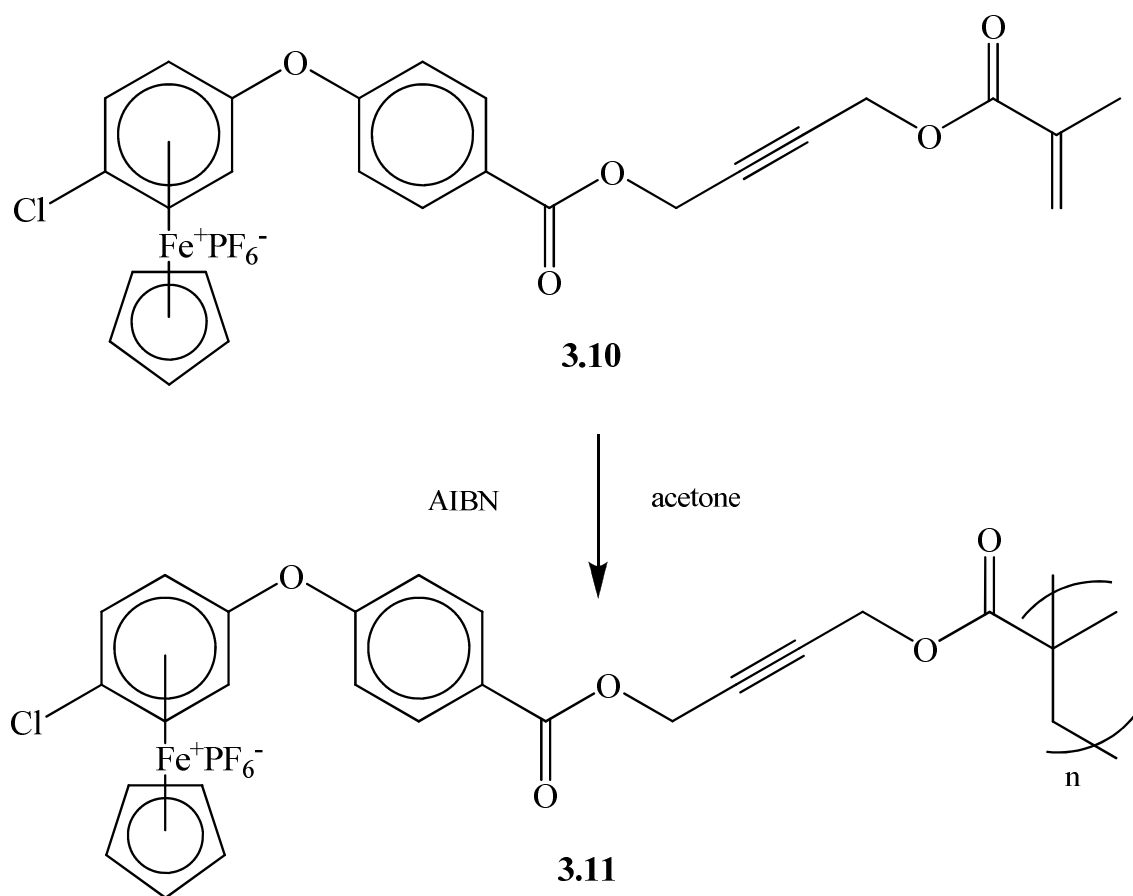


Figure 3.20: APT ^{13}C NMR spectrum of complex **3.10** in acetone- d_6 .

3.3.5 Polymerization of a methacrylate monomer containing a single η^6 -arene- η^5 -cyclopentadienyliron(II) moiety

Radical polymerization of complex **3.10** was initiated with AIBN, giving polymer **3.11** (Scheme 3.9). The molecular weight of this polymer was not determined directly due to the incompatibility of the cationic cyclopentadienyliron unit with the GPC column, however the polymerization was confirmed using NMR spectroscopies. The ^1H NMR spectrum (Figure 3.21) shows that the olefinic peaks of the methacrylate monomer have disappeared as well as a broadening of the resonances as is typical for polymers.



Scheme 3.9: Synthesis of polymer 3.11.

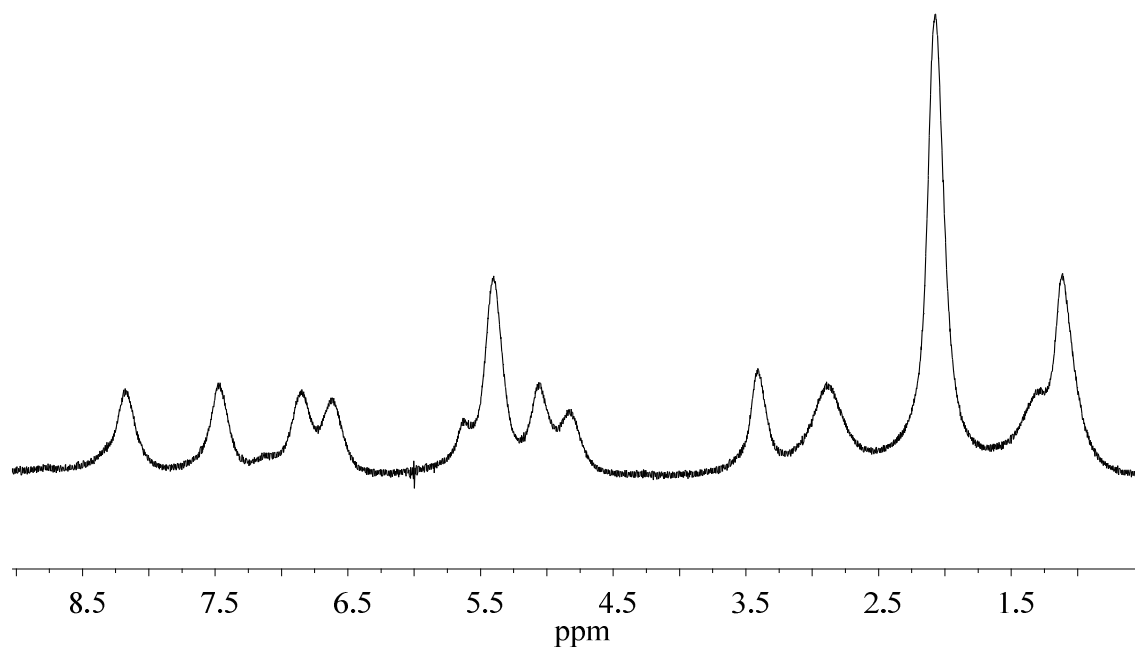
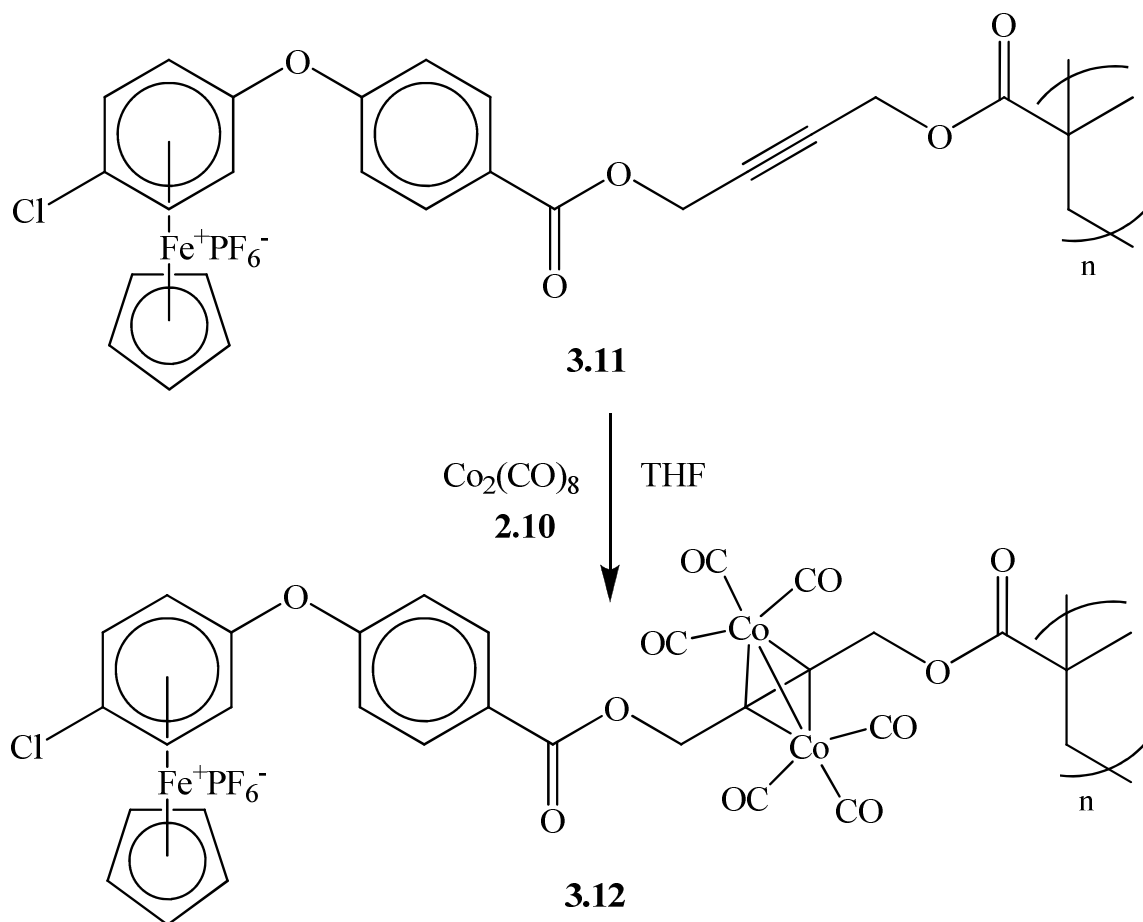


Figure 3.21: ^1H NMR spectrum of polymer **3.11**.

3.3.6 Coordination of cobalt carbonyl to a methacrylate polymer monomer containing a single η^6 -arene- η^5 -cyclopentadienyliron(II) moiety

Polymer **3.11** was reacted with cobalt carbonyl in a THF/DMF solution, giving polymer **3.12** (Scheme 3.10). It was more difficult to purify and analyze this polymer than previously mentioned cobalt containing complexes due to insolubility issues. The IR spectrum for this compound showed peaks at 2103, 2063 and 2032 cm^{-1} indicating partial incorporation of the cobalt carbonyl; however, these bands were not as intense as in the previous cobalt-containing

polymers. The IR spectrum also lacked a peak at $\sim 1830\text{ cm}^{-1}$ for the bridging carbonyls of dicobalt octacarbonyl.



Scheme 3.10: Synthesis of polymer **3.12**.

3.4 Molecular weight determination of polymers

As in chapter 2 the ferrocene based polymer could be put directly into the GPC, while the organic analogues of complexes **3.8** and **3.11** needed to be made (Table 3.1). For the ferrocene polymer **3.4** the $\overline{M}_w = 19\,100$ and $\overline{M}_n = 15\,200$, which is approximately 52 and 42 monomeric units respectively. Pyrolysis at $200\text{ }^\circ\text{C}$ was used to remove the cationic cyclopentadienyliron from polymers **3.8** and **3.11**, where the soluble portions of the polymers were then analyzed by

GPC. The molecular weights of the organic analogues were then used to calculate the molecular weight of the ferrocene and cobalt containing polymer. At best the soluble portions of these polymers can be called oligomers having \overline{M}_w s and \overline{M}_n s ranging from 2 - 9 monomeric units. Unfortunately the soluble portions of the polymer analogues were only 5 - 7 % of the polymer that was pyrolysed, suggesting that higher molecular weight polymers were produced as well.

Table 3.1: Molecular weight data for polymers

Polymer	\overline{M}_w , units	\overline{M}_n , units	PDI
3.4	19 100, 52	15 200, 42	1.3
3.5**	33 900	27 400	1.3
3.8*	3 244, 3	2 342, 2	1.4
3.11*	5 840, 9	5 266, 8	1.1

* The molecular weights of the polymers are estimated from molecular weights of the soluble portions of their analogs after removal of the cationic cyclopentadienyliron moieties. **

Estimated from the molecular weight of the cobalt carbonyl free precursor polymer.

3.5 Thermal analysis of polymers

Thermal analysis of polymers was conducted using TGA and DSC. The TGA data for the polymers is tabulated in

Table 3.2. It can clearly be seen that the cationic organoiron polymers **3.8** and **3.11** began degrade at between 215 and 250 °C due to the decomposition of the cation iron moiety. The cobalt containing analogue **3.9** showed the decomposition of the alkyne-hexacarbonyldicobalt moieties at 120 – 200 °C. For compound **3.12** there was little evidence of the evolution of the

carbonyl groups, this is likely due to only having partial inclusion of the cobalt carbonyl. The ferrocene based polymers were stable up to 263 °C (**3.4**) and 138 °C (**3.5**) due to the decomposition of the ester and alkyne-hexacarbonyldicobalt respectively.

Table 3.2: Thermogravimetric analysis of polymermethacrylates.

Polymer	Step 1 (°C), %	Step 2 (°C), %	Step 3 (°C), %	Step 4 (°C), %
3.4	263 – 309, 14 %	371 – 446, 22%	622 – 673, 9.1 %	
3.5	138 – 189, 10 %	354 – 526, 64 %		
3.8	216 – 247, 21 %	502 – 576, 47 %	600 – 900, 10%	
3.9	120-200, 4 %	216 – 251, 10%	320 – 383, 20 %	400 – 900, 12%
3.11	218 – 250, 29 %	940 – 994, 12 %		
3.12	209 – 246, 15 %	407 – 445, 17 %	707 – 780, 8 %	

Differential scanning calorimetry showed that the polymers displayed glass transition temperatures between 78 and 138 °C (Table 3.3). No glass transition temperatures could be found for the alkyne-hexacarbonyldicobalt containing polymers until after the carbonyl groups had been thermally driven off.

Table 3.3: Differential scanning calorimetry of organoiron polymethacrylates.

Polymer	T _g (°C)	T _g [*] (°C)
3.4	78	
3.5	Not found	92
3.8	86	
3.9	Not found	92
3.11	130	
3.12	Not found	138

T_g^{*} was taken from a second run, after the CO groups had been removed.

3.6 Summary

A number of polymethacrylates containing two different organometallic moieties were prepared. The polymers possessed a combination of either ferrocene and Co₂(CO)₆ or cationic cyclopentadienyliron moieties and Co₂(CO)₆. They were prepared by coordinating Co₂(CO)₆ with pre-prepared organoiron polymethacrylates containing alkyne moieties. The cobalt moieties were added post polymerization since the alkyne Co₂(CO)₆ complexes were found to be incompatible with radical polymerization. Gel permeation chromatography indicated that the polymers possessed MWs between 3 244 and 33 900, with PDIs between 1.1 and 1.4. Thermal analysis showed the polymers displayed glass transition temperatures between 78 and 138 °C.

3.7 Detailed experimental

All reactions and complexes containing a η^6 -aryl- η^5 -cyclopentadienyl iron hexafluorophosphate moiety were kept in the dark to prevent decomposition.

Synthesis of complex 3.2

Compound **2.6** (1.087 g, 3.4 mmol), methacrylic acid (**3.1**) (0.40 mL, 4.7 mmol), DCC (0.8145 g, 3.95 mmol), DMAP (0.4893 g, 4 mmol), 15 mL DCM were stirred under nitrogen for 18 hours. The reaction was then cooled to -10 °C and a fine white precipitate of DCU was filtered out of the solution. The filtrate was diluted with 150 mL of DCM, washed with 200 mL of 1.2 M HCl solution, dried with MgSO₄ and the DCM was removed *in vacuo* leaving an orange liquid that was purified using silica chromatography using ether:hexanes 6:4 as the eluent. The solvent mixture was removed *in vacuo* leaving an orange liquid with a yield of 0.8851 g (71 % yield).

¹H NMR (400 MHz, CDCl₃) δ = 6.14 (dq, J =1.6, 1.0, 1H), 5.58 (p, J =1.6, 1H), 4.84 (t, J =1.8, 2H), 4.82 (NFO t, J =1.9, 2H), 4.80 (t, J =1.8, 2H), 4.40 (NFO t, J =1.9, 2H), 4.22 (s, 5H), 1.92 (dd, J =1.5, 1.0, 3H). ¹H NMR (400 MHz, acetone) δ = 6.10 (dq, J =1.6, 1.0 1H), 5.67 (p, J =1.6, 1H), 4.90 (t, J =1.8, 2H), 4.87 (t, J =1.8, 2H), 4.80 (NFO t, J =1.9, 2H), 4.48 (NFO t, J =1.9, 2H), 4.26 (s, 5H), 1.91 (dd, J =1.5, 1.0 3H)

¹³C NMR (101 MHz, CDCl₃) δ = 171.27, 166.76, 135.77, 126.82, 81.69, 80.56, 71.85, 70.50, 70.08, 69.95, 52.63, 51.88, 18.49.

IR 1714 cm⁻¹ (C=O)

Synthesis of complex 3.3

In a N₂ environment, complex **3.2** (0.3676 g, 1 mmol) was dissolved in THF and 0.4205 g (1.2 mmol) of Co₂(CO)₈ (**2.10**) was added to this stirring solution. Upon the addition of Co₂(CO)₈, the solution turned from orange to red accompanied with the evolution of CO from the solution. After 1 hour the evolution of CO₂ stopped. However, the solution was allowed to stir for an additional 5-12 hours to ensure the full incorporation of the cobalt. The THF was removed in vacuo and the red residue was dissolved in 100 mL of acetone, after 5 min a small amount of brown precipitate formed, which was filtered from the solution. The acetone was then removed in vacuo leaving 0.6299 g (97 % yield) of a dark red solid. Crystals suitable for X-ray diffraction were then grown by slow evaporation from acetone.

¹H NMR (400 MHz, acetone-*d*₆) δ = 6.20 (dq, *J*=1.6, 1.0, 1H), 5.71 (p, *J*=1.6, 1H), 5.54 (s, 2H), 5.51 (s, 2H), 4.85 – 4.83 (NFO t, 2H), 4.50 – 4.48 (NFO t, 2H), 4.25 (s, 5H), 1.98 (dd, *J*=1.6, 1.0, 3H).

¹³C NMR (101 MHz, acetone-*d*₆) δ = 171.71, 167.40, 137.13, 126.53, 91.69, 72.37, 71.78, 70.95, 70.61, 65.82, 65.76, 18.49.

IR 1713 cm⁻¹ (C=O), 2022 cm⁻¹, 2053 cm⁻¹, 2096 cm⁻¹ (CoC≡O)

Synthesis of polymer 3.4

Complex 3.2 (0.4630 g, 0.71 mmol) and 0.0181 g (0.11 mmol) of AIBN and 2 mL of DMF were stirred for 18 hours at 70 °C. The contents of the reaction flask were then added to 100 mL of methanol and placed in the freezer. The precipitate was then collected and washed further with methanol to remove the lower molecular weight monomers and polymers

^1H NMR (400 MHz, CDCl_3) δ = 4.85 (br. s, 4H), 4.65 (br. s, 2H), 4.42 (br. s, 2H), 4.22 (br. s, 5H), 1.84 (br. s, 2H), 1.60 (br. s, 2H), 1.07 (br. s, 1H), 0.93 (br. s, 1H).

IR 1714 (C=O)

Synthesis of polymer 3.5

Under nitrogen, polymer **3.4** (0.0712 g) was dissolved in 30 mL dry THF and dicobalt octacarbonyl (0.0651 g) was added. After 30 minutes of stirring carbon monoxide stopped evolving from the reaction. The reaction was concentrated to 10 mL of THF and 50 mL of acetone was added. A small amount of precipitate was filtered from the solution and the solvent was removed from the filtrate *in vacuo*.

^1H NMR (400 MHz, CDCl_3) δ = 5.35 (br. s, 2H), 5.06 (br. s, 2H), 4.83 (br. s, 2H), 4.40 (br. s, 2H), 4.20 (br. s, 5H), 2.02 (br. s, 1H), 1.64 (br. s, 2H), 1.38 (br. s, 1H), 1.05 (br. s, 1H), 0.82 (br. s, 0H).

IR 1712 (C=O), 2023 cm^{-1} , 2054 cm^{-1} , 2096 cm^{-1} (CoC \equiv O)

Synthesis of complex 3.7

Complex **2.17** (1.1887 g, 1 mmol) was dissolved in 20 mL DCM, 15 drops of pyridine and methacryloyl chloride (**3.6**) (0.21 mL, 2 mmol) were added. The reaction mixture was stirred for 18 hours under N_2 in the dark. After 18 hours the solvent was removed *in vacuo* to give a yellow film. The film was dissolved in acetone and precipitated into H_2O with 0.173 g NH_4PF_6 . The light yellow precipitate was collected and allowed to dry under reduced pressure for 24 hours.

1.1551 g, (98 % yield).

^1H NMR (400 MHz, acetone- d_6) δ = 7.48 (d, J =8.8, 4H), 7.33 (d, J =8.8, 4H), 6.81 (d, J =6.4, 4H), 6.51 (d, J =6.4, 4H), 6.10 (dd, J =1.5, 1.0, 1H), 5.72 – 5.68 (m, 1H), 5.45 – 5.33 (m, 10H), 4.84 (t, J =1.8, 2H), 4.75 (t, J =1.8, 2H), 2.59 – 2.53 (m, 2H), 2.27-2.21 (m, 2H), 1.92 (dd, J =1.6, 1.0, 3H), 1.76 (s, 3H).

^{13}C NMR (101 MHz, acetone- d_6) δ = 173.00, 166.11, 152.37, 147.98, 136.89, 134.03, 130.75, 126.77, 121.41, 105.07, 88.02, 81.83, 81.73, 80.62, 77.37, 52.80, 52.58, 46.44, 37.18, 29.73, 27.94, 18.38.

IR 1730 cm^{-1} (C=O)

Synthesis of polymer 3.8

Complex **3.7** (1.1439, 0.9 mmol) and AIBN (0.0381 g, 0.30 mmol) were dissolved in acetone (10 ml) and refluxed under N_2 for 18 hours. The reaction was then quenched in 100 mL of 1.2 M HCl containing NH_4PF_6 collected via filtration. The precipitate was triturated in DCM to remove unreacted monomer. The residual polymer was redissolved in acetone and precipitated into ether, giving 0.9926 g of polymer.

^1H NMR (400 MHz, acetone- d_6) δ = 7.47 (br. s, 4H), 7.31 (br. s, 4H), 6.75 (br. s, 4H), 6.44 (br. s, 4H), 5.33 (br. s, 10H), 4.74 (br. s, 4H), 2.54 (br. s, 3H), 2.23 (br. s, 3H), 1.73 (br. s, 4H), 1.47 – 0.79 (m, 4H).

IR 1732 cm^{-1} broad (C=O)

Synthesis of polymer 3.9

Polymer **3.8** (0.2586 g), THF (15 mL) and 0.1330 g (0.4 mmol) $\text{Co}_2(\text{CO})_8$ (**2.10**) were combined in an inert atmosphere chamber. To the rapidly stirring solution 1 mL of DMF was

added to dissolve the polymer and rapid evolution of gas occurred, the reaction mixture was stirred for 18 hours under N₂. The THF was removed *in vacuo* and the residual reaction mixture precipitated into ether. The precipitated was collected and dissolved into acetone to facilitate the removal of unwanted cobalt carbonyl by products. The solution was filtered through celite several times to remove the unwanted precipitated. The acetone was removed *en vacuo* to yield 0.2519 g of the pure polymer.

¹H NMR (400 MHz, acetone-*d*₆) δ = 7.47 (bs, 4H), 7.32 (bs, 4H), 6.82 (m, 4H), 6.51 (m, 4H), 5.37 (m, 12H), 4.74 (s, 2H), 2.56 (s, 3H), 2.25 (s, 3H), 1.75 (bs, 4H), 1.50 – 0.79 (m, 3H).

IR 2098 cm⁻¹, 2057 cm⁻¹, 2026 cm⁻¹ (C≡O), 1737 cm⁻¹ (C=O)

Synthesis of complex 3.10

Complex **2.23** (1.08 g, 2 mmol) was dissolved in 20 mL DCM, 15 drops of pyridine and methacryloyl chloride (0.37 mL, 4 mmol) (**3.6**) were added. The reaction mixture was stirred for 18 hours under N₂ in the dark. After 18 hours the solvent was removed *in vacuo* to give a yellow film. The film was dissolved in acetone and precipitated into H₂O with NH₄PF₆. The light yellow precipitate was collected and allowed to dry under reduced pressure for 24 hours. The yield was 1.0761 g (83 % yield).

¹H NMR (400 MHz, acetone-*d*₆) δ = 8.17 (d, *J*=8.7, 2H), 7.48 (d, *J*=8.7, 2H), 6.87 (d, *J*=6.8, 2H), 6.66 (d, *J*=6.8, 2H), 6.11 (s, 1H), 5.75 – 5.68 (m, 1H), 5.42 (s, 5H), 5.06 (t, *J*=1.7, 2H), 4.88 (t, *J*=1.6, 2H), 1.96 – 1.90 (m, 3H).

¹³C NMR (101 MHz, acetone-*d*₆) δ = 166.04, 165.18, 158.73, 136.87, 133.33, 132.47, 132.12, 130.96, 129.39, 128.41, 126.74, 121.35, 105.61, 88.19, 82.16, 81.53, 80.92, 78.79, 53.41, 52.79, 18.39. DCU at 31.98, 30.76, 26.12, 25.42, 25.20, 24.69.

IR 1735 cm^{-1} , 1730 cm^{-1} (C=O)

Synthesis of polymer 3.11

Complex **3.10** (0.4244 g, 0.6 mmol) and AIBN (0.0277 g, 0.2 mmol) were dissolved in acetone (5 ml) and refluxed under N_2 for 18 hours. The reaction was then quenched in 100 mL of 1.2 M HCl containing NH_4PF_6 collected via filtration. The precipitate was triturated in DCM to remove unreacted monomer and low molecular weight oligomers. The residual polymer was re-dissolved in acetone and precipitated into ether. Yielding 0.4114 g of polymer.

^1H NMR (400 MHz, acetone- d_6) δ = 8.15 (br. s, 1H), 7.44 (br. s, 1H), 6.82 (br. s, 1H), 6.59 (br. s, 1H), 5.38 (br. s, 3H), 5.04 (br. s, 1H), 4.79 (br. s, 1H), 3.39 (br. s, 2H), 2.09 (br. s, 5H), 1.09 (br. s, 4H).

IR 1737 cm^{-1} (C=O)

Synthesis of polymer 3.12

Polymer **3.11** (0.0498 g, 0.07 mmol), THF (15 mL) and $\text{Co}_2(\text{CO})_8$ (**2.10**) (0.0535 g, 0.16 mmol) were combined in an inert atmosphere chamber. To the rapidly stirring solution 1 mL of DMF was added to dissolve the polymer and rapid evolution of gas occurred, the reaction mixture was stirred for 18 hours under N_2 . The THF was removed *in vacuo* and the residual reaction mixture precipitated into ether. The precipitated was collected and dissolved into acetone to facilitate the removal of an unwanted precipitate. The solution was filtered through celite several times to remove the precipitate and acetone was removed *in vacuo* to yield 0.0273 g of the polymer.

IR 1720 cm^{-1} (C=O), 2103 cm^{-1} , 2063 cm^{-1} , 2032 cm^{-1} (CoC \equiv O)

Pyrolysis of complexes 3.8 and 3.11

Polymers **3.8** and **3.11** were individually placed in a pyrolysis chamber at 200 °C under vacuum for 30 min. The polymers were then triturated with water, filtered and allowed to dry for 24 hours over vacuum. Preparation for GPC involved dissolving the polymers in THF and filtering through a 45 micron nylon filter, before injection onto the column.

Chapter 4: Condensation polymers

4.1 Introduction

Condensation polymerization is a powerful tool that can attach monomers together via a condensation reaction. Perhaps the most well known condensation polymerization is that between adipic acid and 1,6-hexanediamine that produces nylon-6,6. As was discussed in chapter 1, η^6 -halo-arene- η^5 -cyclopentadienyliron(II) hexafluorophosphate salts are highly susceptible to nucleophilic aromatic substitution to form ethers, thioethers and di-substituted amines.^{12, 17, 18, 21, 21} This high susceptibility to nucleophilic aromatic substitution means that the incorporation of η^6 -halo-arene- η^5 -cyclopentadienyliron(II) hexafluorophosphate salts into various monomers can allow for the formation of a large number of condensation polymers.^{12, 20, 48, 71}

Work performed by previous members of the Abd-El-Aziz group has shown that there are two main strategies that use η^6 -arene- η^5 -cyclopentadienyliron(II) hexafluorophosphate salts to afford condensation polymers.^{12, 20, 48, 71-74} The first strategy uses various aliphatic and aromatic dithiols, as well as, aromatic diol complexes that are reacted with η^6 -p-dichlorobenzene- η^5 -cyclopentadienyliron(II) hexafluorophosphate to afford various polymers of the form in Figure 4.1. The second strategy requires the synthesis of molecules with two terminal η^6 -chloro-arene- η^5 -cyclopentadienyliron(II) hexafluorophosphate salts which could then be reacted with various dithiols, diamines, or diphenols to give polymers of the form in Figure 4.2.^{12, 48, 75} Figures 4.1 and 4.2 show that many different polymers can be synthesized and numerous moieties can be incorporated, with azo dyes and ferrocene providing only two of the possible examples.

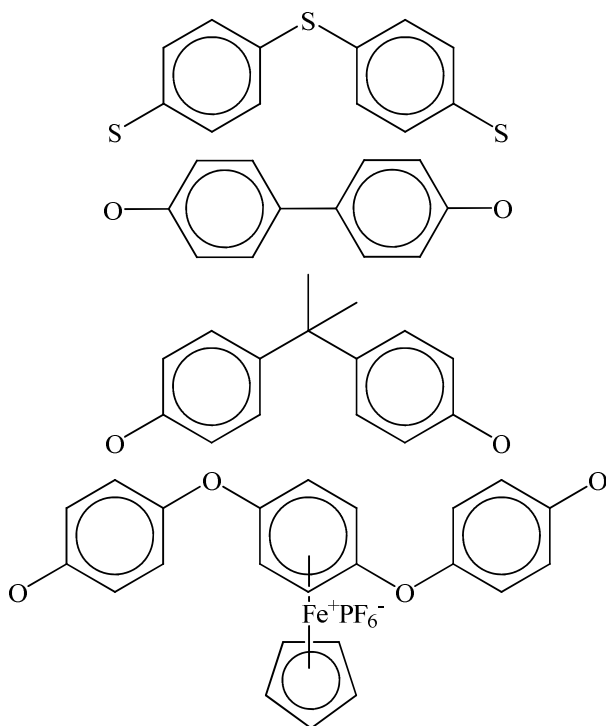
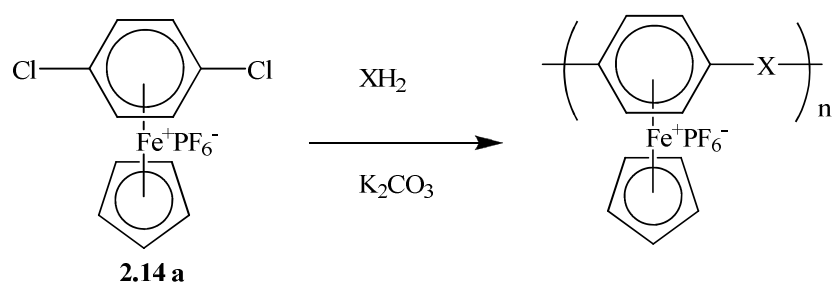


Figure 4.1: Previously reported condensation polymers of η^6 -arene- η^5 -cyclopentadienyliron(II) hexafluorophosphate salts.

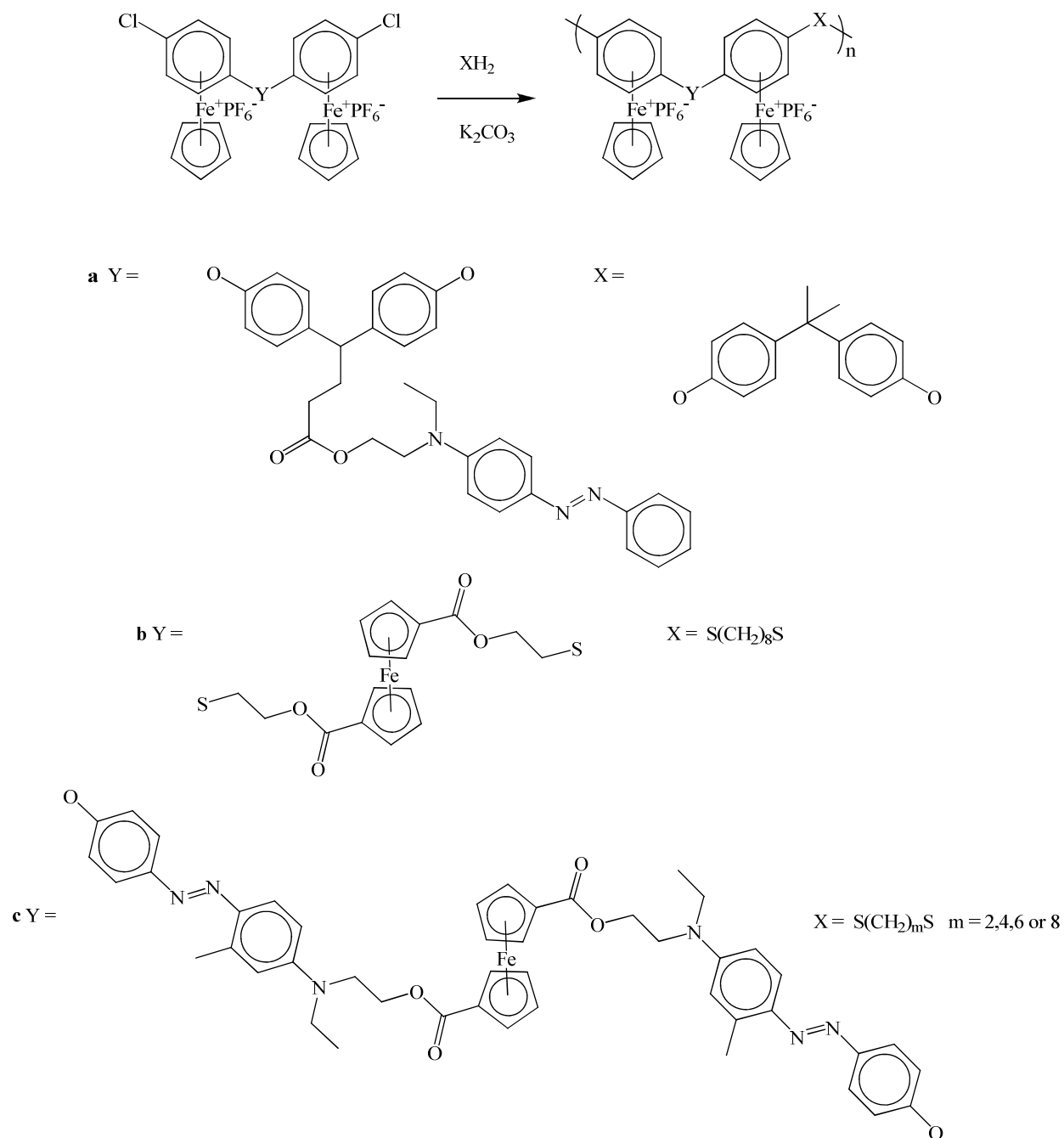


Figure 4.2: Previously reported condensation polymers of η^6 -arene- η^5 -cyclopentadienyliron(II) hexafluorophosphate salts.

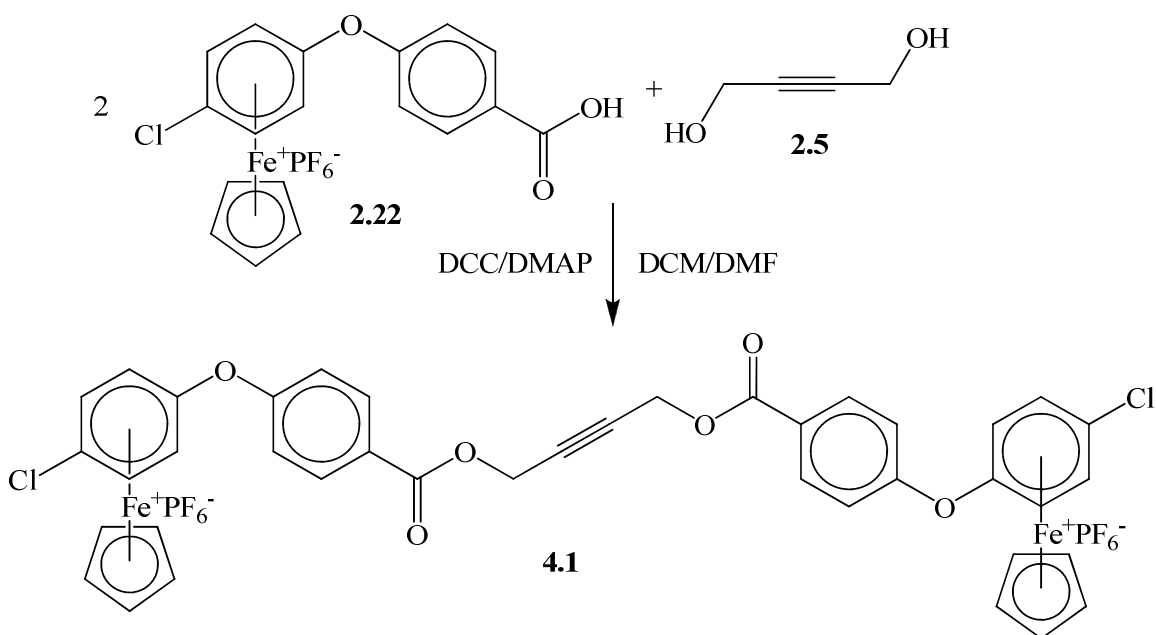
In this chapter, monomers containing alkyne groups or alkyne coordinated dicobalt hexacarbonyl moieties with two terminal η^6 -chloro-arene- η^5 -cyclopentadienyliron(II)

hexafluorophosphate salts will be reacted with dithiols and bisphenol A to give condensation polymers via the second strategy.

4.2 Synthesis and characterization of condensation polymers containing η^6 -arene- η^5 -cyclopentadienyliron(II) and cobalt carbonyl

4.2.1 Synthesis of a monomer containing η^6 -arene- η^5 -cyclopentadienyliron(II) and alkyne moieties

An alkyne-containing complex with two terminal η^6 -chloro-arene- η^5 -cyclopentadienyliron(II) hexafluorophosphate salts (**4.1**) was prepared through the reaction of 2-butyne-1,4-diol (**2.5**) with two equivalents of complex **2.22** (Scheme 4.1). This complex is quite similar to that of **2.23** where only one of the alcohols of the 2-butyne-1,4-diol were reacted.



Scheme 4.1: Synthesis of complex **4.1**.

The ^1H NMR spectrum for complex **4.1** shows all of the expected resonances and confirms that the 2-butyne-1,4-diol has been reacted through both alcohols (Figure 4.3). Identification of the methylene resonances for these two complexes are very similar and spectrally the main differences between these complexes is that for **4.1** the methylenes appear as a singlet at 5.11 ppm rather than two sets of triplets at 5.01 and 4.26 ppm. The non-complexed arene hydrogens resonate as doublets at 8.12 and 7.45 ppm, while the complexed arene hydrogens resonate as doublets at 6.85 and 6.57 ppm. The cyclopentadienyliron hydrogens resonate as a sharp singlet at 5.30 ppm.

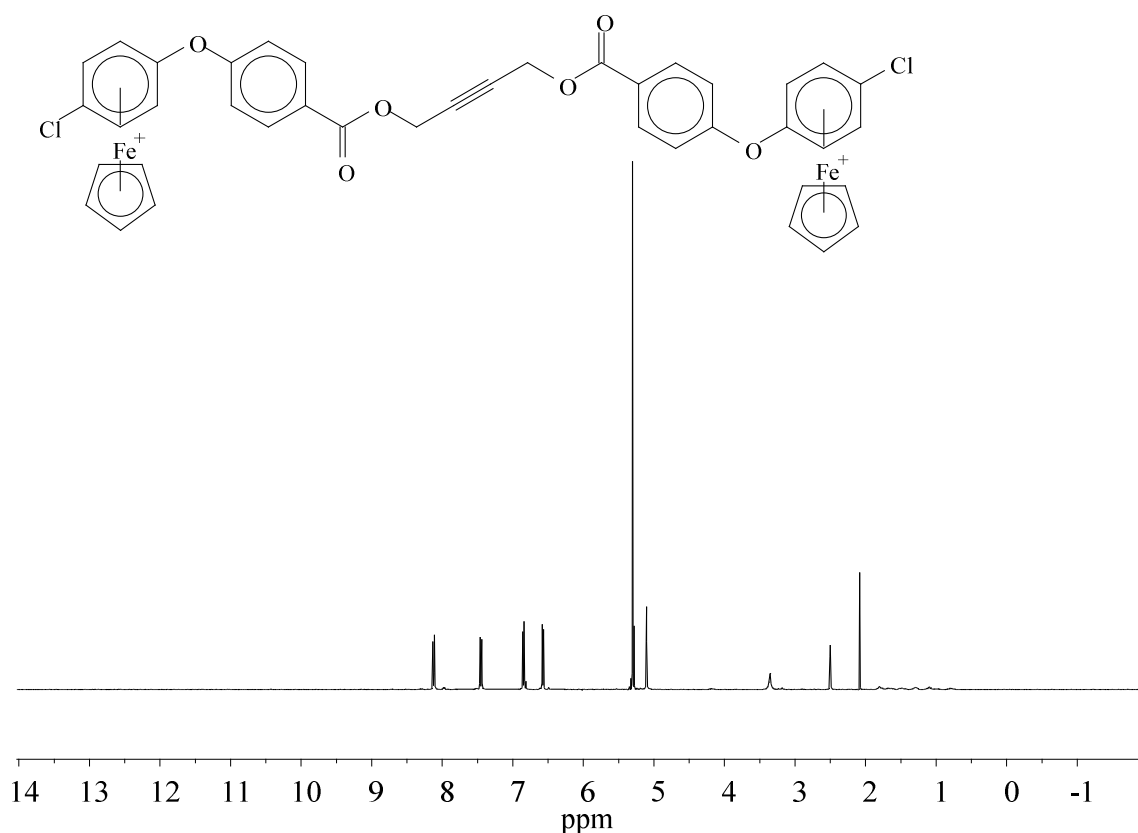


Figure 4.3: ^1H NMR spectrum of complex **4.1** in $\text{DMSO}-d_6$.

The ^{13}C NMR spectrum for complex **4.1** contains all of the expected peaks (Figure 4.4). This spectrum is also very similar to that of complex **2.17**, with a similar pattern of peaks. The

resonance for the carbonyl carbon appears at 164.17 ppm. The non-complexed arenes have resonances at 157.65, 132.16, 130.44 and 120.37. While the complexed arene has resonances at 126.44, 104.11, 86.92 and 77.75 ppm. The complexed cyclopentadiene appears at 79.58 ppm and the alkyne carbons resonate at 81.34 ppm. The methylenes were found at 52.70 ppm. There is also a small amount of DCU and DCC present in the sample, 154.13, 135.50, 53.60, 49.01, 31.28, 30.31, 25.51, 25.10, 24.93 and 24.07 ppm. The typical process used for the removal of DCU involves dissolving the sample in small amounts of acetone or DCM, followed by cooling to -10 °C for 2 hours followed by filtering out any DCU crystals formed. Unfortunately complex **4.1** was not as soluble in acetone or DCM as previous complexes making it necessary to use slightly more solvent and resulting in the retention of a small amount of impurities.

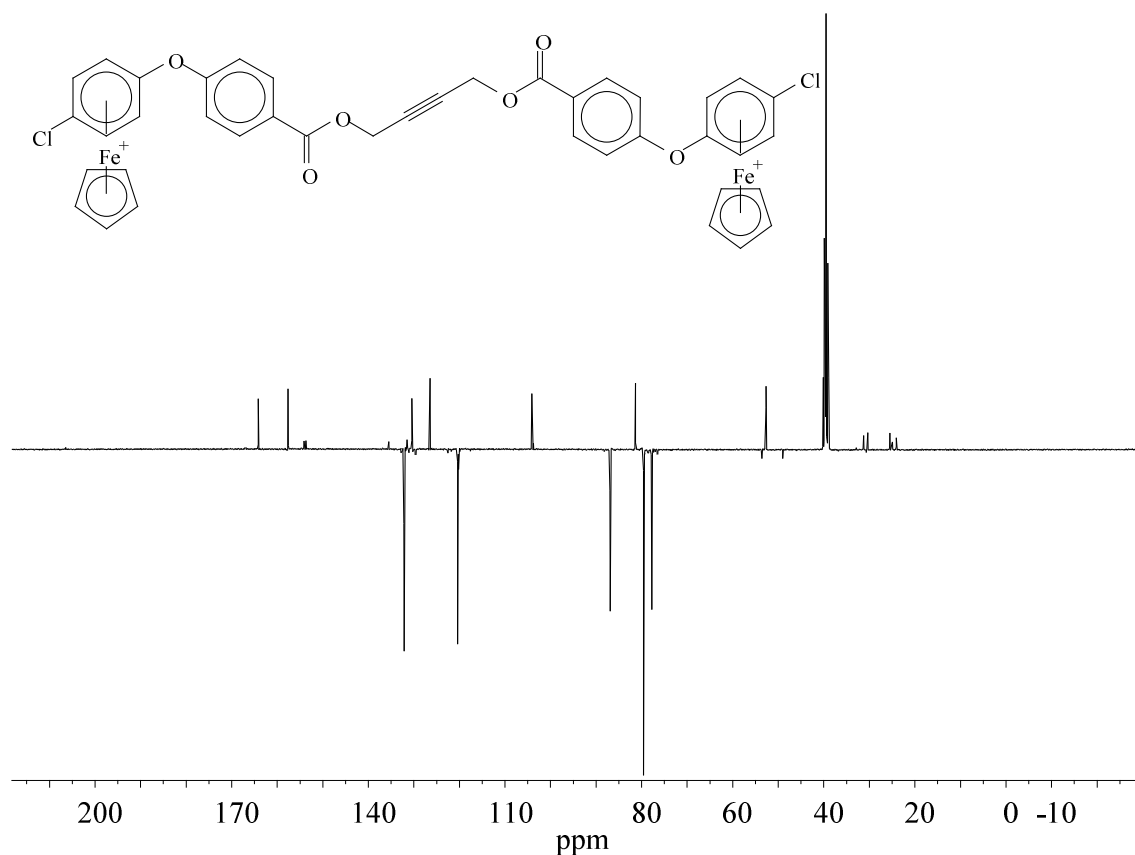
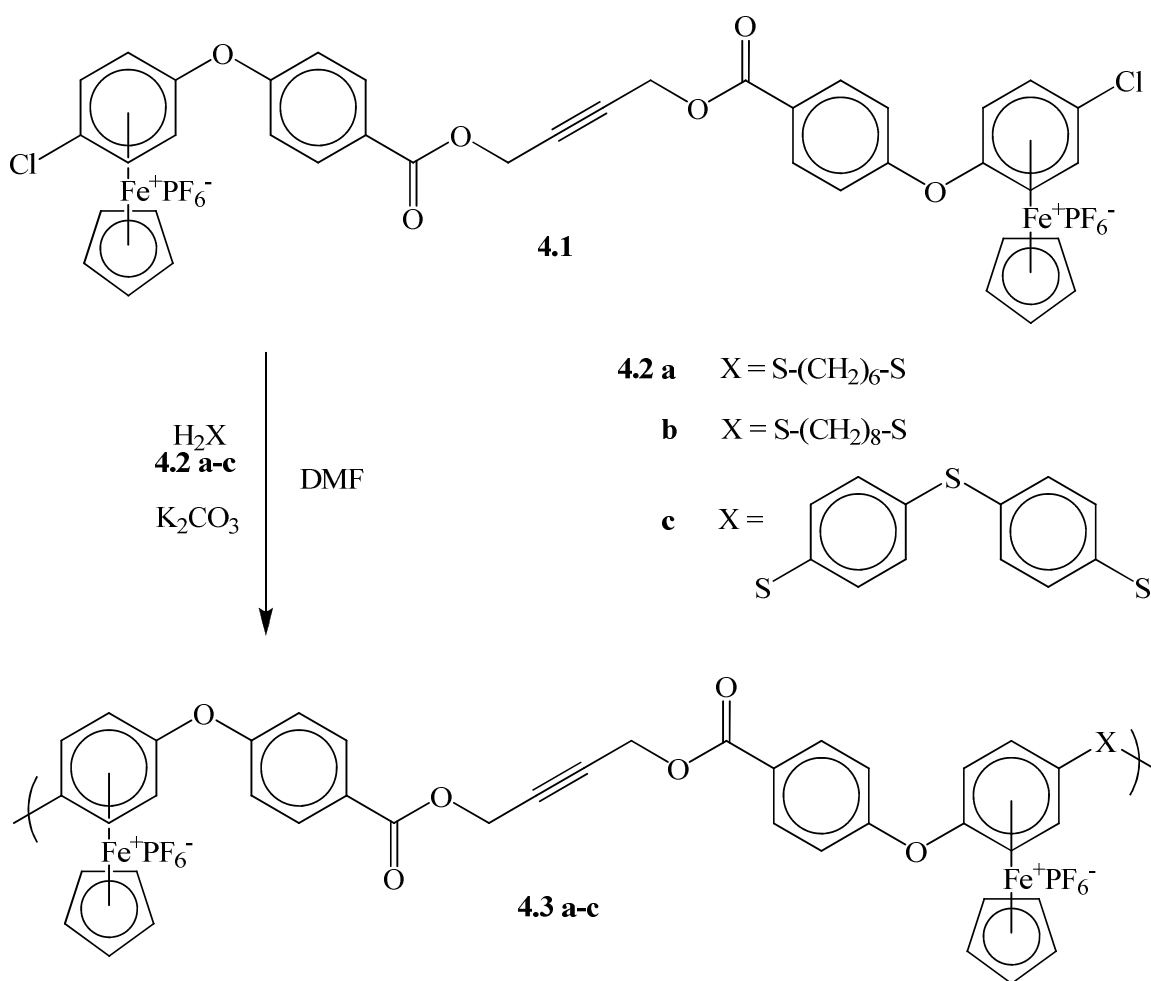


Figure 4.4: APT ^{13}C NMR spectrum of complex **4.1** in $\text{DMSO-}d_6$.

4.2.2 Condensation polymerization of a monomer containing η^6 -arene- η^5 -cyclopentadienyliron(II) and alkyne moieties with dithiol linkers

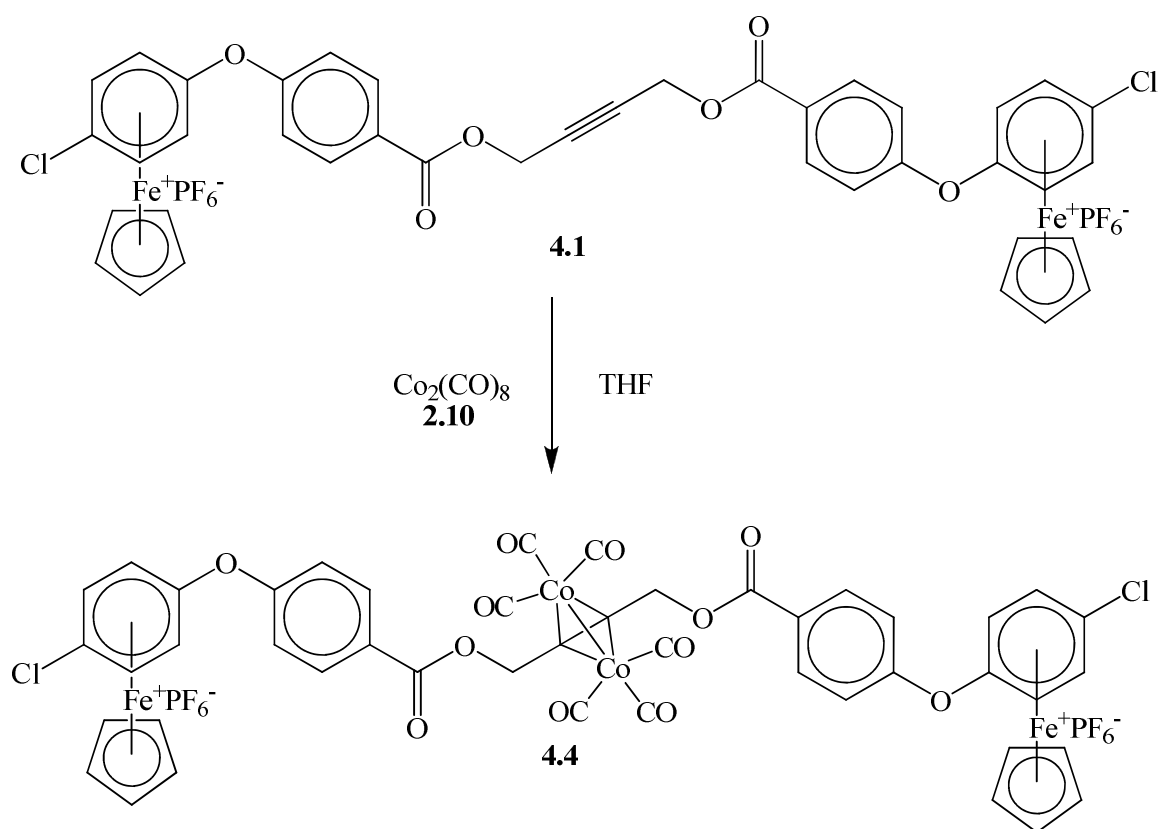
Condensation of complex **4.1** with various dithiols **4.2 a-c** produced polymers **4.3 a-c** (Scheme 4.2). These polymers showed a significant change in solubility compared to the monomers. While the monomers had been soluble in DCM, acetone, DMSO, and acetonitrile, the polymers would not dissolve in these solvents. Due to these insolubility issues no NMR spectral analysis or molecular weight determination could be done on polymers **4.3 a-c**.



Scheme 4.2: Synthesis of polymers **4.3 a-c**.

4.2.3 Coordination of cobalt carbonyl to a monomer containing η^6 -arene- η^5 -cyclopentadienyliron(II) and alkyne moieties

Dicobalt octacarbonyl was coordinated to the alkyne of complex **4.1** to give monomer **4.4** which contained η^6 -arene- η^5 -cyclopentadienyliron(II) and dicobalt hexacarbonyl alkyne moieties (Scheme 4.3). The complexes were isolated as red solids and characterized through NMR and IR spectroscopies.



Scheme 4.3: Synthesis of complex **4.4**.

^1H NMR spectrum of complex **4.4** shows the inclusion of the cobalt carbonyl with the downfield shift of the methylene protons to 5.67 ppm (Figure 4.5). The ^{13}C NMR spectrum also confirms the full inclusion of the cobalt carbonyl with the shift of the methylene resonance to 55.7 ppm and the shift of the alkyne carbon resonance to 90.1 ppm (Figure 4.6). There is also the

appearance of a resonance at 200 ppm due to the Co-CO carbons. Neither of the NMR spectra for this compound are pure, both contain the DCU and DCC peaks that were present in the starting material as well as a very small amount of material that did not have complex **2.22** attached to both sides of the 2-butyne-1,4-diol (**2.5**).

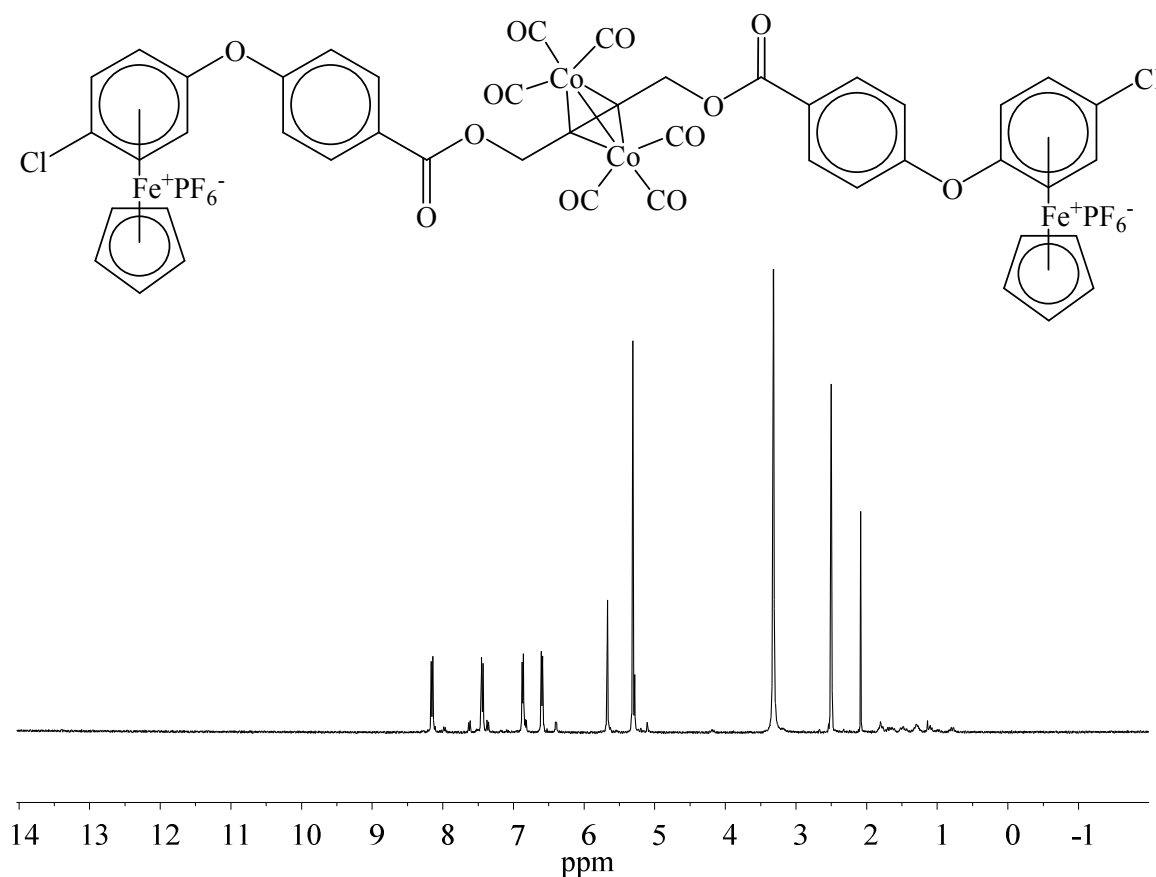


Figure 4.5: ^1H NMR of complex **4.4** in $\text{DMSO-}d_6$.

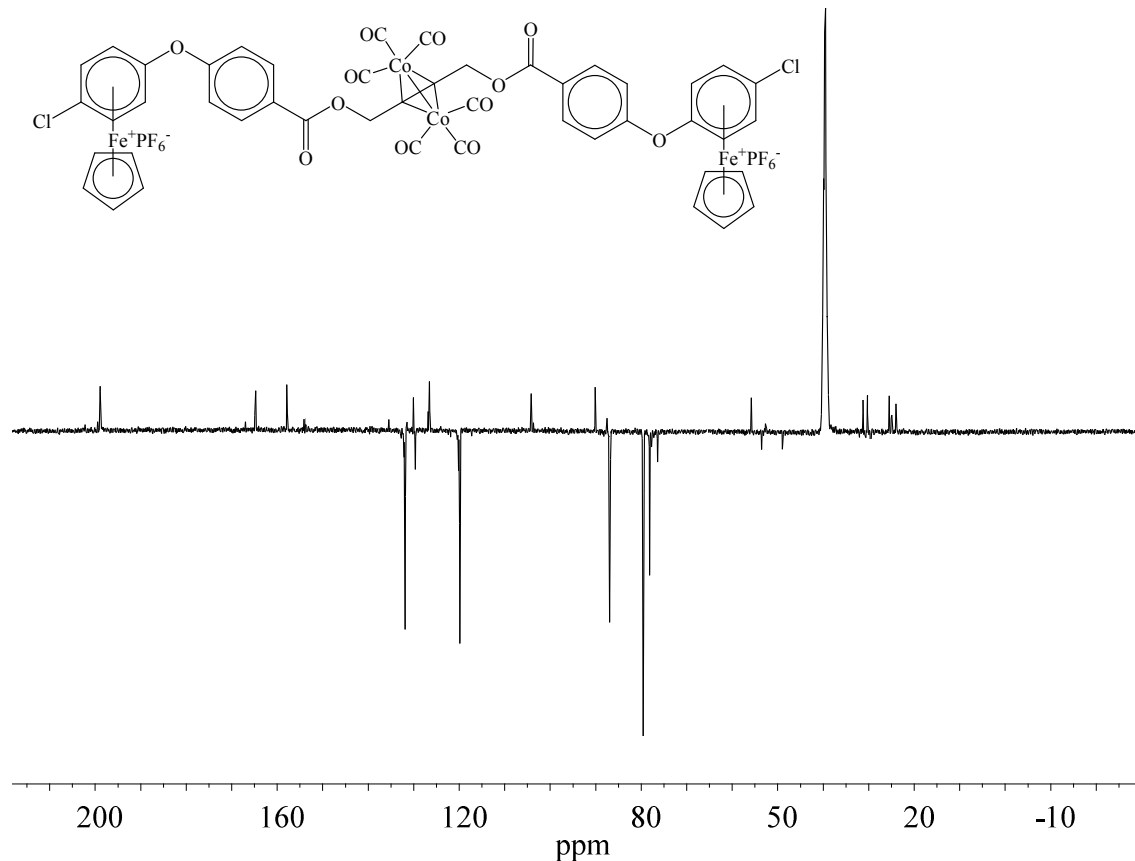


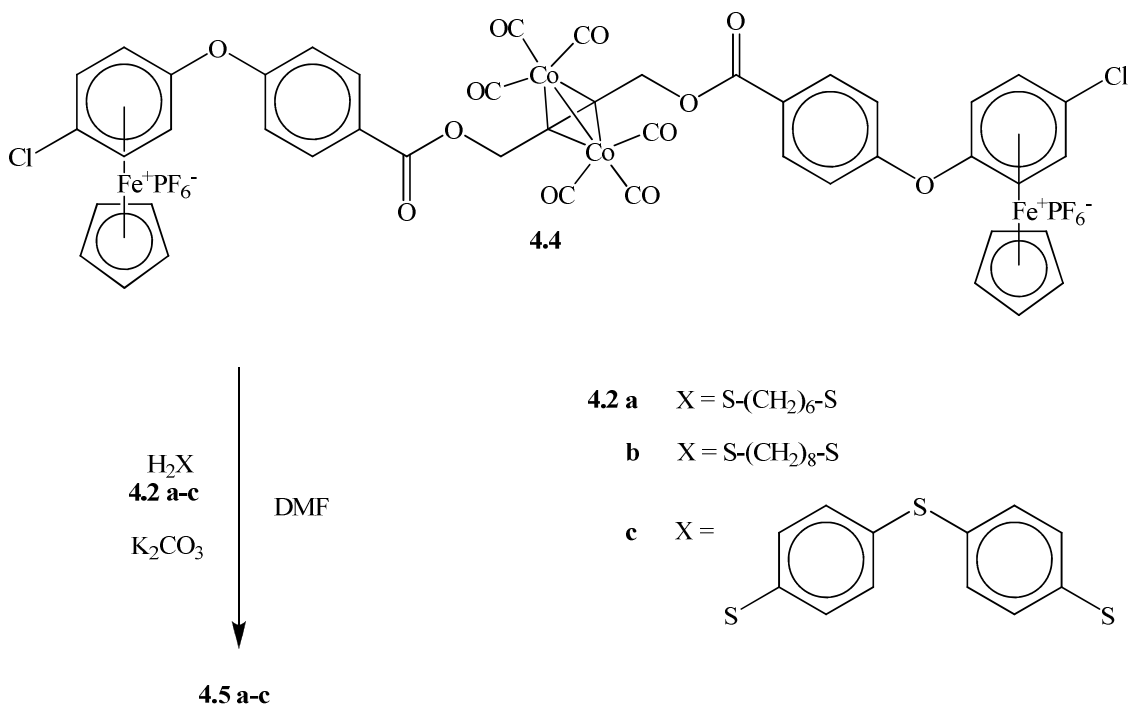
Figure 4.6: APT ^{13}C NMR spectrum of complex **4.4** in $\text{DMSO-}d_6$.

The IR of complex **4.4** shows the appearance of the three characteristic cobalt carbonyl bands at 2097, 2057 and 2037 cm^{-1} .

4.2.4 Condensation polymerization of a monomer containing η^6 -arene- η^5 -cyclopentadienyliron(II) and dicobalt hexacarbonyl moieties with dithiol linkers

Polymerization of complex **4.4** was attempted using the same linking dinucleophiles as used for the cobalt free complex **4.1** (Scheme 4.4). The polymers produced from reactions with dithiol linkers were not as expected; these insoluble polymers were yellow in appearance and

lacked the three characteristic IR cobalt carbonyl bands, indicating the decomposition of the alkyne cobalt carbonyl complex. Studies on similar compounds are currently underway to determine if the decomposition of the alkyne cobalt carbonyl complex results in the restoration of the triple bond.



Scheme 4.4: Synthesis of polymers **4.5 a-c**.

4.3 Thermal analysis of polymers

The polymers were analyzed by both DSC and TGA to determine their thermal properties. All of the polymers were stable up to approximately 200 °C where the cationic cyclopentadienyliron complex decomposed. This decomposition, while significant, is not truly representative of the polymer degradation since the cationic cyclopentadienyliron moieties are pendent to the backbone of the polymer. The polymer backbones of the polymers did not begin to degrade until approximately 400 °C. The TGA data is tabulated in Table 4.1.

Table 4.1: Thermogravimetric analysis of polymers.

Polymer	Step 1	Step 2	Step 3	Step 4
4.3 a	237 – 279, 17%	372 – 423, 37%	875 – 1000, 10%	
4.3 b	202 – 240, 18%	386 – 429, 33%	500 – 1000, 15%	
4.3 c	216 – 232, 13%	438 – 492, 22%	512 – 1000, 20%	
4.5 a	209 – 259, 15%	381 - 431, 21%	570 – 623, 14%	695 – 1000, 12%
4.5 b	163 – 174, 3%	204 – 227, 10%	396 – 495, 56%	
4.5 c	214 – 254, 16%	421 – 516, 16%	750 – 987, 23%	

DSC showed that the polymers displayed reproducible glass transition temperatures between 100 °C and 130 °C (Table 4.2). As glass transitions are exclusive to polymers and large oligomers, the presence of these phase transitions indicates that the polymerization reactions did work.

Table 4.2: Differential scanning calorimetry of polymers.

Polymer	T _g (°C)
4.3 a	125
4.3 b	107
4.3 c	107
4.5 a	123
4.5 b	101
4.5 c	130

4.4 Cyclic voltammetry of complexes

The electrochemical properties of complexes **4.1** and **4.4** were studied using cyclic voltammetry. The complexes showed behaviour similar to those described previously. Complex **4.1** showed a reversible redox couple at $E_{1/2} = -1.42$ V due to the reversible reduction of cationic cyclopentadienyliron moiety. Complex **4.4** displayed two electrochemical processes, the first, a irreversible reduction at -1.25 V due to the cobalt centres and a reversible reduction at $E_{1/2} = -1.44$ V.

Table 4.3: Cyclic voltammetry of monomers.

Complex	$E_{1/2}$	$E_{p,c}$
4.1	-1.42	
4.4	-1.44	-1.25

4.5 Summary

This project developed the synthetic methodology to prepare an alkyne containing organoiron complex where the alkyne moiety is sandwiched between two η^6 -chloroarene- η^5 -cyclopentadienyliron(II) moieties. The terminal chloro groups on the cyclopentadienyliron complexes allowed for polycondensation with a number of dithiols which gave highly insoluble materials. The materials showed glass transition temperatures from 100 °C - 130 °C and thermal gravimetric analysis showed the the polymers were thermally stable up to ~ 200 °C where the cationic cyclopentadienyliron moieties decomposed. The organoiron alkyne complex reacted with dicobalt octacarbonyl to generate a tetrametallic species containing both iron and cobalt. This complex was also reacted with dithiols in the presence of K_2CO_3 to generate insoluble

materials. IR analysis showed that the polymerization conditions led to the decomposition of the alkyne-hexacarbonyldicobalt moiety.

4.6 Detailed experimental

All reactions and complexes containing a η^6 -aryl- η^5 -cyclopentadienyl iron hexafluorophosphate moiety were kept in the dark to prevent decomposition.

Synthesis of complex 4.1

Complex **2.22** (4.3529 g, 8.5 mmol), 2-butyne-1,4-diol (**2.5**) (0.2841 g, 3.5 mmol), DCC (1.8540 g, 9 mmol), DMAP (1.1432, 9 mmol), 15 mL DCM and 5 mL DMF were stirred for 18 hours, in the dark, under nitrogen. The reaction was then placed in the freezer for 3 h and filtered to remove DCU. DCM (50 mL) was added to the filtrate which was then washed twice with 200 mL of 1.2 M HCl and 4 mmol of NH_4PF_6 . The organic layer was dried using magnesium sulphate followed by gravity filtration. The DCM was removed from the filtrate using a rotary evaporator, leaving a mixture of product and DCU in DMF. This mixture was placed in the freezer for 3 hours, resulting in the precipitation of DCU crystals which were then filtered out. The filtrate was then added to 200 mL of water and 4 mmol of NH_4PF_6 forming a yellow precipitate, which was collected in a Buchner funnel and dried over vacuum. In cases where there was still DCU in the product, the product was dissolved in a minimal amount of DCM and placed in the freezer until the DCU crystallized. The DCU crystals were then filtered out of the solution and the DCM was removed *in vacuo*. 3.097 g (82 % yield).

^1H NMR (400 MHz, $\text{DMSO-}d_6$) δ = 8.12 (d, $J=8.9$, 4H), 7.45 (d, $J=8.9$, 4H), 6.85 (d, $J=6.9$, 4H), 6.57 (d, $J=6.9$, 4H), 5.30 (s, 10H), 5.11 (s, 4H). ^1H NMR (400 MHz, $\text{acetone-}d_6$) δ = 8.19 (d,

$J=8.7$, 4H), 7.49 (d, $J=8.7$, 4H), 6.89 (d, $J=7.0$, 4H), 6.67 (d, $J=7.0$, 4H), 5.44 (s, 5H), 5.10 (s, 4H).

^{13}C NMR (101 MHz, DMSO- d_6) δ = 164.17, 157.65, 132.16, 130.44, 126.44, 120.37, 104.11, 86.92, 81.34, 79.58, 77.75, 52.70. DCU and DCC = 154.13, 135.50, 53.60, 49.01, 31.28, 30.31, 25.51, 25.10, 24.93, 24.07.

IR 1727 cm^{-1} (C=O)

Synthesis of polymers 4.3 a-d

Complex **4.1** (0.2 mmol), the appropriate linker **4.2 a-d** (0.2 mmol), and K_2CO_3 (5 mmol) were stirred in 2 mL of DMF, under N_2 , at 55 °C until they became viscous, typically 48-72 hours. The reaction was then dissolved in an additional 5 mL of DMF and slowly added to H_2O (200 mL) and NH_4PF_6 (0.4 mmol) forming a precipitate that was collected by filtration and washed with 20 mL of water.

4.3 a 0.1987 g, IR 1721 cm^{-1} (C=O)

4.3 b 0.2191 g, IR 1718 cm^{-1} (C=O)

4.3 c 0.2245 g, IR 1737 cm^{-1} (C=O)

Synthesis of complex 4.4

In a N_2 environment, 2.1589 g (2 mmol) of complex **4.1** and 1.0382 g (3 mmol) of Co_2CO_8 were stirred in 10 mL of dry THF for 10 hours, for the first half hour gas was evolved from the reaction. The THF was removed in vacuo and the complex was dissolved in acetone. After 20 min a precipitate was formed and filtered out. The filtrate was then slowly added to

100 mL of water and 4 mmol of NH_4PF_6 , forming a precipitate which was collected. Once the product was dry it appeared as a red solid with 2.5934 g yield (95 % yield).

^1H NMR (400 MHz, $\text{DMSO-}d_6$) δ = 8.15 (d, $J=8.7$, 4H), 7.44 (d, $J=8.7$, 4H), 6.86 (d, $J=6.8$, 4H), 6.60 (d, $J=6.8$, 4H), 5.67 (s, 4H), 5.30 (d, $J=10.6$, 10H), 2.08 (s, 3H).

^{13}C NMR (101 MHz, $\text{DMSO-}d_6$) δ = 198.92, 164.71, 157.87, 131.87, 130.06, 126.53, 119.87, 104.15, 90.12, 86.96, 79.58, 78.18, 55.77. DCC and DCU = 154.08, 135.47, 53.55, 48.95, 31.24, 30.27, 25.47, 25.06, 24.89, 24.03.

IR 2097 cm^{-1} , 2057 cm^{-1} , 2037 cm^{-1} ($\text{C}\equiv\text{O}$), 1716 cm^{-1} ($\text{C}=\text{O}$)

Synthesis of polymers 4.5 a-c

0.05 mmol of complex **4.4**, 0.05 mmol of the appropriate linker **4.2 a-d**, and 5 mmol of K_2CO_3 were stirred in 1 mL of DMF, under N_2 , at 55-60 $^\circ\text{C}$ until they became viscous 48-72 hours. Once the reaction became viscous it was dissolved in an additional 5 mL of DMF and slowly added to 200 mL of H_2O and 1 mmol of NH_4PF_6 , forming a precipitate that was collected by filtration and washed with 20 mL of water.

4.5 a 0.0678 g yield, IR 1741 cm^{-1} ($\text{C}=\text{O}$)

4.5 b 0.0567 g yield, IR 1728 cm^{-1} ($\text{C}=\text{O}$)

4.5 c 0.0501 g yield, IR 1736 cm^{-1} ($\text{C}=\text{O}$)

Chapter 5: Preliminary work with polysiloxanes

5.1 Introduction

Polysiloxanes, often referred to as silicones, is a class of polymeric materials well known for their their flexible backbone, thermal stability, durability, resistance to biological degradation and insulation properties.⁷⁶ Due to these useful properties, polysiloxanes have found applications as lubricants, adhesives, mechanical tubing, gaskets, medical implants, medical tools and electrical insulators. Two popular uses of polysiloxanes are in the manufacturing of contact lenses and the children's toy Silly Putty™. Also the low carbon content of polysiloxanes has made them desirable precursors for conducting ceramic materials.

A very convenient chemical reaction for the preparation of functionalized siloxanes and polysiloxanes is hydrosilation. Hydrosilation (aka hydrosilylation) is a term that refers to the addition of an organic or inorganic silicon hydride across a double bond (Figure 5.1). The reaction is quite versatile with respect to the X and Y substituents, which can include alkyl, aryl, alkoxy, acyloxy and halogen. The first mention of this type of reaction was made in a patent by Miller and Schreiber in 1945.^{77, 78} Their method required extreme temperatures of 610-720 °C, which potentially could lead to the decomposition of starting materials. Hydrosilation catalysts are often used to alleviate the issue of starting material degradation.⁷⁷

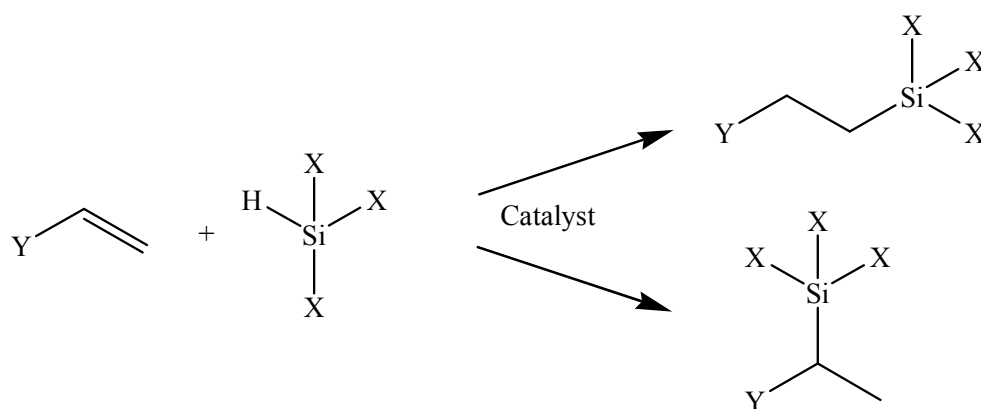


Figure 5.1: Hydrosilylation of a terminal alkene.

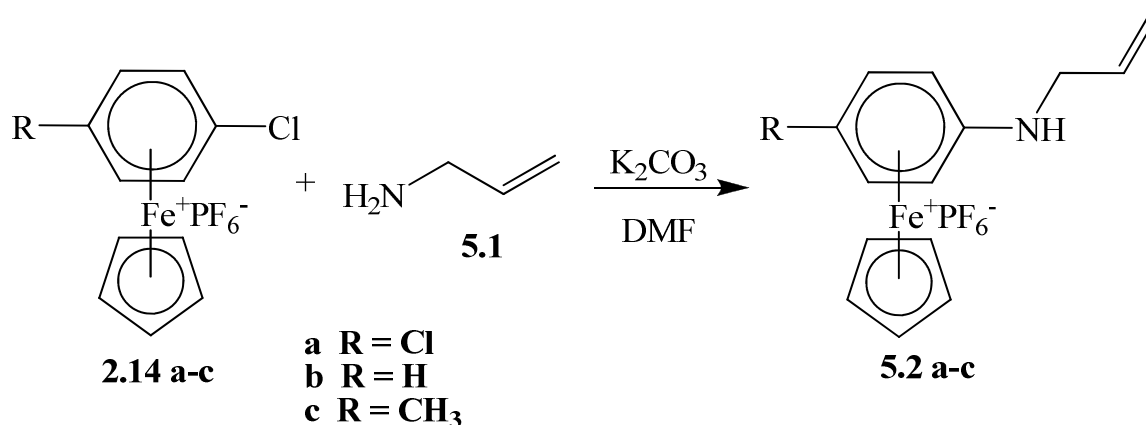
Most transition metal catalysts that have been developed to mediate hydrosilylation reactions give the products according to the anti-Markovnikov rule,⁷⁹ though some palladium catalysts are known to give the α -adduct of the product. The mechanism of the catalyzed hydrosilylation reaction is quite complex and can be different depending on the catalyst, reactants and experimental conditions, meaning that the mechanism has not been elucidated for many of the reactants.⁸⁰ Unfortunately, transition metal catalyzed hydrosilylation is often accompanied by side reactions such as oligomerization, polymerization, isomerization hydrogenation of alkenes and dehydrogenation of silicon hydrides.⁷⁹

This chapter details the synthesis of three polysiloxanes which contain η^6 -aryl- η^5 cyclopentadienyliron(II) hexafluorophosphate moieties. This project lays the foundation for future work within the Abd-El-Aziz group with polysiloxanes and the incorporation of transition metals.

5.2 Synthesis and characterization of polysiloxanes containing η^6 -arene- η^5 -cyclopentadienyliron

5.2.1 Nucleophilic substitution of η^6 -halo-arene- η^5 -cyclopentadienyliron with allylamine

Complexes **5.2 a-c** were synthesized via nucleophilic aromatic substitution of three different η^6 -chlorobenzene- η^5 -cyclopentadienyliron(II) hexafluorophosphate complexes (**2.14 a-c**) with allylamine (**5.1**) (Scheme 5.1). All three complexes appeared red in colour as has been seen previously for complexed anilines.⁸¹ All three complexes were highly soluble in ether, acetone, THF, DCM, DMF and DMSO.



Scheme 5.1: Synthesis of complexes **5.2 a-c**.

Interestingly, even with a large excess of the amine, disubstitution of complex **2.14 a** does not occur. This has also been observed in previous attempts to prepare disubstituted amine complexes and phenylenediamine derivatives, where the formation of a zwitterion is predicted in basic solutions (Figure 5.2).⁸¹ The deprotonation of the amine results in a negative charge on the aromatic ring increasing its electron density and preventing a reaction with a second amine.

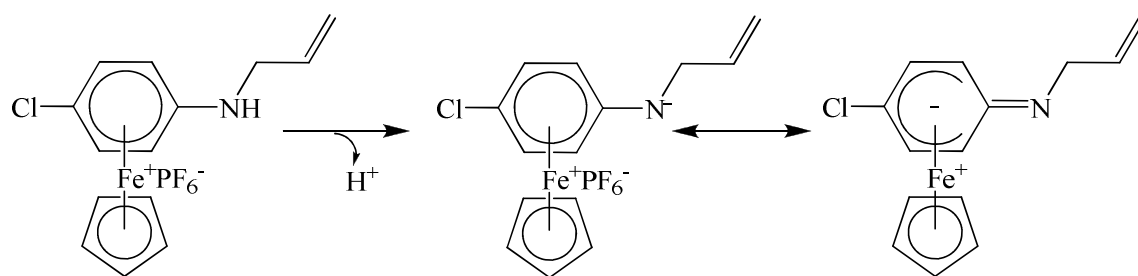


Figure 5.2: Deprotonation of the amine group to form a zwitterion.

The ^1H NMR spectra of all three complexes are quite similar, therefore only complex **5.2 b** will be explored in detail. Figure 5.3 shows the ^1H NMR spectrum of **5.2 b**, as can clearly be seen all of the expected resonances appear. At 6.23 ppm there is the broad singlet of the lone hydrogen on the nitrogen. Directly upfield, at 6.17 ppm is a doublet of doublets due to two of the hydrogens of the complexed arene. At 5.95-6.08 ppm is a multiplet that integrates for two hydrogens. This multiplet is actually the overlapping resonances of the internal allylic hydrogen and the hydrogen of the complexed arene which is para to the nitrogen. The doublet at 5.86 is due to the final two hydrogens of the complexed arene. At 5.40 and 5.27 ppm are two doublets of quartets due to the terminal allyl hydrogens. At 4.99 ppm is the cyclopentadiene resonance and at 4.00 is a triplet of triplets due to the methylene.

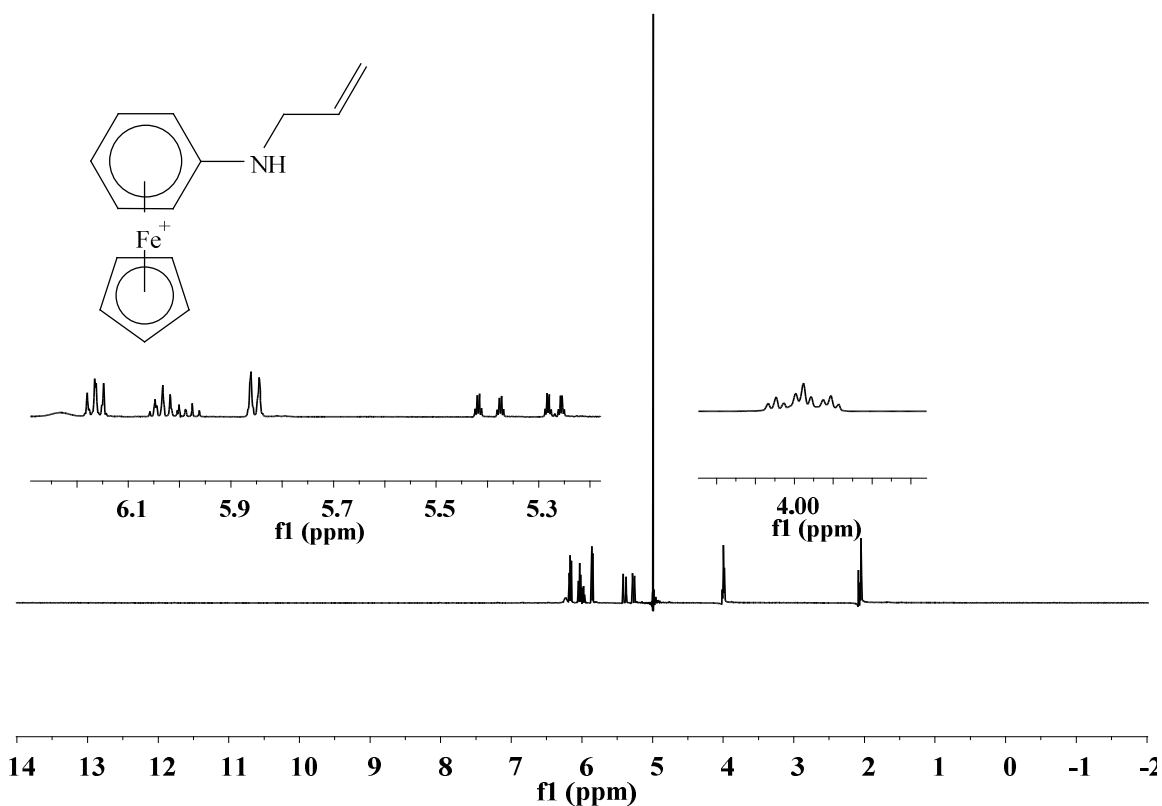


Figure 5.3: ¹H NMR spectrum of complex **5.2 b** in acetone-*d*₆.

The ¹³C NMR spectra of each complex also appear as expected, due to their similarity only the spectra for **5.2 b** will be presented in detail. Figure 5.4 shows the ¹³C NMR of complex **5.2 b**, at 135 ppm and 118 ppm are the α and β allyl carbons respectively, while the small resonance at 127 is due to the lone quaternary carbon of the complexed arene. The remaining resonances of the complexed arene are located at 87, 81 and 69 ppm. The cyclopentadienyl carbons can be seen at 76 ppm and the final carbon resonance due to the CH₂ is at 46 ppm.

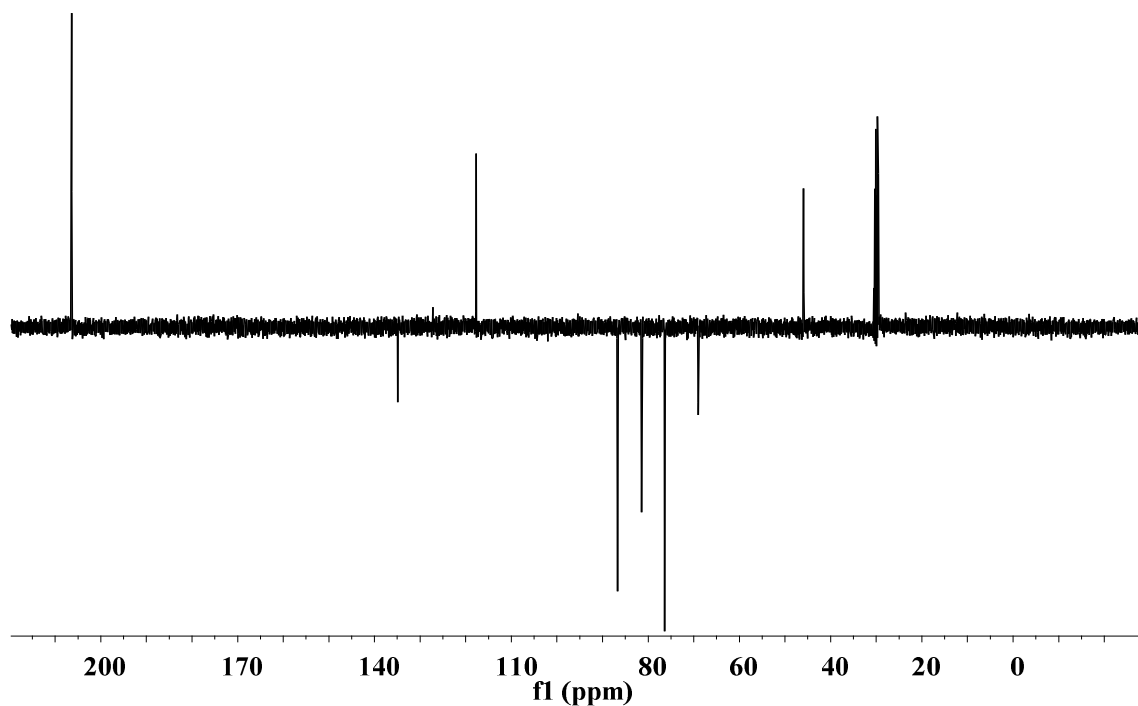
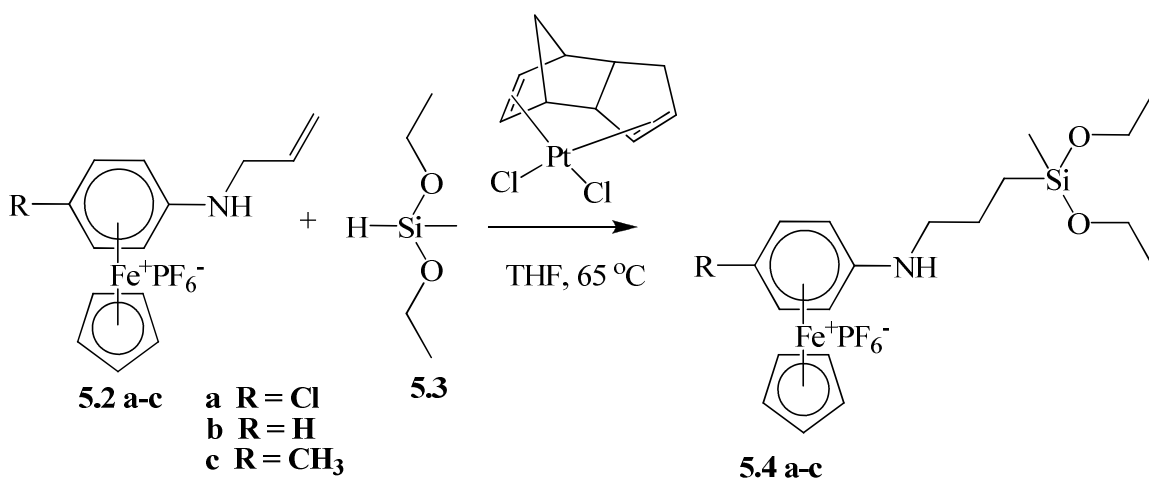


Figure 5.4: APT ^{13}C NMR spectrum of complex **5.2 b** in acetone- d_6 .

5.2.2 Hydrosilation of allylamine complexes with methyldiethoxysilane

Hydrosilation of complexes **5.2 a-c** was performed with methyldiethoxysilane using dicyclopentadienyplatinum dichloride as the catalyst in THF (Scheme 5.2). While two different hydrosilation isomers are possible, only one product is evident in the NMR spectra. Complexes **5.4 a-c** are quite fragile as even atmospheric moisture will start to cleave the ethoxy groups from the Si. As a result, the pure compound must be under anhydrous conditions.



Scheme 5.2: Synthesis of complexes **5.4 a-c**.

Spectroscopically all three compounds (**5.4 a-c**) are quite similar to each other, the only differences being due to the R group on the complexed aromatic. For this reason only **5.4 b** will be described in great detail.

¹H NMR of complex **5.4 b** indicates the successful incorporation of the methyl diethoxysilyl moiety (Figure 5.5). The disappearance of the allylic resonances, as well as, the lack of a Si-H peak between 4 and 5 ppm, indicates that the hydrosilylation reaction went to completion. Three peaks associated with the incorporation of the methyl diethoxy silane group are clearly seen in the spectrum, with the methyl resonance at 0.11 ppm and the ethoxy resonances at 3.77 and 1.17 ppm. The resonances due to the internal propyl group appeared at 0.65, 1.8 and 3.3 ppm. However, the multiplicity of these resonances was complicated by the overlapping of the major and minor product peaks.

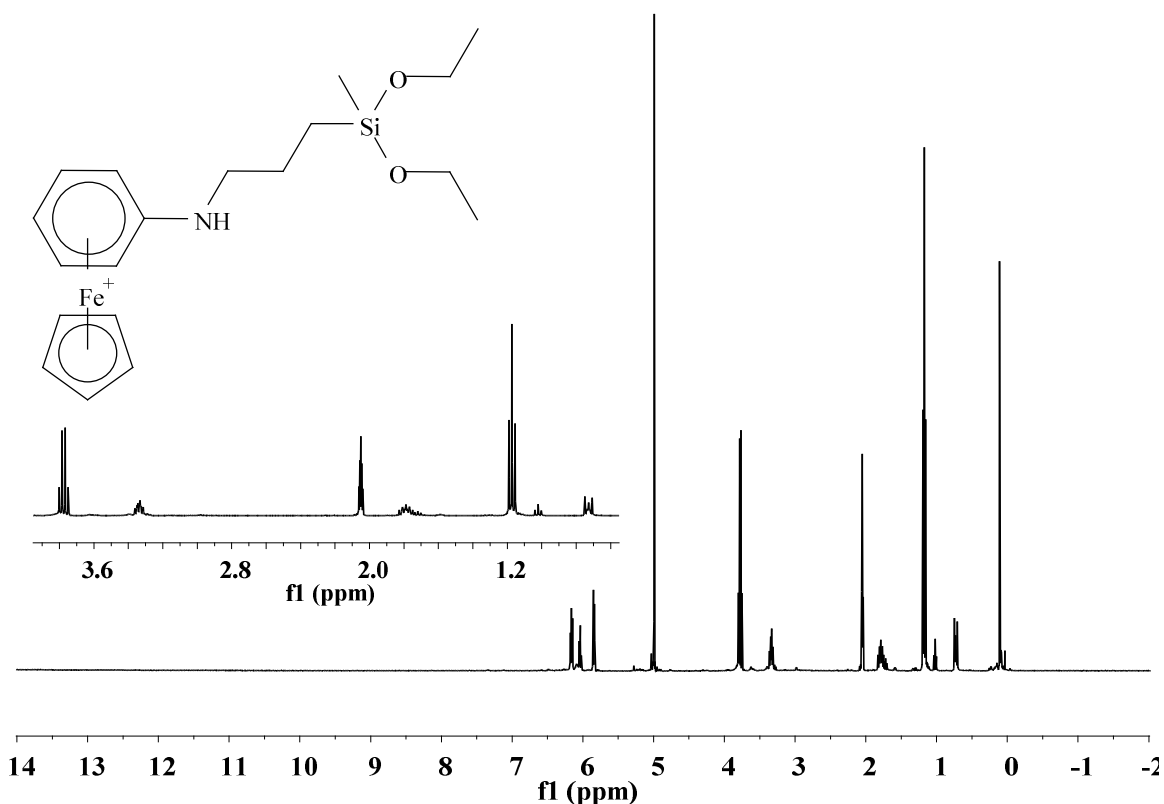


Figure 5.5: ^1H NMR spectrum of complex **5.4 b** in acetone- d_6 .

The ^{13}C NMR spectrum (Figure 5.6) of complex **5.4 b** presents a slightly less complicated picture than the ^1H NMR spectrum. Each of the eleven expected carbon resonances can be seen clearly. The reaction is confirmed through the disappearance of the allylic hydrogens at 135 and 118 ppm (for complex **5.2 b**) and the three internal propyl carbons of complex **5.4 b** resonate at 58.68, 23.17, and 12.00 ppm. At 46.43 and 18.91 ppm are the ethoxy carbons and at -4.71 ppm is the methyl group attached to the silicon.

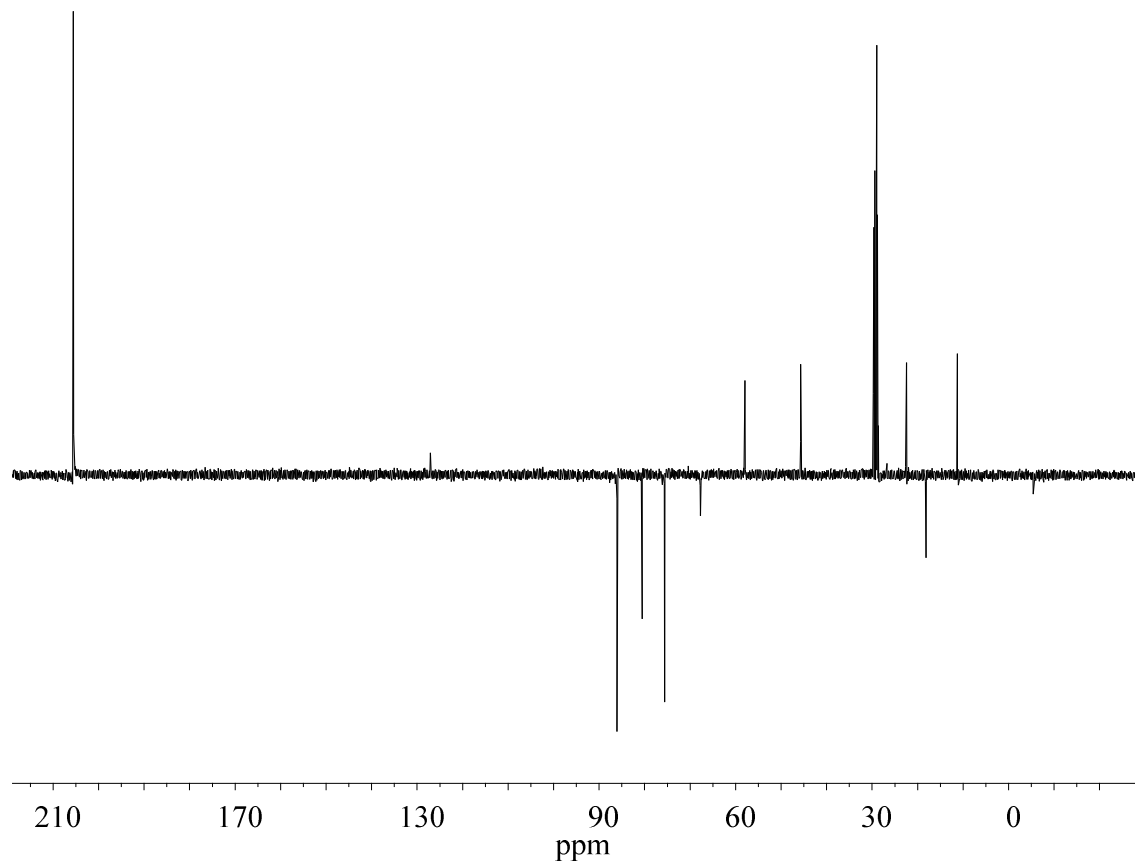
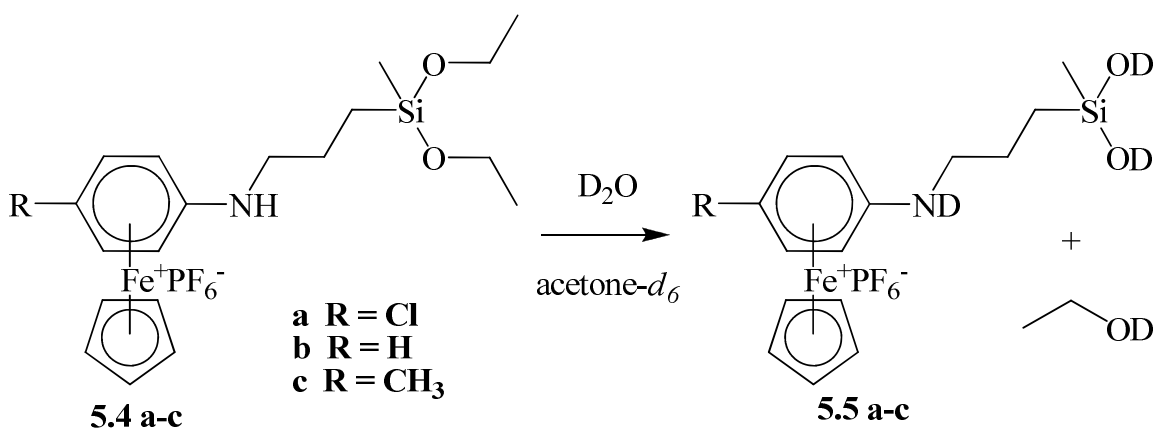


Figure 5.6: APT ^{13}C NMR spectrum of complex **5.4 b** in acetone- d_6 .

5.2.3 Cleavage of ethoxy groups from complexes **5.4 a-c**

Cleavage of the ethoxy groups can be accomplished through the addition of water to complexes **5.4 a-c**, giving the silanol adducts **5.5 a-c** and ethanol (Scheme 5.3, shows the conversion of the major product only). Attempts to isolate **5.5 a-c** have so far been unsuccessful due to the polymerization of these highly reactive monomers. However, the cleavage of the ethoxy groups can be observed using NMR spectroscopy. Figure 5.8 shows the time lapse ^1H NMR spectra of the reaction of complex **5.4 b** with D_2O . The bottom spectrum is of **5.4 b** prior to the addition of a drop of D_2O , the other spectra in ascending order are from 1 min., 3 min., 5

min. and 20 min. after addition of D₂O. It is important to note that the addition of D₂O to the NMR tube, caused a slight shift in the ¹H resonances (see Figure 5.8 before and after 1 min.). When comparing these spectra, the region from 3.5 - 4.0 ppm is particularly interesting; before any D₂O was added the quartet of the ethoxy group was seen at ~3.8 ppm. One minute after addition, a broad peak at ~3.6 ppm is observed which represents the free ethanol, at the 3 minute mark the resonance at ~3.6 ppm had intensified into a clear quartet and the peak at ~3.8 ppm had shrunk. After 20 min. the ethoxy peaks were completely lost and the ethanol peak is the only one that appears in that region. Figure 5.8 also shows just how reactive the silanol complexes are, by 20 min. into the reaction two broadened resonances can be seen for the methyl group between 0.0 and 0.2 ppm, this is possibly due to the formation of dimers as the monomers begin to react with each other.



Scheme 5.3: Cleavage of ethoxy groups from complexes **5.4 a-c**.

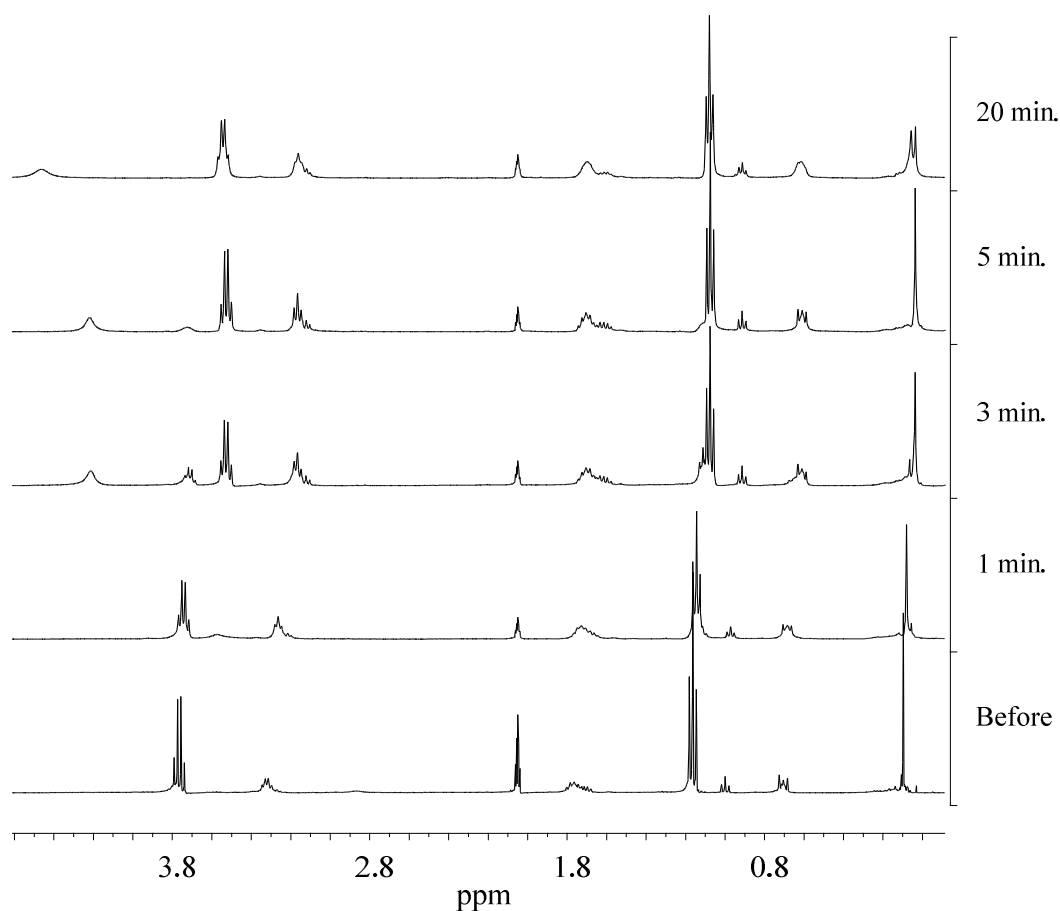
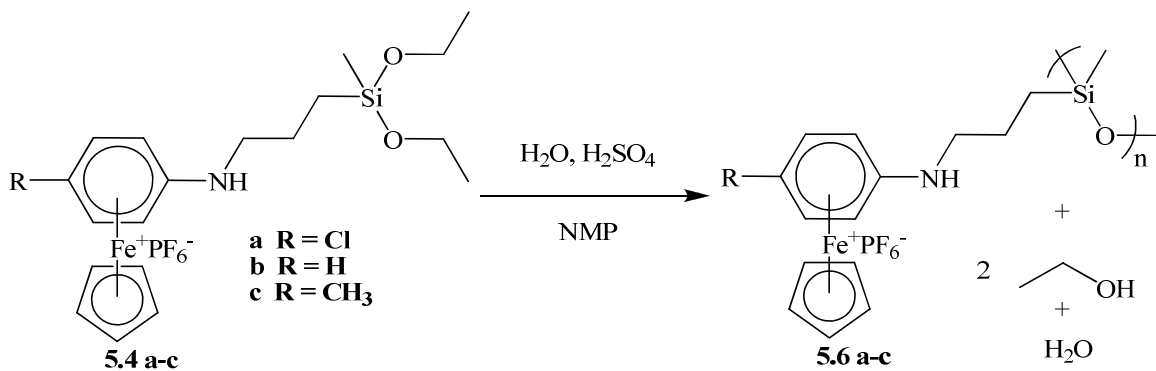


Figure 5.7: ^1H NMR spectral visualization of the cleavage of the ethoxy groups from complex **5.4 b** through a reaction with D_2O in acetone- d_6 .

5.2.4 Polymerization

Due to the reactivity of the silanol groups, cleavage of the ethoxy groups and polymerization were done in a one pot process (Scheme 5.4). Water was added to solutions of the monomers to cleave off the ethoxy groups and H_2SO_4 was used to catalyze the polymerization. After 15 hours trimethylchloro silane was added to cap the polymer ends. The molecular weights of these polymers could not be determined as the iron free analogues were insoluble in THF.



Scheme 5.4: Synthesis of polymers **5.6 a-c**.

The ^1H NMR spectrum for polymer **5.6 b** can be seen in Figure 5.. As can be seen there is a distinct broadening of the proton resonances which is characteristic of polymers. Also, it is clear upon comparison with the starting complex **5.4 b** that the resonances due to the ethoxy groups at 3.77 and 1.17 ppm have disappeared. The loss of the ethoxy groups is also evident in the ^{13}C NMR spectrum (Figure 5.) as there are no carbon resonances at either 46.43 or 18.91 ppm.

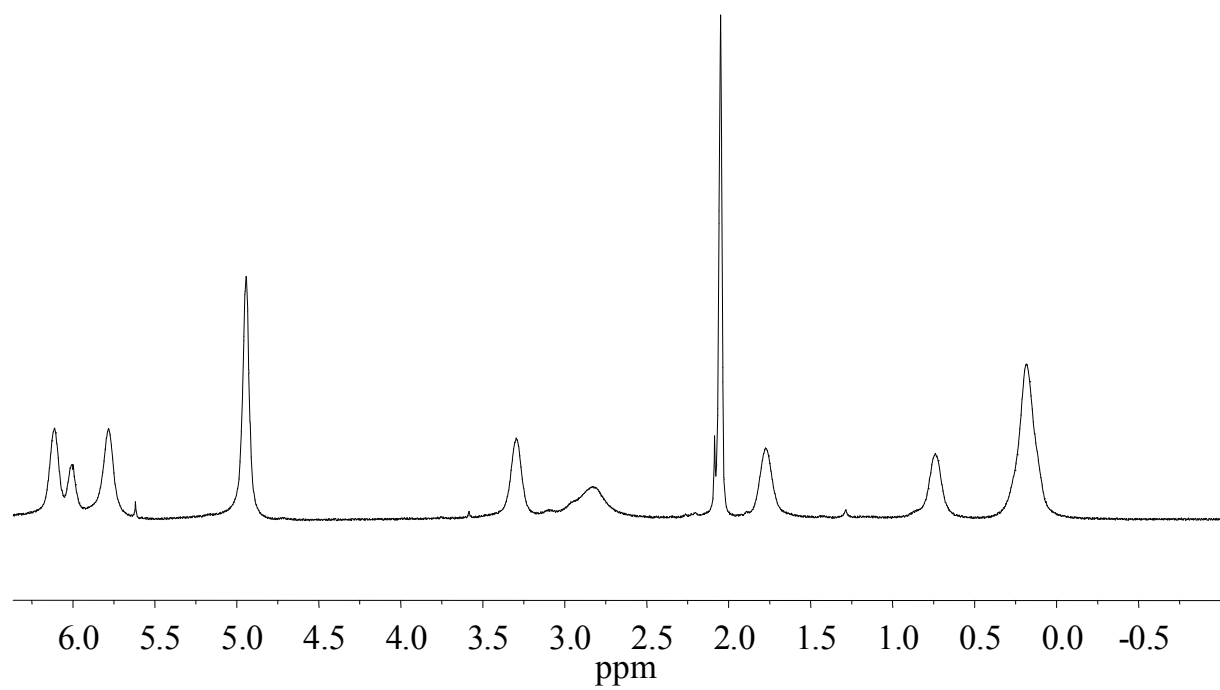


Figure 5.8: ^1H NMR spectrum of polymer **5.6 b** in acetone- d_6 .

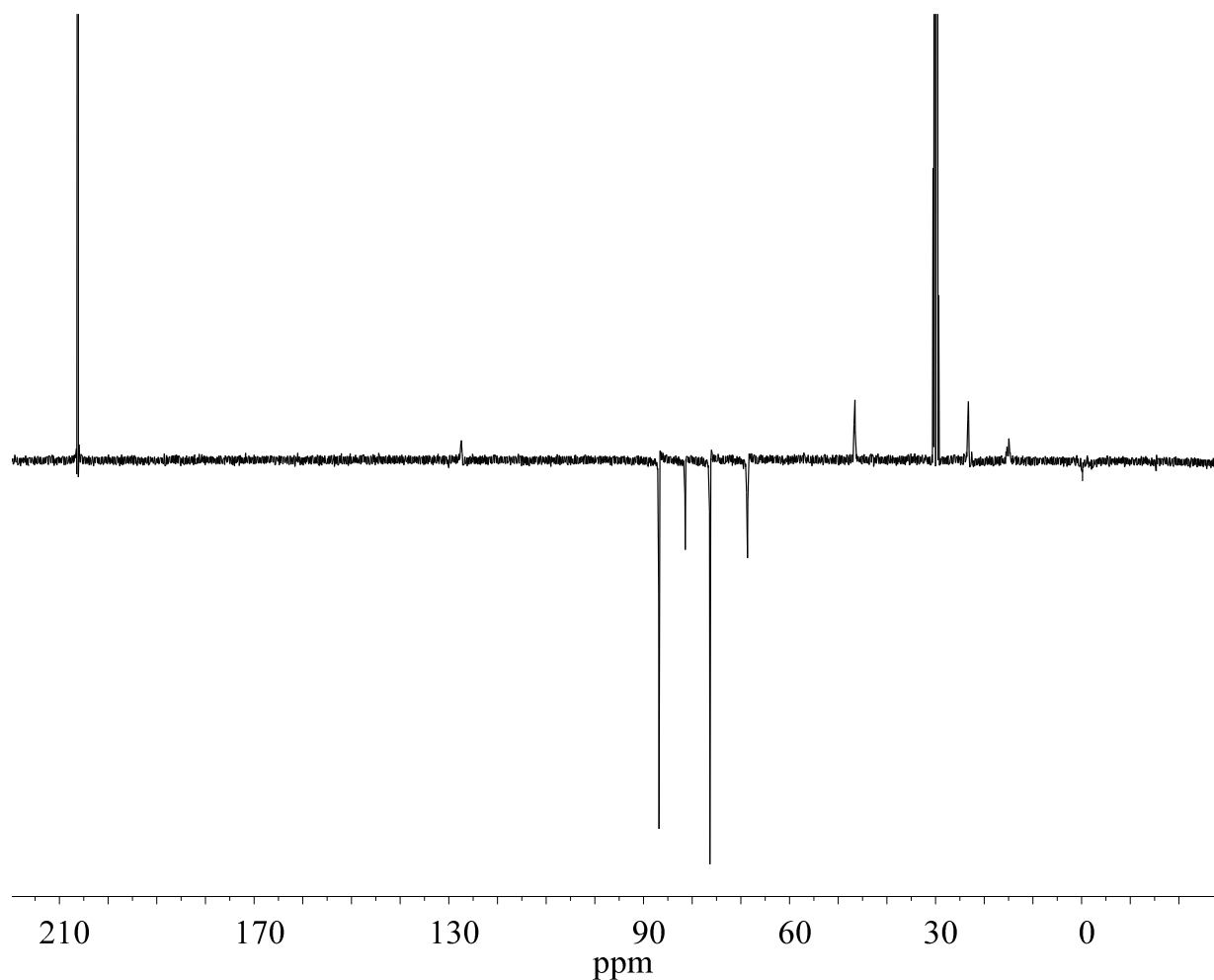


Figure 5.9: APT ^{13}C NMR spectrum of polymer **5.6 b** in acetone- d_6 .

5.3 Thermal analysis of polymers

Polymers **5.6 a-c** were analyzed by both DSC and TGA to determine their thermal properties. From the TGA data tabulated in Table 5.1, all of the polymers were stable up to approximately 200 °C where the cationic cyclopentadienyliron complex decomposed. This decomposition, while significant, is not truly representative of the polymer degradation since the

cationic cyclopentadienyliron moieties are pendent to the backbone of the polymer. The polymer backbones of the polymers did not begin to degrade until approximately 400 °C.

Table 5.1: Thermogravimetric analysis of polymers **5.6 a-c**.

Polymer	Step 1 (°C), %	Step 2 (°C), %	Step 3 (°C), %
5.6 a	199 – 245, 33%	400 – 481, 13%	500 – 1000, 10%
5.6 b	205 – 246, 32%	399 – 470, 16%	950 – 998, 13%
5.6 c	122-248, 60%	757 – 842, 30%	

Differential scanning calorimetry showed that polymers **5.6 a-c** displayed reproducible glass transition temperatures between 80 °C and 111 °C (Table 5.2). As glass transitions are exclusive to polymers and large oligomers, the presence of these phase transitions indicates that the polymerization reactions did work.

Table 5.2: Differential scanning calorimetry of polymers **5.6 a-c**.

Polymer	T _g (°C)
5.6 a	95
5.6 b	111
5.6 c	80

5.4 Cyclic voltammetry of complexes

Electrochemical analysis of some of the allyl and silyl containing complexes showed that the reversible reduction of the iron complexes occurred at more negative E_{1/2s} (Table 5.3) than

seen in previous chapters for the oxygen substituted arene complexes. This is characteristic of cyclopentadienyliron arene complexes containing electron donating substituents.

Table 5.3: Cyclic voltammetry of complexes.

Complex	1 st E _{1/2}	2 nd E _{1/2}
5.2 a	-1.82	-1.96
5.2 b	-1.86	
5.2 c	-1.86	
5.4 a	-1.80	-1.98
5.4 b	-1.88	
5.4 c	-1.87	

5.5 Summary

A number of new cationic organoiron complexes containing amines were prepared from the reaction of haloarene coordinated cyclopentadienyliron complexes and allyl amine. The presence of the allylic group allowed for the incorporation of methyldiethylsilane via hydrosilylation using a platinum catalyst. This reaction allowed for the isolation of cationic organoiron silanes that were highly moisture sensitive. The silane complexes were converted into cationic organometallic polysiloxanes through the acid catalyzed condensation of the organometallic silanols generated *in situ*. The polymers possessed glass transition temperatures from 80-111 °C and were thermally stable up to 163-200 °C.

5.6 Detailed experimental

All reactions and complexes containing a η^6 -aryl- η^5 -cyclopentadienyl iron hexafluorophosphate moiety were kept in the dark to prevent decomposition.

General procedure for the synthesis of complexes 5.2 a-c

The appropriate η^6 -aryl- η^5 -cyclopentadienyl iron hexafluorophosphate (5.0 mmol) complex (**2.14 a-c**) was stirred under nitrogen with allylamine (14 mmol) and K_2CO_3 (14 mmol) in DMSO (15 mL) for 5-18 hours. The reaction was then quenched in a 1.2 M HCl solution and the product was extracted with DCM. The DCM/product mixture was washed twice with 150 mL of water and dried with $MgSO_4$. After filtering out the $MgSO_4$, the DCM was removed from the pure product *in vacuo*.

5.2 a: 1.43 g, red oil (66 % yield).

1H NMR (400 MHz, acetone- d_6) δ = 6.51 (d, $J=7.0$, 2H), 6.38 (s, 1H), 6.05 – 5.93 (m, 1H), 5.91 (d, $J=7.0$, 2H), 5.39 (dq, $J=17.2$, 1.6, 1H), 5.30 – 5.25 (m, 1H), 5.08 (s, 5H), 3.98 (tt, $J=5.6$, 1.5, 2H).

^{13}C NMR (101 MHz, acetone- d_6) δ = 134.83, 127.36, 118.41, 102.29, 87.35, 79.21, 68.15, 46.52.

IR 3418 cm^{-1} (N-H)

5.2 b: 1.49 g, red oil (75% yield).

1H NMR (400 MHz, acetone- d_6) δ = 6.23 (s, 1H), 6.17 (dd, $J=6.9$, 5.7, 2H), 6.08 – 5.95 (m, 2H), 5.86 (d, $J=6.8$, 2H), 5.40 (dq, $J=17.2$, 1.7, 1H), 5.27 (dq, $J=10.3$, 1.5, 1H), 4.99 (s, 5H), 4.00 (tt, $J=5.6$, 1.6, 2H).

^{13}C NMR (101 MHz, acetone- d_6) δ = 134.92, 127.17, 117.70, 86.72, 81.45, 76.38, 69.05, 45.97.

IR 3421 cm^{-1} (N-H)

5.2 c: 1.88 g, red oil (91 % yield).

^1H NMR (400 MHz, acetone- d_6) δ = 6.11 (s, 1H), 6.08 (d, $J=6.9$, 2H), 6.05 – 5.94 (m, 1H), 5.78 (d, $J=6.9$, 2H), 5.38 (dq, $J=17.2$, 1.7, 1H), 5.25 (dq, $J=10.3$, 1.5, 1H), 4.94 (s, 5H), 3.96 (tt, $J=5.6$, 1.6, 2H), 2.40 (s, 3H).

^{13}C NMR (101 MHz, acetone- d_6) δ = 135.40, 126.45, 118.01, 97.15, 87.37, 77.32, 68.81, 46.50, 20.18.

IR 3409 cm^{-1} (N-H)

General hydrosilation procedures used to produce complexes 5.4 a-c

The appropriate precursor complex (**5.2 a, b or c**) (4 mmol), methyldiethoxysilane (8mmol) and 3 mg of dicyclopentadienylplatinum dichloride were stirred under nitrogen in dry THF (50 mL) at 55-60 °C for 20 hours. The THF and excess methyldiethoxysilane were removed *in vacuo*. The residual red oil was then dissolved in acetone and poured into 300 mL of diethyl ether forming a red oil which was then isolated.

5.4 a: 2.11 g (93 % yield).

^1H NMR (400 MHz, acetone- d_6) δ = 6.50 (d, $J=6.7$, 2H), 6.24 (s, 1H), 5.89 (d, $J=6.8$, 2H), 5.08 (s, 5H), 3.77 (q, $J=7.0$, 4H), 3.38 – 3.25 (m, 2H), 1.82-1.65 (m, 2H), 1.17 (t, $J=7.0$, 6H), 1.00 (t, $J=7.4$, 1H), 0.75-0.65 (m, 2H), 0.10 – 0.05 (m, 3H).

^{13}C NMR (101 MHz, acetone- d_6) δ = 128.03, 102.41, 87.93, 80.12, 68.91, 59.08, 47.02, 23.19, 18.93, 12.01, -4.75.

IR 3408 cm^{-1} (N-H)

5.4 b: 2.09 (98 % yield).

^1H NMR (400 MHz, acetone- d_6) δ = 6.19 (dd, $J=6.9, 5.8$, 2H), 6.09 (s, 1H), 6.04 (t, $J=5.9$, 1H), 5.84 (d, $J=6.9$, 2H), 4.99 (s, 5H), 3.77 (q, $J=7.0$, 4H), 3.37 – 3.26 (m, 2H), 1.85 – 1.68 (m, 2H), 1.17 (t, $J=7.0$, 6H), 1.02 (t, $J=7.3$, 0H), 0.77 – 0.68 (m, 2H), 0.13 – 0.07 (m, 3H).

^{13}C NMR (101 MHz, acetone- d_6) δ = 127.77, 86.78, 81.28, 76.30, 68.42, 58.68, 46.43, 23.17, 18.91, 12.00, -4.71.

IR 3409 cm^{-1} (N-H)

5.4 c: 2.08 g (95 % yield).

^1H NMR (400 MHz, acetone- d_6) δ = 6.06 (d, $J=6.8$, 2H), 5.92 (s, 1H), 5.75 (d, $J=6.8$, 2H), 4.92 (s, 5H), 3.77 (q, $J=7.0$, 4H), 3.33 – 3.22 (m, 2H), 2.40 (s, 3H), 1.82 – 1.66 (m, 2H), 1.17 (t, $J=7.0$, 4H), 1.00 (t, $J=7.4$, 0H), 0.75 – 0.67 (m, 2H), 0.11 – 0.08 (m, 3H).

^{13}C NMR (101 MHz, acetone- d_6) δ = 126.61, 96.54, 87.01, 76.82, 67.75, 58.66, 46.55, 23.16, 19.81, 18.90, 11.97, -4.68.

IR 3410 cm^{-1} (N-H)

General polymerization procedures to produce polymers 5.6 a-c

Complexes **5.4 a-c** were individually dissolved in 4 mL NMP and .5 mL of water was added, these solutions were allowed to stir for 20 min. The ethanol and excess water were then distilled off of the reactions. Three drops of concentrated sulphuric acid was added and the reactions were stirred at 50 °C under reduced pressure for 48 hours. Trimethylchlorosilane dissolved in 10 mL of THF was then added to the reactions and was allowed to stir for three hours.

5.6 a: ^1H NMR (400 MHz, acetone- d_6) δ = 6.45 (br. s, 2H), 5.85 (br. s, 2H), 5.00 (s, 5H), 3.28 (br. s, 2H), 1.79 (br. s, 2H), 0.67 (br. s, 2H), 0.05 (br. s, 5H). Not soluble enough for a ^{13}C NMR spectrum.

IR 3412 cm^{-1} (N-H)

5.6 b: ^1H NMR (400 MHz, acetone- d_6) δ = 6.11 (br. s, 2H), 6.00 (br. s, 1H), 5.78 (br. s, 2H), 4.94 (br. s, 5H), 3.30 (br. s, 2H), 1.78 (br. s, 2H), 0.74 (br. s, 2H), 0.18 (br. s, 4H).

^{13}C NMR (101 MHz, acetone- d_6) δ = 127.49, 86.81, 81.44, 76.36, 68.67, 46.59, 23.22, 15.43, 14.91, -0.22.

IR 3407 cm^{-1} (N-H)

5.6 c: ^1H NMR (400 MHz, acetone- d_6) δ = 6.04 (br. s, 2H), 5.79 (br. s, 2H), 4.92 (br. s, 5H), 3.35 (br. s, 2H), 2.39 (br. s, 3H), 1.84 (br. s, 2H), 0.81 (br. s, 2H), 0.21 (br. s, 4H).

^{13}C NMR (101 MHz, acetone- d_6) δ = 125.67, 95.86, 86.28, 76.10, 67.16, 45.93, 22.67, 19.11, 14.27, 1.35, -0.97.

IR 3406 cm^{-1} (N-H)

General demetallation procedures to produce analogues of the polymers 5.6 a-c

Polymers **5.6 a-c** (0.1-0.2 g) were placed in a pyrolysis chamber under vacuum at 250°C for twenty minutes. The organic analogues of polymers **5.6 a-c** were found to be insoluble in THF, which prevent molecular weight determination.

Chapter 6: General conclusions

The synthetic methodology for the incorporation of organoiron and organocobalt into polymers was explored. Three different polynorbornene and three different polymethacrylate based polymers which contained alkyne-hexacarbonyldicobalt and either η^6 -(haloarene)- η^5 -cyclopentadienyliron(II) hexafluorophosphate or ferrocene moieties were synthesized and characterized. Norbornene monomers which contained organoiron and organocobalt were successfully polymerized using ring opening metathesis polymerization. The soluble portions of the polynorbornene based polymers possessed molecular weights ranging from 49 500 - 55 300 and PDIs of 1.2-1.9 (estimated from the GPC analysis of their cationic iron free analogues). Radical polymerization of methacrylate monomers which contained η^6 -(haloarene)- η^5 -cyclopentadienyliron(II) hexafluorophosphate moieties as well as alkyne functional groups, allowed for the coordination of dicobalt hexacarbonyl post polymerization. The soluble portions of the polymethacrylate polymers which contained organoiron possessed weight averaged molecular weights ranging from 3 244 – 19 100 and PDIs of 1.1 - 1.4 (estimated from GPC analysis of the cationic iron analogues).

Thermal analysis of the polynorbornene and the polymethacrylate based polymers was quite interesting. Thermal gravimetric analysis indicated the the carbonyl groups of the alkyne-hexacarbonyldicobalt moieties were driven from the polymers at 130-220 °C. While the cationic cyclopentadiene groups degraded at 200-250 °C. Through differential scanning calorimetry the glass transition temperatures of polynorbornenes containing alkyne-hexacarbonyldicobalt either could not be determined or were around 62 °C; however, once the carbon monoxide had been thermally freed from the polymers, the glass transition temperatures ranged from 82 – 92 °C. Prior to addition of cobalt carbonyl the poly methacrylates, displayed glass transition

temperatures between 78 and 130 °C. Once cobalt carbonyl was added to these polymers, no glass transition temperatures could be found until after the carbonyl groups had been thermally driven off; however, once this occurred, the glass transitions ranged from 92 – 138 °C.

In chapter 4, a monomer containing η^6 -(haloarene)- η^5 -cyclopentadienyliron(II) hexafluorophosphate moieties as well as alkyne functional groups was polymerized using various dithiol linking groups. These polymers were too insoluble to add cobalt post polymerization and their molecular weights could not be determined. A monomer which contained both η^6 -(haloarene)- η^5 -cyclopentadienyliron(II) hexafluorophosphate and alkyne-hexacarbonyldicobalt moieties was also combined with various dithiol linking groups. IR spectral analysis of these polymers indicated a complete loss of the $\text{CoC}\equiv\text{O}$ bands, indicating that the condensation polymerization conditions are not compatible with alkyne-hexacarbonyldicobalt complexes. Thermal gravimetric analysis of these polymers indicated that the polymers were thermally stable to 200 - 250 °C where the cationic cyclopentadienyliron moiety was cleaved. The glass transition temperatures of these polymers ranged from 100 – 130 °C.

Chapter 5 detailed the synthesis and characterization of three siloxane based polymers which contained η^6 -(arene)- η^5 -cyclopentadienyliron(II) hexafluorophosphate moieties. These polymers were thermally stable up to approximately 200 °C where the η^6 -(arene)- η^5 -cyclopentadienyliron decomposed and possessed glass transition temperatures that ranged from 95-111 °C.

Chapter 7: References

- (1) Kealy, T. J.; Pauson, P. L. *Nature (London, U. K.)* **1951**, *168*, 1039-1040.
- (2) Pauson, P. L. *Journal of Organometallic Chemistry* **2001**, *637-639*, 3-6.
- (3) Wilkinson, G.; Rosenblum, M.; Whiting, M. C.; Woodward, R. B. *J. Am. Chem. Soc.* **1952**, *74*, 2125-2126.
- (4) Rinehart, K. L.; Motz, K. L.; Moon, S. *J. Am. Chem. Soc.* **1957**, *79*, 2749-2754.
- (5) Bublitz, D. E.; Rinehart, K. L., Jr. *Org. React.* **1969**, *17*, 1-154.
- (6) Astruc, D. In *Organometallic chemistry and Catalysis*; Springer-Verlag: New York, 2007; p 608.
- (7) Szafran, Z.; Pike, R. M.; Singh, M. M. In *Preparation and use of ferrocene*; Microscale inorganic chemistry: A complete laboratory experience; John Wiley & Sons, Inc.: New York, US, 1991; pp 302-313.
- (8) Tsierkezos, N. *Journal of Solution Chemistry* **2007**, *36*, 289-302.
- (9) Bond, A. M.; Oldham, K. B.; Snook, G. A. *Anal. Chem.* **2000**, *72*, 3492-3496.
- (10) Zanello, P. In *Inorganic Electrochemistry: Theory, Practice and Application*; The Royal Society of Chemistry: UK, 2003; p 615.
- (11) Arimoto, F. S.; Haven, A. C. *J. Am. Chem. Soc.* **1955**, *77*, 6295-6297.

- (12) Abd-El-Aziz, A. S.; Todd, E. K. *Coord. Chem. Rev.*, **2003**, *246*, 3-52.
- (13) Nguyen, P.; Gomez-Elipe, P.; Manners, I. *Chem. Rev.* **1999**, *99*, 1515-1548.
- (14) Hudson, R. D. A. *J. Organomet. Chem.* **2001**, *637-639*, 47-69.
- (15) Kalennikov, E. A.; Bochkov, G. I.; Kirilenko, Y. K.; Kaushanskii, D. A. *Fibre Chemistry* **1974**, *6*, 153-156.
- (16) Nesmeyanov, A. N.; Vol'kenau, N. A.; Bolesova, I. N. *Tetrahedron Lett.* **1963**, *4*, 1725-1729.
- (17) Litvak, V. V.; Filatova, L. S.; Khalikova, N. U.; Shteingarts, V. D. *Zh. Org. Khim.* **1980**, *16*, 336-342.
- (18) Gomes, P. C. B.; Vichi, E. J. S.; Moran, P. J. S.; Federman Neto, A.; Maroso, M. L.; Miller, J. *Organometallics* **1996**, *15*, 3198-3203.
- (19) Nesmeyanov, A. N.; Vol'kenau, N. A.; Petrovskii, P. V.; Kotova, L. S.; Petrakova, V. A.; Denisovich, L. T. *J. Organomet. Chem.* **1981**, *210*, 103-113.
- (20) Abd-El-Aziz, A. S. *Coord. Chem. Rev.*, **2002**, *233-234*, 177-191.
- (21) Abd-El-Aziz, A. S.; Bernardin, S. *Coord. Chem. Rev.*, **2000**, *203*, 219-267.
- (22) Chrisope, D. R.; Park, K. M.; Schuster, G. B. *J. Am. Chem. Soc.* **1989**, *111*, 6195-6201.
- (23) Boyd, D. C.; Bohling, D. A.; Mann, K. R. *J. Am. Chem. Soc.* **1985**, *107*, 1641-1644.

- (24) Nesmeyanov, A. N.; Vol'kenau, N. A.; Shilovtseva, L. S. *Dokl. Akad. Nauk SSSR* **1970**, *190*, 857.
- (25) Nesmeyanov, A. N.; Leshcheva, I. F.; Ustynyuk, Y. A.; Sirotkina, E. I.; Bolesova, I. N.; Isaeva, L. S.; Vol'kenau, N. A. *J. Organomet. Chem.* **1970**, *22*, 689-696.
- (26) Sternberg, H. W.; Greenfield, H.; Friedel, R. A.; Wotiz, J.; Markby, R.; Wender, I. *J. Am. Chem. Soc.* **1954**, *76*, 1457-1458.
- (27) Saha, M.; Nicholas, K. M. *J. Org. Chem.* **1984**, *49*, 417-422.
- (28) Al-Badri, Z.; Tew, G. N. *Macromolecules* **2008**, *41*, 4173-4179.
- (29) Dickson, R. S.; Fraser, P. J. In *Compounds derived from alkynes and carbonyl complexes of cobalt*. Stone, F. G. A., West, R., Eds.; Advances in organometallic chemistry; Academic Press, inc.: NY, 1974; Vol. 12, pp 323-371.
- (30) Silverstein, R. M.; Webster, F. X.; Kiemle, D. J. In *Spectrometric Identification of Organic Compounds 7th ed.* John Wiley & Sons, Inc.: United States, 2005; p 502.
- (31) Miinea, L. A.; Sessions, L. B.; Ericson, K. D.; Glueck, D. S.; Grubbs, R. B. *Macromolecules* **2004**, *37*, 8967-8972.
- (32) Shi, J.; Tong, B.; Li, Z.; Shen, J.; Zhao, W.; Fu, H.; Zhi, J.; Dong, Y.; Haeussler, M.; Lam, J. W. Y.; Tang, B. Z. *Macromolecules* **2007**, *40*, 8195-8204.
- (33) Pangborn, A. B.; Giardello, M. A.; Grubbs, R. H.; Rosen, R. K.; Timmers, F. J. *Organometallics* **1996**, *15*, 1518-1520.

- (34) Janiak, C.; Lassahn, P. G. *Macromol. Rapid Commun.* **2001**, *22*, 479-492.
- (35) Bielawski, C. W.; Grubbs, R. H. *Prog. Polym. Sci.* **2007**, *32*, 1-29.
- (36) Toste, F. D.; Chatterjee, A. K.; Grubbs, R. H. *Pure Appl. Chem.* **2002**, *74*, 7-10.
- (37) Li, H.; Tong, H.; Wang, C.; Song, L.; Zhang, W.; Zhu, X. *Lizi Jiaohuan Yu Xifu* **2005**, *21*, 358-364.
- (38) Sutthasupa, S.; Sanda, F.; Masuda, T. *Macromolecules* **2008**, *41*, 305-311.
- (39) Abd-El-Aziz, A. S.; Edel, A. L.; May, L. J.; Epp, K. M.; Hutton, H. M. *Can. J. Chem.* **1999**, *77*, 1797-1809.
- (40) Abd-El-Aziz, A. S.; Edel, A. L.; Epp, K. M.; Hutton, H. M. *New J. Chem.* **1999**, *23*, 569-571.
- (41) Malenfant, P. R. L.; Peters, A.; Wan, J. Patent Application Country: Application: US; Patent Country: US Patent 2008039589, 2008.
- (42) Katsumata, T.; Shiotsuki, M.; Sanda, F.; Masuda, T. *Polymer* **2009**, *50*, 1389-1394.
- (43) Cotton, F. A.; Reid, A. H. Jr., *Acta Crystallographica Section C* **1985**, *41*, 686-688.
- (44) Smulik, J. A.; Diver, S. T. *Org. Lett.* **2000**, *2*, 2271-2274.
- (45) Lippstreu, J. J.; Straub, B. F. *J. Am. Chem. Soc.* **2005**, *127*, 7444-7457.
- (46) Nandi, S.; Winter, H. H. *Macromolecules* **2005**, *38*, 4447-4455.

- (47) Neukamm, M. A.; Pinto, A.; Metzler-Nolte, N. *Chem. Commun.* **2008**, 232-234.
- (48) Abd-El-Aziz, A. S.; Afifi, T. H.; Budakowski, W. R.; Friesen, K. J.; Todd, E. K. *Macromolecules* **2002**, *35*, 8929-8932.
- (49) Gottlieb, H. E.; Kotlyar, V.; Nudelman, A. *J. Org. Chem.* **1997**, *62*, 7512-7515.
- (50) Abd-El-Aziz, A. S.; Carruthers, S. A.; Todd, E. K.; Afifi, T. H.; Gavina, J. M. A. *J. Polym. Sci., Part A: Polym. Chem.* **2005**, *43*, 1382-1396.
- (51) Manning, D. D.; Strong, L. E.; Hu, X.; Beck, P. J.; Kiessling, L. L. *Tetrahedron* **1997**, *53*, 11937-11952.
- (52) Abd-El-Aziz, A. S.; May, L. J.; Hurd, J. A.; Okasha, R. M. *J. Polym. Sci., Part A: Polym. Chem.* **2001**, *39*, 2716-2722.
- (53) Nuyken, O.; Lattermann, G. In *Polymers of acrylic acid, methacrylic acid, maleic acid and their derivatives*. Kricheldorf, H. R., Ed.; Handbook of polymer synthesis, Part A; Marcel Dekker inc.: New York, 1992; pp 223-315.
- (54) Moad, G.; Solomon, D. In *The chemistry of radical polymerization*; Elsevier Ltd.: CA, 2006; p 429.
- (55) Abd-El-Aziz, A. S.; Carraher, C. E.; Pittman, C. U.; Zeldin, M., Eds.; In *Macromolecules containing metal and metal-like elements, Transition metal-containing polymers*; Wiley-Interscience: New Jersey, 2005; Vol. 6, p 219.

- (56) Archer, R. D. In *Inorganic and Organometallic Polymers*; Wiley-VHC: New York, 2001; p 247.
- (57) Manners, I. *Science* **2001**, *294*, 1664-1666.
- (58) Pittman, C. U., Jr.; Voges, R. L.; Jones, W. B. *Macromolecules* **1971**, *4*, 291-297.
- (59) Pittman, C. U., Jr.; Voges, R. L.; Jones, W. B. *Macromolecules* **1971**, *4*, 298-302.
- (60) Pittman, C. U., Jr.; Lai, J. C.; Vanderpool, D. P.; Good, M.; Prado, R. *Macromolecules* **1970**, *3*, 746-754.
- (61) Pittman, C. U., Jr.; Lai, J. C.; Vanderpool, D. P. *Macromolecules* **1970**, *3*, 105-107.
- (62) Pittman, C. U., Jr.; Lai, J. C.; Vanderpool, D. P.; Good, M.; Prados, R. In *In Polymers of ferrocenylmethyl acrylate and ferrocenylmethyl methacrylate and their ferricinium salts*.
Section Title: Synthetic High Polymers; 1971; pp 97-124.
- (63) Abd-El-Aziz, A. S.; Todd, E. K.; Ma, G.; DiMartino, J. J. *Inorg. Organomet. Polym.* **2000**, *10*, 265-272.
- (64) Abd-El-Aziz, A. S.; Todd, E. K. *Macromol. Chem. Phys.* **2004**, *205*, 418-429.
- (65) Abd-El-Aziz, A. S.; Todd, E. K.; Ma, G.; DiMartino, J. J. *Inorg. Organomet. Polym.* **2000**, *10*, 265-272.
- (66) Abd-El-Aziz, A. S.; Todd, E. K.; Okasha, R. M. *Macromol. Containing Met. Met. -Like Elem.* **2004**, *2*, 233-273.

- (67) Abd-El-Aziz, A. S.; Shipman, P. O.; Neeland, E. G.; Corkery, T. C.; Mohammed, S.; Harvey, P. D.; Mohamed, H. M.; Bedair, A. H.; El-Agrody, A. M.; Aguiar, P. M.; Kroeker, S. *Macromol. Chem. Phys.* **2008**, *209*, 84-103.
- (68) Abd-El-Aziz, A. S.; Todd, E. K.; Ma, G.; DiMartino, J. J. *Inorg. Organomet. Polym.* **2000**, *10*, 265-272.
- (69) Thorn, D. L.; Hoffmann, R. *Inorg. Chem.* **1978**, *17*, 126-140.
- (70) Brusey, S. A.; Banide, E. V.; Dörrich, S.; O'Donohue, P.; Ortin, Y.; Müller-Bunz, H.; Long, C.; Evans, P.; McGlinchey, M. J. *Organometallics* **2009**, *28*, 6308-6319.
- (71) Abd-El-Aziz, A. S.; de Denus, C. R.; Todd, E. K.; Bernardin, S. A. *Macromolecules* **2000**, *33*, 5000-5005.
- (72) Abd-El-Aziz, A. S.; Todd, E. K.; Okasha, R. M.; Shipman, P. O.; Wood, T. E. *Macromolecules* **2005**, *38*, 9411-9419.
- (73) Abd-El-Aziz, A. S. *Macromol. Rapid Commun.* **2002**, *23*, 995-1031.
- (74) Abd-El-Aziz, A.; Todd, E.; Shipman, P. *Polymer News* **2005**, *30*, 202-212.
- (75) Abd-El-Aziz, A. S.; Okasha, R. M.; Shipman, P. O.; Afifi, T. H. *Macromol. Rapid Commun.* **2004**, *25*, 1497-1503.
- (76) Rahimi, A.; Shokrolahi, P. *Int. J. Inorg. Mat.* **2001**, *3*, 843-847.
- (77) Meals, R. N. *Pure Appl. Chem.* **1966**, *13*, 141-157.

- (78) Miller, H. C.; Schreiber, R. S. U.S. Patent 2,379,821, July 3, 1945.
- (79) Matisons, J.; In *Hydrosilylation: A Comprehensive Review on Recent Advances*; Marciniak, B., Ed.; Springer: UK, 2008; Vol. 1, p 408.
- (80) Binet, C.; Dumont, M.; Fitremann, J.; Gineste, S.; Laurent, E.; Marty, J.; Mauzac, M.; Mingotaud, A.; Moukarzel, W.; Palaprat, G.; Zadoina, L. *Silicon Based Polymers* **2008**, 135-151.
- (81) Abd-El-Aziz, A. S.; Bernardin, S. A.; Tran, K. *Tetrahedron Lett.* **1999**, 40, 1835-1838.

Chapter 8: Appendices

Crystallographic data was measured, elucidated and reported by Brian Patrick at the University of British Columbia in Vancouver.

8.1 X-ray structure report for complex 2.6

Data Collection

A red plate crystal of $C_{15}H_{14}O_3Fe$ having approximate dimensions of 0.12 x 0.20 x 0.45 mm was mounted on a glass fiber. All measurements were made on a Bruker X8 APEX II diffractometer with graphite monochromated Mo-K α radiation. The data were collected at a temperature of $-170.0 \pm 0.1^\circ C$ to a maximum 2θ value of 56.0° . Data were collected in a series of ϕ and ω scans in 0.50° oscillations with 5.0-second exposures. The crystal-to-detector distance was 40.00 mm.

Data Reduction

Of the 21477 reflections that were collected, 3041 were unique ($R_{int} = 0.037$); equivalent reflections were merged. Data were collected and integrated using the Bruker SAINT¹ software package. The linear absorption coefficient, μ , for Mo-K α radiation is 11.96 cm^{-1} . Data were corrected for absorption effects using the multi-scan technique (SADABS²), with minimum and maximum transmission coefficients of 0.712 and 0.866, respectively. The data were corrected for Lorentz and polarization effects.

Structure Solution and Refinement

The structure was solved by direct methods³. The material crystallizes with disorder in the position of the hydroxyl group. The disorder was modeled in two orientations. All non-hydrogen atoms were refined anisotropically. The hydroxyl hydrogen atom was located in a

difference map and refined isotropically. All C-H hydrogen atoms were placed in calculated positions but were not refined. The final cycle of full-matrix least-squares refinement⁴ on F^2 was based on 3041 reflections and 236 variable parameters and converged (largest parameter shift was 0.00 times its esd) with unweighted and weighted agreement factors of:

$$R1 = \Sigma ||F_o| - |F_c|| / \Sigma |F_o| = 0.039$$

$$wR2 = [\Sigma (w (F_o^2 - F_c^2)^2) / \Sigma w(F_o^2)^2]^{1/2} = 0.075$$

The standard deviation of an observation of unit weight⁵ was 1.02. The weighting scheme was based on counting statistics. The maximum and minimum peaks on the final difference Fourier map corresponded to 0.82 and $-0.25 \text{ e}^-/\text{\AA}^3$, respectively.

Neutral atom scattering factors were taken from Cromer and Waber⁶. Anomalous dispersion effects were included in F_{calc} ⁷; the values for $\Delta f'$ and $\Delta f''$ were those of Creagh and McAuley⁸. The values for the mass attenuation coefficients are those of Creagh and Hubbell⁹. All refinements were performed using the SHELXTL¹⁰ crystallographic software package of Bruker-AXS.

References

- (1) SAINT. Version 7.60A. Bruker AXS Inc., Madison, Wisconsin, USA. (1997-2009).
- (2) SADABS. Bruker Nonius area detector scaling and absorption correction - V2008/1, Bruker AXS Inc., Madison, Wisconsin, USA (2008).
- (3) SIR97 - Altomare A., Burla M.C., Camalli M., Cascarano G.L., Giacovazzo C. , Guagliardi A., Moliterni A.G.G., Polidori G., Spagna R. (1999) J. Appl. Cryst. 32, 115-119.
- (4) Least Squares function minimized:

$$\Sigma w(F_o^2 - F_c^2)^2$$

(5) Standard deviation of an observation of unit weight:

$$[\Sigma w(F_o^2 - F_c^2)^2 / (N_o - N_v)]^{1/2}$$

where: N_o = number of observations

N_v = number of variables

(6) Cromer, D. T. & Waber, J. T.; "International Tables for X-ray Crystallography", Vol. IV, The Kynoch Press, Birmingham, England, Table 2.2 A (1974).

(7) Ibers, J. A. & Hamilton, W. C.; Acta Crystallogr., 17, 781 (1964).

(8) Creagh, D. C. & McAuley, W.J. ; "International Tables for Crystallography", Vol C, (A.J.C. Wilson, ed.), Kluwer Academic Publishers, Boston, Table 4.2.6.8, pages 219-222 (1992).

(9) Creagh, D. C. & Hubbell, J.H.; "International Tables for Crystallography", Vol C, (A.J.C. Wilson, ed.), Kluwer Academic Publishers, Boston, Table 4.2.4.3, pages 200-206 (1992).

(10) SHELXTL Version 5.1. Bruker AXS Inc., Madison, Wisconsin, USA. (1997).

EXPERIMENTAL DETAILS

A. Crystal Data

Empirical Formula	$C_{15}H_{14}O_3Fe$
Formula Weight	298.11
Crystal Color, Habit	red, plate
Crystal Dimensions	0.12 X 0.20 X 0.45 mm
Crystal System	orthorhombic

Lattice Type	primitive
Lattice Parameters	$a = 7.3827(4) \text{ \AA}$ $b = 17.1286(8) \text{ \AA}$ $c = 19.9355(10) \text{ \AA}$ $\alpha = 90^\circ$ $\beta = 90^\circ$ $\gamma = 90^\circ$ $V = 2520.9(2) \text{ \AA}^3$
Space Group	<i>P bca</i> (#61)
Z value	8
D _{calc}	1.571 g/cm ³
F ₀₀₀	1232.00
$\mu(\text{MoK}\alpha)$	11.96 cm ⁻¹
B. Intensity Measurements	
Diffractometer	Bruker X8 APEX II
Radiation	MoK α ($\lambda = 0.71073 \text{ \AA}$) graphite monochromated
Data Images	809 exposures @ 5.0 seconds
Detector Position	40.00 mm
$2\theta_{\text{max}}$	56.0 $^\circ$
No. of Reflections Measured	Total: 21477 Unique: 3041 ($R_{\text{int}} = 0.037$)

Corrections	Absorption ($T_{\min} = 0.712$, $T_{\max} = 0.866$)
	Lorentz-polarization
C. Structure Solution and Refinement	
Structure Solution	Direct Methods (SIR97)
Refinement	Full-matrix least-squares on F^2
Function Minimized	$\Sigma w (F_o^2 - F_c^2)^2$
Least Squares Weights	$w=1/(\sigma^2(F_o^2)+(0.0384P)^2+ 1.2522P)$
Anomalous Dispersion	All non-hydrogen atoms
No. Observations ($I>0.00\sigma(I)$)	3041
No. Variables	236
Reflection/Parameter Ratio	12.89
Residuals (refined on F^2 , all data): R1; wR2	0.039; 0.075
Goodness of Fit Indicator	1.02
No. Observations ($I>2.00\sigma(I)$)	2487
Residuals (refined on F): R1; wR2	0.028; 0.069
Max Shift/Error in Final Cycle	0.00
Maximum peak in Final Diff. Map	0.82 e ⁻ /Å ³
Minimum peak in Final Diff. Map	-0.25 e ⁻ /Å ³

Table 2. Atomic coordinates ($\times 10^4$) and equivalent isotropic displacement parameters ($\text{\AA}^2 \times 10^3$) for aa004. U(eq) is defined as one third of the trace of the orthogonalized U_{ij} tensor.

	x	y	z	U (eq)	occ
C (1)	4300 (50)	1900 (20)	1363 (19)	30 (5)	0.42 (4)
C (2)	3380 (40)	2574 (17)	1562 (18)	40 (6)	0.42 (4)
C (3)	2150 (40)	2352 (15)	2043 (13)	35 (6)	0.42 (4)
C (4)	2400 (30)	1540 (15)	2176 (14)	37 (6)	0.42 (4)
C (5)	3680 (40)	1277 (12)	1735 (16)	31 (5)	0.42 (4)
C (1B)	4240 (40)	2078 (17)	1316 (15)	35 (4)	0.58 (4)
C (2B)	3060 (30)	2626 (14)	1628 (10)	25 (2)	0.58 (4)
C (3B)	2080 (30)	2215 (12)	2143 (10)	25 (2)	0.58 (4)
C (4B)	2600 (30)	1438 (10)	2113 (11)	35 (4)	0.58 (4)
C (5B)	3960 (30)	1350 (12)	1625 (13)	38 (5)	0.58 (4)
C (6)	1107 (2)	1497 (1)	225 (1)	21 (1)	
C (7)	168 (3)	2184 (1)	411 (1)	27 (1)	
C (8)	-1009 (2)	2007 (1)	950 (1)	30 (1)	
C (9)	-830 (2)	1204 (1)	1104 (1)	26 (1)	
C (10)	489 (2)	884 (1)	656 (1)	20 (1)	
C (11)	1220 (2)	91 (1)	695 (1)	20 (1)	
C (12)	3508 (2)	-753 (1)	299 (1)	23 (1)	
C (13)	4667 (2)	-802 (1)	892 (1)	24 (1)	
C (14)	5591 (2)	-838 (1)	1379 (1)	25 (1)	
O (1)	696 (2)	-422 (1)	1065 (1)	25 (1)	
O (2)	2600 (2)	-7 (1)	262 (1)	21 (1)	
C (15)	6713 (3)	-892 (1)	1987 (1)	32 (1)	0.703 (4)
O (3)	8064 (3)	-298 (1)	2055 (1)	34 (1)	0.703 (4)
C (15B)	6713 (3)	-892 (1)	1987 (1)	32 (1)	0.297 (4)
O (3B)	8277 (6)	-1277 (3)	1835 (3)	35 (2)	0.297 (4)
Fe (1)	1601 (1)	1745 (1)	1209 (1)	17 (1)	

Table 3. Bond lengths [Å] and angles [deg] for aa004.

C(1)-C(5)	1.38(3)
C(1)-C(2)	1.39(4)
C(1)-Fe(1)	2.03(4)
C(1)-H(1)	0.9500
C(2)-C(3)	1.37(3)
C(2)-Fe(1)	2.06(3)
C(2)-H(2)	0.9500
C(3)-C(4)	1.43(3)
C(3)-Fe(1)	2.00(3)
C(3)-H(3)	0.9500
C(4)-C(5)	1.37(3)
C(4)-Fe(1)	2.05(3)
C(4)-H(4)	0.9500
C(5)-Fe(1)	2.02(3)
C(5)-H(5)	0.9500
C(1B)-C(5B)	1.41(3)
C(1B)-C(2B)	1.43(3)
C(1B)-Fe(1)	2.04(3)
C(1B)-H(1B)	0.9500
C(2B)-C(3B)	1.44(3)
C(2B)-Fe(1)	2.03(2)
C(2B)-H(2B)	0.9500
C(3B)-C(4B)	1.39(2)
C(3B)-Fe(1)	2.06(2)
C(3B)-H(3B)	0.9500
C(4B)-C(5B)	1.40(2)
C(4B)-Fe(1)	2.02(2)
C(4B)-H(4B)	0.9500
C(5B)-Fe(1)	2.04(2)
C(5B)-H(5B)	0.9500
C(6)-C(7)	1.414(3)
C(6)-C(10)	1.432(2)
C(6)-Fe(1)	2.0396(17)
C(6)-H(6)	0.9500
C(7)-C(8)	1.415(3)
C(7)-Fe(1)	2.0539(18)
C(7)-H(7)	0.9500
C(8)-C(9)	1.417(3)
C(8)-Fe(1)	2.0446(18)
C(8)-H(8)	0.9500
C(9)-C(10)	1.431(2)
C(9)-Fe(1)	2.0307(18)
C(9)-H(9)	0.9500
C(10)-C(11)	1.464(2)
C(10)-Fe(1)	2.0161(17)
C(11)-O(1)	1.209(2)
C(11)-O(2)	1.346(2)
C(12)-O(2)	1.446(2)
C(12)-C(13)	1.461(3)
C(12)-H(12A)	0.9900
C(12)-H(12B)	0.9900
C(13)-C(14)	1.190(3)
C(14)-C(15)	1.470(3)
C(15)-O(3)	1.432(3)

C (15) -H (15A)	0.9900
C (15) -H (15B)	0.9900
O (3) -H (3O)	0.92 (6)
O (3B) -H (3O2)	0.87 (10)
C (5) -C (1) -C (2)	109 (3)
C (5) -C (1) -Fe (1)	69.8 (19)
C (2) -C (1) -Fe (1)	71.1 (18)
C (5) -C (1) -H (1)	125.5
C (2) -C (1) -H (1)	125.5
Fe (1) -C (1) -H (1)	124.8
C (3) -C (2) -C (1)	107 (3)
C (3) -C (2) -Fe (1)	68.1 (15)
C (1) -C (2) -Fe (1)	69.0 (19)
C (3) -C (2) -H (2)	126.4
C (1) -C (2) -H (2)	126.7
Fe (1) -C (2) -H (2)	127.6
C (2) -C (3) -C (4)	108 (2)
C (2) -C (3) -Fe (1)	72.4 (14)
C (4) -C (3) -Fe (1)	71.0 (15)
C (2) -C (3) -H (3)	125.9
C (4) -C (3) -H (3)	125.7
Fe (1) -C (3) -H (3)	122.4
C (5) -C (4) -C (3)	106.8 (18)
C (5) -C (4) -Fe (1)	69.4 (17)
C (3) -C (4) -Fe (1)	67.7 (15)
C (5) -C (4) -H (4)	126.5
C (3) -C (4) -H (4)	126.7
Fe (1) -C (4) -H (4)	127.0
C (4) -C (5) -C (1)	109 (2)
C (4) -C (5) -Fe (1)	71.4 (17)
C (1) -C (5) -Fe (1)	70.5 (18)
C (4) -C (5) -H (5)	125.6
C (1) -C (5) -H (5)	125.6
Fe (1) -C (5) -H (5)	125.5
C (5B) -C (1B) -C (2B)	108 (2)
C (5B) -C (1B) -Fe (1)	69.9 (14)
C (2B) -C (1B) -Fe (1)	69.1 (14)
C (5B) -C (1B) -H (1B)	126.3
C (2B) -C (1B) -H (1B)	126.0
Fe (1) -C (1B) -H (1B)	126.4
C (1B) -C (2B) -C (3B)	107.3 (19)
C (1B) -C (2B) -Fe (1)	69.9 (15)
C (3B) -C (2B) -Fe (1)	70.3 (12)
C (1B) -C (2B) -H (2B)	126.4
C (3B) -C (2B) -H (2B)	126.3
Fe (1) -C (2B) -H (2B)	125.2
C (4B) -C (3B) -C (2B)	107.3 (16)
C (4B) -C (3B) -Fe (1)	68.5 (12)
C (2B) -C (3B) -Fe (1)	68.4 (11)
C (4B) -C (3B) -H (3B)	126.2
C (2B) -C (3B) -H (3B)	126.4
Fe (1) -C (3B) -H (3B)	128.2
C (3B) -C (4B) -C (5B)	109.4 (14)
C (3B) -C (4B) -Fe (1)	71.6 (11)
C (5B) -C (4B) -Fe (1)	70.7 (12)
C (3B) -C (4B) -H (4B)	125.4

C (5B) -C (4B) -H (4B)	125.2
Fe (1) -C (4B) -H (4B)	124.4
C (4B) -C (5B) -C (1B)	108.3 (18)
C (4B) -C (5B) -Fe (1)	68.8 (12)
C (1B) -C (5B) -Fe (1)	69.8 (14)
C (4B) -C (5B) -H (5B)	126.0
C (1B) -C (5B) -H (5B)	125.7
Fe (1) -C (5B) -H (5B)	126.4
C (7) -C (6) -C (10)	107.31 (16)
C (7) -C (6) -Fe (1)	70.34 (10)
C (10) -C (6) -Fe (1)	68.45 (10)
C (7) -C (6) -H (6)	126.3
C (10) -C (6) -H (6)	126.3
Fe (1) -C (6) -H (6)	126.4
C (6) -C (7) -C (8)	108.75 (16)
C (6) -C (7) -Fe (1)	69.24 (10)
C (8) -C (7) -Fe (1)	69.45 (11)
C (6) -C (7) -H (7)	125.6
C (8) -C (7) -H (7)	125.6
Fe (1) -C (7) -H (7)	127.3
C (7) -C (8) -C (9)	108.44 (17)
C (7) -C (8) -Fe (1)	70.16 (10)
C (9) -C (8) -Fe (1)	69.13 (10)
C (7) -C (8) -H (8)	125.8
C (9) -C (8) -H (8)	125.8
Fe (1) -C (8) -H (8)	126.5
C (8) -C (9) -C (10)	107.41 (17)
C (8) -C (9) -Fe (1)	70.19 (10)
C (10) -C (9) -Fe (1)	68.75 (10)
C (8) -C (9) -H (9)	126.3
C (10) -C (9) -H (9)	126.3
Fe (1) -C (9) -H (9)	126.3
C (9) -C (10) -C (6)	108.09 (15)
C (9) -C (10) -C (11)	124.94 (16)
C (6) -C (10) -C (11)	126.57 (16)
C (9) -C (10) -Fe (1)	69.84 (10)
C (6) -C (10) -Fe (1)	70.21 (9)
C (11) -C (10) -Fe (1)	119.99 (12)
O (1) -C (11) -O (2)	122.92 (16)
O (1) -C (11) -C (10)	126.01 (16)
O (2) -C (11) -C (10)	111.07 (15)
O (2) -C (12) -C (13)	111.33 (14)
O (2) -C (12) -H (12A)	109.4
C (13) -C (12) -H (12A)	109.4
O (2) -C (12) -H (12B)	109.4
C (13) -C (12) -H (12B)	109.4
H (12A) -C (12) -H (12B)	108.0
C (14) -C (13) -C (12)	179.1 (2)
C (13) -C (14) -C (15)	179.0 (2)
C (11) -O (2) -C (12)	115.29 (13)
O (3) -C (15) -C (14)	115.17 (17)
O (3) -C (15) -H (15A)	108.5
C (14) -C (15) -H (15A)	108.5
O (3) -C (15) -H (15B)	108.5
C (14) -C (15) -H (15B)	108.5
H (15A) -C (15) -H (15B)	107.5
C (15) -O (3) -H (3O)	109 (3)

C (3) -Fe (1) -C (10)	156.4 (8)
C (3) -Fe (1) -C (4B)	47.1 (8)
C (10) -Fe (1) -C (4B)	116.5 (5)
C (3) -Fe (1) -C (5)	67.7 (10)
C (10) -Fe (1) -C (5)	107.6 (7)
C (4B) -Fe (1) -C (5)	32.4 (10)
C (3) -Fe (1) -C (9)	120.1 (7)
C (10) -Fe (1) -C (9)	41.41 (7)
C (4B) -Fe (1) -C (9)	107.2 (5)
C (5) -Fe (1) -C (9)	122.8 (7)
C (3) -Fe (1) -C (1)	66.9 (12)
C (10) -Fe (1) -C (1)	125.3 (10)
C (4B) -Fe (1) -C (1)	62.6 (11)
C (5) -Fe (1) -C (1)	39.7 (10)
C (9) -Fe (1) -C (1)	160.3 (10)
C (3) -Fe (1) -C (2B)	33.5 (10)
C (10) -Fe (1) -C (2B)	169.5 (6)
C (4B) -Fe (1) -C (2B)	68.5 (8)
C (5) -Fe (1) -C (2B)	71.4 (9)
C (9) -Fe (1) -C (2B)	148.0 (6)
C (1) -Fe (1) -C (2B)	47.4 (11)
C (3) -Fe (1) -C (6)	160.5 (8)
C (10) -Fe (1) -C (6)	41.34 (7)
C (4B) -Fe (1) -C (6)	150.5 (6)
C (5) -Fe (1) -C (6)	123.5 (8)
C (9) -Fe (1) -C (6)	69.41 (7)
C (1) -Fe (1) -C (6)	110.4 (10)
C (2B) -Fe (1) -C (6)	130.1 (6)
C (3) -Fe (1) -C (1B)	64.8 (11)
C (10) -Fe (1) -C (1B)	130.6 (8)
C (4B) -Fe (1) -C (1B)	68.2 (10)
C (5) -Fe (1) -C (1B)	48.2 (10)
C (9) -Fe (1) -C (1B)	169.0 (8)
C (1) -Fe (1) -C (1B)	9.0 (15)
C (2B) -Fe (1) -C (1B)	41.0 (9)
C (6) -Fe (1) -C (1B)	109.2 (8)
C (3) -Fe (1) -C (5B)	70.2 (10)
C (10) -Fe (1) -C (5B)	109.0 (6)
C (4B) -Fe (1) -C (5B)	40.5 (7)
C (5) -Fe (1) -C (5B)	9.2 (12)
C (9) -Fe (1) -C (5B)	130.0 (6)
C (1) -Fe (1) -C (5B)	31.5 (11)
C (2B) -Fe (1) -C (5B)	68.2 (9)
C (6) -Fe (1) -C (5B)	118.3 (7)
C (1B) -Fe (1) -C (5B)	40.3 (7)
C (3) -Fe (1) -C (8)	106.7 (7)
C (10) -Fe (1) -C (8)	68.83 (7)
C (4B) -Fe (1) -C (8)	128.9 (7)
C (5) -Fe (1) -C (8)	158.8 (8)
C (9) -Fe (1) -C (8)	40.68 (8)
C (1) -Fe (1) -C (8)	158.8 (10)
C (2B) -Fe (1) -C (8)	116.0 (7)
C (6) -Fe (1) -C (8)	68.53 (8)
C (1B) -Fe (1) -C (8)	149.8 (8)
C (5B) -Fe (1) -C (8)	168.0 (7)
C (3) -Fe (1) -C (4)	41.3 (9)
C (10) -Fe (1) -C (4)	120.4 (7)

C (4B) -Fe (1) -C (4)	7.4 (11)
C (5) -Fe (1) -C (4)	39.2 (9)
C (9) -Fe (1) -C (4)	105.8 (6)
C (1) -Fe (1) -C (4)	66.3 (12)
C (2B) -Fe (1) -C (4)	65.7 (9)
C (6) -Fe (1) -C (4)	157.2 (8)
C (1B) -Fe (1) -C (4)	71.0 (10)
C (5B) -Fe (1) -C (4)	46.8 (10)
C (8) -Fe (1) -C (4)	123.2 (7)

Symmetry transformations used to generate equivalent atoms:

Table 4. Anisotropic displacement parameters ($\text{\AA}^2 \times 10^3$) for aa004.
 The anisotropic displacement factor exponent takes the form:
 $-2 \pi^2 [h^2 a^{*2} U_{11} + \dots + 2 h k a^* b^* U_{12}]$

	U11	U22	U33	U23	U13	U12
C (1)	11 (3)	54 (11)	24 (9)	-6 (7)	-1 (5)	-6 (6)
C (2)	46 (13)	18 (6)	56 (12)	5 (6)	-36 (9)	-14 (8)
C (3)	38 (10)	37 (9)	31 (11)	-20 (7)	-11 (7)	21 (7)
C (4)	24 (4)	69 (16)	17 (4)	4 (7)	4 (3)	-9 (7)
C (5)	27 (7)	18 (5)	46 (11)	6 (6)	-15 (6)	-1 (5)
C (1B)	20 (5)	69 (12)	18 (3)	1 (7)	-5 (3)	-15 (6)
C (2B)	21 (4)	26 (4)	27 (3)	4 (3)	-12 (3)	-5 (3)
C (3B)	26 (4)	35 (5)	12 (3)	-2 (3)	3 (2)	-6 (4)
C (4B)	61 (10)	20 (3)	25 (6)	6 (3)	-17 (6)	-6 (4)
C (5B)	27 (6)	48 (11)	38 (8)	-26 (6)	-20 (5)	21 (7)
C (6)	21 (1)	22 (1)	21 (1)	-1 (1)	-7 (1)	-3 (1)
C (7)	27 (1)	21 (1)	33 (1)	-2 (1)	-15 (1)	1 (1)
C (8)	16 (1)	27 (1)	48 (1)	-12 (1)	-9 (1)	4 (1)
C (9)	14 (1)	27 (1)	37 (1)	-7 (1)	2 (1)	-3 (1)
C (10)	15 (1)	20 (1)	24 (1)	-3 (1)	-2 (1)	-3 (1)
C (11)	16 (1)	21 (1)	21 (1)	-4 (1)	0 (1)	-4 (1)
C (12)	23 (1)	18 (1)	29 (1)	-4 (1)	3 (1)	3 (1)
C (13)	22 (1)	18 (1)	31 (1)	0 (1)	5 (1)	-1 (1)
C (14)	23 (1)	20 (1)	34 (1)	4 (1)	5 (1)	-1 (1)
O (1)	23 (1)	21 (1)	31 (1)	2 (1)	4 (1)	-5 (1)
O (2)	22 (1)	18 (1)	24 (1)	-1 (1)	4 (1)	1 (1)
C (15)	29 (1)	33 (1)	34 (1)	10 (1)	-2 (1)	-4 (1)
O (3)	36 (1)	38 (1)	27 (1)	0 (1)	0 (1)	-7 (1)
C (15B)	29 (1)	33 (1)	34 (1)	10 (1)	-2 (1)	-4 (1)
O (3B)	19 (2)	46 (3)	42 (3)	21 (2)	4 (2)	-1 (2)
Fe (1)	14 (1)	18 (1)	18 (1)	-3 (1)	-1 (1)	0 (1)

Table 5. Hydrogen coordinates ($\times 10^4$) and isotropic displacement parameters ($\text{Å}^2 \times 10^3$) for aa004.

	x	y	z	U (eq)
H (1)	5204	1876	1025	36
H (2)	3569	3087	1397	48
H (3)	1285	2682	2252	42
H (4)	1791	1240	2508	44
H (5)	4073	752	1692	37
H (1B)	5071	2185	964	43
H (2B)	2936	3163	1517	29
H (3B)	1224	2435	2446	29
H (4B)	2121	1029	2381	42
H (5B)	4579	879	1521	45
H (6)	1985	1452	-121	26
H (7)	305	2682	207	32
H (8)	-1787	2366	1170	36
H (9)	-1468	928	1444	31
H (12A)	4252	-829	-109	28
H (12B)	2593	-1175	315	28
H (15A)	5906	-871	2383	38
H (15B)	7321	-1407	1990	38
H (15C)	6995	-363	2156	38
H (15D)	6047	-1178	2342	38
H (3O)	8900 (80)	-350 (30)	1720 (30)	95 (18)
H (3O2)	8950 (110)	-960 (50)	1600 (40)	29 (19)

Table 6. Torsion angles [deg] for aa004.

C (5)-C (1)-C (2)-C (3)	-2 (4)
Fe (1)-C (1)-C (2)-C (3)	57.7 (19)
C (5)-C (1)-C (2)-Fe (1)	-60 (3)
C (1)-C (2)-C (3)-C (4)	4 (3)
Fe (1)-C (2)-C (3)-C (4)	62.3 (19)
C (1)-C (2)-C (3)-Fe (1)	-58 (2)
C (2)-C (3)-C (4)-C (5)	-5 (3)
Fe (1)-C (3)-C (4)-C (5)	59 (2)
C (2)-C (3)-C (4)-Fe (1)	-63.2 (19)
C (3)-C (4)-C (5)-C (1)	3 (4)
Fe (1)-C (4)-C (5)-C (1)	61 (2)
C (3)-C (4)-C (5)-Fe (1)	-58 (2)
C (2)-C (1)-C (5)-C (4)	-1 (4)
Fe (1)-C (1)-C (5)-C (4)	-61 (2)
C (2)-C (1)-C (5)-Fe (1)	61 (2)
C (5B)-C (1B)-C (2B)-C (3B)	1 (3)
Fe (1)-C (1B)-C (2B)-C (3B)	60.7 (14)
C (5B)-C (1B)-C (2B)-Fe (1)	-59.6 (18)
C (1B)-C (2B)-C (3B)-C (4B)	-3 (2)
Fe (1)-C (2B)-C (3B)-C (4B)	57.6 (15)
C (1B)-C (2B)-C (3B)-Fe (1)	-60.4 (17)
C (2B)-C (3B)-C (4B)-C (5B)	3 (2)
Fe (1)-C (3B)-C (4B)-C (5B)	61.0 (16)
C (2B)-C (3B)-C (4B)-Fe (1)	-57.6 (13)
C (3B)-C (4B)-C (5B)-C (1B)	-3 (3)
Fe (1)-C (4B)-C (5B)-C (1B)	58.8 (18)
C (3B)-C (4B)-C (5B)-Fe (1)	-61.5 (16)
C (2B)-C (1B)-C (5B)-C (4B)	1 (3)
Fe (1)-C (1B)-C (5B)-C (4B)	-58.2 (16)
C (2B)-C (1B)-C (5B)-Fe (1)	59.1 (18)
C (10)-C (6)-C (7)-C (8)	0.3 (2)
Fe (1)-C (6)-C (7)-C (8)	-58.34 (13)
C (10)-C (6)-C (7)-Fe (1)	58.67 (11)
C (6)-C (7)-C (8)-C (9)	-0.5 (2)
Fe (1)-C (7)-C (8)-C (9)	-58.70 (13)
C (6)-C (7)-C (8)-Fe (1)	58.21 (12)
C (7)-C (8)-C (9)-C (10)	0.4 (2)
Fe (1)-C (8)-C (9)-C (10)	-58.89 (12)
C (7)-C (8)-C (9)-Fe (1)	59.34 (13)
C (8)-C (9)-C (10)-C (6)	-0.2 (2)
Fe (1)-C (9)-C (10)-C (6)	-60.04 (12)
C (8)-C (9)-C (10)-C (11)	172.94 (16)
Fe (1)-C (9)-C (10)-C (11)	113.14 (16)
C (8)-C (9)-C (10)-Fe (1)	59.80 (12)
C (7)-C (6)-C (10)-C (9)	-0.06 (19)
Fe (1)-C (6)-C (10)-C (9)	59.81 (12)
C (7)-C (6)-C (10)-C (11)	-173.10 (16)
Fe (1)-C (6)-C (10)-C (11)	-113.23 (17)
C (7)-C (6)-C (10)-Fe (1)	-59.87 (12)
C (9)-C (10)-C (11)-O (1)	7.5 (3)
C (6)-C (10)-C (11)-O (1)	179.44 (17)
Fe (1)-C (10)-C (11)-O (1)	92.81 (19)
C (9)-C (10)-C (11)-O (2)	-171.98 (16)
C (6)-C (10)-C (11)-O (2)	-0.1 (2)

Fe (1) -C (10) -C (11) -O (2)	-86.70 (16)
O (2) -C (12) -C (13) -C (14)	47 (13)
C (12) -C (13) -C (14) -C (15)	64 (22)
O (1) -C (11) -O (2) -C (12)	-4.1 (2)
C (10) -C (11) -O (2) -C (12)	175.39 (13)
C (13) -C (12) -O (2) -C (11)	-74.61 (19)
C (13) -C (14) -C (15) -O (3)	-168 (14)
C (2) -C (3) -Fe (1) -C (10)	163.7 (17)
C (4) -C (3) -Fe (1) -C (10)	46 (2)
C (2) -C (3) -Fe (1) -C (4B)	110.8 (18)
C (4) -C (3) -Fe (1) -C (4B)	-6.5 (16)
C (2) -C (3) -Fe (1) -C (5)	80.7 (17)
C (4) -C (3) -Fe (1) -C (5)	-36.6 (13)
C (2) -C (3) -Fe (1) -C (9)	-163.3 (14)
C (4) -C (3) -Fe (1) -C (9)	79.4 (14)
C (2) -C (3) -Fe (1) -C (1)	37.4 (17)
C (4) -C (3) -Fe (1) -C (1)	-79.9 (16)
C (2) -C (3) -Fe (1) -C (2B)	-9 (3)
C (4) -C (3) -Fe (1) -C (2B)	-126 (2)
C (2) -C (3) -Fe (1) -C (6)	-48 (3)
C (4) -C (3) -Fe (1) -C (6)	-165.7 (16)
C (2) -C (3) -Fe (1) -C (1B)	27.8 (16)
C (4) -C (3) -Fe (1) -C (1B)	-89.5 (15)
C (2) -C (3) -Fe (1) -C (5B)	71.2 (15)
C (4) -C (3) -Fe (1) -C (5B)	-46.1 (13)
C (2) -C (3) -Fe (1) -C (8)	-121.1 (16)
C (4) -C (3) -Fe (1) -C (8)	121.6 (12)
C (2) -C (3) -Fe (1) -C (4)	117 (2)
C (9) -C (10) -Fe (1) -C (3)	45.5 (18)
C (6) -C (10) -Fe (1) -C (3)	164.5 (18)
C (11) -C (10) -Fe (1) -C (3)	-74.0 (18)
C (9) -C (10) -Fe (1) -C (4B)	86.3 (8)
C (6) -C (10) -Fe (1) -C (4B)	-154.8 (7)
C (11) -C (10) -Fe (1) -C (4B)	-33.3 (8)
C (9) -C (10) -Fe (1) -C (5)	120.0 (9)
C (6) -C (10) -Fe (1) -C (5)	-121.1 (9)
C (11) -C (10) -Fe (1) -C (5)	0.5 (9)
C (6) -C (10) -Fe (1) -C (9)	118.93 (15)
C (11) -C (10) -Fe (1) -C (9)	-119.51 (18)
C (9) -C (10) -Fe (1) -C (1)	160.2 (13)
C (6) -C (10) -Fe (1) -C (1)	-80.9 (13)
C (11) -C (10) -Fe (1) -C (1)	40.7 (13)
C (9) -C (10) -Fe (1) -C (2B)	-157 (4)
C (6) -C (10) -Fe (1) -C (2B)	-38 (4)
C (11) -C (10) -Fe (1) -C (2B)	83 (4)
C (9) -C (10) -Fe (1) -C (6)	-118.93 (15)
C (11) -C (10) -Fe (1) -C (6)	121.56 (18)
C (9) -C (10) -Fe (1) -C (1B)	169.5 (11)
C (6) -C (10) -Fe (1) -C (1B)	-71.6 (11)
C (11) -C (10) -Fe (1) -C (1B)	50.0 (11)
C (9) -C (10) -Fe (1) -C (5B)	129.6 (8)
C (6) -C (10) -Fe (1) -C (5B)	-111.5 (8)
C (11) -C (10) -Fe (1) -C (5B)	10.1 (8)
C (9) -C (10) -Fe (1) -C (8)	-37.79 (12)
C (6) -C (10) -Fe (1) -C (8)	81.14 (12)
C (11) -C (10) -Fe (1) -C (8)	-157.30 (16)
C (9) -C (10) -Fe (1) -C (4)	79.1 (8)

C (6) -C (10) -Fe (1) -C (4)	-161.9 (8)
C (11) -C (10) -Fe (1) -C (4)	-40.4 (8)
C (3B) -C (4B) -Fe (1) -C (3)	6.9 (17)
C (5B) -C (4B) -Fe (1) -C (3)	-112.2 (15)
C (3B) -C (4B) -Fe (1) -C (10)	-152.2 (10)
C (5B) -C (4B) -Fe (1) -C (10)	88.7 (11)
C (3B) -C (4B) -Fe (1) -C (5)	126.7 (19)
C (5B) -C (4B) -Fe (1) -C (5)	8 (2)
C (3B) -C (4B) -Fe (1) -C (9)	-108.5 (11)
C (5B) -C (4B) -Fe (1) -C (9)	132.4 (10)
C (3B) -C (4B) -Fe (1) -C (1)	89.8 (15)
C (5B) -C (4B) -Fe (1) -C (1)	-29.3 (14)
C (3B) -C (4B) -Fe (1) -C (2B)	37.8 (10)
C (5B) -C (4B) -Fe (1) -C (2B)	-81.3 (12)
C (3B) -C (4B) -Fe (1) -C (6)	173.0 (9)
C (5B) -C (4B) -Fe (1) -C (6)	53.9 (15)
C (3B) -C (4B) -Fe (1) -C (1B)	82.1 (13)
C (5B) -C (4B) -Fe (1) -C (1B)	-37.0 (11)
C (3B) -C (4B) -Fe (1) -C (5B)	119.1 (15)
C (3B) -C (4B) -Fe (1) -C (8)	-68.9 (12)
C (5B) -C (4B) -Fe (1) -C (8)	172.0 (9)
C (3B) -C (4B) -Fe (1) -C (4)	-28 (8)
C (5B) -C (4B) -Fe (1) -C (4)	-148 (9)
C (4) -C (5) -Fe (1) -C (3)	38.5 (13)
C (1) -C (5) -Fe (1) -C (3)	-80.2 (19)
C (4) -C (5) -Fe (1) -C (10)	-116.9 (13)
C (1) -C (5) -Fe (1) -C (10)	124.5 (18)
C (4) -C (5) -Fe (1) -C (4B)	-4.9 (19)
C (1) -C (5) -Fe (1) -C (4B)	-124 (2)
C (4) -C (5) -Fe (1) -C (9)	-73.9 (15)
C (1) -C (5) -Fe (1) -C (9)	167.5 (17)
C (4) -C (5) -Fe (1) -C (1)	119 (2)
C (4) -C (5) -Fe (1) -C (2B)	74.1 (14)
C (1) -C (5) -Fe (1) -C (2B)	-44.6 (18)
C (4) -C (5) -Fe (1) -C (6)	-159.6 (11)
C (1) -C (5) -Fe (1) -C (6)	81.8 (19)
C (4) -C (5) -Fe (1) -C (1B)	114.0 (19)
C (1) -C (5) -Fe (1) -C (1B)	-5 (3)
C (4) -C (5) -Fe (1) -C (5B)	143 (9)
C (1) -C (5) -Fe (1) -C (5B)	24 (8)
C (4) -C (5) -Fe (1) -C (8)	-40 (3)
C (1) -C (5) -Fe (1) -C (8)	-158.8 (19)
C (1) -C (5) -Fe (1) -C (4)	-119 (2)
C (8) -C (9) -Fe (1) -C (3)	80.5 (9)
C (10) -C (9) -Fe (1) -C (3)	-160.7 (9)
C (8) -C (9) -Fe (1) -C (10)	-118.77 (16)
C (8) -C (9) -Fe (1) -C (4B)	130.4 (7)
C (10) -C (9) -Fe (1) -C (4B)	-110.8 (7)
C (8) -C (9) -Fe (1) -C (5)	162.0 (10)
C (10) -C (9) -Fe (1) -C (5)	-79.2 (10)
C (8) -C (9) -Fe (1) -C (1)	-174 (3)
C (10) -C (9) -Fe (1) -C (1)	-55 (3)
C (8) -C (9) -Fe (1) -C (2B)	53.7 (12)
C (10) -C (9) -Fe (1) -C (2B)	172.4 (12)
C (8) -C (9) -Fe (1) -C (6)	-80.63 (13)
C (10) -C (9) -Fe (1) -C (6)	38.14 (10)
C (8) -C (9) -Fe (1) -C (1B)	-166 (4)

C (10) -C (9) -Fe (1) -C (1B)	-47 (4)
C (8) -C (9) -Fe (1) -C (5B)	169.2 (9)
C (10) -C (9) -Fe (1) -C (5B)	-72.0 (9)
C (10) -C (9) -Fe (1) -C (8)	118.77 (16)
C (8) -C (9) -Fe (1) -C (4)	122.9 (8)
C (10) -C (9) -Fe (1) -C (4)	-118.4 (8)
C (5) -C (1) -Fe (1) -C (3)	82.4 (18)
C (2) -C (1) -Fe (1) -C (3)	-37.1 (17)
C (5) -C (1) -Fe (1) -C (10)	-74 (2)
C (2) -C (1) -Fe (1) -C (10)	166.2 (17)
C (5) -C (1) -Fe (1) -C (4B)	30.2 (16)
C (2) -C (1) -Fe (1) -C (4B)	-89 (2)
C (2) -C (1) -Fe (1) -C (5)	-120 (3)
C (5) -C (1) -Fe (1) -C (9)	-33 (4)
C (2) -C (1) -Fe (1) -C (9)	-152 (2)
C (5) -C (1) -Fe (1) -C (2B)	115 (2)
C (2) -C (1) -Fe (1) -C (2B)	-4 (2)
C (5) -C (1) -Fe (1) -C (6)	-118.3 (17)
C (2) -C (1) -Fe (1) -C (6)	122 (2)
C (5) -C (1) -Fe (1) -C (1B)	157 (13)
C (2) -C (1) -Fe (1) -C (1B)	38 (11)
C (5) -C (1) -Fe (1) -C (5B)	-7 (2)
C (2) -C (1) -Fe (1) -C (5B)	-127 (3)
C (5) -C (1) -Fe (1) -C (8)	159 (2)
C (2) -C (1) -Fe (1) -C (8)	39 (4)
C (5) -C (1) -Fe (1) -C (4)	37.3 (16)
C (2) -C (1) -Fe (1) -C (4)	-82 (2)
C (1B) -C (2B) -Fe (1) -C (3)	124 (2)
C (3B) -C (2B) -Fe (1) -C (3)	7 (2)
C (1B) -C (2B) -Fe (1) -C (10)	-39 (4)
C (3B) -C (2B) -Fe (1) -C (10)	-157 (3)
C (1B) -C (2B) -Fe (1) -C (4B)	81.2 (15)
C (3B) -C (2B) -Fe (1) -C (4B)	-36.6 (11)
C (1B) -C (2B) -Fe (1) -C (5)	46.7 (16)
C (3B) -C (2B) -Fe (1) -C (5)	-71.1 (13)
C (1B) -C (2B) -Fe (1) -C (9)	169.4 (14)
C (3B) -C (2B) -Fe (1) -C (9)	51.6 (19)
C (1B) -C (2B) -Fe (1) -C (1)	9 (2)
C (3B) -C (2B) -Fe (1) -C (1)	-108.6 (19)
C (1B) -C (2B) -Fe (1) -C (6)	-71.8 (16)
C (3B) -C (2B) -Fe (1) -C (6)	170.4 (9)
C (3B) -C (2B) -Fe (1) -C (1B)	-117.8 (18)
C (1B) -C (2B) -Fe (1) -C (5B)	37.5 (14)
C (3B) -C (2B) -Fe (1) -C (5B)	-80.3 (12)
C (1B) -C (2B) -Fe (1) -C (8)	-154.8 (13)
C (3B) -C (2B) -Fe (1) -C (8)	87.4 (12)
C (1B) -C (2B) -Fe (1) -C (4)	88.6 (16)
C (3B) -C (2B) -Fe (1) -C (4)	-29.2 (11)
C (7) -C (6) -Fe (1) -C (3)	-42 (2)
C (10) -C (6) -Fe (1) -C (3)	-161 (2)
C (7) -C (6) -Fe (1) -C (10)	118.74 (15)
C (7) -C (6) -Fe (1) -C (4B)	169.3 (11)
C (10) -C (6) -Fe (1) -C (4B)	50.6 (11)
C (7) -C (6) -Fe (1) -C (5)	-163.0 (8)
C (10) -C (6) -Fe (1) -C (5)	78.3 (8)
C (7) -C (6) -Fe (1) -C (9)	80.54 (12)
C (10) -C (6) -Fe (1) -C (9)	-38.20 (10)

C (7) -C (6) -Fe (1) -C (1)	-120.5 (11)
C (10) -C (6) -Fe (1) -C (1)	120.7 (11)
C (7) -C (6) -Fe (1) -C (2B)	-69.8 (9)
C (10) -C (6) -Fe (1) -C (2B)	171.5 (9)
C (7) -C (6) -Fe (1) -C (1B)	-111.0 (8)
C (10) -C (6) -Fe (1) -C (1B)	130.2 (8)
C (7) -C (6) -Fe (1) -C (5B)	-154.1 (7)
C (10) -C (6) -Fe (1) -C (5B)	87.1 (7)
C (7) -C (6) -Fe (1) -C (8)	36.82 (11)
C (10) -C (6) -Fe (1) -C (8)	-81.92 (11)
C (7) -C (6) -Fe (1) -C (4)	162.4 (16)
C (10) -C (6) -Fe (1) -C (4)	43.6 (16)
C (5B) -C (1B) -Fe (1) -C (3)	88.7 (16)
C (2B) -C (1B) -Fe (1) -C (3)	-30.2 (15)
C (5B) -C (1B) -Fe (1) -C (10)	-69.7 (17)
C (2B) -C (1B) -Fe (1) -C (10)	171.3 (10)
C (5B) -C (1B) -Fe (1) -C (4B)	37.2 (12)
C (2B) -C (1B) -Fe (1) -C (4B)	-81.7 (15)
C (5B) -C (1B) -Fe (1) -C (5)	7 (2)
C (2B) -C (1B) -Fe (1) -C (5)	-112 (2)
C (5B) -C (1B) -Fe (1) -C (9)	-30 (5)
C (2B) -C (1B) -Fe (1) -C (9)	-149 (4)
C (5B) -C (1B) -Fe (1) -C (1)	-13 (11)
C (2B) -C (1B) -Fe (1) -C (1)	-132 (13)
C (5B) -C (1B) -Fe (1) -C (2B)	119 (2)
C (5B) -C (1B) -Fe (1) -C (6)	-111.3 (14)
C (2B) -C (1B) -Fe (1) -C (6)	129.7 (12)
C (2B) -C (1B) -Fe (1) -C (5B)	-119 (2)
C (5B) -C (1B) -Fe (1) -C (8)	168.5 (13)
C (2B) -C (1B) -Fe (1) -C (8)	50 (2)
C (5B) -C (1B) -Fe (1) -C (4)	44.5 (15)
C (2B) -C (1B) -Fe (1) -C (4)	-74.4 (15)
C (4B) -C (5B) -Fe (1) -C (3)	46.1 (12)
C (1B) -C (5B) -Fe (1) -C (3)	-74.0 (15)
C (4B) -C (5B) -Fe (1) -C (10)	-108.9 (10)
C (1B) -C (5B) -Fe (1) -C (10)	131.1 (14)
C (1B) -C (5B) -Fe (1) -C (4B)	-120.1 (19)
C (4B) -C (5B) -Fe (1) -C (5)	-26 (8)
C (1B) -C (5B) -Fe (1) -C (5)	-146 (9)
C (4B) -C (5B) -Fe (1) -C (9)	-67.1 (13)
C (1B) -C (5B) -Fe (1) -C (9)	172.8 (13)
C (4B) -C (5B) -Fe (1) -C (1)	124 (3)
C (1B) -C (5B) -Fe (1) -C (1)	4 (3)
C (4B) -C (5B) -Fe (1) -C (2B)	81.9 (12)
C (1B) -C (5B) -Fe (1) -C (2B)	-38.2 (15)
C (4B) -C (5B) -Fe (1) -C (6)	-153.1 (9)
C (1B) -C (5B) -Fe (1) -C (6)	86.8 (15)
C (4B) -C (5B) -Fe (1) -C (1B)	120.1 (19)
C (4B) -C (5B) -Fe (1) -C (8)	-31 (4)
C (1B) -C (5B) -Fe (1) -C (8)	-151 (3)
C (4B) -C (5B) -Fe (1) -C (4)	5.4 (16)
C (1B) -C (5B) -Fe (1) -C (4)	-114.7 (19)
C (7) -C (8) -Fe (1) -C (3)	123.2 (8)
C (9) -C (8) -Fe (1) -C (3)	-117.0 (8)
C (7) -C (8) -Fe (1) -C (10)	-81.38 (11)
C (9) -C (8) -Fe (1) -C (10)	38.45 (11)
C (7) -C (8) -Fe (1) -C (4B)	171.0 (7)

C (9) -C (8) -Fe (1) -C (4B)	-69.2 (7)
C (7) -C (8) -Fe (1) -C (5)	-166 (2)
C (9) -C (8) -Fe (1) -C (5)	-46 (2)
C (7) -C (8) -Fe (1) -C (9)	-119.83 (16)
C (7) -C (8) -Fe (1) -C (1)	54 (3)
C (9) -C (8) -Fe (1) -C (1)	174 (3)
C (7) -C (8) -Fe (1) -C (2B)	88.5 (6)
C (9) -C (8) -Fe (1) -C (2B)	-151.7 (6)
C (7) -C (8) -Fe (1) -C (6)	-36.85 (11)
C (9) -C (8) -Fe (1) -C (6)	82.98 (12)
C (7) -C (8) -Fe (1) -C (1B)	54.8 (17)
C (9) -C (8) -Fe (1) -C (1B)	174.6 (17)
C (7) -C (8) -Fe (1) -C (5B)	-163 (3)
C (9) -C (8) -Fe (1) -C (5B)	-44 (3)
C (7) -C (8) -Fe (1) -C (4)	165.3 (9)
C (9) -C (8) -Fe (1) -C (4)	-74.9 (9)
C (5) -C (4) -Fe (1) -C (3)	-119.2 (19)
C (5) -C (4) -Fe (1) -C (10)	80.5 (14)
C (3) -C (4) -Fe (1) -C (10)	-160.4 (12)
C (5) -C (4) -Fe (1) -C (4B)	21 (8)
C (3) -C (4) -Fe (1) -C (4B)	140 (9)
C (3) -C (4) -Fe (1) -C (5)	119.2 (19)
C (5) -C (4) -Fe (1) -C (9)	122.9 (13)
C (3) -C (4) -Fe (1) -C (9)	-117.9 (13)
C (5) -C (4) -Fe (1) -C (1)	-37.8 (14)
C (3) -C (4) -Fe (1) -C (1)	81.4 (16)
C (5) -C (4) -Fe (1) -C (2B)	-90.0 (14)
C (3) -C (4) -Fe (1) -C (2B)	29.2 (14)
C (5) -C (4) -Fe (1) -C (6)	49 (2)
C (3) -C (4) -Fe (1) -C (6)	167.7 (14)
C (5) -C (4) -Fe (1) -C (1B)	-46.1 (14)
C (3) -C (4) -Fe (1) -C (1B)	73.1 (14)
C (5) -C (4) -Fe (1) -C (5B)	-7.7 (17)
C (3) -C (4) -Fe (1) -C (5B)	111.5 (17)
C (5) -C (4) -Fe (1) -C (8)	163.8 (11)
C (3) -C (4) -Fe (1) -C (8)	-77.0 (14)

Table 7. Hydrogen Bonds

Donor H...A	--- H...A	H....Acceptor ..01	[ARU] [1655.01]	D - H 0.91 (6)	H...A 1.87 (6)	D...A 2.778 (3)	D - 177 (5)
O3	--H3O	..01	[1655.01]	0.91 (6)	1.87 (6)	2.778 (3)	177 (5)

Translation of ARU-code to Equivalent Position Code

[1655.] = 1+x,y,z

8.2 X-ray structure report for complex 3.3

Data Collection

A red prism crystal of $C_{25}H_{18}O_{10}FeCo_2$ having approximate dimensions of 0.22 x 0.25 x 0.40 mm was mounted on a glass fiber. All measurements were made on a Bruker X8 APEX II diffractometer with graphite monochromated Mo-K α radiation. The data were collected at a temperature of $-100.0 \pm 0.1^\circ C$ to a maximum 2θ value of 56.0° . Data were collected in a series of ϕ and ω scans in 0.50° oscillations with 5.0-second exposures. The crystal-to-detector distance was 36.00 mm.

Data Reduction

Of the 27275 reflections that were collected, 6187 were unique ($R_{int} = 0.026$); equivalent reflections were merged. Data were collected and integrated using the Bruker SAINT¹ software package. The linear absorption coefficient, μ , for Mo-K α radiation is 18.85 cm^{-1} . Data were corrected for absorption effects using the multi-scan technique (SADABS²), with minimum and maximum transmission coefficients of 0.560 and 0.661, respectively. The data were corrected for Lorentz and polarization effects.

Structure Solution and Refinement

The structure was solved by direct methods³. The material crystallizes with disorder about the C16 – C17 bond, with the acetylenic and methyl carbons exchanging positions. All non-hydrogen atoms were refined anisotropically. All C-H hydrogen atoms were placed in calculated positions but were not refined. The final cycle of full-matrix least-squares refinement⁴ on F^2 was based on 6187 reflections and 364 variable parameters and converged (largest parameter shift was 0.00 times its esd) with unweighted and weighted agreement factors of:

$$R1 = \Sigma ||F_o| - |F_c|| / \Sigma |F_o| = 0.033$$

$$wR2 = [\Sigma (w (F_o^2 - F_c^2)^2) / \Sigma w(F_o^2)^2]^{1/2} = 0.059$$

The standard deviation of an observation of unit weight⁵ was 1.02. The weighting scheme was based on counting statistics. The maximum and minimum peaks on the final difference Fourier map corresponded to 0.32 and $-0.32 \text{ e}^-/\text{\AA}^3$, respectively. Neutral atom scattering factors were taken from Cromer and Waber⁶. Anomalous dispersion effects were included in F_{calc} ⁷; the values for $\Delta f'$ and $\Delta f''$ were those of Creagh and McAuley⁸. The values for the mass attenuation coefficients are those of Creagh and Hubbell⁹. All refinements were performed using the SHELXTL¹⁰ crystallographic software package of Bruker-AXS.

References

- (1) SAINT. Version 7.60A. Bruker AXS Inc., Madison, Wisconsin, USA. (1997-2009).
- (2) SADABS. Bruker Nonius area detector scaling and absorption correction - V2008/1, Bruker AXS Inc., Madison, Wisconsin, USA (2008).
- (3) SIR97 - Altomare A., Burla M.C., Camalli M., Cascarano G.L., Giacovazzo C. , Guagliardi A., Moliterni A.G.G., Polidori G., Spagna R. (1999) J. Appl. Cryst. 32, 115-119.

(4) Least Squares function minimized:

$$\Sigma w(F_o^2 - F_c^2)^2$$

(5) Standard deviation of an observation of unit weight:

$$[\Sigma w(F_o^2 - F_c^2)^2 / (N_o - N_v)]^{1/2}$$

where: N_O = number of observations

N_V = number of variables

(6) Cromer, D. T. & Waber, J. T.; "International Tables for X-ray Crystallography", Vol. IV, The Kynoch Press, Birmingham, England, Table 2.2 A (1974).

(7) Ibers, J. A. & Hamilton, W. C.; Acta Crystallogr., 17, 781 (1964).

(8) Creagh, D. C. & McAuley, W.J. ; "International Tables for Crystallography", Vol C, (A.J.C. Wilson, ed.), Kluwer Academic Publishers, Boston, Table 4.2.6.8, pages 219-222 (1992).

(9) Creagh, D. C. & Hubbell, J.H.; "International Tables for Crystallography", Vol C, (A.J.C. Wilson, ed.), Kluwer Academic Publishers, Boston, Table 4.2.4.3, pages 200-206 (1992).

(10) SHELXTL Version 5.1. Bruker AXS Inc., Madison, Wisconsin, USA. (1997).

EXPERIMENTAL DETAILS

A. Crystal Data

Empirical Formula	$C_{25}H_{18}O_{10}FeCo_2$
Formula Weight	652.10
Crystal Color, Habit	red, prism
Crystal Dimensions	0.22 X 0.25 X 0.40 mm
Crystal System	monoclinic

Lattice Type	primitive
Lattice Parameters	$a = 13.7682(4) \text{ \AA}$ $b = 12.9640(4) \text{ \AA}$ $c = 15.5095(5) \text{ \AA}$ $\alpha = 90^\circ$ $\beta = 111.513(1)^\circ$ $\gamma = 90^\circ$ $V = 2575.45(4) \text{ \AA}^3$
Space Group	$P 2_1/n$ (#14)
Z value	4
D _{calc}	1.682 g/cm ³
F ₀₀₀	1312.00
$\mu(\text{MoK}\alpha)$	18.85 cm ⁻¹
B. Intensity Measurements	
Diffractometer	Bruker X8 APEX II
Radiation	MoK α ($\lambda = 0.71073 \text{ \AA}$) graphite monochromated
Data Images	1233 exposures @ 5.0 seconds
Detector Position	36.00 mm
$2\theta_{\text{max}}$	56.1 $^\circ$
No. of Reflections Measured	Total: 27275 Unique: 6187 ($R_{\text{int}} = 0.026$)

Corrections	Absorption ($T_{\min} = 0.560$, $T_{\max} = 0.661$)
	Lorentz-polarization
C. Structure Solution and Refinement	
Structure Solution	Direct Methods (SIR97)
Refinement	Full-matrix least-squares on F^2
Function Minimized	$\Sigma w (F_o^2 - F_c^2)^2$
Least Squares Weights	$w=1/(\sigma^2(F_o^2)+(0.0270P)^2+ 0.8904P)$
Anomalous Dispersion	All non-hydrogen atoms
No. Observations ($I>0.00\sigma(I)$)	6187
No. Variables	364
Reflection/Parameter Ratio	17.00
Residuals (refined on F^2 , all data): R1; wR2	0.033; 0.059
Goodness of Fit Indicator	1.02
No. Observations ($I>2.00\sigma(I)$)	5213
Residuals (refined on F): R1; wR2	0.023; 0.056
Max Shift/Error in Final Cycle	0.00
Maximum peak in Final Diff. Map	0.32 e ⁻ /Å ³
Minimum peak in Final Diff. Map	-0.32 e ⁻ /Å ³

Table 2. Atomic coordinates ($\times 10^4$) and equivalent isotropic displacement parameters ($\text{\AA}^2 \times 10^3$) for aa001_0m. U(eq) is defined as one third of the trace of the orthogonalized U_{ij} tensor.

	x	y	z	U(eq)	occ
C(1)	5465(2)	2939(2)	-3651(2)	61(1)	
C(2)	6178(2)	2842(2)	-2727(2)	48(1)	
C(3)	7170(2)	2770(2)	-2753(2)	55(1)	
C(4)	7088(3)	2820(2)	-3668(2)	73(1)	
C(5)	6044(3)	2924(2)	-4228(2)	75(1)	
C(6)	6258(1)	5344(1)	-2600(1)	28(1)	
C(7)	5674(1)	5487(1)	-3557(1)	34(1)	
C(8)	6374(1)	5494(1)	-4035(1)	34(1)	
C(9)	7401(1)	5359(1)	-3383(1)	28(1)	
C(10)	7333(1)	5262(1)	-2489(1)	23(1)	
C(11)	8211(1)	5011(1)	-1637(1)	23(1)	
C(12)	8690(1)	4537(2)	-62(1)	28(1)	
C(13)	8217(1)	4542(1)	653(1)	23(1)	
C(14)	8419(1)	4366(1)	1552(1)	24(1)	
C(15)	9247(1)	4001(2)	2414(1)	30(1)	
C(16)	9517(1)	3744(1)	3986(1)	30(1)	
C(17)	9097(2)	3893(1)	4738(1)	31(1)	0.59(2)
C(18)	9848(14)	3687(15)	5671(6)	41(3)	0.59(2)
C(19)	8096(10)	4186(12)	4548(11)	52(3)	0.59(2)
C(17B)	9097(2)	3893(1)	4738(1)	31(1)	0.41(2)
C(18B)	7996(10)	4177(17)	4465(13)	40(4)	0.41(2)
C(19B)	9760(20)	3760(20)	5622(10)	45(5)	0.41(2)
C(20)	5926(1)	4072(1)	-276(1)	29(1)	
C(21)	7348(1)	2585(1)	561(1)	32(1)	
C(22)	6464(1)	3686(2)	1685(1)	35(1)	
C(23)	6743(1)	6228(1)	108(1)	32(1)	
C(24)	8757(2)	6526(2)	1432(1)	39(1)	
C(25)	7175(2)	5987(2)	2074(1)	38(1)	
O(1)	9116(1)	4950(1)	-1561(1)	35(1)	
O(2)	7887(1)	4839(1)	-928(1)	26(1)	
O(3)	8859(1)	4088(1)	3159(1)	29(1)	
O(4)	10351(1)	3372(1)	4096(1)	55(1)	
O(5)	5251(1)	4210(1)	-957(1)	45(1)	
O(6)	7612(1)	1808(1)	394(1)	49(1)	
O(7)	6140(1)	3604(1)	2254(1)	58(1)	
O(8)	6163(1)	6518(1)	-574(1)	45(1)	
O(9)	9468(1)	7037(1)	1585(1)	62(1)	
O(10)	6868(1)	6184(1)	2634(1)	63(1)	
Fe(1)	6497(1)	4127(1)	-3327(1)	24(1)	
Co(1)	7027(1)	3868(1)	802(1)	22(1)	
Co(2)	7661(1)	5663(1)	1165(1)	25(1)	

Table 3. Bond lengths [Å] and angles [deg] for aa001_0m.

C(1)-C(5)	1.402(4)
C(1)-C(2)	1.415(3)
C(1)-Fe(1)	2.030(2)
C(1)-H(1)	0.9500
C(2)-C(3)	1.384(3)
C(2)-Fe(1)	2.0331(19)
C(2)-H(2)	0.9500
C(3)-C(4)	1.383(4)
C(3)-Fe(1)	2.034(2)
C(3)-H(3)	0.9500
C(4)-C(5)	1.386(4)
C(4)-Fe(1)	2.032(2)
C(4)-H(4)	0.9500
C(5)-Fe(1)	2.034(2)
C(5)-H(5)	0.9500
C(6)-C(7)	1.416(2)
C(6)-C(10)	1.429(2)
C(6)-Fe(1)	2.0342(16)
C(6)-H(6)	0.9500
C(7)-C(8)	1.415(3)
C(7)-Fe(1)	2.0548(18)
C(7)-H(7)	0.9500
C(8)-C(9)	1.416(2)
C(8)-Fe(1)	2.0596(17)
C(8)-H(8)	0.9500
C(9)-C(10)	1.429(2)
C(9)-Fe(1)	2.0465(16)
C(9)-H(9)	0.9500
C(10)-C(11)	1.465(2)
C(10)-Fe(1)	2.0194(15)
C(11)-O(1)	1.2099(18)
C(11)-O(2)	1.3480(17)
C(12)-O(2)	1.4456(18)
C(12)-C(13)	1.477(2)
C(12)-H(12A)	0.9900
C(12)-H(12B)	0.9900
C(13)-C(14)	1.338(2)
C(13)-Co(2)	1.9436(15)
C(13)-Co(1)	1.9444(15)
C(14)-C(15)	1.481(2)
C(14)-Co(1)	1.9518(15)
C(14)-Co(2)	1.9550(16)
C(15)-O(3)	1.4438(18)
C(15)-H(15A)	0.9900
C(15)-H(15B)	0.9900
C(16)-O(4)	1.199(2)
C(16)-O(3)	1.3459(19)
C(16)-C(17)	1.491(2)
C(17)-C(19)	1.354(12)
C(17)-C(18)	1.462(11)
C(18)-H(18A)	0.9800
C(18)-H(18B)	0.9800
C(18)-H(18C)	0.9800

C (19) -H (19A)	0.9500
C (19) -H (19B)	0.9500
C (18B) -H (18D)	0.9800
C (18B) -H (18E)	0.9800
C (18B) -H (18F)	0.9800
C (19B) -H (19C)	0.9500
C (19B) -H (19D)	0.9500
C (20) -O (5)	1.135 (2)
C (20) -Co (1)	1.8174 (17)
C (21) -O (6)	1.132 (2)
C (21) -Co (1)	1.7962 (19)
C (22) -O (7)	1.131 (2)
C (22) -Co (1)	1.8196 (17)
C (23) -O (8)	1.131 (2)
C (23) -Co (2)	1.8163 (18)
C (24) -O (9)	1.133 (2)
C (24) -Co (2)	1.800 (2)
C (25) -O (10)	1.126 (2)
C (25) -Co (2)	1.8182 (18)
Co (1) -Co (2)	2.4767 (3)

C (5) -C (1) -C (2)	107.4 (2)
C (5) -C (1) -Fe (1)	69.98 (13)
C (2) -C (1) -Fe (1)	69.75 (11)
C (5) -C (1) -H (1)	126.3
C (2) -C (1) -H (1)	126.3
Fe (1) -C (1) -H (1)	125.6
C (3) -C (2) -C (1)	107.6 (2)
C (3) -C (2) -Fe (1)	70.16 (12)
C (1) -C (2) -Fe (1)	69.48 (12)
C (3) -C (2) -H (2)	126.2
C (1) -C (2) -H (2)	126.2
Fe (1) -C (2) -H (2)	125.7
C (4) -C (3) -C (2)	108.5 (2)
C (4) -C (3) -Fe (1)	70.03 (14)
C (2) -C (3) -Fe (1)	70.07 (12)
C (4) -C (3) -H (3)	125.7
C (2) -C (3) -H (3)	125.7
Fe (1) -C (3) -H (3)	125.8
C (3) -C (4) -C (5)	108.8 (2)
C (3) -C (4) -Fe (1)	70.20 (13)
C (5) -C (4) -Fe (1)	70.13 (14)
C (3) -C (4) -H (4)	125.6
C (5) -C (4) -H (4)	125.6
Fe (1) -C (4) -H (4)	125.7
C (4) -C (5) -C (1)	107.6 (2)
C (4) -C (5) -Fe (1)	70.00 (14)
C (1) -C (5) -Fe (1)	69.66 (13)
C (4) -C (5) -H (5)	126.2
C (1) -C (5) -H (5)	126.2
Fe (1) -C (5) -H (5)	125.8
C (7) -C (6) -C (10)	107.50 (14)
C (7) -C (6) -Fe (1)	70.51 (10)
C (10) -C (6) -Fe (1)	68.80 (9)
C (7) -C (6) -H (6)	126.3
C (10) -C (6) -H (6)	126.3
Fe (1) -C (6) -H (6)	126.0

C (8) -C (7) -C (6)	108.44 (15)
C (8) -C (7) -Fe (1)	70.07 (10)
C (6) -C (7) -Fe (1)	68.96 (10)
C (8) -C (7) -H (7)	125.8
C (6) -C (7) -H (7)	125.8
Fe (1) -C (7) -H (7)	126.8
C (7) -C (8) -C (9)	108.52 (14)
C (7) -C (8) -Fe (1)	69.70 (10)
C (9) -C (8) -Fe (1)	69.33 (9)
C (7) -C (8) -H (8)	125.7
C (9) -C (8) -H (8)	125.7
Fe (1) -C (8) -H (8)	126.8
C (8) -C (9) -C (10)	107.49 (14)
C (8) -C (9) -Fe (1)	70.33 (9)
C (10) -C (9) -Fe (1)	68.42 (9)
C (8) -C (9) -H (9)	126.3
C (10) -C (9) -H (9)	126.3
Fe (1) -C (9) -H (9)	126.6
C (9) -C (10) -C (6)	108.05 (13)
C (9) -C (10) -C (11)	124.69 (14)
C (6) -C (10) -C (11)	126.96 (13)
C (9) -C (10) -Fe (1)	70.45 (9)
C (6) -C (10) -Fe (1)	69.91 (9)
C (11) -C (10) -Fe (1)	120.41 (11)
O (1) -C (11) -O (2)	123.16 (14)
O (1) -C (11) -C (10)	125.63 (14)
O (2) -C (11) -C (10)	111.20 (12)
O (2) -C (12) -C (13)	107.39 (12)
O (2) -C (12) -H (12A)	110.2
C (13) -C (12) -H (12A)	110.2
O (2) -C (12) -H (12B)	110.2
C (13) -C (12) -H (12B)	110.2
H (12A) -C (12) -H (12B)	108.5
C (14) -C (13) -C (12)	143.25 (14)
C (14) -C (13) -Co (2)	70.39 (9)
C (12) -C (13) -Co (2)	131.18 (12)
C (14) -C (13) -Co (1)	70.22 (9)
C (12) -C (13) -Co (1)	135.20 (12)
Co (2) -C (13) -Co (1)	79.14 (5)
C (13) -C (14) -C (15)	142.47 (14)
C (13) -C (14) -Co (1)	69.62 (9)
C (15) -C (14) -Co (1)	134.03 (13)
C (13) -C (14) -Co (2)	69.48 (10)
C (15) -C (14) -Co (2)	134.41 (12)
Co (1) -C (14) -Co (2)	78.68 (6)
O (3) -C (15) -C (14)	108.06 (12)
O (3) -C (15) -H (15A)	110.1
C (14) -C (15) -H (15A)	110.1
O (3) -C (15) -H (15B)	110.1
C (14) -C (15) -H (15B)	110.1
H (15A) -C (15) -H (15B)	108.4
O (4) -C (16) -O (3)	122.92 (15)
O (4) -C (16) -C (17)	124.51 (16)
O (3) -C (16) -C (17)	112.56 (14)
C (19) -C (17) -C (18)	124.1 (9)
C (19) -C (17) -C (16)	121.4 (6)
C (18) -C (17) -C (16)	114.5 (7)

C (17) -C (19) -H (19A)	120.0
C (17) -C (19) -H (19B)	120.0
H (19A) -C (19) -H (19B)	120.0
H (18D) -C (18B) -H (18E)	109.5
H (18D) -C (18B) -H (18F)	109.5
H (18E) -C (18B) -H (18F)	109.5
H (19C) -C (19B) -H (19D)	120.0
O (5) -C (20) -Co (1)	178.62 (16)
O (6) -C (21) -Co (1)	174.69 (16)
O (7) -C (22) -Co (1)	177.24 (18)
O (8) -C (23) -Co (2)	175.56 (16)
O (9) -C (24) -Co (2)	176.99 (18)
O (10) -C (25) -Co (2)	179.5 (2)
C (11) -O (2) -C (12)	115.66 (11)
C (16) -O (3) -C (15)	114.81 (12)
C (10) -Fe (1) -C (1)	153.37 (9)
C (10) -Fe (1) -C (4)	125.90 (11)
C (1) -Fe (1) -C (4)	67.31 (12)
C (10) -Fe (1) -C (2)	118.05 (7)
C (1) -Fe (1) -C (2)	40.77 (9)
C (4) -Fe (1) -C (2)	67.08 (10)
C (10) -Fe (1) -C (5)	163.58 (11)
C (1) -Fe (1) -C (5)	40.37 (11)
C (4) -Fe (1) -C (5)	39.88 (12)
C (2) -Fe (1) -C (5)	67.88 (9)
C (10) -Fe (1) -C (6)	41.29 (6)
C (1) -Fe (1) -C (6)	119.00 (10)
C (4) -Fe (1) -C (6)	162.26 (11)
C (2) -Fe (1) -C (6)	106.04 (8)
C (5) -Fe (1) -C (6)	154.77 (12)
C (10) -Fe (1) -C (3)	106.74 (8)
C (1) -Fe (1) -C (3)	67.51 (10)
C (4) -Fe (1) -C (3)	39.77 (11)
C (2) -Fe (1) -C (3)	39.77 (9)
C (5) -Fe (1) -C (3)	67.24 (11)
C (6) -Fe (1) -C (3)	124.66 (9)
C (10) -Fe (1) -C (9)	41.13 (6)
C (1) -Fe (1) -C (9)	164.41 (9)
C (4) -Fe (1) -C (9)	109.36 (10)
C (2) -Fe (1) -C (9)	153.61 (8)
C (5) -Fe (1) -C (9)	127.36 (9)
C (6) -Fe (1) -C (9)	69.05 (7)
C (3) -Fe (1) -C (9)	120.47 (8)
C (10) -Fe (1) -C (7)	68.56 (7)
C (1) -Fe (1) -C (7)	108.47 (9)
C (4) -Fe (1) -C (7)	156.64 (11)
C (2) -Fe (1) -C (7)	125.81 (9)
C (5) -Fe (1) -C (7)	121.89 (11)
C (6) -Fe (1) -C (7)	40.53 (7)
C (3) -Fe (1) -C (7)	162.07 (9)
C (9) -Fe (1) -C (7)	68.15 (7)
C (10) -Fe (1) -C (8)	68.43 (6)
C (1) -Fe (1) -C (8)	127.42 (9)
C (4) -Fe (1) -C (8)	122.73 (10)
C (2) -Fe (1) -C (8)	163.78 (9)
C (5) -Fe (1) -C (8)	110.39 (9)
C (6) -Fe (1) -C (8)	68.26 (7)

C (3) -Fe (1) -C (8)	155.86 (9)
C (9) -Fe (1) -C (8)	40.34 (7)
C (7) -Fe (1) -C (8)	40.23 (7)
C (21) -Co (1) -C (20)	97.46 (8)
C (21) -Co (1) -C (22)	103.97 (8)
C (20) -Co (1) -C (22)	105.67 (7)
C (21) -Co (1) -C (13)	96.25 (7)
C (20) -Co (1) -C (13)	106.29 (7)
C (22) -Co (1) -C (13)	139.26 (7)
C (21) -Co (1) -C (14)	99.60 (7)
C (20) -Co (1) -C (14)	143.69 (7)
C (22) -Co (1) -C (14)	100.95 (7)
C (13) -Co (1) -C (14)	40.16 (6)
C (21) -Co (1) -Co (2)	145.56 (6)
C (20) -Co (1) -Co (2)	100.24 (6)
C (22) -Co (1) -Co (2)	99.34 (6)
C (13) -Co (1) -Co (2)	50.42 (5)
C (14) -Co (1) -Co (2)	50.72 (5)
C (24) -Co (2) -C (23)	101.80 (9)
C (24) -Co (2) -C (25)	101.16 (9)
C (23) -Co (2) -C (25)	105.98 (8)
C (24) -Co (2) -C (13)	97.80 (7)
C (23) -Co (2) -C (13)	100.42 (7)
C (25) -Co (2) -C (13)	143.32 (8)
C (24) -Co (2) -C (14)	98.92 (8)
C (23) -Co (2) -C (14)	137.77 (7)
C (25) -Co (2) -C (14)	105.51 (8)
C (13) -Co (2) -C (14)	40.13 (6)
C (24) -Co (2) -Co (1)	146.26 (6)
C (23) -Co (2) -Co (1)	95.93 (6)
C (25) -Co (2) -Co (1)	101.20 (6)
C (13) -Co (2) -Co (1)	50.45 (4)
C (14) -Co (2) -Co (1)	50.60 (5)

Symmetry transformations used to generate equivalent atoms:

Table 4. Anisotropic displacement parameters ($\text{\AA}^2 \times 10^3$) for aa001_0m.
The anisotropic displacement factor exponent takes the form:
 $-2 \pi^2 [h^2 a^{*2} U_{11} + \dots + 2 h k a^* b^* U_{12}]$

	U11	U22	U33	U23	U13	U12
C (1)	51 (1)	38 (1)	74 (2)	1 (1)	1 (1)	-22 (1)
C (2)	74 (2)	31 (1)	43 (1)	4 (1)	26 (1)	-18 (1)
C (3)	58 (1)	22 (1)	71 (2)	10 (1)	6 (1)	1 (1)
C (4)	115 (2)	28 (1)	106 (2)	-7 (1)	76 (2)	6 (1)
C (5)	153 (3)	30 (1)	32 (1)	-12 (1)	22 (2)	-24 (2)
C (6)	28 (1)	30 (1)	24 (1)	-2 (1)	8 (1)	4 (1)
C (7)	32 (1)	32 (1)	30 (1)	2 (1)	1 (1)	7 (1)
C (8)	47 (1)	27 (1)	21 (1)	5 (1)	5 (1)	-5 (1)
C (9)	36 (1)	26 (1)	22 (1)	0 (1)	11 (1)	-8 (1)
C (10)	27 (1)	20 (1)	20 (1)	-1 (1)	8 (1)	-3 (1)
C (11)	26 (1)	26 (1)	20 (1)	-2 (1)	10 (1)	-4 (1)
C (12)	19 (1)	48 (1)	16 (1)	3 (1)	7 (1)	4 (1)
C (13)	18 (1)	30 (1)	21 (1)	-1 (1)	8 (1)	1 (1)
C (14)	20 (1)	31 (1)	21 (1)	-1 (1)	7 (1)	2 (1)
C (15)	24 (1)	49 (1)	19 (1)	3 (1)	9 (1)	10 (1)
C (16)	37 (1)	30 (1)	21 (1)	2 (1)	6 (1)	3 (1)
C (17)	46 (1)	26 (1)	21 (1)	1 (1)	12 (1)	-5 (1)
C (18)	58 (5)	43 (6)	14 (3)	1 (3)	2 (3)	-8 (4)
C (19)	71 (6)	66 (7)	19 (3)	10 (3)	18 (3)	12 (5)
C (17B)	46 (1)	26 (1)	21 (1)	1 (1)	12 (1)	-5 (1)
C (18B)	37 (5)	60 (9)	39 (9)	-3 (5)	31 (5)	1 (4)
C (19B)	58 (7)	32 (7)	50 (10)	5 (6)	28 (7)	-8 (6)
C (20)	23 (1)	33 (1)	31 (1)	1 (1)	12 (1)	-2 (1)
C (21)	29 (1)	35 (1)	28 (1)	1 (1)	6 (1)	0 (1)
C (22)	29 (1)	44 (1)	31 (1)	3 (1)	11 (1)	-6 (1)
C (23)	35 (1)	25 (1)	35 (1)	0 (1)	14 (1)	4 (1)
C (24)	42 (1)	36 (1)	41 (1)	-6 (1)	17 (1)	-3 (1)
C (25)	37 (1)	43 (1)	32 (1)	-7 (1)	12 (1)	2 (1)
O (1)	23 (1)	61 (1)	24 (1)	2 (1)	11 (1)	-2 (1)
O (2)	19 (1)	44 (1)	16 (1)	2 (1)	6 (1)	2 (1)
O (3)	28 (1)	41 (1)	17 (1)	4 (1)	10 (1)	7 (1)
O (4)	49 (1)	81 (1)	28 (1)	10 (1)	7 (1)	33 (1)
O (5)	29 (1)	62 (1)	35 (1)	8 (1)	1 (1)	1 (1)
O (6)	53 (1)	37 (1)	52 (1)	-8 (1)	13 (1)	9 (1)
O (7)	51 (1)	92 (1)	41 (1)	5 (1)	29 (1)	-15 (1)
O (8)	49 (1)	38 (1)	40 (1)	7 (1)	8 (1)	14 (1)
O (9)	55 (1)	50 (1)	86 (1)	-21 (1)	32 (1)	-23 (1)
O (10)	65 (1)	91 (1)	43 (1)	-21 (1)	31 (1)	7 (1)
Fe (1)	29 (1)	21 (1)	20 (1)	0 (1)	8 (1)	-3 (1)
Co (1)	20 (1)	27 (1)	20 (1)	1 (1)	8 (1)	1 (1)
Co (2)	25 (1)	28 (1)	22 (1)	-2 (1)	10 (1)	0 (1)

Table 5. Hydrogen coordinates ($\times 10^4$) and isotropic displacement parameters ($\text{Å}^2 \times 10^3$) for aa001_0m.

	x	y	z	U (eq)
H (1)	4728	3003	-3844	73
H (2)	6008	2828	-2186	58
H (3)	7800	2699	-2231	66
H (4)	7655	2789	-3878	87
H (5)	5772	2976	-4885	90
H (6)	5985	5309	-2120	34
H (7)	4938	5565	-3830	41
H (8)	6186	5576	-4685	40
H (9)	8022	5338	-3515	33
H (12A)	9282	5027	106	34
H (12B)	8952	3839	-118	34
H (15A)	9425	3274	2343	36
H (15B)	9884	4425	2551	36
H (18A)	9525	3837	6125	61
H (18B)	10463	4127	5794	61
H (18C)	10058	2961	5720	61
H (19A)	7843	4269	5037	62
H (19B)	7646	4308	3925	62
H (18D)	7820	4249	5020	60
H (18E)	7559	3638	4064	60
H (18F)	7870	4833	4128	60
H (19C)	9523	3860	6119	53
H (19D)	10468	3580	5747	53

Table 6. Torsion angles [deg] for aa001_0m.

C(5)-C(1)-C(2)-C(3)	0.0(2)
Fe(1)-C(1)-C(2)-C(3)	-60.09(15)
C(5)-C(1)-C(2)-Fe(1)	60.12(15)
C(1)-C(2)-C(3)-C(4)	0.0(2)
Fe(1)-C(2)-C(3)-C(4)	-59.67(16)
C(1)-C(2)-C(3)-Fe(1)	59.66(15)
C(2)-C(3)-C(4)-C(5)	0.0(3)
Fe(1)-C(3)-C(4)-C(5)	-59.71(17)
C(2)-C(3)-C(4)-Fe(1)	59.70(15)
C(3)-C(4)-C(5)-C(1)	0.0(3)
Fe(1)-C(4)-C(5)-C(1)	-59.73(16)
C(3)-C(4)-C(5)-Fe(1)	59.75(16)
C(2)-C(1)-C(5)-C(4)	0.0(3)
Fe(1)-C(1)-C(5)-C(4)	59.94(17)
C(2)-C(1)-C(5)-Fe(1)	-59.98(15)
C(10)-C(6)-C(7)-C(8)	0.0(2)
Fe(1)-C(6)-C(7)-C(8)	-59.11(13)
C(10)-C(6)-C(7)-Fe(1)	59.08(11)
C(6)-C(7)-C(8)-C(9)	-0.2(2)
Fe(1)-C(7)-C(8)-C(9)	-58.61(12)
C(6)-C(7)-C(8)-Fe(1)	58.43(13)
C(7)-C(8)-C(9)-C(10)	0.3(2)
Fe(1)-C(8)-C(9)-C(10)	-58.52(11)
C(7)-C(8)-C(9)-Fe(1)	58.84(13)
C(8)-C(9)-C(10)-C(6)	-0.34(19)
Fe(1)-C(9)-C(10)-C(6)	-60.06(11)
C(8)-C(9)-C(10)-C(11)	173.77(15)
Fe(1)-C(9)-C(10)-C(11)	114.05(16)
C(8)-C(9)-C(10)-Fe(1)	59.72(12)
C(7)-C(6)-C(10)-C(9)	0.23(19)
Fe(1)-C(6)-C(10)-C(9)	60.40(11)
C(7)-C(6)-C(10)-C(11)	-173.71(16)
Fe(1)-C(6)-C(10)-C(11)	-113.54(16)
C(7)-C(6)-C(10)-Fe(1)	-60.17(12)
C(9)-C(10)-C(11)-O(1)	7.3(3)
C(6)-C(10)-C(11)-O(1)	-179.71(17)
Fe(1)-C(10)-C(11)-O(1)	93.54(19)
C(9)-C(10)-C(11)-O(2)	-171.95(15)
C(6)-C(10)-C(11)-O(2)	1.0(2)
Fe(1)-C(10)-C(11)-O(2)	-85.72(15)
O(2)-C(12)-C(13)-C(14)	179.6(2)
O(2)-C(12)-C(13)-Co(2)	-65.14(18)
O(2)-C(12)-C(13)-Co(1)	56.6(2)
C(12)-C(13)-C(14)-C(15)	-3.9(4)
Co(2)-C(13)-C(14)-C(15)	-137.7(3)
Co(1)-C(13)-C(14)-C(15)	137.2(3)
C(12)-C(13)-C(14)-Co(1)	-141.1(3)
Co(2)-C(13)-C(14)-Co(1)	85.16(4)
C(12)-C(13)-C(14)-Co(2)	133.7(3)
Co(1)-C(13)-C(14)-Co(2)	-85.16(4)
C(13)-C(14)-C(15)-O(3)	176.9(2)
Co(1)-C(14)-C(15)-O(3)	-65.5(2)
Co(2)-C(14)-C(15)-O(3)	58.9(2)
O(4)-C(16)-C(17)-C(19)	-170.8(8)

O (3) -C (16) -C (17) -C (19)	10.1 (8)
O (4) -C (16) -C (17) -C (18)	8.6 (8)
O (3) -C (16) -C (17) -C (18)	-170.5 (8)
O (1) -C (11) -O (2) -C (12)	-2.1 (2)
C (10) -C (11) -O (2) -C (12)	177.18 (14)
C (13) -C (12) -O (2) -C (11)	171.49 (14)
O (4) -C (16) -O (3) -C (15)	-1.6 (3)
C (17) -C (16) -O (3) -C (15)	177.55 (14)
C (14) -C (15) -O (3) -C (16)	177.50 (14)
C (9) -C (10) -Fe (1) -C (1)	-169.52 (18)
C (6) -C (10) -Fe (1) -C (1)	-50.8 (2)
C (11) -C (10) -Fe (1) -C (1)	71.0 (2)
C (9) -C (10) -Fe (1) -C (4)	78.06 (14)
C (6) -C (10) -Fe (1) -C (4)	-163.25 (13)
C (11) -C (10) -Fe (1) -C (4)	-41.40 (16)
C (9) -C (10) -Fe (1) -C (2)	158.90 (11)
C (6) -C (10) -Fe (1) -C (2)	-82.41 (12)
C (11) -C (10) -Fe (1) -C (2)	39.44 (15)
C (9) -C (10) -Fe (1) -C (5)	51.6 (3)
C (6) -C (10) -Fe (1) -C (5)	170.2 (3)
C (11) -C (10) -Fe (1) -C (5)	-67.9 (3)
C (9) -C (10) -Fe (1) -C (6)	-118.68 (14)
C (11) -C (10) -Fe (1) -C (6)	121.85 (16)
C (9) -C (10) -Fe (1) -C (3)	117.42 (12)
C (6) -C (10) -Fe (1) -C (3)	-123.89 (11)
C (11) -C (10) -Fe (1) -C (3)	-2.04 (15)
C (6) -C (10) -Fe (1) -C (9)	118.68 (14)
C (11) -C (10) -Fe (1) -C (9)	-119.46 (16)
C (9) -C (10) -Fe (1) -C (7)	-80.90 (11)
C (6) -C (10) -Fe (1) -C (7)	37.79 (10)
C (11) -C (10) -Fe (1) -C (7)	159.64 (14)
C (9) -C (10) -Fe (1) -C (8)	-37.51 (10)
C (6) -C (10) -Fe (1) -C (8)	81.18 (10)
C (11) -C (10) -Fe (1) -C (8)	-156.97 (14)
C (5) -C (1) -Fe (1) -C (10)	-163.33 (19)
C (2) -C (1) -Fe (1) -C (10)	-45.0 (3)
C (5) -C (1) -Fe (1) -C (4)	-37.59 (16)
C (2) -C (1) -Fe (1) -C (4)	80.70 (17)
C (5) -C (1) -Fe (1) -C (2)	-118.3 (2)
C (2) -C (1) -Fe (1) -C (5)	118.3 (2)
C (5) -C (1) -Fe (1) -C (6)	160.86 (15)
C (2) -C (1) -Fe (1) -C (6)	-80.85 (16)
C (5) -C (1) -Fe (1) -C (3)	-80.82 (17)
C (2) -C (1) -Fe (1) -C (3)	37.47 (15)
C (5) -C (1) -Fe (1) -C (9)	43.1 (4)
C (2) -C (1) -Fe (1) -C (9)	161.4 (3)
C (5) -C (1) -Fe (1) -C (7)	117.84 (16)
C (2) -C (1) -Fe (1) -C (7)	-123.87 (14)
C (5) -C (1) -Fe (1) -C (8)	77.12 (19)
C (2) -C (1) -Fe (1) -C (8)	-164.59 (13)
C (3) -C (4) -Fe (1) -C (10)	71.70 (17)
C (5) -C (4) -Fe (1) -C (10)	-168.65 (13)
C (3) -C (4) -Fe (1) -C (1)	-81.62 (17)
C (5) -C (4) -Fe (1) -C (1)	38.04 (15)
C (3) -C (4) -Fe (1) -C (2)	-37.21 (15)
C (5) -C (4) -Fe (1) -C (2)	82.44 (16)
C (3) -C (4) -Fe (1) -C (5)	-119.7 (2)

C (3) -C (4) -Fe (1) -C (6)	33.1 (4)
C (5) -C (4) -Fe (1) -C (6)	152.7 (3)
C (5) -C (4) -Fe (1) -C (3)	119.7 (2)
C (3) -C (4) -Fe (1) -C (9)	114.71 (15)
C (5) -C (4) -Fe (1) -C (9)	-125.64 (15)
C (3) -C (4) -Fe (1) -C (7)	-165.75 (19)
C (5) -C (4) -Fe (1) -C (7)	-46.1 (3)
C (3) -C (4) -Fe (1) -C (8)	157.44 (13)
C (5) -C (4) -Fe (1) -C (8)	-82.91 (17)
C (3) -C (2) -Fe (1) -C (10)	-82.53 (15)
C (1) -C (2) -Fe (1) -C (10)	158.94 (14)
C (3) -C (2) -Fe (1) -C (1)	118.5 (2)
C (3) -C (2) -Fe (1) -C (4)	37.21 (17)
C (1) -C (2) -Fe (1) -C (4)	-81.32 (18)
C (3) -C (2) -Fe (1) -C (5)	80.53 (17)
C (1) -C (2) -Fe (1) -C (5)	-38.00 (17)
C (3) -C (2) -Fe (1) -C (6)	-125.42 (14)
C (1) -C (2) -Fe (1) -C (6)	116.04 (15)
C (1) -C (2) -Fe (1) -C (3)	-118.5 (2)
C (3) -C (2) -Fe (1) -C (9)	-50.3 (2)
C (1) -C (2) -Fe (1) -C (9)	-168.88 (18)
C (3) -C (2) -Fe (1) -C (7)	-165.27 (13)
C (1) -C (2) -Fe (1) -C (7)	76.20 (17)
C (3) -C (2) -Fe (1) -C (8)	167.6 (2)
C (1) -C (2) -Fe (1) -C (8)	49.1 (3)
C (4) -C (5) -Fe (1) -C (10)	34.3 (4)
C (1) -C (5) -Fe (1) -C (10)	153.0 (3)
C (4) -C (5) -Fe (1) -C (1)	-118.6 (2)
C (1) -C (5) -Fe (1) -C (4)	118.6 (2)
C (4) -C (5) -Fe (1) -C (2)	-80.26 (16)
C (1) -C (5) -Fe (1) -C (2)	38.37 (15)
C (4) -C (5) -Fe (1) -C (6)	-160.89 (18)
C (1) -C (5) -Fe (1) -C (6)	-42.3 (3)
C (4) -C (5) -Fe (1) -C (3)	-37.08 (15)
C (1) -C (5) -Fe (1) -C (3)	81.55 (16)
C (4) -C (5) -Fe (1) -C (9)	74.73 (17)
C (1) -C (5) -Fe (1) -C (9)	-166.64 (13)
C (4) -C (5) -Fe (1) -C (7)	160.34 (14)
C (1) -C (5) -Fe (1) -C (7)	-81.03 (16)
C (4) -C (5) -Fe (1) -C (8)	117.06 (15)
C (1) -C (5) -Fe (1) -C (8)	-124.32 (14)
C (7) -C (6) -Fe (1) -C (10)	118.64 (14)
C (7) -C (6) -Fe (1) -C (1)	-84.77 (13)
C (10) -C (6) -Fe (1) -C (1)	156.58 (11)
C (7) -C (6) -Fe (1) -C (4)	168.6 (3)
C (10) -C (6) -Fe (1) -C (4)	50.0 (3)
C (7) -C (6) -Fe (1) -C (2)	-126.91 (12)
C (10) -C (6) -Fe (1) -C (2)	114.45 (11)
C (7) -C (6) -Fe (1) -C (5)	-54.9 (2)
C (10) -C (6) -Fe (1) -C (5)	-173.54 (18)
C (7) -C (6) -Fe (1) -C (3)	-166.24 (12)
C (10) -C (6) -Fe (1) -C (3)	75.12 (13)
C (7) -C (6) -Fe (1) -C (9)	80.48 (11)
C (10) -C (6) -Fe (1) -C (9)	-38.17 (9)
C (10) -C (6) -Fe (1) -C (7)	-118.64 (14)
C (7) -C (6) -Fe (1) -C (8)	37.03 (11)
C (10) -C (6) -Fe (1) -C (8)	-81.61 (10)

C (4) -C (3) -Fe (1) -C (10)	-126.58 (17)
C (2) -C (3) -Fe (1) -C (10)	113.97 (13)
C (4) -C (3) -Fe (1) -C (1)	81.07 (19)
C (2) -C (3) -Fe (1) -C (1)	-38.38 (14)
C (2) -C (3) -Fe (1) -C (4)	-119.5 (2)
C (4) -C (3) -Fe (1) -C (2)	119.5 (2)
C (4) -C (3) -Fe (1) -C (5)	37.17 (17)
C (2) -C (3) -Fe (1) -C (5)	-82.29 (16)
C (4) -C (3) -Fe (1) -C (6)	-168.34 (16)
C (2) -C (3) -Fe (1) -C (6)	72.21 (15)
C (4) -C (3) -Fe (1) -C (9)	-83.94 (18)
C (2) -C (3) -Fe (1) -C (9)	156.61 (12)
C (4) -C (3) -Fe (1) -C (7)	161.5 (3)
C (2) -C (3) -Fe (1) -C (7)	42.1 (3)
C (4) -C (3) -Fe (1) -C (8)	-52.1 (3)
C (2) -C (3) -Fe (1) -C (8)	-171.57 (17)
C (8) -C (9) -Fe (1) -C (10)	-119.00 (14)
C (8) -C (9) -Fe (1) -C (1)	43.3 (4)
C (10) -C (9) -Fe (1) -C (1)	162.3 (3)
C (8) -C (9) -Fe (1) -C (4)	118.14 (14)
C (10) -C (9) -Fe (1) -C (4)	-122.86 (14)
C (8) -C (9) -Fe (1) -C (2)	-164.61 (18)
C (10) -C (9) -Fe (1) -C (2)	-45.6 (2)
C (8) -C (9) -Fe (1) -C (5)	77.18 (16)
C (10) -C (9) -Fe (1) -C (5)	-163.82 (14)
C (8) -C (9) -Fe (1) -C (6)	-80.69 (11)
C (10) -C (9) -Fe (1) -C (6)	38.31 (9)
C (8) -C (9) -Fe (1) -C (3)	160.54 (12)
C (10) -C (9) -Fe (1) -C (3)	-80.47 (13)
C (8) -C (9) -Fe (1) -C (7)	-37.02 (10)
C (10) -C (9) -Fe (1) -C (7)	81.98 (10)
C (10) -C (9) -Fe (1) -C (8)	119.00 (14)
C (8) -C (7) -Fe (1) -C (10)	81.52 (11)
C (6) -C (7) -Fe (1) -C (10)	-38.48 (10)
C (8) -C (7) -Fe (1) -C (1)	-126.67 (12)
C (6) -C (7) -Fe (1) -C (1)	113.33 (12)
C (8) -C (7) -Fe (1) -C (4)	-51.3 (3)
C (6) -C (7) -Fe (1) -C (4)	-171.3 (2)
C (8) -C (7) -Fe (1) -C (2)	-168.63 (11)
C (6) -C (7) -Fe (1) -C (2)	71.37 (13)
C (8) -C (7) -Fe (1) -C (5)	-84.25 (14)
C (6) -C (7) -Fe (1) -C (5)	155.75 (13)
C (8) -C (7) -Fe (1) -C (6)	120.00 (15)
C (8) -C (7) -Fe (1) -C (3)	159.5 (2)
C (6) -C (7) -Fe (1) -C (3)	39.5 (3)
C (8) -C (7) -Fe (1) -C (9)	37.11 (10)
C (6) -C (7) -Fe (1) -C (9)	-82.89 (11)
C (6) -C (7) -Fe (1) -C (8)	-120.00 (15)
C (7) -C (8) -Fe (1) -C (10)	-81.88 (11)
C (9) -C (8) -Fe (1) -C (10)	38.22 (9)
C (7) -C (8) -Fe (1) -C (1)	73.33 (15)
C (9) -C (8) -Fe (1) -C (1)	-166.57 (13)
C (7) -C (8) -Fe (1) -C (4)	158.42 (15)
C (9) -C (8) -Fe (1) -C (4)	-81.48 (16)
C (7) -C (8) -Fe (1) -C (2)	34.9 (3)
C (9) -C (8) -Fe (1) -C (2)	155.0 (3)
C (7) -C (8) -Fe (1) -C (5)	115.67 (15)

C (9) -C (8) -Fe (1) -C (5)	-124.22 (14)
C (7) -C (8) -Fe (1) -C (6)	-37.29 (10)
C (9) -C (8) -Fe (1) -C (6)	82.81 (10)
C (7) -C (8) -Fe (1) -C (3)	-164.7 (2)
C (9) -C (8) -Fe (1) -C (3)	-44.6 (2)
C (7) -C (8) -Fe (1) -C (9)	-120.10 (14)
C (9) -C (8) -Fe (1) -C (7)	120.10 (14)
O (6) -C (21) -Co (1) -C (20)	102.0 (18)
O (6) -C (21) -Co (1) -C (22)	-149.8 (18)
O (6) -C (21) -Co (1) -C (13)	-5.4 (18)
O (6) -C (21) -Co (1) -C (14)	-45.8 (18)
O (6) -C (21) -Co (1) -Co (2)	-18.6 (18)
O (5) -C (20) -Co (1) -C (21)	-97 (7)
O (5) -C (20) -Co (1) -C (22)	156 (7)
O (5) -C (20) -Co (1) -C (13)	2 (7)
O (5) -C (20) -Co (1) -C (14)	21 (8)
O (5) -C (20) -Co (1) -Co (2)	54 (7)
O (7) -C (22) -Co (1) -C (21)	132 (4)
O (7) -C (22) -Co (1) -C (20)	-126 (4)
O (7) -C (22) -Co (1) -C (13)	15 (4)
O (7) -C (22) -Co (1) -C (14)	29 (4)
O (7) -C (22) -Co (1) -Co (2)	-22 (4)
C (14) -C (13) -Co (1) -C (21)	-97.49 (11)
C (12) -C (13) -Co (1) -C (21)	50.31 (17)
Co (2) -C (13) -Co (1) -C (21)	-170.39 (6)
C (14) -C (13) -Co (1) -C (20)	162.83 (10)
C (12) -C (13) -Co (1) -C (20)	-49.37 (18)
Co (2) -C (13) -Co (1) -C (20)	89.93 (7)
C (14) -C (13) -Co (1) -C (22)	22.46 (16)
C (12) -C (13) -Co (1) -C (22)	170.26 (16)
Co (2) -C (13) -Co (1) -C (22)	-50.43 (13)
C (12) -C (13) -Co (1) -C (14)	147.8 (2)
Co (2) -C (13) -Co (1) -C (14)	-72.89 (9)
C (14) -C (13) -Co (1) -Co (2)	72.89 (9)
C (12) -C (13) -Co (1) -Co (2)	-139.31 (19)
C (13) -C (14) -Co (1) -C (21)	88.32 (11)
C (15) -C (14) -Co (1) -C (21)	-56.51 (16)
Co (2) -C (14) -Co (1) -C (21)	160.44 (6)
C (13) -C (14) -Co (1) -C (20)	-28.59 (16)
C (15) -C (14) -Co (1) -C (20)	-173.43 (14)
Co (2) -C (14) -Co (1) -C (20)	43.53 (13)
C (13) -C (14) -Co (1) -C (22)	-165.29 (11)
C (15) -C (14) -Co (1) -C (22)	49.88 (17)
Co (2) -C (14) -Co (1) -C (22)	-93.17 (7)
C (15) -C (14) -Co (1) -C (13)	-144.8 (2)
Co (2) -C (14) -Co (1) -C (13)	72.12 (9)
C (13) -C (14) -Co (1) -Co (2)	-72.12 (9)
C (15) -C (14) -Co (1) -Co (2)	143.05 (18)
O (9) -C (24) -Co (2) -C (23)	-101 (4)
O (9) -C (24) -Co (2) -C (25)	150 (4)
O (9) -C (24) -Co (2) -C (13)	1 (4)
O (9) -C (24) -Co (2) -C (14)	42 (4)
O (9) -C (24) -Co (2) -Co (1)	19 (4)
O (8) -C (23) -Co (2) -C (24)	132 (2)
O (8) -C (23) -Co (2) -C (25)	-122 (2)
O (8) -C (23) -Co (2) -C (13)	32 (2)
O (8) -C (23) -Co (2) -C (14)	14 (2)

O (8) -C (23) -Co (2) -Co (1)	-19 (2)
O (10) -C (25) -Co (2) -C (24)	166 (100)
O (10) -C (25) -Co (2) -C (23)	60 (25)
O (10) -C (25) -Co (2) -C (13)	-74 (25)
O (10) -C (25) -Co (2) -C (14)	-91 (25)
O (10) -C (25) -Co (2) -Co (1)	-39 (25)
C (14) -C (13) -Co (2) -C (24)	94.61 (11)
C (12) -C (13) -Co (2) -C (24)	-50.32 (15)
Co (1) -C (13) -Co (2) -C (24)	167.31 (7)
C (14) -C (13) -Co (2) -C (23)	-161.79 (10)
C (12) -C (13) -Co (2) -C (23)	53.28 (15)
Co (1) -C (13) -Co (2) -C (23)	-89.10 (7)
C (14) -C (13) -Co (2) -C (25)	-26.11 (17)
C (12) -C (13) -Co (2) -C (25)	-171.04 (14)
Co (1) -C (13) -Co (2) -C (25)	46.58 (14)
C (12) -C (13) -Co (2) -C (14)	-144.93 (19)
Co (1) -C (13) -Co (2) -C (14)	72.69 (9)
C (14) -C (13) -Co (2) -Co (1)	-72.69 (9)
C (12) -C (13) -Co (2) -Co (1)	142.38 (16)
C (13) -C (14) -Co (2) -C (24)	-91.54 (11)
C (15) -C (14) -Co (2) -C (24)	53.40 (17)
Co (1) -C (14) -Co (2) -C (24)	-163.82 (7)
C (13) -C (14) -Co (2) -C (23)	27.21 (15)
C (15) -C (14) -Co (2) -C (23)	172.15 (14)
Co (1) -C (14) -Co (2) -C (23)	-45.08 (12)
C (13) -C (14) -Co (2) -C (25)	164.17 (10)
C (15) -C (14) -Co (2) -C (25)	-50.89 (17)
Co (1) -C (14) -Co (2) -C (25)	91.88 (7)
C (15) -C (14) -Co (2) -C (13)	144.9 (2)
Co (1) -C (14) -Co (2) -C (13)	-72.29 (9)
C (13) -C (14) -Co (2) -Co (1)	72.29 (9)
C (15) -C (14) -Co (2) -Co (1)	-142.77 (18)
C (21) -Co (1) -Co (2) -C (24)	-6.00 (15)
C (20) -Co (1) -Co (2) -C (24)	-125.81 (13)
C (22) -Co (1) -Co (2) -C (24)	126.27 (13)
C (13) -Co (1) -Co (2) -C (24)	-23.08 (13)
C (14) -Co (1) -Co (2) -C (24)	29.71 (13)
C (21) -Co (1) -Co (2) -C (23)	115.70 (11)
C (20) -Co (1) -Co (2) -C (23)	-4.10 (7)
C (22) -Co (1) -Co (2) -C (23)	-112.03 (8)
C (13) -Co (1) -Co (2) -C (23)	98.63 (8)
C (14) -Co (1) -Co (2) -C (23)	151.42 (8)
C (21) -Co (1) -Co (2) -C (25)	-136.68 (12)
C (20) -Co (1) -Co (2) -C (25)	103.52 (8)
C (22) -Co (1) -Co (2) -C (25)	-4.41 (8)
C (13) -Co (1) -Co (2) -C (25)	-153.75 (9)
C (14) -Co (1) -Co (2) -C (25)	-100.96 (8)
C (21) -Co (1) -Co (2) -C (13)	17.07 (11)
C (20) -Co (1) -Co (2) -C (13)	-102.73 (8)
C (22) -Co (1) -Co (2) -C (13)	149.34 (8)
C (14) -Co (1) -Co (2) -C (13)	52.79 (8)
C (21) -Co (1) -Co (2) -C (14)	-35.71 (11)
C (20) -Co (1) -Co (2) -C (14)	-155.51 (8)
C (22) -Co (1) -Co (2) -C (14)	96.56 (8)
C (13) -Co (1) -Co (2) -C (14)	-52.79 (8)